A SIMULATION MODEL OF CLASTIC SEDIMENTARY PROCESSES

A DISSERTATION

Submitted to the Department of Applied Earth Sciences
and the Committee on Graduate Studies

of Stanford University

in partial fulfillment of the requirements
for the degree of
Doctor of Philosophy

by

Daniel Matias Tetzlaff

May 1, 1987

I certify that I have read this thesis and that in my opinion it is fully adequate, in scope and quality, as a dissertation for the degree of Doctor of Philosophy.

John W Harbaugh

(Principal Adviser)

I certify that I have read this thesis and that in my opinion it is fully adequate, in scope and quality, as a dissertation for the degree of Doctor of Philosophy.

Stephan Alan Graham

I certify that I have read this thesis and that in my opinion it is fully adequate, in scope and quality, as a dissertation for the degree of Doctor of Philosophy.

Jeffrey R. Koseff

(Civil Engineering)

Approved for the University Committee
on Graduate Studies:

Elizabeth Closs Traugott

Dean of Graduate Studies

Table of Contents

Table of Figures

Index of Tables

ABSTRACT

This dissertation describes SEDSIM, a computer model that simulates erosion, transport, and deposition of clastic sediments by free-surface flow in natural environments. SEDSIM is deterministic and is applicable to sedimentary processes in rivers, deltas, continental shelves, submarine canyons, and turbidite fans. The model is used to perform experiments in clastic sedimentation. Computer experimentation is limited by the machine power available. However, computer experimentation is free from scaling problems associated with laboratory experiments, such as simulations in tanks or flumes containing sediment. SEDSIM responds to information provided to it at the outset of a simulation experiment; including initial topography, preexisting subsurface configuration, physical parameters of fluid and sediment, and characteristics of sediment sources.

SEDSIM was developed in three stages: The first stage involved a "flow-only" model. The flow-defining equations, the Navier-Stokes equations, were integrated vertically and modified to incorporate eddy viscosity rather than kinematic viscosity, yielding a simplified depth-mean flow model. A "particle-cell" numerical was applied, resulting in a model that is able to handle both steady and unsteady flow over an arbitrary topography. In the second stage, criteria governing sediment erosion, transport, and deposition for a single sediment type were incorporated into algorithms that simulate periods of time of geological significance. In the third stage, the model was expanded to deal with up to four arbitrary particle sizes and densities of clastic sediments, and their mixtures in any proportions.

Extensive computer graphics are incorporated in SEDSIM to display the three-dimensional geometry of simulated deposits in the form of successions of contour maps, perspective diagrams (including stereographic pairs), arrow plots of current velocities, and cross sections of any azimuth orientation, that display the sediment age and composition of the sequences of deposits that have been formed in the simulation experiment.

SEDSIM works realistically with processes involving wide channel shifting and topographic changes. Example applications include a Cretaceous sequence in the National Petroleum Reserve in Alaska, known mainly from seismic sections, and a sequence of Tertiary age in the Golden Meadow oil field of Louisiana, known principally from well logs. These examples illustrate how SEDSIM can be used in making geologic interpretations.

I conclude that simulation models can become useful tools in interpreting modern as well as ancient clastic deposits, and in predicting the shapes and orientation of specific sedimentary units in such deposits.

ACKNOWLEDGMENTS

I am grateful to Texaco Inc. for providing the financial support for this project. Donald F. Beaumont, Richard E. Byrd, Michael Zeitlin, and Martin Perlmutter of Texaco, were particularly supportive in funding decisions as well as in providing valuable ideas and personal encouragement.

Gould Inc. donated a PowerNode 9080 computer system, on which most of the computer-intensive runs were made. The speed and versatility of this machine allowed me to perform some runs that would have been impractical on computers of lesser capabilities. I am indebted to James Enking, Stephen Coles, Robert Leaf, and Shirley Scardino, of Gould, who helped arrange the donation of the PowerNode 9080.

Early development of SEDSIM involved a Gould/SEL 32/77 computer donated by Arco Exploration Company, and maintained by Gould. Arco Exploration Company and Arco Alaska Inc. provided funds for the study involving the Cretaceous sequence described in Chapter 5, used as one of two test applications of SEDSIM.

I am indebted to the faculty of Stanford's School of Earth Sciences and the School of Engineering for guidance in this project, particularly to Dr. John W. Harbaugh, my academic advisor, who provided constant encouragement to develop new ideas, and carefully reviewed the manuscript. Dr. Stephen A. Graham, of the Department of Applied Earth Sciences and Dr. David Larue of the Department of Geology contributed their knowledge of sedimentology in evaluating SEDSIM's performance. Members of the Department of Civil Engineering also assisted me in my research: Dr. Joseph Franzini guided quantitative aspects, and Dr. Jeffrey Koseff evaluated the modeling methods employed. Dr. Ralph Cheng, of the U.S. Geological Survey, provided valuable suggestions at an early stage of the project.

I wish to extend my appreciation to my office colleagues at Stanford: Robert Laudati and Paul Martinez made the well log correlations shown in Chapter V, and are currently working on extensions to the model; Norman Scott thoroughly tested the computer program; Klaus Bitzer suggested extensions and new applications; Claudio Bettini, Phillip Kushner and Luis Ramos provided sustained encouragement.

The support given by my wife, Alicia I. Tetzlaff, is beyond thanks. She typed the entire manuscript several times over, served as a diligent manager of the PowerNode 9080 computer system, and was my inseparable partner all the time.

Chapter I
INTRODUCTION

Simulation, as employed here, is the process of creating a mathematical model of an actual system and performing experiments with the model that imitate the actual system's behavior. Employing this meaning, simulation involves a broad set of techniques, applied in every field of science, and treated by many authors. General and comprehensive treatises regarding simulation are provided by Chorafas (1965) and by Shannon (1975).

Examples of simulation in the earth sciences include representation of flow in groundwater reservoirs and in oil and gas reservoirs, flood routing and river-stage calculations, and sedimentation modeling.

CLASSIFICATION OF SIMULATION MODELS

Table 1 classifies various simulation models with respect to whether they are experimental or theoretical, probabilistic or deterministic, non-dimensional, one-, two-, or three-dimensional, static or dynamic. While such a classification scheme is neither thorough nor exhaustive, it ranks SEDSIM's principal features within a spectrum of other models.

Table 1: Classification of simulation models

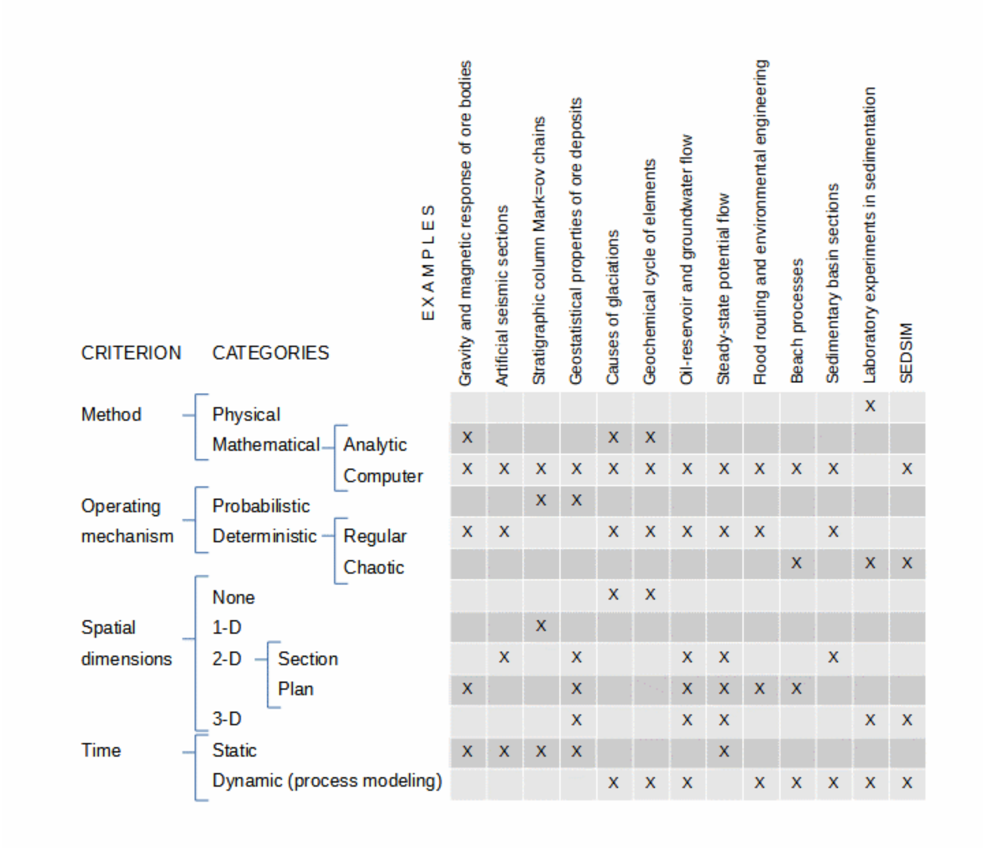

			EXAMPLES												
CRITERION	CATEGORIES		Gravity and magnetic response of ore bodies	Artificial seismic sections	Stratigraphic column Mark=ov chains	Geostatistical properties of ore deposits	Causes of glaciations	Geochemical cycle of elements	Oil-reservoir and groundwater flow	Steady-state potential flow	Flood routing and environmental engineering	Beach processes	Sedimentary basin sections	Laboratory experiments in sedimentation	SEDSIM
Method	Physical													X	
	Mathematical	Analytic	X				X	X							
		Computer	X	X	X	X	X	X	X	X	X	X	X		X
Operating mechanism	Probabilistic				X	X									
	Deterministic	Regular	X	X			X	X	X	X	X		X		
		Chaotic										X		X	X
Spatial dimensions	None						X	X							
	1-D				X										
	2-D	Section		X		X			X	X			X		
		Plan	X			X			X	X	X	X			
	3-D					X			X	X				X	X
Time	Static		X	X	X	X				X					
	Dynamic (process modeling)						X	X	X		X	X	X	X	X

Broadly, simulation models can be divided into two groups, namely (1) physical models, that embody small-scale versions of actual physical processes, such as flumes or sand-filled tanks in a sedimentation laboratory, and (2) mathematical models, in which relationships are represented as equations and logic statements, generally as computer programs.

Physical models have an advantage in that they directly represent the same phenomena as the actual system, but are often hindered because some of the physical variables represented cannot be scaled downward or upward. Mathematical models, on the other hand, do not suffer from scaling limitations, but their fidelity may be limited by the simplification necessary for treatment by computer, particularly the subdivision of a continuous medium into a finite number of cells or steps.

Simulation models may contain elements of chance, as when cause-and-effect relationships are influenced or governed by probability distributions, (for example, sedimentary sequences represented by Markov chains), or they can be totally deterministic. However, even if a simulation model is entirely deterministic, when each stateof the system leads unequivocally to the next. Certain simple deterministic systems, however, can generate apparently random behavior, because small uncertainties in the system's state may result in significant uncertainties in the model's later states (Schuster, 1985,Crutchfield et al.,1986) > SEDSIM is deterministic but can show such apparently random or "chaotic" behavior. For example, When simulating the development of a braided stream beginning with a straight channel, minor changes in flow may later cause a significant deviation in the channel. If initial conditions are changed, no matter how slightly, the later form of the channel may be significantly different. Even though it contains no elements designed to cause it to behave in a random fashion, such a model is random in the sense that its behavior can only be predicted if the initial state is known in perfect detail.

Simulation models can be classified according to number of dimensions. Some models are dimensionless, such as models that simulate the geologic cycle of a chemical element without regard for geographic or spatial distribution. Models that simulate sedimentary sequences in the form of a stratigraphic column are one-dimensional. SEDSIM represents flow in two horizontal dimensions, but flow depth is also taken into account. Therefore, from the standpoint of flow simulation, SEDSIM can be considered a "two-plus-" dimensional model. But SEDSIM is three-dimensional in simulating sedimentation, because it reproduces the full spatial distribution of sedimentary deposits.

If time is represented in a simulation model, it can be called a dynamic model or process model. Dynamic models are important in earth sciences because they may provide an insight into the past events that produced features observed at present. For example, the nature and magnitude of processes that filled an evaporite basin can be analyzed with dynamic models. Simulation experiments can be performed under various hypothesized flow circulation patterns in the basin, and with different sea water inflow conditions, until the actual stratigraphic configuration can be reproduced by the model. Harbaugh and Bonham-Carter (1970) provided a synoptic view of the use of dynamic models in geology. SEDSIM is truly dynamic. It does indeed permit the realization of experiments that can not only shed light on the processes that generated a clastic sequence, but also predict the configuration of sedimentary deposits between or beyond areas for which information is available, as for example, in an oil field where wells provide only local information.

SEDIMENTARY PROCESS MODELING

Simulation of sedimentation is difficult because of the complexity of the systems represented. Although a model can be much simpler than the real system, the model should represent all basic relationships between the system's components of specific interest. Such goal, however, may be difficult to attain in complex systems. Analytical solutions for systems of equations that govern flow and clastic sedimentation may not be feasible. Even numerical methods consume a large amount of computer time for relatively simple models. Some models of processes that transport clastic sediments work satisfactorily, as described below, but in general they are restricted to particular sedimentary environments or conditions, or they simulate only short periods of time.

We need process models that can simulate clastic processes in large sedimentary systems over extended periods of time. Such models could be used in at least three major applications:

(1) To better understand mechanisms that create depositional sedimentary features, particularly the reciprocal interaction between flow and topographic configuration.

(2) To reconstruct the depositional history of a sedimentary sequence and to predict its configuration beyond the locations where it can be observed, as in wells or outcrops. For example, there may be several alternative hypotheses concerning ancient geographic conditions that influenced the deposition of the sedimentary sequence observed in a well. A process model can be used to simulate the consequences that stem from each of the alternative hypotheses. Flow rates, sediment input, and basin slope can be adjusted until the simulated deposits and observed deposits are in suitable accord. If a feasible model can be established, it can be considered for use in predicting the sedimentary deposits in locations where geological or geophysical information is lacking.

(3) To predict the short term future behavior of fluvial systems, as for example in dealing with engineering problems posed by erosion and deposition along river banks or man-made channels, and sedimentation in reservoirs. Although procedures exist that adequately handle some of these problems, few procedures are useful in cases where channel shifts and other major topographic changes take place.

The challenge in simulating sedimentation processes lies chiefly in the fact that medium or large scale sedimentary features are not the result of isolated processes, but instead have been produced by the interactions between flow, sediment transport, and topography resulting from erosion and deposition.

While we have a good understanding of how flow causes erosion, transport, and deposition, and conversely how topographic features affect flow, the mutual interaction of these processes is known mostly conceptually. While my study does not further the principles of sediment transport, it does focus on the role of sedimentary processes within a coherent system, which can be monitored quantitatively. One of the benefits of my work has been to find an optimum compromise between the fidelity of simulation models, and the computing power available, so that computer modeling can be genuinely helpful in explaining the origin of sedimentary features and in predicting the behavior of sedimentary systems.

REVIEW OF PREVIOUS WORK

Many quantitative models that focus on various aspects of sedimentation have been described. Only a few simulation models that are closely relevant to SEDSIM will be reviewed here. The models described below were chosen because they are deterministic, and utilize an "integrated system" approach in dealing with the interaction of flow, topography and sedimentation, rather than treating isolated phenomena.

Strahler's graded stream model

Some theoretical sedimentation simulation models were developed by quantitative geomorphologists. Strahler (1952) described a one-dimensional model to simulate the evolution of a graded river's profile. He observed that at any particular time, the relationship between elevation of the river bed and distance from the head is given by an exponential function. Strahler also postulated that the rate at which the stream profile is lowered at a given point is proportional to the slope at that point. By formulating these two relationships as a set of equations, he expressed the graded stream's profile as a function of time (Fig. 1).

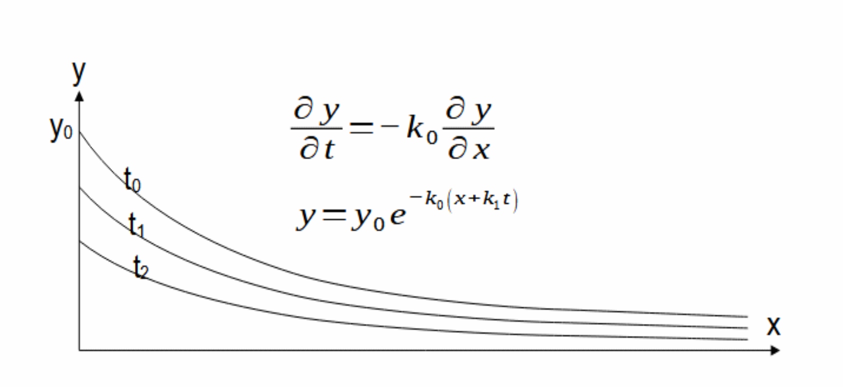

Figure 1: Profiles of graded rivers produced in accordance with Strahler's (1952) model. Y_0 is elevation of stream head at time 0. Profiles are shown at arbitrary time units 0, 1, and 2.

Strahler's model also can be used to perform simple "experiments". By modifying the resistance to erosion of the underlying bedrock, different stream profiles are produced. Although Strahler did not use computers, it would be easy to represent his conceptual model as a computer program that would calculate stream profiles in cases in which the bedrock resistance changes along the river's course, or tributaries flow into the main channel at certain points. Although simple, Strahler's model incorporates principles present in many dynamic simulation models.

Hydrologic Engineering Center model

Computer simulation models have been devised to deal with engineering applications of processes that involve scour and deposition in man-made channels and reservoirs. A particularly useful model was developed by the Hydrologic Engineering Center (HEC) of the U.S. Army

Corps of Engineers (Thomas, 1976). The computer program, called HEC-6, calculates flow conditions in a river or channel, and predicts erosion, transport and deposition of clastic sediment.

Program input consists of information on channel geometry, water discharge, and sediment characteristics. Channel geometry is specified by a series of vertical transverse cross sections. The horizontal location of the stream's bed is assumed to be fixed (Fig. 2), so lateral shifting of a channel cannot be represented. The floodplain through which the river flows is also fixed. A steady discharge can be specified for each of a number of consecutive time periods. Discharge is treated as steady within each period, but is allowed to change from one period to the next, thus permitting representation of a seasonal variation in the hydrograph. Sediment input is specified as the amount of each sediment type that the river is supplied with at its upstream end. The composition of material present in the river bed must also be specified. HEC-6 can represent up to fifteen grain size classes of clastic sediment, ranging from clay to gravel.

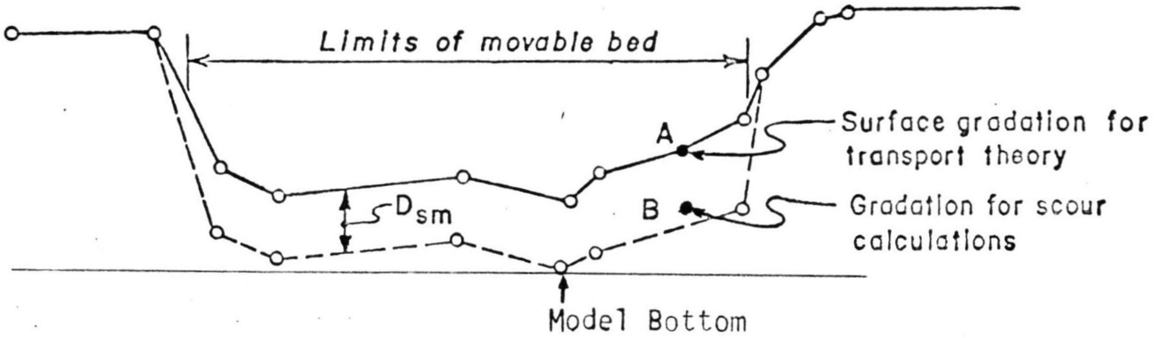
Limits of movable bed
A
Surface gradation for transport theory
D_{sm}
B
Gradation for scour calculations
Model Bottom

Figure 2: Cross section used by sedimentation program HEC-6 to represent river bed. Only central section of channel (movable bed) is subject to erosion and deposition. When scour occurs, every point of movable bed drops by same amount (D_{sm}) unless bottom level is reached, below which scour cannot occur due to presence of hypothetical hard surface. Model assumes specific sediment composition at surface of channel and different composition underneath channel. Thus, rudimentary bedforms can be simulated. From Thomas (1976).

HEC-6 calculates flow employing equations for open channel steady flow that are solved in steps for each of a series of river segments that extend between predefined cross sections. The user can choose one of three possible bed-transport equations. The elevation of an entire cross section is raised or lowered to reflect erosion or deposition. Therefore, bedforms can be simulated in rudimentary fashion. Although no record is kept of the vertical variation of the resulting deposits, HEC-6 contains a provision to simulate "armoring" (the natural process by which a channel acquires a lining of gravel-size material when finer sediment is washed away), and the subsequent destruction of the layer of armor. HEC-6 also provides for sediment consolidation (hardening) with time, but not for compaction (volume reduction). HEC-6 has proven useful in engineering applications involving simulated periods of time up to a few years.

Harbaugh and Bonham-Carter’s continental shelf model

Another model relevant to my project was developed by Harbaugh and Bonham-Carter (1970), to represent sedimentation on a continental shelf. It is based on a conceptual model by Sloss (1962). Harbaugh and Bonham-Carter’s model assumes that the continental shelf can be represented as a series of columns that extend from the shore toward a basin (Fig. 3a).

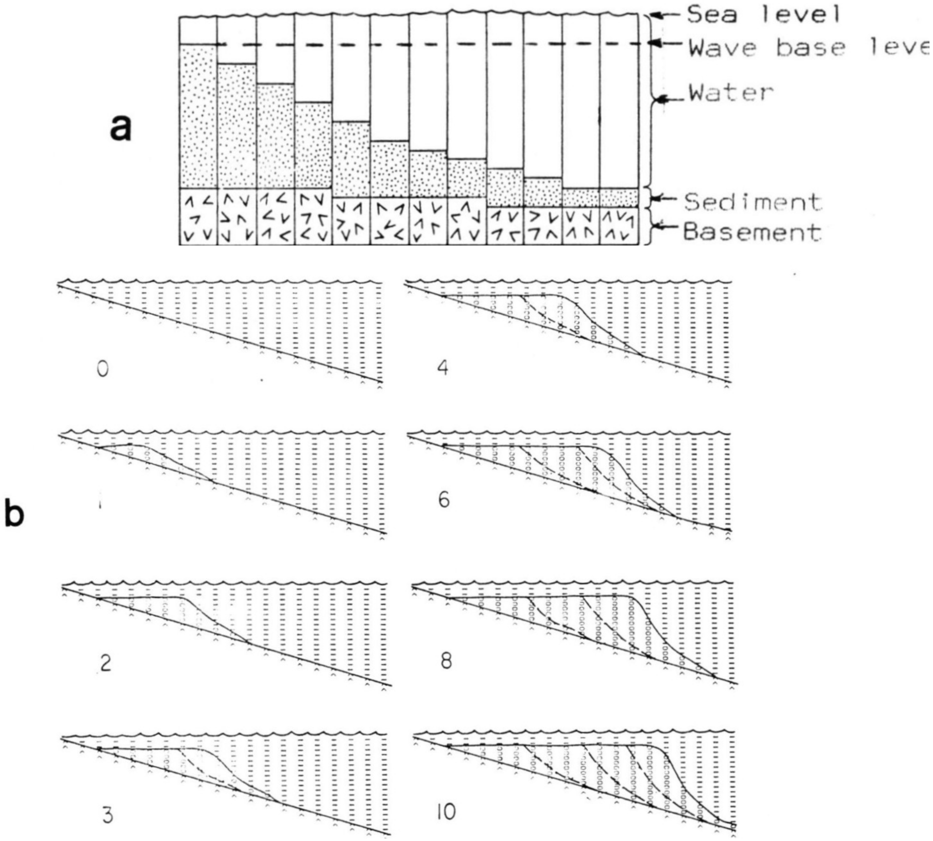

Figure 3: (a) Diagram showing subdivision of section of sedimentary basin into series of vertical cells representing water, sediment, and basement. From Harbaugh and Bonham Carter (1970). (b) Sequence of sections produced by Harbaugh and Bonham Carter's (1970) model.

The model is thus two dimensional, and is represented only in cross section. The model assumes that sedimentation on a continental shelf proceeds in te basin from a source on shore. A fraction, k, is retained in the cell nearest to shore and the rest (1-k) is carried into the next cell. The constant, k, may be likened to a “decay” constant, in regulating dispersion of sediment. However, sedimentation cannot take place above a level specified as the wave-base. Therefore, if the amount of sediment available for deposition exceeds the amount needed to fill to wave-base level, then only enough sediment to reach the wave-base level is deposited and the rest is carried to the next cell where the process is repeated.

Harbaugh and Bonham-Carter’s model produces sigmoidally shaped deposits that strongly resemble those formed on continental shelves (Fig. 3b). The model also can treat several sediment types at a time, by assigning each type a specific value of k. The proportion of each type is specified for input during each time. A mixture of sediment types is thus availabe for deposition in each cell.

Another interesting feature of Harbaugh and Bonham-Carter’s model is its capability of simulating crustal subsidence due to sediment load. Subsidence rate can be kept constant throughout the entire cross section, or it can be represented locally, within each column, as a function of sediment load in that column (Fig. 3c). A time lag also can be introduced so that subsidence occurs only after a certain number of time increments have elapsed. Experiments incorporating two sediment types and time-lag subsidence produce cyclic interfingering of coarse and fine deposits (Fig. 3d), emphasizing that interfingering need not be caused by variations in source, but also can arise solely because of lag in subsidence as the system responds to load.

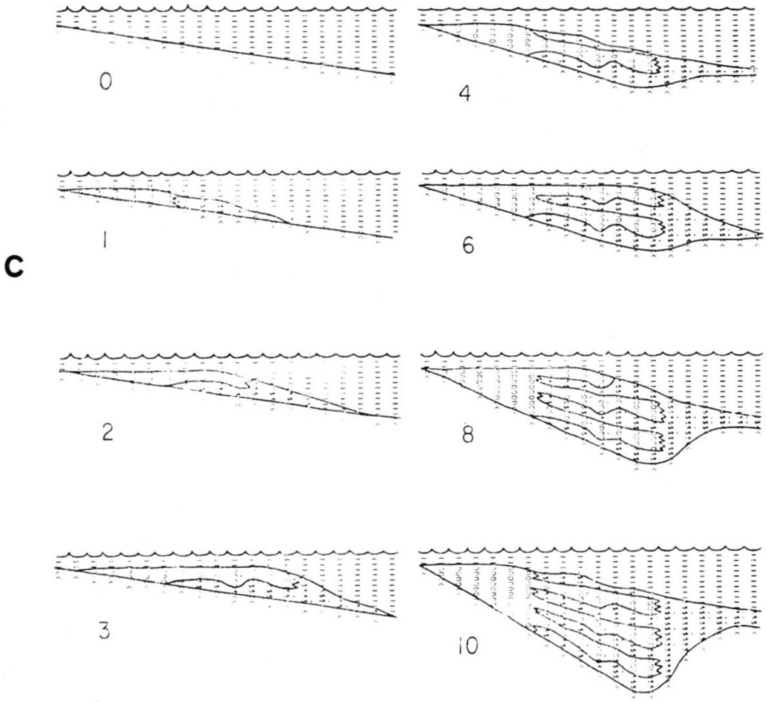

Figure 3 (cont.): (c) Section showing response of Harbaugh and Bonham Carter's (1970) model using two different grain izes. Subsidence is proportional to amount of sediment deposited in each column, but subsidence lags behind deposition until three time increments have elapsed, causing deposits of different grin sizes to interfinger with each other.

Bonham-Carter and Sutherland’s jet-flow delta model

Bonham-Carter and Sutherland (1968) developed a model that simulates deltaic sedimentation in three-dimensions. The model incorporates river width and depth, discharge rate, composition and quantity of the river’s sediment load, and the sedimentary basin’s geometry. The model utilizes equations of open-channel steady flow and assumes that as the river enters the sea,

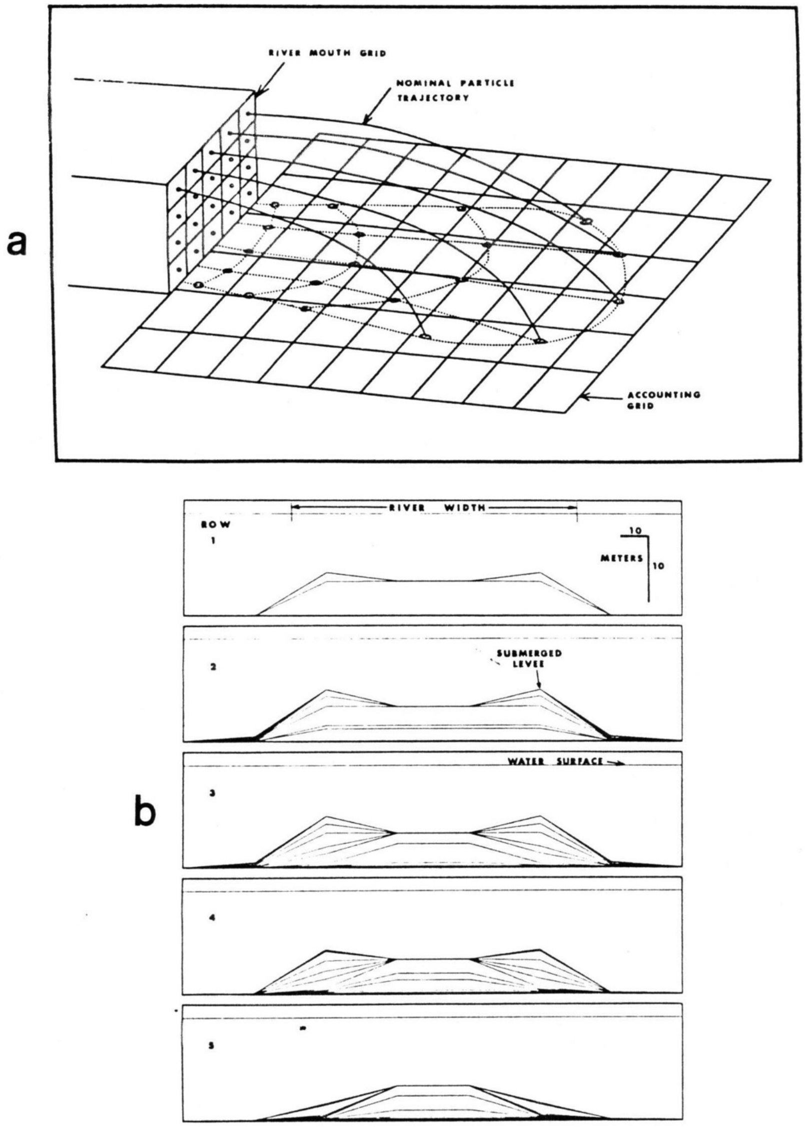

Figure 4: (a) Sediment-particle trajectories calculated by Bonham-Carter and Sutherland's (1968) model of deltaic deposits. Trajectories result from flow velocity and particle's fall velocity. When particles reach bottom of flow, they are assumed to fall vertically through still water before coming to rest on bottom. Accounting grid represents thickness of resulting deposits by adding number of statistical aggregates of particles that fall within a cell. (b) Set of transverse sections through deltaic deposits at progressively increasing distances from river mouth. Time lines showing position of water-sediment interface at successive intervals of time reveal development of submerged levees.

the resulting flow velocity distribution is that of a “plane jet”. Sediment particles are assumed to be distributed throughout the river channel’s section according to empirical functions relating sediment load, depth and velocity. The model allows use of several sediment types. Grain diameter and density define each sediment type. By considering fall velocity, horizontal flow velocities, and lateral transport of sediment, the model calculates the trajectories of particles as they leave the river mouth and thus determines the positions of individual particles as they settle (Fig. 4a). The “particles” considered in the model actually represent a large number of individual sediment grains. Deposit thickness is determined by the density of particles that settle per unit area. The results realistically represent deltaic lobes, levees and mouth bars (Figs. 4b and 4c). The flow can also be made to oscillate from side to side as it leaves the river mouth, thereby simulating the effect of longshore currents.

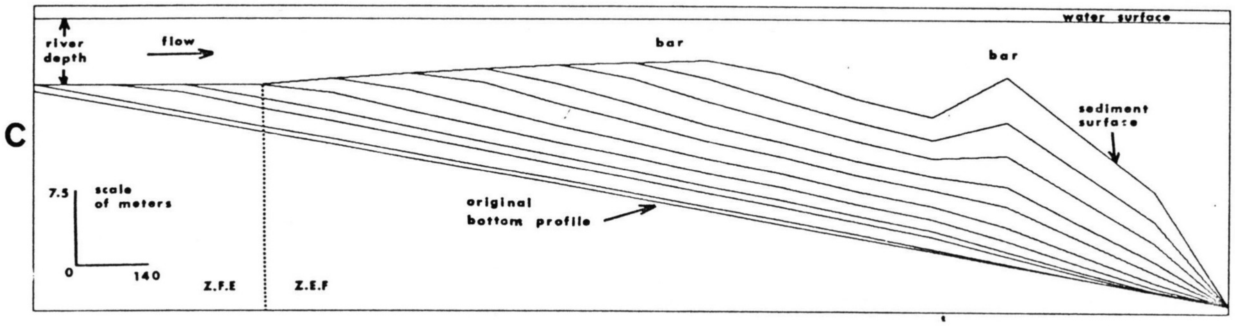

Figure 4 (cont.): (c) Longitudinal section through deltaic deposits produced by Bonham Carter and Sutherland's (1968) model. Time lines reveal progressive development of river-mouth bar. Experiment is different from that shown in Figure 4b.

Bridge’s Meandering stream model

Various authors deal with models of meandering streams. Particularly notable is the work of Bridge (1975). His model that utilizes widely accepted empirical formulas that relate a river’s hydraulic regime with the geometry of its meanders. The model contains modules that simulate the plan form of meanders, the shapes of channel cross sections, the nature and occurrence of cut-offs (which are treated probabilistically), discharge during seasonal high-water periods, and long-term aggradation. Valley slope, discharge, and sediment characteristics are provided as input data to the computer program. Output consists of vertical cross sections, that can be directly compared with sedimentary sequences. The model is particularly useful in interpreting the sedimentary sequences produced by combinations of channel migration, aggradation, and seasonal discharge variations (Fig.5). Bridge’s model does not allow lateral migration of an entire meander belt, and does not simulate overbank deposits. Therefore, the model is useful for simulating relatively short pieces of a stratigraphic record. The model has been successfully used in analyzing primary sedimentary features in Devonian sediments of Britain and in North America.

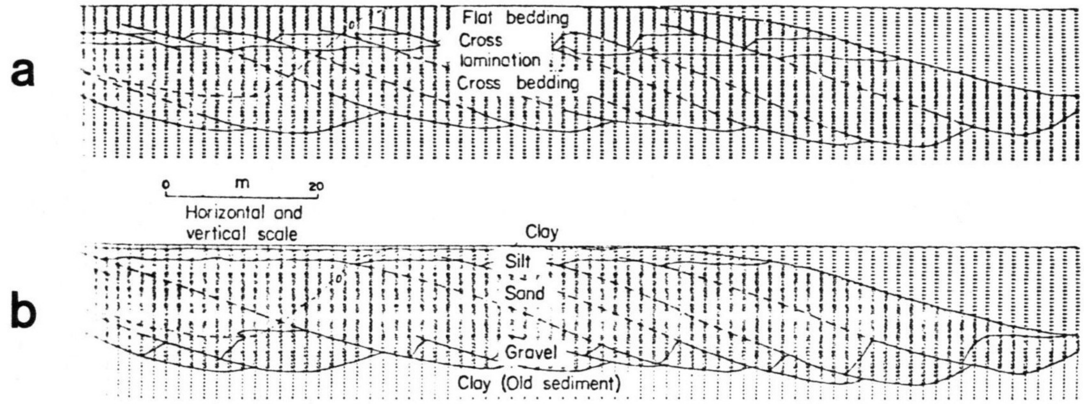

Figure 5: Sections through simulated deposits of meandering rivers produced by Bridge's (1975) model. Section represents Devonian fluvial deposits. Time lines are drawn over computer printouts. (a) Distribution of sedimentary structures, (b) distribution of sediment particle sizes.

GENERAL SCIENTIFIC PROCEDURE IN DEVELOPING SEDSIM

Creation of an effective simulation model of a physical process (Harbaugh, 1970, Hockney and Eastwood, 1981, Fischer, 1981) involves a general sequence of steps as follows:

1. Observe physical phenomena
2. Devise mathematical model
3. Develop numerical approximation
4. Write computer program
5. Conduct computer experiments

The physical phenomena that SEDSIM simulates are open-channel steady flow and open-channel unsteady flow, and the erosion, transport, and deposition of clastic sediments by flow. SEDSIM is not concerned with chemical or organogenic sediments, although it could be expanded to incorporate such processes. It accepts sea level changes and tectonic processes as “outside input”. For example faults and subsidence can be specified to occur at designated times and rates, but SEDSIM, per se, does not predict faulting and subsidence. However, SEDSIM’s modular organization permits it to be linked with simulation models of other processes, such as faulting and subsidence.

Most existing sedimentation simulation models either do not simulate flow (they only represent sediment transport) or they utilize steady flow open channel formulas, generally requiring a constant channel cross section. SEDSIM however, utilizes a more general, if less accurate approach, permitting unsteady flow and irregular channels.

Adaptation of Navier-Stokes equations

The mathematical flow model used by SEDSIM is based on a simplification of the Navier-Stokes equations. The Navier-Stokes equations completely describe flow in three dimensions in differential form. These equations cannot be incorporated into a computer program because they provide a complete description of every portion of the flow, requiring perfect knowledge of the system in order to be applicable. Adaptation of the Navier-Stokes equations is described in Chapter II.

Through two main simplifications it is possible to integrate the Navier-Stokes equations to yield a generalized open channel flow model. The model is applicable to channels whose cross section is irregular, or varies along the length of the channel, or to channels that merge (as for example river tributaries) or diverge (as delta distributaries).

The most important simplification involves the assumption that flow velocity is essentially constant from channel bottom to surface. This may seem to be an unwarranted assumption, given that actual flow velocity changes throughout the depth of any channel. However, if appropriate sediment-load formulas are devised, the effect of flow on sedimentation will still be realistic. Although it is possible to utilize less restrictive assumptions regarding the flow velocity profile (the procedure is outlined in Chapter II), the “constant profile” assumption was chosen because it simplifies computation.

The second simplification involves replacement of the fluid’s kinematic viscosity (actual physical viscosity of the fluid) by its eddy viscosity (apparent viscosity resulting from turbulence). The effect of eddy viscosity is then unfolded into two components: friction between fluid and bottom, and friction within the fluid. This method yields two parameters that are calibrated using existing semiempirical formulas for open channel flow. The parameters are not totally independent of flow conditions and may require adjustment for different environments.

The system of equations that results from applying these simplifications describes flow in two horizontal dimensions, but takes into account variations in depth of the flow. The method yields two parameters that are calibrated using existing semiempirical formulas for open chanel flow. The parameter are not totally independent of flow conditions and may require adjustment for different environment

Equations governing erosion, transport, and deposition of sediment are then added to this system. Any of a number of criteria defining erosion or deposition rates as a function of flow parameters can be used.

Eulerian representation

Flow equations can have two distinct representations: *Eulerian* and *Lagrangian*. Each method gives rise to a different numerical method to solve the flow equations. In Eulerian representation (Fig. 6a), flow is described by specific parameters (such as velocity, acceleration, and density) at points that are fixed in space. Eulerian representation is convenient for steady flow because flow velocity and acceleration do not change at points fixed in space. Therefore, steady flow models are generally based on an Eulerian method, employing a fixed grid. Methods of “discretizing” flow in mathematical descriptions that involve fixed grids include finite-difference methods (Richtmeyer and Morton, 1967), and finite-element methods (Strang and Fix, 1973).

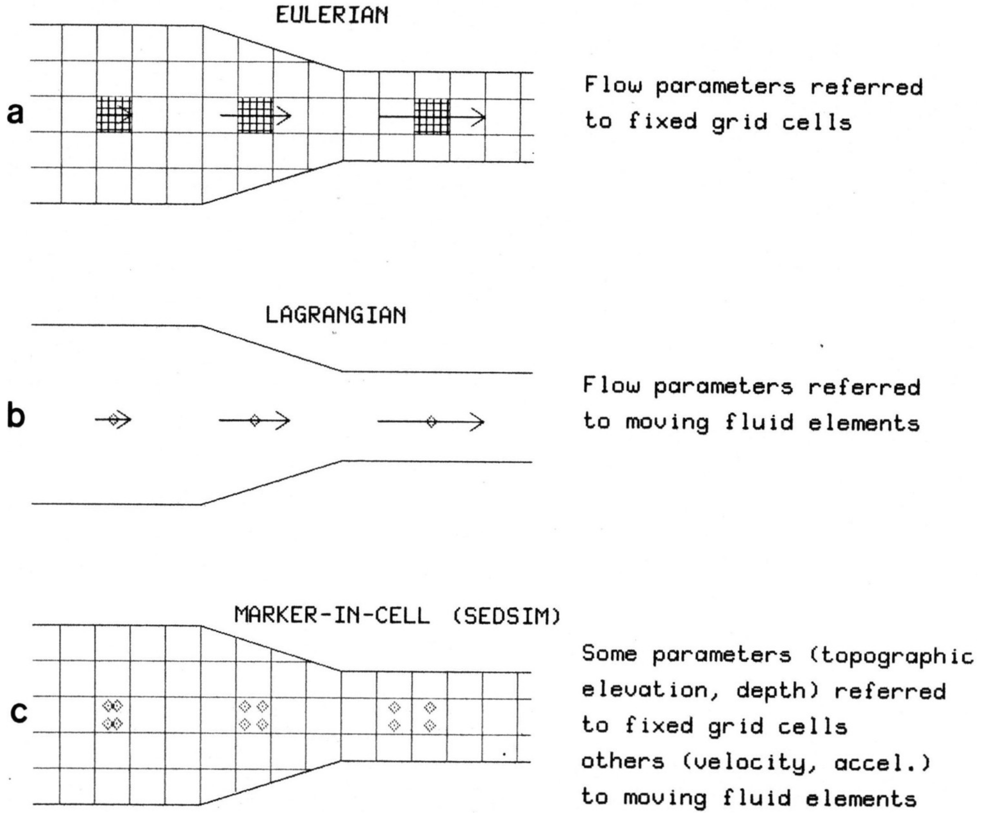
EULERIAN
a
Flow parameters referred to fixed grid cells
LAGRANGIAN
b
Flow parameters referred to moving fluid elements
MARKER-IN-CELL (SEDSIM)
c
Some parameters (topographic elevation, depth) referred to fixed grid cells
others (velocity, accel.) to moving fluid elements

Figure 6: Schematic map view of channel that narrows downstream, illustrating three different procedures for numerical representation of flow: (a) Eulerian method utilizes fixed grid, and is most effective for steady flow, (b) Lagrangian method refers all flow parameters to moving fluid elements, (c) Marker-in-cell technique uses markers or fluid elements representing small portions of fluid to simulate steady flow and transport, but retains fixed grid for some flow parameters to facilitate computations.

Lagrangian representation

In a Lagrangian representation there is no fixed grid, and therefore finite-difference and finite-element methods are not used. Instead, flow parameters are represented with respect to the moving fluid as a frame of reference (Fig. 6b). Lagrangian representation causes some difficulty because approximating the flow equations numerically requires defining a grid that can be continuously deformed, or using a large number of small portions of fluid ("fluid elements" or "particles") whose positions and velocities must be recalculated at each time step. Lagrangian representation, however, is equally appropriate to handle steady as well as unsteady flow. Furthermore, with Eulerian representation, even in steady flow, substances transported in the flow (such as suspended sediment) often tend to artificially diffuse. "Artificial diffusion" may occur in the computations because the numerical algorithm causes the transported substance to be split between grid cells, thus causing it to appear to diffuse (Roache, 1972). The use of moving fluid elements in Lagrangian representation makes it easier to eliminate artificial diffusion.

Marker-in-cell method

A model using a Lagrangian approach can sometimes be made shorter and more efficient if it is combined with a fixed grid in order to handle properties of the flow that need not be known in fine detail (Fig. 6c). Such a mixed method is called the "marker-in-cell" method (Harlow, 1964), or "particle-cell" method (Hockney and Eastwood, 1981). Harlow (1964) described the use of the marker-in-cell technique to simulate free surface flow in a vertical cross section. His model was applied to simulate the breaking of a dam, and the opening of a sluice gate. Marker-in-cell techniques are also incorporated in models that simulate flow in two horizontal dimensions (Cheng, 1983). Fully three-dimensional models utilizing the marker-in-cell method are extremely lengthy, and are mostly applied to problems in particle physics (Buneman et al., 1980).

SEDSIM uses a marker-in-cell technique in two-horizontal dimensions. Flow velocity and sediment load are represented at points that move with the fluid (Fig. 6c). A two-dimensional square grid is used to represent flow-depth and topographic elevation. A three-dimensional grid represents the subsurface configuration of sedimentary deposits. Grid parameters and fluid-element parameters are updated in cycles representing time increments of a few seconds duration. Such short time increments would make calculations involving sedimentation through intervals of geologic time prohibitive because of the vast amount of arithmetic. Therefore, erosion and sedimentation are calculated in longer time increments whose length depends on the properties and scale of the system being simulated.

Computer Program SEDSIM

Computer program SEDSIM, written in FORTRAN 77, is modular in construction, consisting of a short main program whose function is to call subroutines that are specialized for each task. The code for the entire program is relatively short, but recursion is high, resulting in lengthy execution times. Therefore the program is typically run in batch mode, and results are written onto a disk file.

An auxiliary interactive program computer is used to generate data files containing the initial topographic grid and parameters describing fluid and sediment. The display of results is handled by another interactive program, that reads the disk file and generates maps, perspectives and cross sections. The graphics program is relatively fast and simple to use. It can generate sequences of contour maps or cross sections which, when drawn in quick succession on a color terminal, represent the history of the sedimentary system, as in "movie" form.

Chapter II
FLOW MODEL

This chapter describes how SEDSIM simulates flow. Simulation of the erosion, transport, and deposition of clastic sediment of uniform grain size is treated in Chapter III, whereas Chapter IV covers the extension of the model to deal with clastic sediment of different grain sizes.

MATHEMATICAL MODEL

SEDSIM simulates flow by use of equations derived from the Navier-Stokes equations. Simplifying assumptions are made that reduce the Navier-Stokes equations to a system that is essentially two-dimensional. The reduction is accomplished by employing "depth-mean" parameters of flow, which are defined as parameters that represent an average of values along a vertical line through the flow. The resulting model is suitable for simulating free-surface flow under a variety of different flow conditions

Navier-Stokes equations

The Navier-Stokes equations consist of the continuity equation (Eq. 1) and the momentum equation (Eq. 2). Together they provide a complete mathematical description of flow for an isotropic Newtonian fluid (i.e., a fluid whose physical properties are the same in all directions, and that follows Newton's laws of motion).

Continuity equation:

The continuity equation incorporates the conservation of mass, and states:

$$\frac{\partial \rho}{\partial t} + \nabla \cdot \rho \vec{q} = 0 \qquad (1)$$

where:

$\rho =$ fluid density
$t =$ time
$\vec{q} =$ flow velocity vector

(Note: For nomenclature and a complete list of mathematical symbols, refer to Appendix B).

Momentum equation:

The momentum equation states:

$$\rho \left(\frac{\partial \vec{q}}{\partial t} + (\vec{q} \cdot \nabla) \vec{q} \right) = -\nabla p + \nabla \cdot \mu U + \rho (\vec{g} + \Omega \vec{q}) \qquad (2)$$

where:
$p=$ pressure
$\mu=$ fluid viscosity
$U=$ NavierStokes tensor:

$$\begin{bmatrix} 2\frac{\partial u}{\partial x}-\frac{2}{3}\nabla\cdot\vec{q} & \frac{\partial u}{\partial y}+\frac{\partial v}{\partial x} & \frac{\partial u}{\partial z}+\frac{\partial w}{\partial x} \\ \frac{\partial u}{\partial y}+\frac{\partial v}{\partial x} & 2\frac{\partial v}{\partial y}-\frac{2}{3}\nabla\cdot\vec{q} & \frac{\partial v}{\partial z}+\frac{\partial w}{\partial y} \\ \frac{\partial u}{\partial z}+\frac{\partial w}{\partial x} & \frac{\partial v}{\partial z}+\frac{\partial w}{\partial y} & 2\frac{\partial w}{\partial z}-\frac{2}{3}\nabla\cdot\vec{q} \end{bmatrix}$$

$u, v, w=$ components of $\vec{q}$ along the x, y, z axes

$\Omega=$ Coriolis tensor:

$$\begin{bmatrix} 0 & 2\omega\sin(\phi) & -2\omega\sin(\phi) \\ \omega\sin(\phi) & 0 & 0 \\ \omega\cos(\phi) & 0 & 0 \end{bmatrix}$$

If the fluid is also homogeneous, incompressible. and remains at constant temperature, the density ρ and the viscosity μ can be considered constant. The Coriolis acceleration, Ω, can be considered very small in the systems studied here, and is therefore ignored. Large-scale marine currents, however, are affected by the Coriolis acceleration, and so the flow model employed by SEDSIM cannot be used in simulating oceanic circulation.

With ρ and μ constant, and Ω equal to 0, the system of Equations (1) and (2) becomes:

$$\nabla\cdot\vec{q}=0 \qquad (3)$$

$$\frac{\partial\vec{q}}{\partial t}+(\vec{q}\cdot\nabla)\vec{q}=-\nabla\phi+\nu\nabla^2\vec{q}+\vec{g} \qquad (4)$$

where:
$\phi=$ ratio of pressure to constant density $=-p/\rho$
$\nu=$ kinematic viscosity $=\mu/\rho$

The solution to the system of Equations (3) and (4) is completely determined when initial conditions and boundary conditions are specified. Initial conditions involve flow at time 0:

$$\vec{q}(x, y, z, t_0)=0 \qquad (5)$$

Boundary conditions for free-surface flow:

Boundary conditions must be specified at the interface between the fluid and its surroundings. This interface is assumed to be either a free surface, or a rigid impermeable surface. "Rigid" is taken to mean that its changes in elevation are negligibly slow as compared with fluid movement.

A free surface can be described by an implicit equation:

$$f(x,y,z,t)=0 \qquad (6)$$

The kinematic equation of the free surface is:

$$u(H)\frac{\partial f}{\partial x}+v(H)\frac{\partial f}{\partial y}+w(H)\frac{\partial f}{\partial z}+\frac{\partial f}{\partial t}=\frac{Df}{Dt} \qquad (7)$$

where:

$H=$free surface elevation with respect to sea level

The rigid impermeable surface is assumed to be a function of x and y, that is, every point in the x-y plane has one and only one elevation (thus prohibiting vertical or overhanging slopes). Further, we assume that the water surface is also a function of x and y, and that the flow is always bounded by a rigid impermeable surface and a free surface. Normally the rigid impermeable surface is the topographic surface (or channel bottom), and the free surface is the air-water interface. Equation (6) then can be expressed as an explicit equation of z:

$$z=H(x,y,z) \qquad (8)$$

Now (7) yields:

$$\frac{\partial h}{\partial t}=\frac{\partial H}{\partial t}=w(H)-u(h)\frac{\partial H}{\partial x}-v(h)\frac{\partial H}{\partial y} \qquad (9)$$

Equation (9) defines the boundary conditions for the free surface of the flow.

At the rigid impermeable boundary, it is reasonable to assume from a physical standpoint that the flow is zero. However, it is possible to make the more general assumption that there is no flow perpendicular to the boundary. This has the advantage of permitting further simplification at a later stage. Thus:

$$\vec{q}\cdot\vec{N}=0 \qquad (10)$$

where:

$\vec{N}=$any vector perpendicular to the boundary

In particular:

$$\vec{N}=\left(\frac{-\partial Z}{\partial x},-\frac{\partial Z}{\partial y},1\right) \qquad (11)$$

where:

$Z=$topographic elevation (with respect to sea level)

Therefore:

$$-u(Z)\frac{\partial Z}{\partial x}-v(Z)\frac{\partial Z}{\partial y}+w(Z)=0 \qquad (12)$$

$$w(Z)=u(Z)\frac{\partial Z}{\partial x}+v(Z)\frac{\partial Z}{\partial y} \qquad (13)$$

Equation (13) defines the boundary condition for the rigid impermeable surface of the flow.

Two-dimensional continuity equation

From the simplified Navier-Stokes continuity equation (3), it is possible to obtain a two-dimensional continuity equation involving horizontal flow velocity and flow depth that applies to a flow that is confined between a rigid and a free surface. From Equation (3):

$$\frac{\partial w}{\partial Z}=-\frac{\partial u}{\partial x}-\frac{\partial v}{\partial y} \qquad (14)$$

Integrating vertically over the depth of the flow:

$$\int_Z^H \frac{\partial w}{\partial z}dz=\int_Z^H\left(-\frac{\partial u}{\partial x}-\frac{\partial v}{\partial y}\right)dz \qquad (15)$$

$$w(H)-w(Z)=\int_Z^H -\frac{\partial u}{\partial x}dz+\int_Z^H -\frac{\partial v}{\partial y}dz \qquad (16)$$

$$w(H)=\int_Z^H -\frac{\partial u}{\partial x}dz+\int_Z^H -\frac{\partial v}{\partial y}dz+w(Z) \qquad (17)$$

Both H and Z are functions of x and y (the horizontal coordinates). Therefore applying Leibnitz' rule:

$$\begin{aligned} w(H)=&-\frac{\partial\left(\int_Z^H u\,dz\right)}{\partial x}+u(H)\frac{\partial H}{\partial x}-u(Z)\frac{\partial Z}{\partial x} \\ &-\frac{\partial\left(\int_Z^H v\,dz\right)}{\partial y}+u(H)\frac{\partial H}{\partial y}-u(Z)\frac{\partial Z}{\partial y}+w(Z) \qquad (18)\end{aligned}$$

It is convenient at this point to define the vertically averaged velocities, as follows:

$$\bar{u}=\frac{1}{H-Z}\int_Z^H u\,dz \qquad (19)$$

$$\bar{v}=\frac{1}{H-Z}\int_Z^H v\,dz \qquad (20)$$

and:

$$Q = \bar{u}i + \bar{v}\,j \qquad (21)$$

where:

$Q =$ vertically averaged horizontal velocity, could also be noted as $\bar{\bar{\vec{q}}}_{xy}$

$i, j =$ vectors of unit length in the direction of the x and y axes respectively.

Then (18) becomes:

$$w(H) = -\frac{\partial(H-Z)\bar{u}}{\partial x} + u(H)\frac{\partial H}{\partial x} - u(Z)\frac{\partial Z}{\partial x}$$
$$-\frac{\partial(H-Z)\bar{v}}{\partial y} + v(H)\frac{\partial H}{\partial y} - u(Z)\frac{\partial Z}{\partial y} + w(Z) \qquad (22)$$

Using (l3) to replace w(Z), and canceling opposite terms:

$$w(H) = -\frac{\partial(H-Z)\bar{u}}{\partial x} + u(H)\frac{\partial H}{\partial x} - \frac{\partial(H-Z)\bar{v}}{\partial y} + v(H)\frac{\partial H}{\partial Z} \qquad (23)$$

Now (23) can be used to replace in (9), which after canceling opposite terms yields:

$$\frac{\partial h}{\partial t} = -\frac{\partial((H-Z)u)}{\partial x} - \frac{\partial((H-Z)v)}{\partial y} \qquad (24)$$

Thus:

$$\frac{\partial h}{\partial t} = \frac{\partial H}{\partial t} = -\nabla \cdot (hQ) \qquad (25)$$

where:

$h =$ fluid depth $= H - Z$

Equation (25) is the continuity equation for the depth-mean model. It says that if the fluid converges, its surface must rise, and vice versa. Equation (25) constitutes the first of two main equations in the simplified two-dimensional flow model.

Two-dimensional momentum equation

The second equation in the flow model is derived from Equation (4). Equation (4) can be rewritten for the components along the x, y, and z axes respectively, as follows:

For the x component:

$$\frac{\partial u}{\partial t} + u\frac{\partial u}{\partial x} + v\frac{\partial u}{\partial y} + w\frac{\partial u}{\partial z} = -\frac{1}{\rho}\frac{\partial p}{\partial x} + \frac{\mu}{\rho}\left(\frac{\partial^2 u}{\partial x^2} + \frac{\partial^2 u}{\partial y^2} + \frac{\partial^2 u}{\partial z^2}\right) \qquad (26)$$

For the y component:

$$\frac{\partial v}{\partial t} + u\frac{\partial v}{\partial x} + v\frac{\partial v}{\partial y} + w\frac{\partial v}{\partial z} = -\frac{1}{\rho}\frac{\partial p}{\partial x} + \frac{\mu}{\rho}\left(\frac{\partial^2 v}{\partial x^2} + \frac{\partial^2 v}{\partial y^2} + \frac{\partial^2 v}{\partial z^2}\right) \qquad (27)$$

For the z (vertical) component:

$$\frac{\partial w}{\partial t}+u\frac{\partial w}{\partial x}+v\frac{\partial w}{\partial y}+w\frac{\partial w}{\partial z}=-\frac{1}{\rho}\frac{\partial p}{\partial x}+\frac{\mu}{\rho}\left(\frac{\partial^2 w}{\partial x^2}+\frac{\partial^2 w}{\partial y^2}+\frac{\partial^2 w}{\partial z^2}\right)+\vec{g} \qquad (28)$$

Equation (28) will not be used further because it is not needed if pressure distribution is considered hydrostatic. Equations (26) and (27) can be integrated with respect to z, yielding respectively:

$$\underset{A}{\int_z^H \frac{\partial u}{\partial t}dz}+\underset{B}{\int_z^H\left(u\frac{\partial u}{\partial x}+v\frac{\partial u}{\partial y}\right)dz}+\underset{C}{\int_z^H w\frac{\partial u}{\partial z}dz}=\underset{D}{\int_z^H-\frac{1}{\rho}\frac{\partial p}{\partial x}dz}+\underset{E}{\int_z^H\frac{\mu}{\rho}\left(\frac{\partial^2 u}{\partial x^2}+\frac{\partial^2 u}{\partial y^2}\right)dz}+\underset{F}{\int_z^H\frac{\mu}{\rho}\frac{\partial^2 u}{\partial x^2}dz} \qquad (29)$$

and

$$\int_z^H \frac{\partial v}{\partial t}dz+\int_z^H\left(u\frac{\partial v}{\partial x}+v\frac{\partial v}{\partial y}\right)dz+\int_z^H w\frac{\partial v}{\partial z}dz=\int_z^H-\frac{1}{\rho}\frac{\partial p}{\partial x}dz+\int_z^H\frac{\mu}{\rho}\left(\frac{\partial^2 v}{\partial x^2}+\frac{\partial^2 v}{\partial y^2}\right)dz+\int_z^H\frac{\mu}{\rho}\frac{\partial^2 v}{\partial x^2}dz \qquad (30)$$

Each term in Equation (29) has been labeled so as to proceed separately with integration. To integrate the terms along the vertical dimension, it is necessary to make an assumption, described next, about vertical variation in flow, because otherwise the system of equations (26), (27), and (28) could not be effectively simplified.

Velocity profile:

The general assumption is made that the flow-velocity profile has the same shape everywhere in the flow. That is, there is a function r (Fig. 7) such that for every point

$$\vec{q}_{xy}(x_0,y_0,z) \;=\; r\left(\frac{z-Z}{H-z}\right)\;Q(x_0,y_0) \qquad (31)$$

where:

$\vec{q}_{xy}=$ horizontal velocity $=ui+vj$

$z=$ vertical coordinate with respect to sea level (within the flow: $Z\leq z\leq H$)

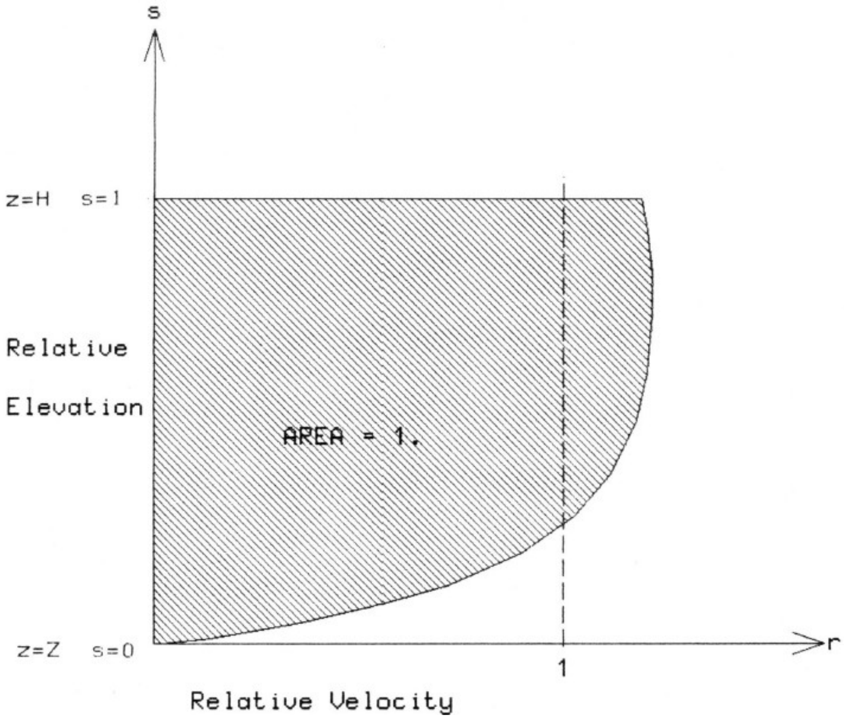

Figure 7: Example of velocity profile. Curve shows relative velocity as function of relative depth. Relative depth (s) is on vertical axis to accord with conventional representation of velocity profiles, and is scaled from 0 at channel bottom, to 1 at water surface. Relative velocity (r) is scaled so that area bounded by curve represents unit area.

Let:

$$s = \left(\frac{z-Z}{H-z}\right) \qquad (32)$$

It follows that:

$$\int_0^1 r(s)\ ds = 1 \qquad (33)$$

The function r is called the velocity profile.

Integration of the momentum equation:

A two-dimensional momentum equation can be derived by integrating Equations (29) and (30) and by making further simplifying assumptions, resulting in the expression represented by Equation (78). The integration is shown term-by-term for Equation (29), and is similar for Equation (30):

Integration of A:

$$A \;=\; \int_{Z}^{H} \frac{\partial u}{\partial t} \; dz \qquad (34)$$

$$A \;=\; \frac{\partial \int_{Z}^{H} \frac{\partial u}{\partial t} \; dz}{\partial t} - u(H)\frac{\partial H}{\partial t} + u(H)\frac{\partial Z}{\partial t} \qquad (35)$$

Assuming that the change in topography with time is very small:

$$A \;=\; \frac{\partial((H-Z)\bar{u})}{\partial t} - u(H)\frac{\partial H}{\partial t} \qquad (36)$$

$$=\; (H-Z)\frac{\partial \bar{u}}{\partial t} + \frac{\partial H}{\partial t}\bar{u} - \frac{\partial H}{\partial t}u(H) \qquad (37)$$

$$=\; (H-Z)\frac{\partial \bar{u}}{\partial t} + \frac{\partial H}{\partial t}\bar{u}(1-r(1)) \qquad (38)$$

$$\alpha = (1-r(1)) \qquad (39)$$

Then:

$$A = h\frac{\partial \bar{u}}{\partial t} + \frac{\partial H}{\partial t}\bar{u}\,\alpha \qquad (40)$$

Integration of B:

$$B = \int_{Z}^{H} \left(u\frac{\partial u}{\partial x} + v\frac{\partial u}{\partial y} \right) dz \qquad (41)$$

$$B = \underbrace{\int_{Z}^{H} u\frac{\partial u}{\partial x} dz}_{B1} + \underbrace{\int_{Z}^{H} v\frac{\partial u}{\partial y} dz}_{B2} \qquad (42)$$

$$B1 = \int_{Z}^{H} u\frac{\partial u}{\partial x} dz = (H-Z)\int_{0}^{1} r(s)\bar{u} \;\; r(s)\frac{\partial \bar{u}}{\partial x} ds \qquad (43)$$

$$B1 \;=\; (H-Z)\bar{u} \;\; r(s)\frac{\partial \bar{u}}{\partial x} \int_{0}^{1} r^{2}(s)\, ds \qquad (44)$$

Let $\beta = \int_{0}^{1} r^{2}(s)\, ds$ (45)

Then, after integrating B2 (Eq. 42) in similar fashion, the following is obtained:

$$B=h(\bar{q}\cdot\nabla)\bar{u}\,\beta \qquad (46)$$

Integration of C:

$$C \;=\; \int_{Z}^{H} w\frac{\partial u}{\partial z}dz \qquad (47)$$

First an expression for w(z) is found:

$$\int_{Z}^{z}\frac{\partial w}{\partial z}dz \;=\; \int_{Z}^{z}\left(-\frac{\partial u}{\partial x}-\frac{\partial v}{\partial y}\right)dz \qquad (48)$$

$$w(z)-w(Z) \;=\; \int_{Z}^{z}\left(-\frac{\partial u}{\partial x}-\frac{\partial v}{\partial y}\right)dz \qquad (49)$$

$$w(z) \;=\; \int_{Z}^{z}\left(-\frac{\partial u}{\partial x}-\frac{\partial v}{\partial y}\right)dz+w(Z) \qquad (50)$$

$$w(z)=-\frac{\partial\int_{Z}^{z}u\,dz}{\partial x}-u(Z)\frac{\partial u}{\partial x}-\frac{\partial\int_{Z}^{z}v\,dz}{\partial y}-v(Z)\frac{\partial v}{\partial y}+w(Z) \qquad (51)$$

$$w(z) \;=\; -\frac{\partial\int_{Z}^{z}u\,dz}{\partial x}\;-\frac{\partial\int_{Z}^{z}v\,dz}{\partial y} \qquad (52)$$

$$a \qquad\qquad b$$

$$a=-\frac{\partial\int_{Z}^{z}\bar{u}\;\;r\left(\frac{z-Z}{H-Z}\right)dz}{\partial x} \qquad (53)$$

$$a=-\frac{\partial(H-Z)\bar{u}\int_{0}^{S}r(s)ds}{\partial x}=-\frac{\partial(H-Z)\bar{u}R(S)}{\partial x} \qquad (54)$$

$$a=-\frac{\partial(H-Z)\bar{u}}{\partial x}R(S)-(H-Z)\bar{u}\frac{\partial R(S)}{\partial x} \qquad (55)$$

A similar expression can be found for b. The derivative of R(S) with respect to x can be expanded as follows:

$$\frac{\partial R(S)}{\partial x}=\frac{\partial R}{\partial S}\frac{\partial S}{\partial x}=r(S)\frac{1}{(H-Z)^{2}}\left(-\frac{\partial Z}{\partial x}(H-Z)-\frac{(z-Z)}{(H-Z)}\frac{\partial H}{\partial x}-\frac{\partial Z}{\partial x}\right) \qquad (56)$$

$$\frac{\partial R(S)}{\partial S}=\frac{r(S)}{(H-Z)}\left(-\frac{\partial Z}{\partial x}-S\frac{\partial(H-Z)}{\partial x}\right) \qquad (57)$$

Applying (57) to (55):

$$a=\left(-\frac{\partial(H-Z)\bar{u}}{\partial x}\right)R(S)-(H-Z)\bar{u}\frac{r(s)}{(H-Z)}\left(-\frac{\partial Z}{\partial x}-S\frac{\partial(H-Z)}{\partial x}\right) \tag{58}$$

$$a=\left(-\frac{\partial(H-Z)}{\partial x}\bar{u}-\frac{\partial\bar{u}}{\partial x}(H-Z)\right)R(S)-r(S)\left(\bar{u}\frac{\partial Z}{\partial x}-\bar{u}S\frac{\partial(H-Z)}{\partial x}\right) \tag{59}$$

Solving similarly for b, and replacing in (52):

$$w(z) \ = \ \nabla\cdot(hQ) \ \ R(S) \ - \ (Q\cdot\nabla)Z \ \ r(S) \ + \ S(Q\cdot\nabla)(H-Z) \tag{60}$$

Replacing in (47):

$$C \ = \ \bar{u}\left(\int_0^1 \nabla\cdot(hQ) \ \ R(S) \ \ r'(S) \ \ dS \ - \ \int_0^1 (Q\cdot\nabla)Z \ \ R(S) \ \ r'(S) \ \ dS \ + \ \int_0^1 (Q\cdot\nabla)h \ \ r'(S) \ \ dS\right) \tag{61}$$

$$C \ = \ \bar{u}\left(\nabla\cdot(hQ)\int_0^1 R(S) \ \ r'(S) \ \ dS \ - \ (Q\cdot\nabla)Z\int_0^1 r(S) \ \ r'(S) \ \ dS \ + \ (Q\cdot\nabla)h\int_0^1 S \ \ r'(S) \ \ dS\right) \tag{62}$$

$$C \ = \ \bar{u}\left(\int_0^1 \nabla\cdot(hQ)\gamma_1 \ - \ \int_0^1 (Q\cdot\nabla)Z\gamma_2 \ + \ \int_0^1 (Q\cdot\nabla)h\gamma_3\right) \tag{63}$$

where:

$$\gamma_1 \ = \ r(1)-\int_0^1 r^2(s)ds$$

$$\gamma_2 \ = \ \frac{1}{2}\left(r^2(1)-r^2(0)\right)$$

$$\gamma_3 \ = \ r(1)-1$$

Integration of D:

$$D \ = \ \int_Z^H -\frac{1}{\rho}\frac{\partial p}{\partial x}dz \tag{64}$$

Assuming hydrostatic conditions, the term in the integral is constant, because:

$$p(z) \ = \ \rho g(H-Z) \tag{65}$$

and therefore:

$$\frac{\partial p(z)}{\partial x} \ = \ \rho g\frac{\partial(H-Z)}{\partial x} \tag{66}$$

Since the vertical coordinate z is independent of x and y:

$$\frac{\partial p(z)}{\partial x} \ = \ \rho g\frac{\partial H}{\partial x} \tag{67}$$

Then:

$$D \;=\; -g\int_{Z}^{H} \frac{\partial H}{\partial x}\,dz \;=\; -g\,h\frac{\partial H}{\partial x} \qquad (68)$$

Integration of E:

$$E \;=\; \frac{\mu}{\rho}\int_{Z}^{H} \;\underset{E1}{\frac{\partial^2 u}{\partial x^2}} \;+\; \underset{E2}{\frac{\partial^2 u}{\partial y^2}}\;\, dz \qquad (69)$$

$$E1 \;=\; \int_{Z}^{H} \;\frac{\partial^2 u}{\partial x^2}\;\, dz \qquad (70)$$

Applying Leibnitz' rule twice:

$$\begin{aligned} E1 \;=\; & (H-Z)\frac{\partial^2 u}{\partial x^2}+2\frac{\partial \bar{u}}{\partial x}\frac{\partial(H-Z)}{\partial x}+\bar{u}\frac{\partial^2(H-Z)}{\partial x^2} \\ & -2\frac{\partial u(H)}{\partial x}\frac{\partial H}{\partial x}-u(H)\frac{\partial^2 H}{\partial x^2}+2\frac{\partial u(Z)}{\partial x}\frac{\partial Z}{\partial x}+u(Z)\frac{\partial^2 Z}{\partial x^2} \end{aligned} \qquad (71)$$

$$E1 \;=\; (H-Z)\frac{\partial^2 \bar{u}}{\partial x^2}+\left(2\frac{\partial \bar{u}}{\partial x}\frac{\partial(H-Z)\epsilon}{\partial x}+\bar{u}\frac{\partial^2(H-Z)\epsilon}{\partial x^2}\right) \qquad (72)$$

where:

$$\epsilon-1-\frac{r(1)H-r(0)Z}{H-Z}$$

Proceeding similarly with E2 the following is obtained:

$$E \;=\; \frac{\mu}{\rho}\left(h\nabla^2\bar{u}+2\left(\nabla(h\epsilon)\cdot\nabla\right)\bar{u}+Q\cdot\nabla^2(h\epsilon)\right) \qquad (73)$$

Integration of F:

$$F \;=\; \frac{\mu}{\rho}\int_{Z}^{H}\left(\frac{\partial^2 u}{\partial z^2}+\frac{\partial^2 v}{\partial z^2}\right)dz \;=\; \frac{1}{(H-Z)}(u+v)\int_{0}^{1}\frac{d^2 r}{d s^2}ds \qquad (74)$$

$$F \;=\; \frac{\mu}{\rho}\frac{Q}{(H-Z)}\left(r'(1)-r'(0)\right) \qquad (75)$$

$$F \;=\; \frac{\mu}{\rho}\frac{Q}{H}\phi \qquad (76)$$

where:

$$\phi \;=\; r'(1)-r'(0)$$

The terms of Equation (30) can be similarly integrated. The integrated form of Equations (29) and (30) can then be combined into a single expression, as follows:

$$h\frac{\partial Q}{\partial t}+\frac{\partial H}{\partial t}Q\alpha+h(Q\cdot\nabla)Q\beta-\frac{\partial H}{\partial t}Q\gamma_1-Q(Q\cdot\nabla)\gamma_2+Q(Q\cdot\nabla)\gamma_3 =$$

$$-hg\nabla H+h\frac{\mu}{\rho}\nabla^2 Q+\frac{\mu}{\rho}\left(2(\nabla(h\epsilon))\cdot\nabla\right)Q+Q\nabla^2(h\epsilon)+\frac{\mu}{\rho}\frac{Q}{h}\phi \qquad (77)$$

After applying (25) and dividing by h:

$$\frac{\partial Q}{\partial t}+\frac{\partial H}{\partial t}\frac{Q}{h}\alpha+(Q\cdot\nabla)Q\beta-\frac{\partial H}{\partial t}\frac{Q}{h}\gamma_1-\frac{Q}{h}(Q\cdot\nabla)\gamma_2+\frac{Q}{h}(Q\cdot\nabla)\gamma_3 =$$

$$-g\nabla H+\frac{\mu}{\rho}\nabla^2 Q+\frac{\mu}{\rho}\frac{1}{h}\left(2(\nabla(h\epsilon))\cdot\nabla\right)Q+Q\nabla^2(h^2\epsilon)+\frac{\mu}{\rho}\frac{Q}{h^2}\phi \qquad (78)$$

where:

$$\begin{aligned}
\alpha &= 1-r(1)\\
\beta &= \int_0^1 r^2(s)\,ds\\
\gamma_1 &= r(1)-\beta\\
\gamma_2 &= \frac{1}{2}\left(r^2(1)-r^2(0)\right)\\
\gamma_3 &= r(1)-1\\
\epsilon &= 1-\frac{1}{(H-Z)}\left(r(1)H-r(0)Z\right)\\
\phi &= r'(1)-r'(0)
\end{aligned}$$

Simplified velocity profiles:

Coefficients α through ϕ in Equation (78) depend on the shape of the velocity profile, defined by function r in Equations (31) and (32). The velocity profile r can be arbitrarily chosen, but additional assumptions about r can further simplify Equation (78). Figure 8 illustrates some possibilities, and Table 2 lists the corresponding coefficients for Equation (78).

Table 2: Coefficients of two-dimensional kinematic equation (Equation 78) for four idealized velocity profiles. Constant profile yields simplest mathematical model.

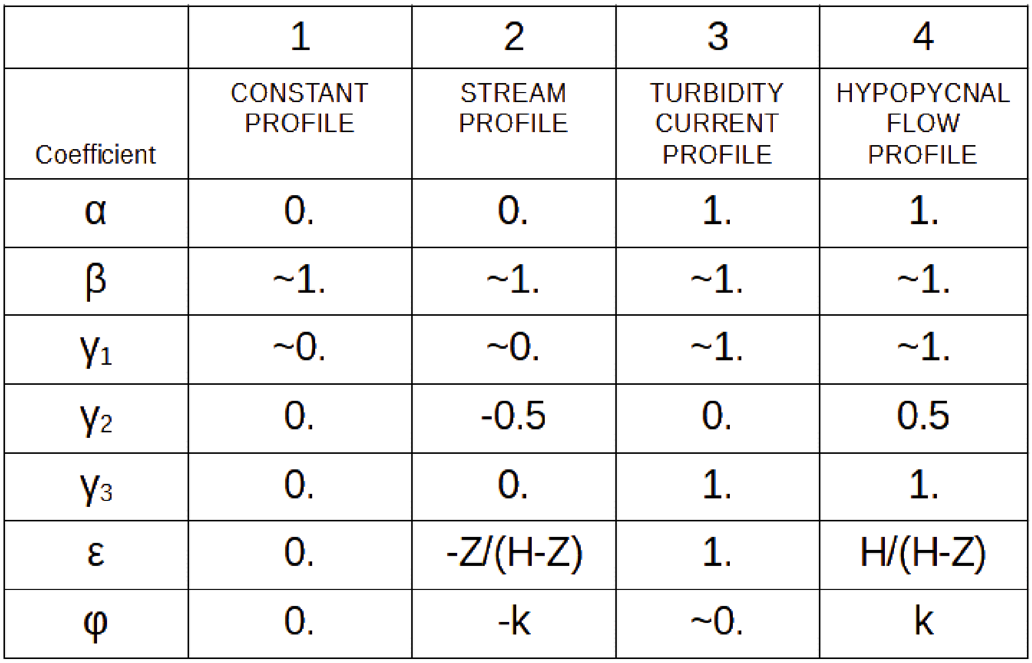

	1	2	3	4
Coefficient	CONSTANT PROFILE	STREAM PROFILE	TURBIDITY CURRENT PROFILE	HYPOPYCNAL FLOW PROFILE
α	0.	0.	1.	1.
β	~1.	~1.	~1.	~1.
γ_1	~0.	~0.	~1.	~1.
γ_2	0.	-0.5	0.	0.5
γ_3	0.	0.	1.	1.
ε	0.	-Z/(H-Z)	1.	H/(H-Z)
φ	0.	-k	~0.	k

In the simplest velocity profile, r is constant with depth (Fig. 8a). Another option (Fig. 8b) involves a profile in which the velocity is zero at the bottom, but immediately above, and for the rest of the profile upwards, is constant. This profile is called the "stream" profile. A third velocity profile (Fig. 8c) involves the assumption that the velocity is zero at both the bottom and top of the flow, but it is constant in between. Such a profile can be called a "turbidite" profile because it approximates the profile of a turbidity current, where there is drag at both the bottom and top of the flow. The turbidity profile is idealized because it ignores vertical motion within the flow, as well as displacement of the surrounding fluid, mixing, and other interactions.

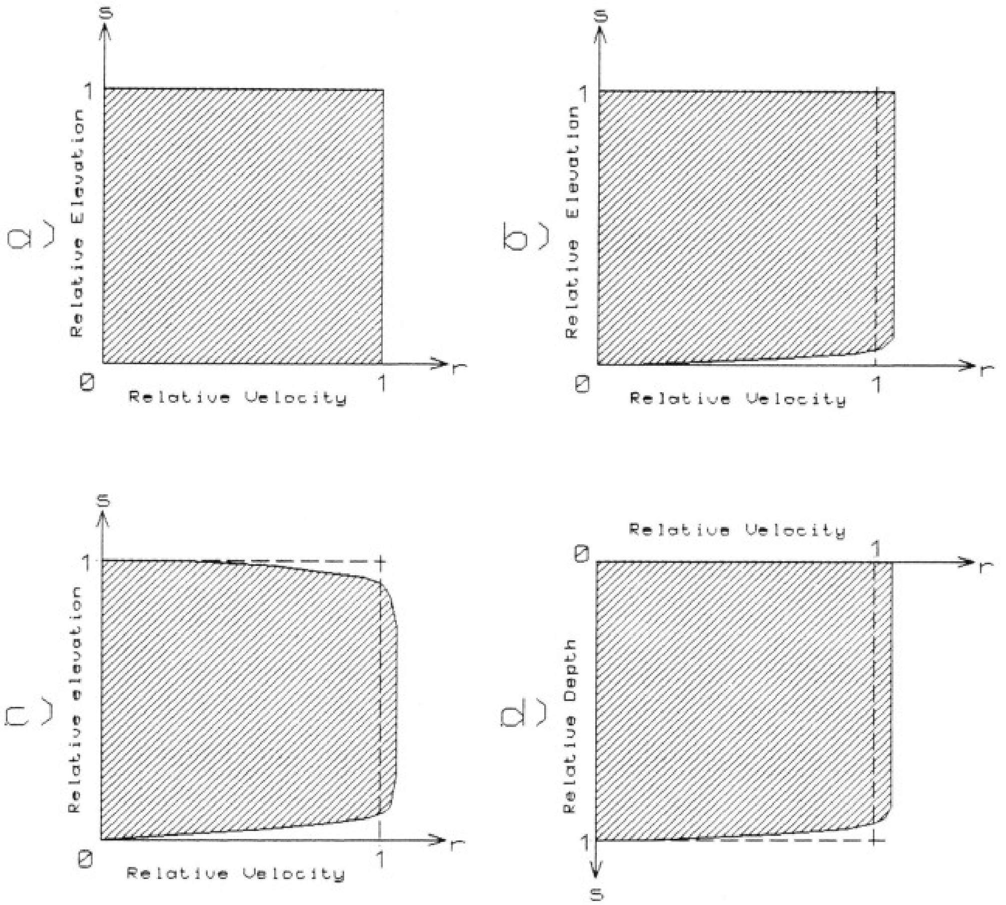

Figure 8: Four different examples of velocity profiles that simplify computations: (a) "Constant" profile, incorporated in SEDSIM. (b) "Stream" profile. (c) "Turbidity" profile. (d) "Hypopycnal flow" profile.

Finally, we can conceive of a profile in which the velocity is zero at the free surface, but is constant throughout the rest of the flow (Fig. 8d). We can invert this profile by assuming that the free surface is at the bottom of the flow, and the rigid surface is at the top, as could be provided by a fluid of low density flowing over a stagnant fluid of slightly higher density. This profile can be called the "hypopicnal-flow" profile, following the nomenclature of Bates (1953) to describe rivers discharging into bodies of water of slightly higher density. For "hypopicnal" flow, topographic elevation Z must be replaced by sea level in the flow equations. This representation of "hypopicnal" flow is idealized because wind, waves, and mixing between the flow and the surrounding fluid are ignored.

When the flow is surrounded by a medium of different density, as in turbidity currents and hypopicnal flow, Equation (78) has to be modified by multiplying gravity by the relative density of the flow with respect to the surrounding medium (R_ρ), namely:

$$R_\rho = |(\rho_1 - \rho_2)/\rho_2| \qquad (79)$$

where:

ρ_1 = density of the flow (river water)

ρ_2 = density of the surrounding fluid (sea water)

The profiles for streams, turbidity currents, and hypopicnal flow at river mouths, shown in Figures 8b, 8c, and 8d respectively, simplify the equations, but computations are still extremely lengthy for complicated flow situations. An even simpler procedure is to utilize the constant profile (Figure Ba) for all three flow situations. The constant profile method is used by SEDSIM, applying Equation (79) For turbidity and hypopicnal flow, and replacing topography by sea level for hypopicnal flow.

From the standpoint of fluid mechanics, the constant profile assumption may be too simple for practical applications. However, other sedimentation simulation models that successfully reproduce sedimentary features are based on even simpler assumptions. For example Bonham-Carter and Sutherland's (1968) jet-flow delta model, described in Chapter l, also assumes a constant velocity profile. Harbaugh and Bonham-Carter's (1970) continental shelf model treats sediment distribution without simulating flow.

Bottom friction:

The constant-profile assumption implies there is no shear in any horizontal plane in the flow, and thus friction is absent within the flow. Friction must be reintroduced at the upper or lower boundaries of the flow for realistic results. Friction is assumed to occur at the lower boundary of the flow in streams, at both the lower and upper boundaries in turbidity currents, and at the lower boundary in hypopicnal flow. Also, in turbidity flow and hypopicnal flow, gravity must be multiplied by relative flow density defined by Equation (79) to account for buoyancy of the flow.

It is convenient to employ empirical or semiempirical formulas to represent friction. In an open channel, bottom friction is proportional to the square of the average flow velocity. Therefore, acceleration due to bottom friction is given by the following formula:

$$a = -c_1 \frac{Q|Q|}{h} \qquad (80)$$

where:

c_1 = bottom friction coefficient

If the flow model is reduced to two horizontal dimensions, it is incorrect to use water viscosity μ in Equation (78), because the model applies only to turbulent flow at a macroscopic level, while μ applies to laminar flow. Therefore it is appropriate to replace μ by a coefficient c_2 that represents the effect of shear between portions of fluid of different horizontal velocities. Assuming a constant-velocity profile, and adding bottom friction, Equation (78) becomes:

$$\frac{\partial Q}{\partial t} + (Q \cdot \nabla) Q = -g \nabla H + \frac{c_2}{\rho} \nabla^2 Q - c_1 \frac{Q|Q|}{h} \qquad (81)$$

in Lagrangian form:

$$\frac{DQ}{Dt} \;=\; -g\nabla H+\frac{c_2}{\rho}\nabla^2 Q-c_1\frac{Q|Q|}{h} \qquad (82)$$

Equation (82) and the continuity equation (Eq. 25) constitute the system of equations on which the flow model for open streams is based. Coefficients c_1 and c_2 need to be calibrated, as explained later. Equation (81) defines acceleration of each element of fluid. The terms on the right side correspond, respectively, to acceleration caused by slope of the water surface, "lateral" friction within the fluid, and friction against the lower or upper boundary of the flow.

To summarize, Equations (25) and (82) have been derived from the Navier-Stokes equations making the following simplifying assumptions:

1. Flow is always confined between a rigid impermeable surface, and a free surface. Neither surface can have vertical or overhanging slopes.
2. Flow velocity is constant along any vertical line through the flow.
3. Pressure distribution is hydrostatic.
4. Friction at the flow boundaries is proportional to flow velocity squared.

Initial conditions and boundary conditions

The flow system must be provided with appropriate initial conditions and boundary conditions. The initial conditions must specify the flow velocity and depth at every point at time 0:

$$Q(x,y,t_0) \;=\; Q_0(x,y) \qquad (83)$$

$$h(x,y,t_0) \;=\; h_0(x,y) \qquad (84)$$

The boundary conditions must be specified at the "shoreline" (the line where the flow depth h becomes zero), as well as at the edges of the area. At the shoreline:

$$h(x,y,t) \;=\; 0 \qquad (85)$$

and therefore

$$\bar{u}_s\frac{\partial h_s}{\partial x}+\bar{v}_s\frac{\partial h_s}{\partial y}+\frac{\partial h_s}{\partial t} \;=\; \frac{Dh_s}{Dt} \;=\; 0 \qquad (86)$$

where:

$\bar{u}_s, \bar{v}_s$ = components of velocity at the shoreline

h_s = flow depth at the shoreline

D = derivative following motion of the fluid

At the edges of the simulated area, we assume that all fluid is removed so as to make flow depth equal to zero. This assumption approximates the physical condition that permits the flow to exit freely at the boundaries:

$$h_e=0 \qquad (87)$$

Sources of fluid at specific geographic points can be provided. being defined by additional boundary conditions. Flow rate at each source is defined as follows:

$$\nabla \cdot \left(h\left(x_{si}, y_{si}\right) Q\left(x_{si}, y_{si}\right)\right)+\frac{\partial h}{\partial t} = F_{si} \qquad (88)$$

where:

x_{si}, y_{si} = coordinates defining geographic position of point source

s_i = source number

F_{si} = flow rate at source s_i

The velocity at each source is provided by:

$$Q\left(x_{si}, y_{si}\right) = Q_{si} \qquad (89)$$

where:

Q_{si} = velocity at source s_i

With the addition of the initial and boundary conditions defined by equations (83) through (89), the flow system is completely defined. The unknowns in the system are flow depths and horizontal flow velocities that are a function of position and time. Conditions for the existence and uniqueness of a solution to the system are not rigorously treated here, but are illustrated by means of examples.

NUMERICAL APPROXIMATION

The solution to a complicated system of partial differential equations is often impossible to find analytically. Numerical methods can then be applied to find an approximate solution. Typically, continuous variables are represented at discrete points. A continuous function defined on a plane, for example, can be substituted by a function whose domain is a finite set of points, or grid, on the plane. Time can be subdivided into a series of intervals or steps. Differential equations can then be replaced by algebraic expressions relating the values of the discrete variables to each other. To find an approximation to the solution, the algebraic expressions are applied to the discrete variables in a series of iterations. Since there are many possible algebraic approximations, criteria are needed to determine the "goodness" of each approximation. The criteria include consistency, accuracy, stability, and efficiency (Hockney and Eastwood, 1981, Lapidus. 1982). Consistency is obtained when the solution obtained from the numerical approximation approaches the exact solution to the differential equations, as discrete intervals (time steps or grid elements) are made very small. Accuracy is a measure of closeness between a value given by an approximate algebraic expression at a point, and the actual value given by the exact solution. Stability is the property that causes errors to decrease as successive iterations are calculated. Efficiency pertains to the ability of the method to reach a suitable approximation to the actual solution in an acceptable number of iterations.

Consistency and stability are the most important properties of a numerical method. When both are met, the method is said to be convergent, because successive application of the algebraic expressions to approximate values over a grid with a mesh of small cells leads to a solution of the original differential equation or set of equations.

Storage is another important property of numerical methods. Storage is the amount of information that needs to be retained when performing the numerical algorithms. Generally. there is a trade-off between storage and efficiency, because some methods can be made more efficient at the expense of "remembering" more information, or vice versa. In a digital computer, storage affects the amount of memory that the program will use, while efficiency, together with the computer's speed, affects execution time.

Static versus dynamic models

In a static system, where time is not represented, only the "spatial variables" need to be placed in discrete form. Thus the solution of a three-dimensional static system can be approximated by a single three-dimensional grid of points distributed through space. In contrast, a dynamic system includes time, and the solution of a three-dimensional dynamic system must be represented by a large number of three-dimensional grids (one for each time increment). The solution also can be regarded as a four-dimensional grid that includes time as the fourth dimension.

Table 3: Steps involved in solving static and dynamic spatial models by successive iterations. In most static spatial models, each iteration produces new grid that is closer to exact solution than preceding grid. When deviation from exact solution is small, last grid is used as solution. Solution of dynamic spatial models contains time as a dimension, and result of each iteration is part of solution. Therefore, result of each iteration must be precise enough to be acceptable as solution for particular time, making dynamic models longer and more difficult to solve.

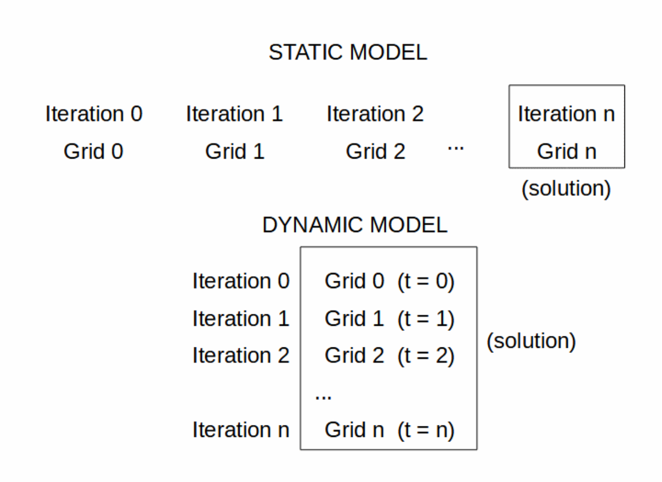

STATIC MODEL

Iteration 0	Iteration 1	Iteration 2		Iteration n
Grid 0	Grid 1	Grid 2	...	Grid n
				(solution)

DYNAMIC MODEL

Iteration 0	Grid 0 (t = 0)	(solution)
Iteration 1	Grid 1 (t = 1)	
Iteration 2	Grid 2 (t = 2)	
	...	
Iteration n	Grid n (t = n)	

Static systems can be solved by taking a grid of approximate values that are iteratively recalculated to approximate a solution. Only the final grid represents the solution (Table 3). In a dynamic system this method is generally not feasible. Dynamic systems must be solved by starting with a grid representing the initial conditions. Iterative calculations are then applied to Find each subsequent state. Greater accuracy and efficiency are required at each iteration because the result of every iteration (not just of the last iteration) is part of the solution.

Therefore dynamic systems are usually lengthier and harder to solve than static systems of comparable spatial extent and detail.

In this study, the system of equations is solved by a particle-mesh method (Hockney and Eastwood, 1981) that employs a grid to represent variables at fixed points such as topographic elevation and flow depth, and "particles" or "fluid elements" to represent variables at points that move with the fluid, such as position. Flow velocity is represented both as a "grid variable" and as a "fluid-element variable".

Grid variables are treated by standard finite-difference methods, for which consistency and stability have been proven (Richtmeyer and Morton, 1967). For algebraic approximations involving the interaction between particle variables and grid variables, consistency and stability are evaluated by means of test runs.

Grid variables

Representation of two-dimensional variables by regular grids may differ according to the shape of the cells in the grid in plan view (the cells may be square, rectangular, triangular, or hexagonal). Also, if the method requires interpolation between grid points, grids may differ according to the interpolation of function. The interpolation of function can be represented graphically by a surface of of varying elevation over a cell. Figure 9 shows several alternative grids. A grid surface should not have discontinuities or jumps at the interfaces that bound cells (i.e. the interpolation function should be continuous if the variable represented is continuous). However, avoiding discontinuities can be in conflict with the desirable property that grid cells have plane surfaces (i.e. linear interpolation functions), so that interpolated values between grid points can be readily calculated.

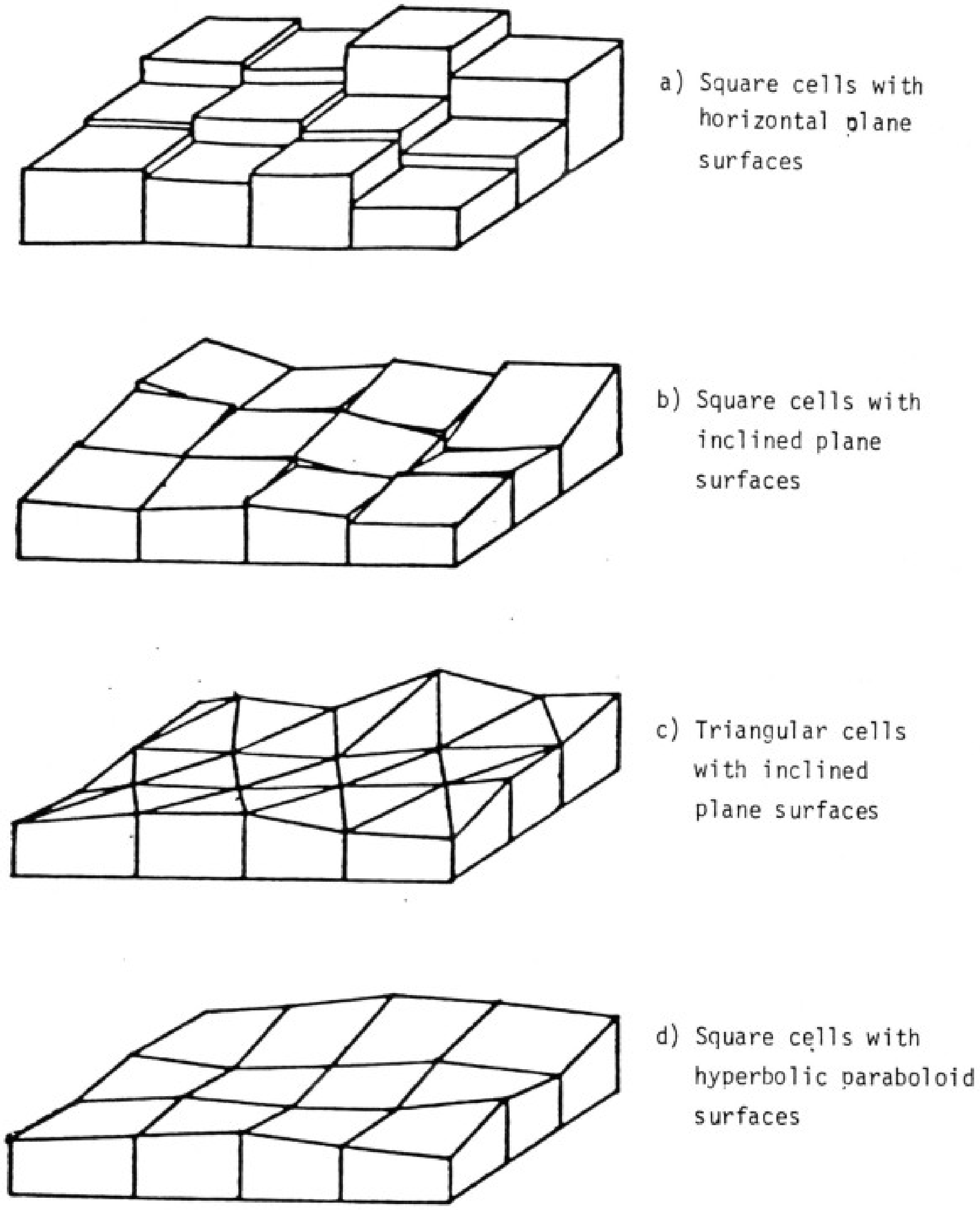
a) Square cells with horizontal plane surfaces
b) Square cells with inclined plane surfaces
c) Triangular cells with inclined plane surfaces
d) Square cells with hyperbolic paraboloid surfaces

Figure 9: Examples of grids with different cell shapes and interpolation functions: (a) Square cells employing constant interpolation function. (b) Square cells employing linear interpolation function. (c) Triangular cells employing linear interpolation function. (d) Square cells employing hyperbolic-paraboloid interpolation function as used by SEDSIM. Hyperbolic paraboloid is simplest second-degree function that exactly fits values at cell corners, becoming linear when one of two variables (x or y) are fixed. Therefore a cell's edges are straight lines that are shared by adjacent cells, and there are no discontinuities between cells.

Two-dimensional regular grids:

A grid with square cells and horizontal cell surfaces is the simplest grid (Fig. 9a). The variable represented takes the same value everywhere within a given cell. Therefore interpolation within each cell is trivial, but there are discontinuities between cells. The discontinuities persist even if the cell surfaces are inclined planes (Fig. 9b), represented by linear interpolation functions within each cell. Triangular cells permit plane surfaces without discontinuities at the edges of cells (Fig. 9c), but triangular cells require trigonometric functions for determining the specific cell in which a given point is located, thus increasing computing effort. If a grid with square cells is to have continuous cell boundaries, each cell's surface must be curved to fit the edges of the cell. Therefore, we lose the advantage of using linear interpolation functions (represented by planar surfaces) if we are to maintain continuity at cell boundaries. The simplest interpolation function that can be used for representing a curved surface that fits the straight edges of a cell that is square or rectangular in plan view is a hyperbolic paraboloid. SEDSIM employs a procedure in which the in-cell values are defined by a hyperbolic paraboloid, which is only slightly lengthier to compute than a linear interpolation function, but provides continuity at cell edges.

Interpolation function:

When values within a grid cell are interpolated with a hyperbolic paraboloid, the values are calculated as follows:

$$z(Z_1,Z_2,Z_3,Z_4,X,Y)=Z_1XY+Z_2(1-X)Y+Z_3X(1-Y)+Z_4(1-X)(1-Y) \qquad (90)$$

where:

z = variable being evaluated
Z_i = value of z at each corner of a cell
X,Y = coordinates of position within cell $(0\le X\le 1,\ 0\le Y\le 1)$

First derivatives along the x and y axes, represented by the slope of the cell's surface, are calculated as follows:

$$\begin{aligned} S_x(Z_1,Z_2,Z_3,Z_4,X,Y)&=(Z_2-Z_1)Y+(Z_3-Z_4)(1-Y)\\ S_y(Z_1,Z_2,Z_3,Z_4,X,Y)&=(Z_3-Z_1)X+(Z_4-Z_2)(1-X)\end{aligned} \qquad (91)$$

where:

S_x,S_y = slopes of z in the x and y directions

Topographic elevation:

In SEDSIM, a value representing topographic elevation is supplied at each grid point. Equations (90) and (91) are used to calculate elevation and slope of the topographic surface between grid points.

Flow depth:

Flow depth is calculated using the number of fluid elements in the vicinity of each grid point (Fig. 10). Fluid elements are assumed to have fixed volume, and therefore the average flow depth over an area, A, can be calculated from the number of fluid elements on that area, the volume of each element, and the size of area A. Although such a relationship is intuitively obvious, it also can be deduced from the continuity equation (Eq. 25). In fact, by integrating Equation (25) over the area of a cell, and then applying Stokes theorem, we obtain:

$$\frac{\partial h}{\partial t} = \frac{1}{A}\oint_{\partial A} h(N\cdot Q)\,dl \qquad (92)$$

where:

A = area of one cell
$\oint$ = curvilinear integral
∂A = perimeter of one cell
N = normal external versor to ∂A
l = length

Then, integration of Equation (92) over a period of time T yields:

$$h_t - h_0 = \frac{1}{A}\int_0^t \left(\oint h(N\cdot Q)\,dl\right)dt \qquad (93)$$

or

$$h_t = h_0 + V/A \qquad (94)$$

where:

V = net volume of fluid that has entered the cell since time 0

Equation (94) can be expressed in discrete algebraic form.

$$h_{i,j} \simeq V_e L_{i,j}/A \qquad (95)$$

where:

$h_{i,j}$ = flow depth at point i,j
V_e = volume of one fluid element
$L_{i,j}$ = number of fluid elements near grid point i,j (Fig. 10)
A = area

In SEDSIM, area A is assumed to be the area "surrounding" each grid point (Fig. 10). Thus a grid representing flow depth can be obtained using (95).

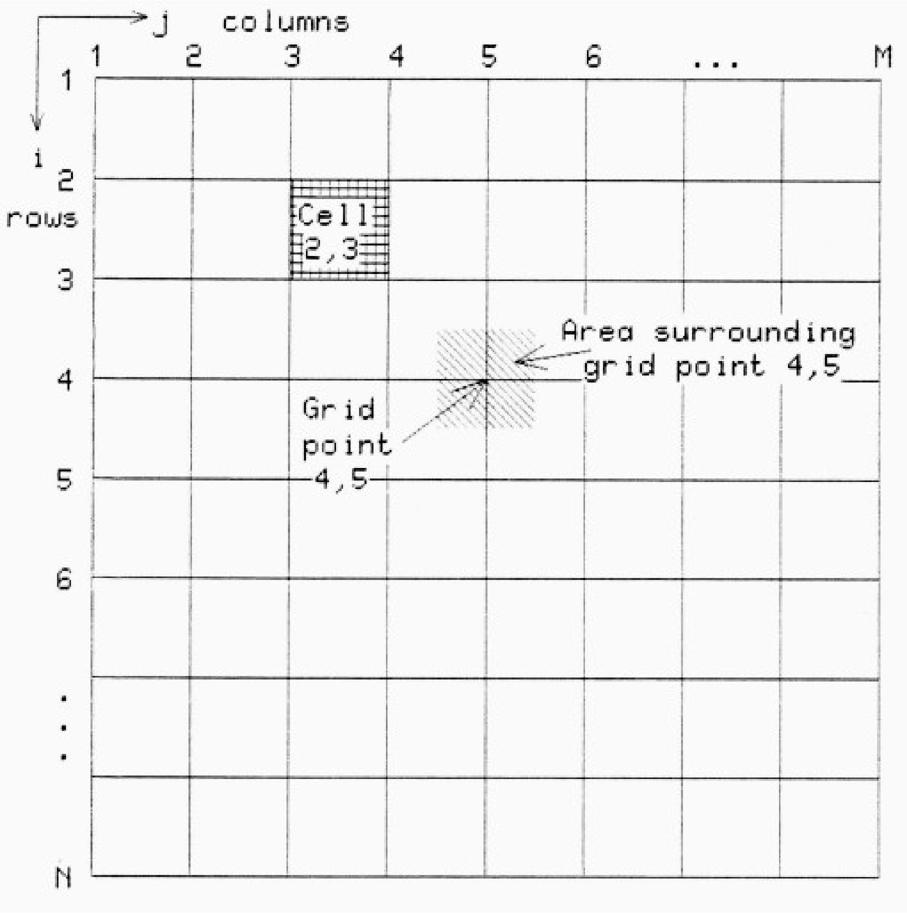

Figure 10: Map view of square grid employed by SEDSIM. Parameters at grid points are calculated by averaging parameters within square area surrounding each grid point.

Velocity:

Flow velocity at each grid point is calculated as the average velocity of the fluid elements in the vicinity of the grid point:

$$Q_{i,j} \;=\; 1/L\sum_{k=1}^{L} Q_k \qquad (96)$$

where:

$Q_{i,j}$ = velocity at grid point i,j

$\sum_{k=1}^{L}$ = summation over k, $1 \le k \le L$

L = number of fluid elements near grid point i,j

Q_k = velovity of fluid element k

The value of $\nabla^2 Q$ can be calculated from the average flow velocity at grid point $(O_{i,j})$, and the average velocity in the surrounding grid points, as is standard in finite-difference schemes:

$$\nabla^2 Q \;=\; \frac{Q_{i,j} - \left(Q_{i,j+1} + Q_{i,j-1} + Q_{i+1,j} + Q_{i-1,j}\right)}{\left(\Delta X\right)^2} \qquad (97)$$

Fluid-element variables

Fluid position and velocity are represented in two horizontal dimensions as a set of moving points or fluid elements. The acceleration of each fluid element can be approximated as follows:

$$\frac{DQ}{Dt} \;\simeq\; \frac{\Delta Q}{\Delta T} \;=\; \frac{Q_{t+1} - Q_t}{\Delta t} \qquad (98)$$

Therefore Equation (82) can be expressed algebraically as follows:

$$\frac{Q_{k,t+1} - Q_{k,t}}{\Delta T} \;=\; g\,S_k(H) \;-\; c_1 \frac{Q_k |Q_k|}{Z_k - H_k} \;+\; \frac{c_2}{\rho} \frac{Q_{i,j} - \left(Q_{i,j+1} + Q_{i,j-1} \;+\; Q_{i+1,j} + Q_{i-1,j}\right)}{\left(\Delta X\right)^2} \qquad (99)$$

where:

H_k = water surface elevation at location of element k

S_k = water surface slope at location of element k

Z_k = topographic elevation at location of element k

Let C be the term on the right side of Equation (99), then the velocity of each fluid element is given by the following expression:

$$Q_{k,t+1} = Q_{k,t} + C \;\; \Delta T \qquad (100)$$

The position of each fluid element is given by:

$$X_{k,t+1} \;=\; X_{k,t} + \frac{Q_{k,t} + Q_{k,t}}{2} \Delta T \qquad (101)$$

where:

$X_{k,t+1}$ = position of fluid element k at time t

$X_{k,t-1}$ = position of fluid element k at time $t-1$

Equations (100) and (101) are used to update velocities and positions of each fluid element at each time increment.

COMPUTER PROGRAM

Computer program SEDCYC1 performs the flow simulation. A number of accessory programs deal with input data preparation, graphic output, and printed output. Figure 11 is a schematic flow chart showing the relationship between the computer programs that are used in running a simulation and displaying its results.

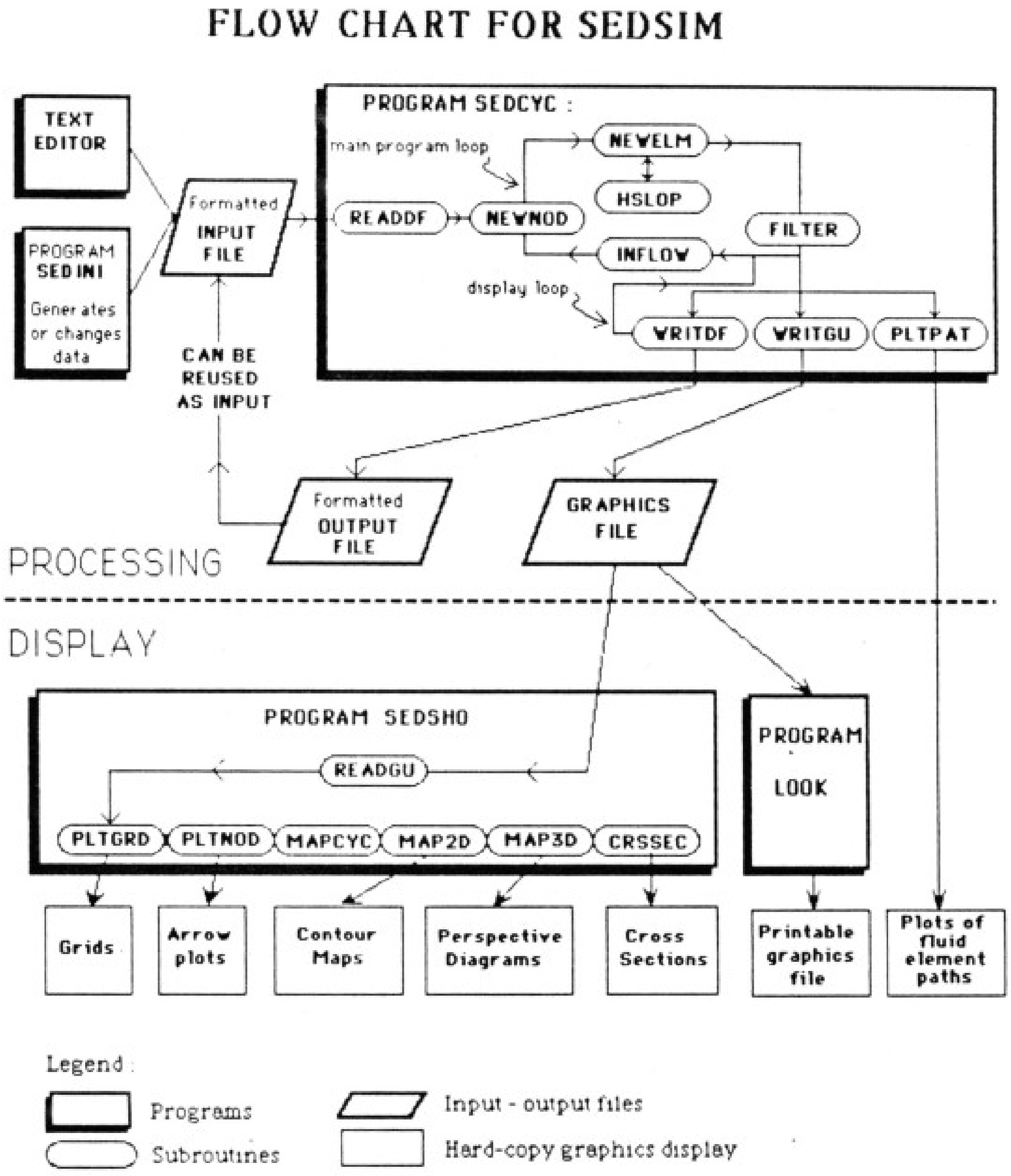

Figure 11: Schematic flow chart of modular programs used to simulate flow in SEDSIM.

An input data file, that contains all the information on the initial state of the system to be simulated, must be provided. An example input file is shown in Table 4, which contains physical parameters, the topographic grid, and the characteristics of the sources of fluid. The input data file can be prepared with the aid of program SEDINI, which is an interactive program capable of generating grids, and writing all pertinent information in the appropriate formats.

Table 4: Sample input data file for program SEDCYC1 involving simulation of flow on inclined plane. File contains headings for every input parameter or grid to facilitate user's understanding of input parameters.

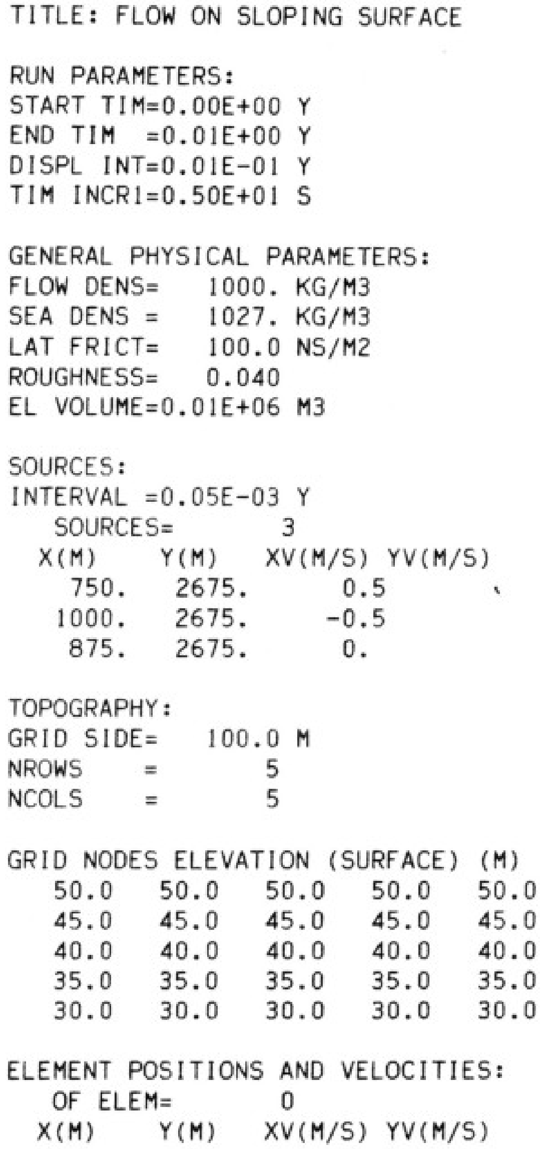

```
TITLE: FLOW ON SLOPING SURFACE

RUN PARAMETERS:
START TIM=0.00E+00 Y
END TIM  =0.01E+00 Y
DISPL INT=0.01E-01 Y
TIM INCR1=0.50E+01 S

GENERAL PHYSICAL PARAMETERS:
FLOW DENS=   1000. KG/M3
SEA DENS =   1027. KG/M3
LAT FRICT=   100.0 NS/M2
ROUGHNESS=   0.040
EL VOLUME=0.01E+06 M3

SOURCES:
INTERVAL =0.05E-03 Y
   SOURCES=        3
  X(M)    Y(M)   XV(M/S) YV(M/S)
    750.   2675.       0.5
   1000.   2675.      -0.5
    875.   2675.       0.

TOPOGRAPHY:
GRID SIDE=   100.0 M
NROWS    =       5
NCOLS    =       5

GRID NODES ELEVATION (SURFACE) (M)
   50.0   50.0   50.0   50.0   50.0
   45.0   45.0   45.0   45.0   45.0
   40.0   40.0   40.0   40.0   40.0
   35.0   35.0   35.0   35.0   35.0
   30.0   30.0   30.0   30.0   30.0

ELEMENT POSITIONS AND VELOCITIES:
   OF ELEM=        0
  X(M)    Y(M)   XV(M/S) YV(M/S)
```

Program cycles

After an input data file has been prepared, computer program SEDCYC1 can be executed. SEDCYC1 First invokes subroutine READDF, which reads the formatted data file. Then it enters the main loop in which each cycle represents a time increment. During each cycle, (1) subroutine NEWNOD updates the grid variables, and (2) subroutine NEWELM updates the particle variables. NEWNOD and NEWELM are executed alternately, a procedure known as the "leapfrog" method (Hockney and Eastwood, 1981).

NEWNOD updates flow velocity and flow depth at each grid point according to Equations (95) and (96). Depth is represented by the number of fluid elements in the area surrounding each grid point (Fig. 10). Subroutine NEWNOD assigns each fluid element to its nearest grid point and then counts the number of elements at each grid point. The number of fluid elements at each grid point, multiplied by the volume of a single element, and divided by the area surrounding each grid point (which is equal to the area of a grid cell), gives the flow depth at that grid point (Equation 95). Similarly, velocity at each grid point is found by averaging the velocities of the elements assigned to that grid point.

Subroutine NEWELM updates fluid-element variables. Each fluid-element variable is determined by its previous value, and the present value of the grid variables (Eqs. 100 and 101). Elevation, flow depth, and velocity need to be known at the location of the particle being updated, and are calculated by interpolation from the nearest grid points. Interpolation is performed by subroutine HSLOP, employing Equations (90) and (91). Grid variables also determine whether turbidity or hypopicnal flow occur, and the program modifies the calculations as described later if necessary.

Optionally, subroutines FILTER and INFLOW can be called inside the main loop. FILTER applies a "time filter" to the grid representing flow to facilitate graphic display of flow velocities and flow depths. A "time filter" is a procedure that averages the value of a variable over a given time. Boundary conditions at the sources are handled by subroutine INFLOW, which provides new fluid elements as specified in the input data file.

At preselected times during the execution of the main loop, subroutine WRITGU is called to write a graphics file containing a "summary" of the current state of the system. The simulated time that elapses between successive calls to WRITGU is controlled by the "display interval" specified in the input data file. The graphics file can be used later to examine the intermediate states of a simulation run with the help of the graphic display program SEDSHO1. When all the cycles are completed, the program calls WRITDF. which writes the complete final state of the system in the same format as the original input. Thus, the results can be used as input for a succeeding run.

Graphic output:

A large amount of information is needed to define the state of the flow model at any specific point in time. Topography, flow velocities, flow depths, and positions of sources of fluid provide the definition. These data are displayed graphically by program SEDSHO1, which reads the graphics file written by SEDCYC1 and converts it for display on a color-graphics terminal or color plotter. The graphics file can grow very large if the simulation run is long and information is requested at short intervals. Therefore the graphics file cannot contain the complete information describing each state of the system. To save space, the graphics file does not include information on individual fluid elements. Instead it includes two grids: one that represents flow velocities, and another one that records flow depths.

SEDSHO1 interactively asks the user what types of displays are desired and what span of time they are to represent. The types of display include topographic contour maps or perspective "fishnet" diagrams, current-velocity plots, and depth plots. It is possible to show a series of flow-velocity plots in quick succession, so as to visualize unsteady flow processes such as turbidity currents in motion, much as a movie or video display.

If a graphics terminal is not available, computer program LOOK can be used. LOOK converts the graphics file into formatted numerical display that can be printed on a line-printer. The printout can also be used to present accurate numerical information on flow velocities and flow depths.

It is often desirable to display information while a simulation run is in progress, rather than wait for the program (SEDCYC1) to complete its run. For example, when short computer experiments are run that involve few fluid elements, visualizing the elements' paths as they move is desirable. The visualization is accomplished by including subroutine PLTPAT with the main program. At each time increment, PLTPAT plots an arrow showing the displacement of each fluid element during that interval. Figures 13 through 15 were generated using PLTPAT. If a color graphics terminal is available, PLTPAT shows the fluid elements' movements on the screen while the simulation program is running.

PROGRAM VERIFICATION

The model was tested at increasing levels of complexity to ensure that simple criteria were met before complicated situations were tested. The simplest tests involve checking for variations of energy and momentum under conditions that are known to conserve energy and momentum.

Experiment to verify conservation of energy

An experiment was performed to verify whether the numerical method that represents flow introduces any spurious loss or gain in energy when no friction is present. Equations (25) and (82) can be shown to conserve energy when friction coefficients c_1 and c_2 are zero. For example, a single fluid element without friction was assumed in an experiment. The fluid element, representing a mass of 100 kg, was allowed to move freely under the effect of slope and gravity, for a simulated time of 500 seconds. The experiment involves a topographic surface shaped as an inverted square pyramid 2000 m on each side and 30 m deep (Fig. 12). The experiment involves time increments of one second. An arrow was drawn after each time increment (using subroutine PLTPAT) to show the path of the fluid element during the succession of time increments in the experiment. The length of each arrow is proportional to the velocity of the element during the corresponding time increment.

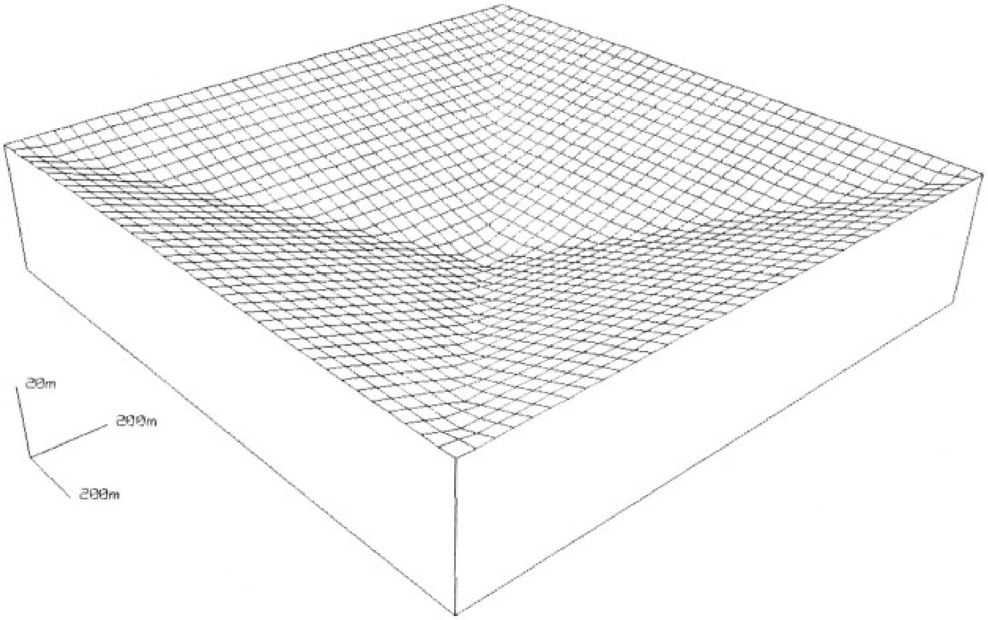

Figure 12: Perspective "fishnet" display of square basin used in simulation experiments involving single fluid element. Basin's sides are 2000 m long, and depth is 30 m. "Fluid elements", each of which represents a small mass of fluid, are allowed to move under influence of gravity in experiments shown in Figures 13 and 14.

The resulting plot is shown in Figure 13. The fluid element moves back and forth over the inverted pyramid without any energy loss or gain, demonstrating that there is no variation in the total energy during the simulated time. When friction is incorporated (Fig. 14), however, the amplitude of movement progressively decreases, and if given enough time, it dies out completely.

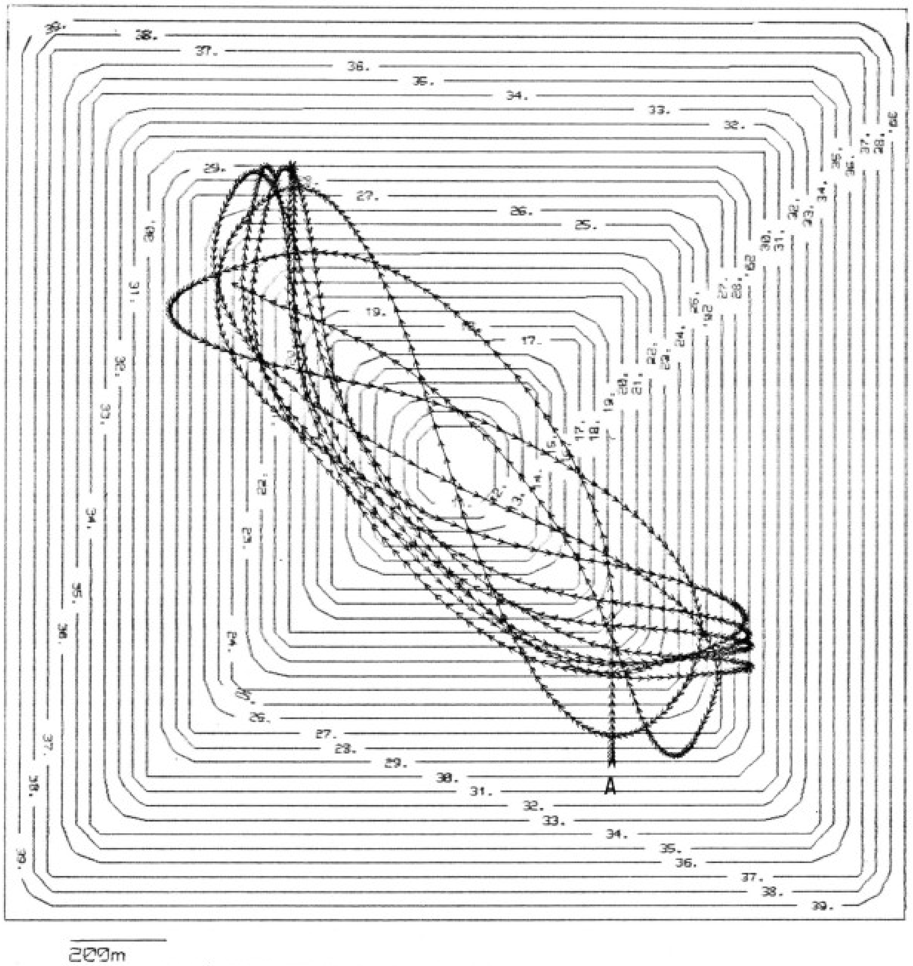

Figure 13: Contour map of basin shown Figure 12 and path of single fluid element after it was released from point A. Friction is assumed to be absent, so element moves back and forth endlessly. Velocity, indicated by arrow lengths, is such that kinetic energy plus potential energy is constant, showing that energy is conserved. Contours are in meters.

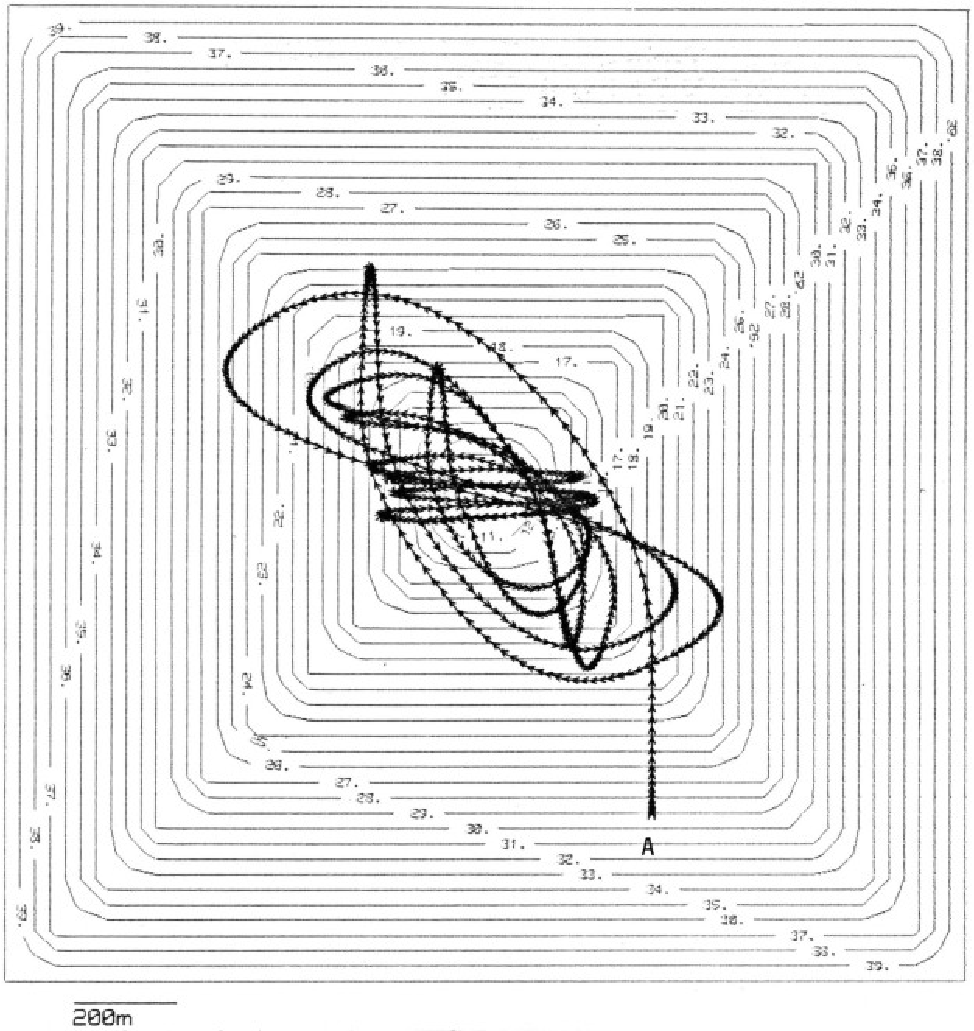

Figure 14: Contour map and path of single fluid element in experiment similar to that in Figure 13, except that fluid element is slowed by friction proportional to square of its velocity. Contours are in meters.

Experiment to verify conservation of momentum

When more than one fluid element is present, elevation of the water surface, and friction of the elements against each other, have an effect on motion. On a horizontal surface that does not provide friction against the fluid, Equations (25) and (82) can be shown to conserve momentum. Conservation of momentum is not represented exactly by the numerical method and computer program if only a single fluid element is present in a cell, but if the numerical method is consistent, momentum should be conserved as smaller fluid elements are used and their average number per cell increases.

The test for conservation of momentum involves an experiment in which two groups of fluid elements are present (Fig. 15). The topography is horizontal and bottom friction is zero. The two groups of fluid elements are released along paths that intersect each other. Momentum is conserved if the center of gravity of the system moves uniformly along a straight line. The centers of gravity of each group for every time increment are shown as red crosses. The total center of gravity is shown as black crosses at each time increment.

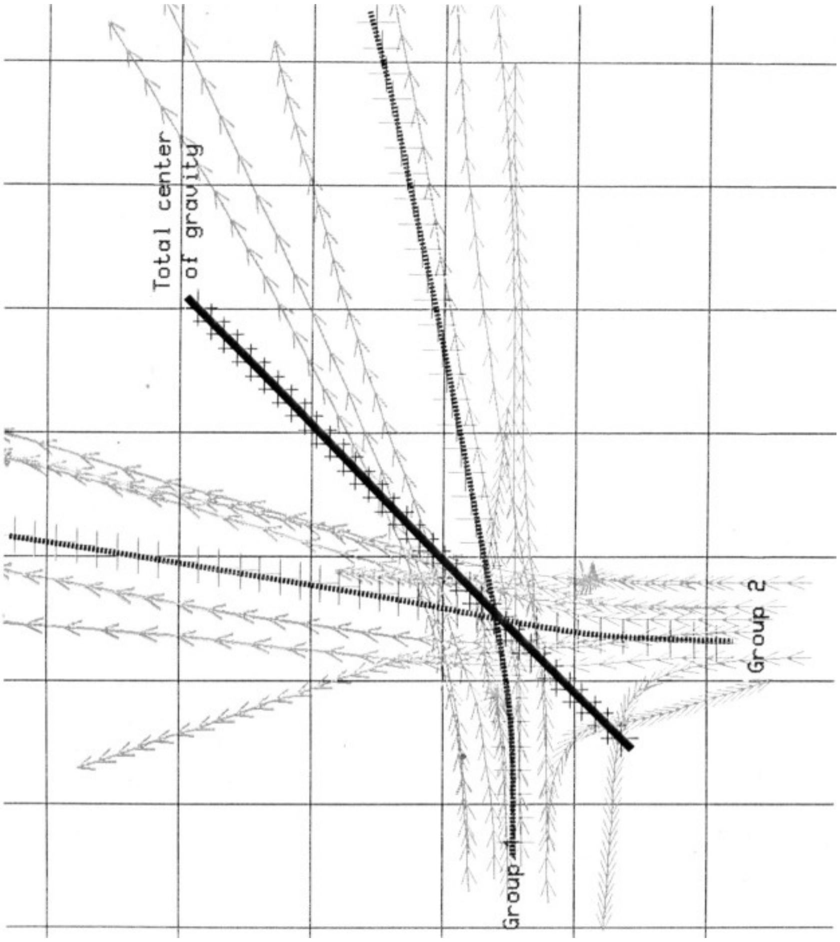

Figure 15: Map view of trajectories of two groups of fluid elements moving on horizontal surface in experiment to test for conservation of momentum. Two groups of fluid elements are released with initial trajectories that intersect each other. Blue arrows show paths of individual elements. Centers of gravity of each group (dashed lines) deviate due to encounter with other group, but overall center of gravity (bold line) moves uniformly along straight path, showing that momentum is conserved.

Fluid elements interact when reaching adjacent cells. The elements tend to repel each other, because of the bulge on the water surface that each one produces. Figure 15 shows that the center of gravity of the system follows a straight line and moves uniformly.

Experiments with only a few fluid elements are not realistic because individual elements are discrete points and cannot deform as a fluid does. For useful applications, a large number of fluid elements must be used.

Estimating the flow model's coefficients

Before proceeding with more realistic examples, it is necessary to find the bottom-friction coefficient c_l and the lateral-friction coefficient c_2. Open-channel steady flow conditions can be used to calibrate the flow model because there are many suitable formulas that describe open-channel steady flow, and there are large amounts of experimental data to validate the existing formulas.

We can find a suitable value for the bottom friction coefficient by postulating a situation in which there is bottom friction, but no "lateral" friction. This condition may be approximated near the center of a wide channel. Under such condition, Equation (82) becomes:

$$\frac{DQ}{Dt} = -g\nabla H - c_1 \frac{Q|Q|}{(H-Z)} \qquad (102)$$

Because the flow is steady, DQ/Dt is zero and therefore:

$$|Q| = \sqrt{g/c_1}\ \sqrt{Sh} \qquad (103)$$

where:

S = slope = $-|\nabla H|$

h = flow depth = $H-Z$

Equation (103) is similar to Chezy's equation, which states:

$$Q_u = C\sqrt{R_h S} \qquad (104)$$

where:

Q_u = uniform flow velocity

C = constant

R_h = hydraulic radius (in a wide channel $R_h = h$)

Though Chezy’s equation applies only to steady flow in channels of regular cross section, it is applied here to find approximate values For SEDSIM's coefficients to be used more general conditions (including turbidity currents and hypopicnal flow) to avoid the necessity of performing physical experiments for calibration.

Bottom-friction coefficient:

Manning’s formula (Manning, 1890) states that the coefficient C can be found by the following expression:

$$c = \frac{r_h^{1/6}}{n} \qquad \text{(SI units)} \qquad (105)$$

where:

n = Manning's roughness coefficient

Values for n can be obtained empirically and depend on the roughness of the material forming the surface of the channel bed. Equating (103) with (104), and substituting (105), the following equation is obtained:

$$c_1 \ = \ g\frac{n^2}{h^{1/3}} \qquad \text{(SI units)} \qquad (106)$$

which yields a value for the model's bottom friction coefficient c$_1$.

Lateral-friction coefficient:

The Chezy-Manning equation, derived from Equations (104) and (105) above, states:

$$Q_u = \frac{1}{n} s^{1/2} R_h^{2/3} \qquad \text{(SI units)} \qquad (107)$$

Equation (107) is one of the most widely used semi-empirical formulas for open-channel steady flow. It can be used to calibrate the lateral-friction coefficient c$_2$ as follows: We can assume a channel of rectangular cross section in which the flow is steady and "parallel" (i.e., there is no significant flow component across the channel). Equation (81) is relatively simple to solve under these circumstances. Manning's equation also applies under such conditions, thereby allowing us to solve for c$_2$. However, if we solve for c$_2$, we find that c$_2$ takes slightly different values for channels of different width. Therefore it is better to find a value of c$_2$ that produces the best overall agreement with Manning’s formula over a range of different channel slopes, widths, depths, and cross-section geometries.

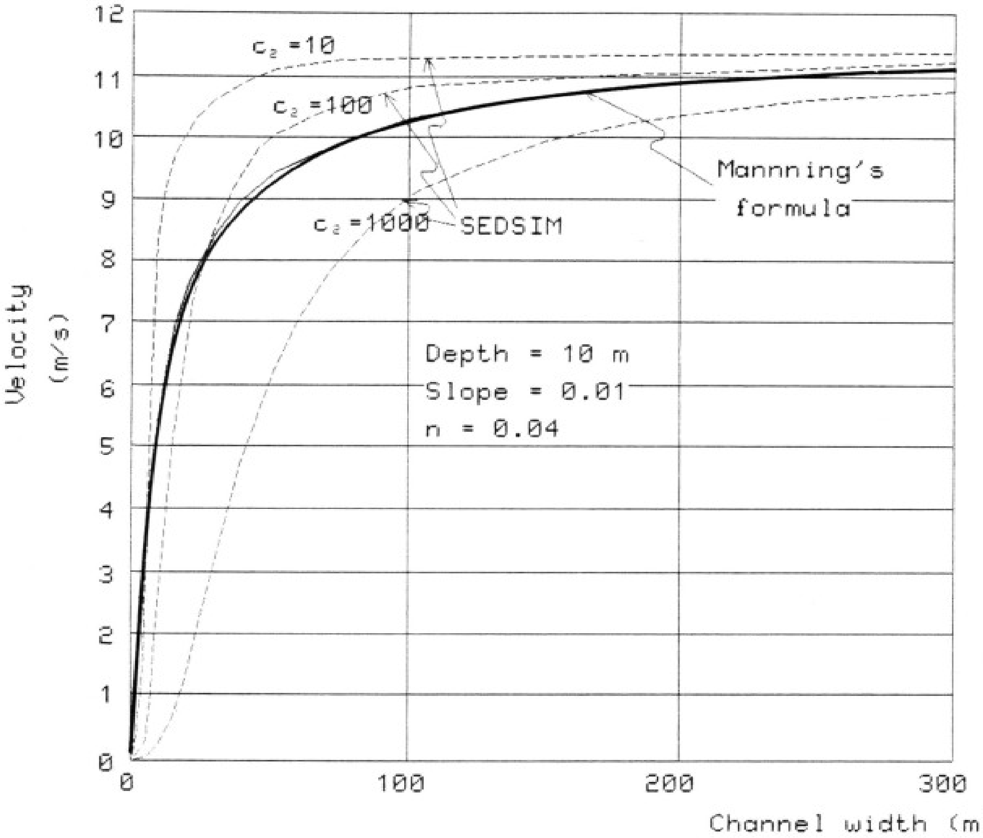

Figure 16: Curves representing average flow velocity (vertical axis) vs. channel width (horizontal axis) for channels of rectangular cross section. Curves provide calibration for lateral friction parameter c2. Depth and slope are constant. Bold curve shows the result of Manning's formula for channels of different widths and constant depth. Dashed lines show curves obtained with SEDSIM's flow formula applied to steady "parallel" flow for various values of c2. Value producing curve that best matches Manning's curve has been chosen for subsequent experiments. Ideally, procedure should be repeated for different depths of channel.

Figure 16 shows how c_2 can be calibrated in a channel of rectangular cross section that is 10 m deep, with a longitudinal slope of 0.01. The dashed curves in Figure 16 show average velocity as a function of channel width, and were calculated using Equation (81) with steady "parallel" flow. Each curve was obtained with a different value of c_2. The bold line shows flow velocity as a function of width according to Manning's formula. For the specific conditions of depth, slope, and roughness used in this graph, a value of approximately 100 kg/(ms) for c_2 produces good agreement with Manning's formula over a wide range of channel widths. For optimum results, c_2 should be recalibrated for different conditions.

The value of c_2 was obtained assuming there was no flow component across the channel. In SEDSIM. however, velocity components across the channel are usually present. The effect is that simulated flow velocities differ slightly from those predicted by assuming steady "parallel" flow.

Testing the calibrated flow model:

Computer experiments were conducted to test the calibrated model's performance under a variety of flow conditions. The arrangement for the experiments is shown in Figure 17. Table 5 and Figure 18 show the results using a trapezoidal channel 100 m wide at the base with the same slope (0.01) that was used to calibrate c_2. Discharge was varied between 100 and 10,000 cubic meters per second, and the results predicted by SEDSIM were compared with those predicted by Manning's formula (Eq. 107), and those resulting from the application of Equations (25) and (81) to steady "parallel" flow. The set of experiments was repeated with a different slope (0.001), and different channel width (200 m), to test the accuracy of SEDSIM's predictions in conditions that are different from those in which the parameters were calibrated, and the results are shown in Table 6 and Figure 19. Although further testing may be needed, in general velocities predicted by SEDSIM for a given discharge rate are within ten percent of the values predicted by Manning's formula. The extent to which the simulated values agree with predictions may be insufficient for certain engineering applications, but the agreement is adequate for SEDSIM's operation, particularly considering SEDSIM's versatility in which flow in irregular channels of arbitrary shape can be simulated.

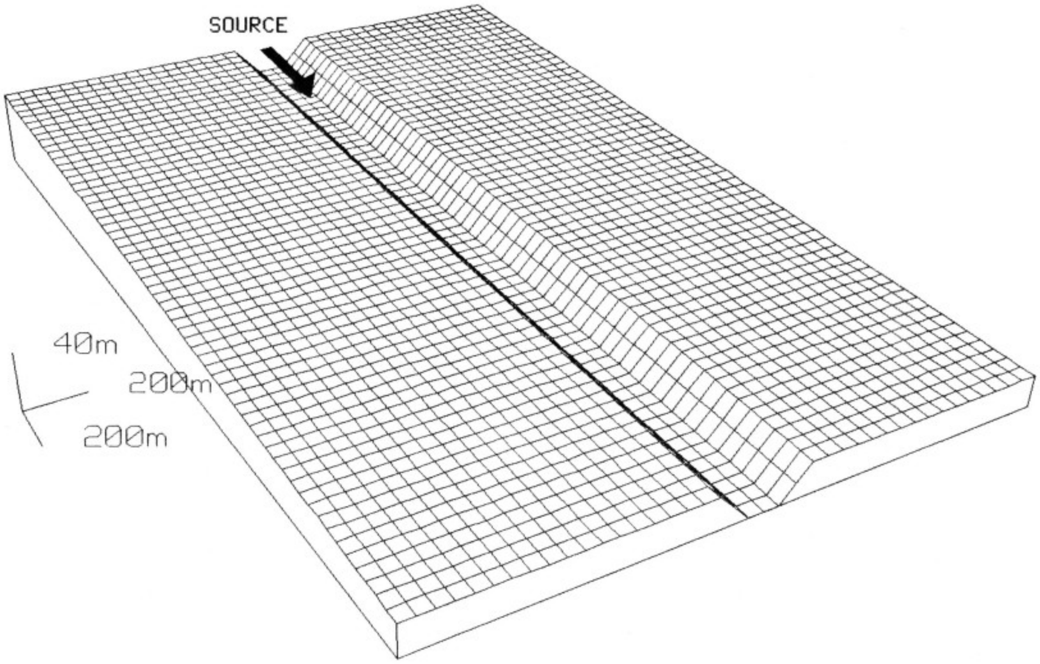

Figure 17: Fishnet diagram showing channel at onset of simulation experiment involving open-channel steady flow.

Table 5: Values of water discharge and corresponding velocities calculated in three different ways: (1) using Manning's formula, (2) using SEDSIM's mathematical model solved for steady "parallel" flow, and (3) using SEDSIM's numerical approximation and computer program with turbulent movement arising from sideways velocity component of fluid elements (only three experiments were performed, and therefore only three values are shown in the rightmost column). Assumptions are that rectangular channel has width of 100 m, slope of 0.01, Manning's n = 0.04, and c2 = 100 kg/(ms). Data are plotted in Figure 18.

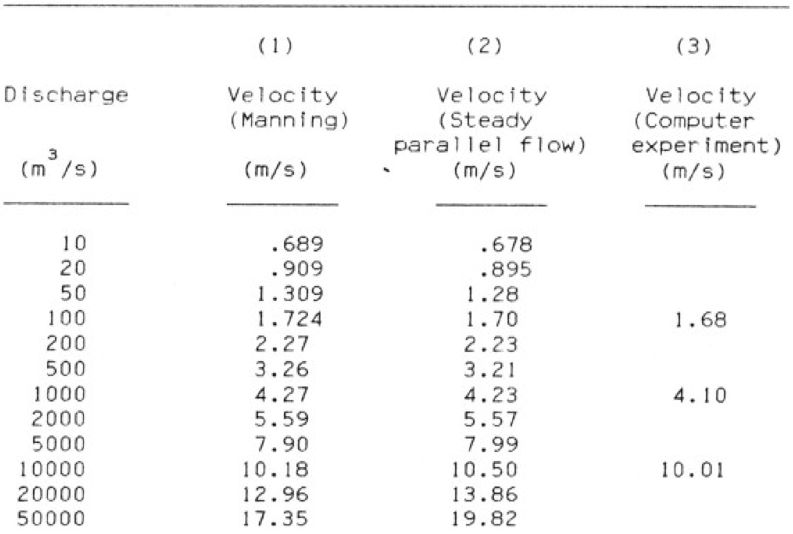

	(1)	(2)	(3)
Discharge	Velocity (Manning)	Velocity (Steady parallel flow)	Velocity (Computer experiment)
(m^3/s)	(m/s)	(m/s)	(m/s)
10	.689	.678	
20	.909	.895	
50	1.309	1.28	
100	1.724	1.70	1.68
200	2.27	2.23	
500	3.26	3.21	
1000	4.27	4.23	4.10
2000	5.59	5.57	
5000	7.90	7.99	
10000	10.18	10.50	10.01
20000	12.96	13.86	
50000	17.35	19.82	

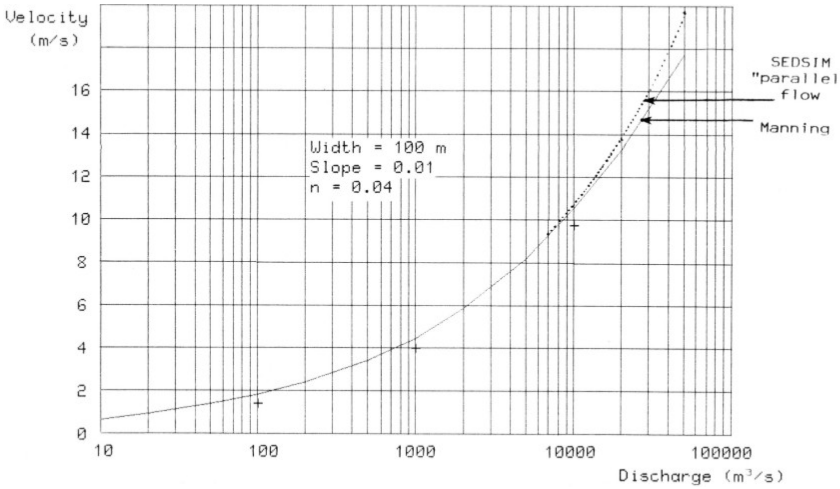

Figure 18: Plot of average flow velocity (vertical axis) vs. discharge rate (horizontal axis) in open channel. Data are listed in Table 5. Curves are based on results of Manning's formula and results of SEDSIM's formula for steady parallel flow. Curves coincide for low values of discharge. Crosses indicate results of computer experiments. Flow conditions are similar to conditions for which SEDSIM's parameters were calibrated.

Table 6: Values of water discharge and corresponding velocities calculated similar to those in Table 5, but for conditions that are substantially different from calibration conditions (as in Table 5, only three values are shown in the rightmost column because only three experiments were performed). Assumptions are that rectangular channel has width of 200 m, slope of 0.01, Manning's n = 0.04, and c2 = 100 kg/(ms). Data are plotted on Figure 19.

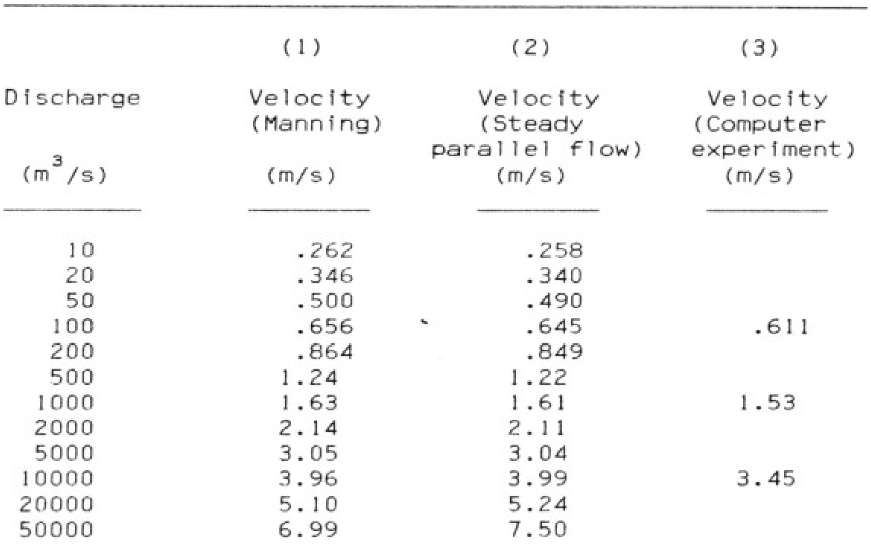

	(1)	(2)	(3)
Discharge	Velocity (Manning)	Velocity (Steady parallel flow)	Velocity (Computer experiment)
(m^3/s)	(m/s)	(m/s)	(m/s)
10	.262	.258	
20	.346	.340	
50	.500	.490	
100	.656	.645	.611
200	.864	.849	
500	1.24	1.22	
1000	1.63	1.61	1.53
2000	2.14	2.11	
5000	3.05	3.04	
10000	3.96	3.99	3.45
20000	5.10	5.24	
50000	6.99	7.50	

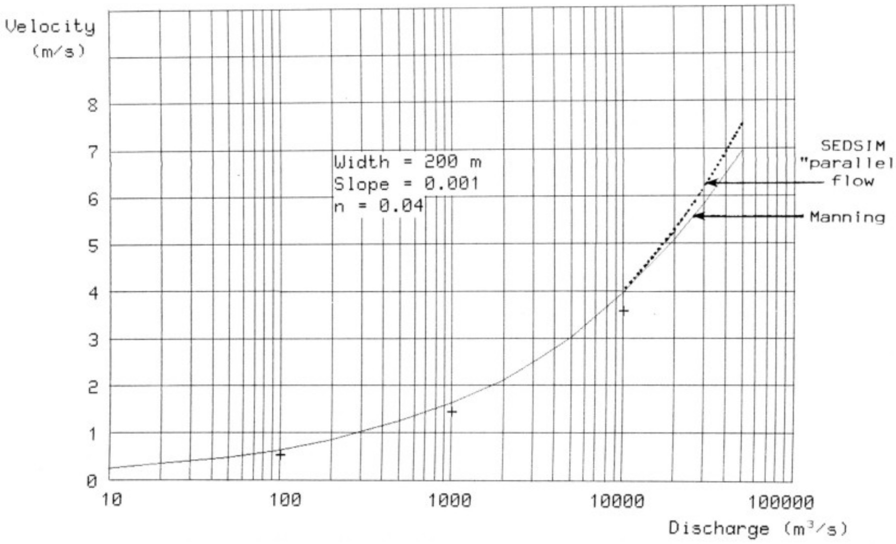

Figure 19: Plot of velocity (vertical axis) versus discharge rate (horizontal axis), similar to plot shown in Figure 18, but assuming wider channel and lower slope. SEDSIM's predicted velocities agree well with Manning's semiempirical formulas.

Channel-bend experiment

SEDCYC1 as calibrated is appropriate for a variety of channels, as for example in a stream channel that is trapezoidal in cross section and contains a bend (Fig. 20). Both ends of the channel in Figure 20 have been partially closed to maintain a relatively high water level. A flow rate has been selected that causes slight overbank flooding adjacent to the downstream part of the channel. The experiment was run for a simulated period of one day, yielding the results shown in Figures 21 and 22. Immediately downstream from the bend in the channel, the flow is asymmetric, with higher velocities near the outside of the bend.

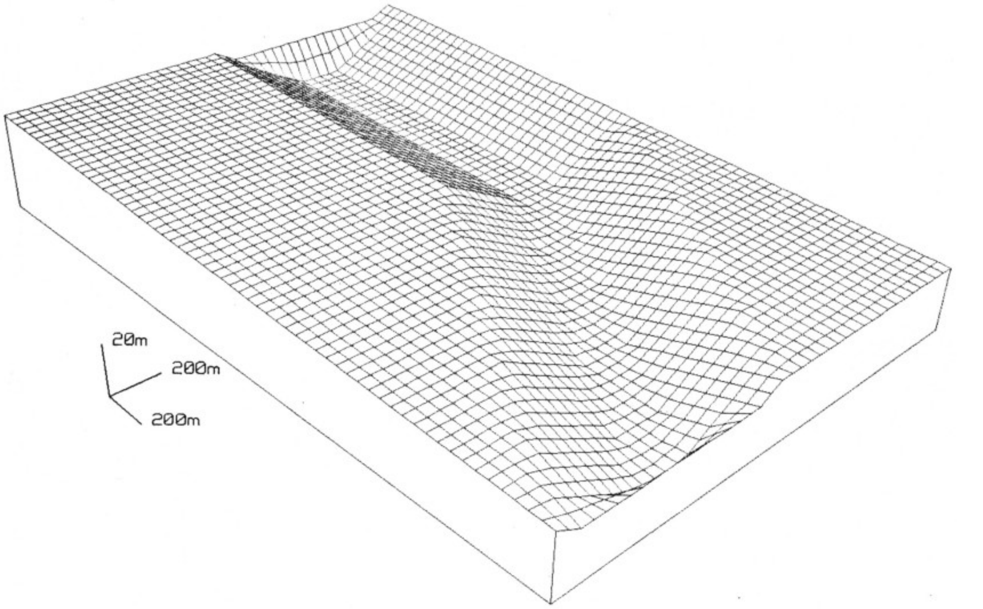

Figure 20: Fishnet diagram of channel that bends. Channel cross section is trapezoidal. "Sills" at ends of channel cause water to be contained within channel, causing high water depth and low flow velocity.

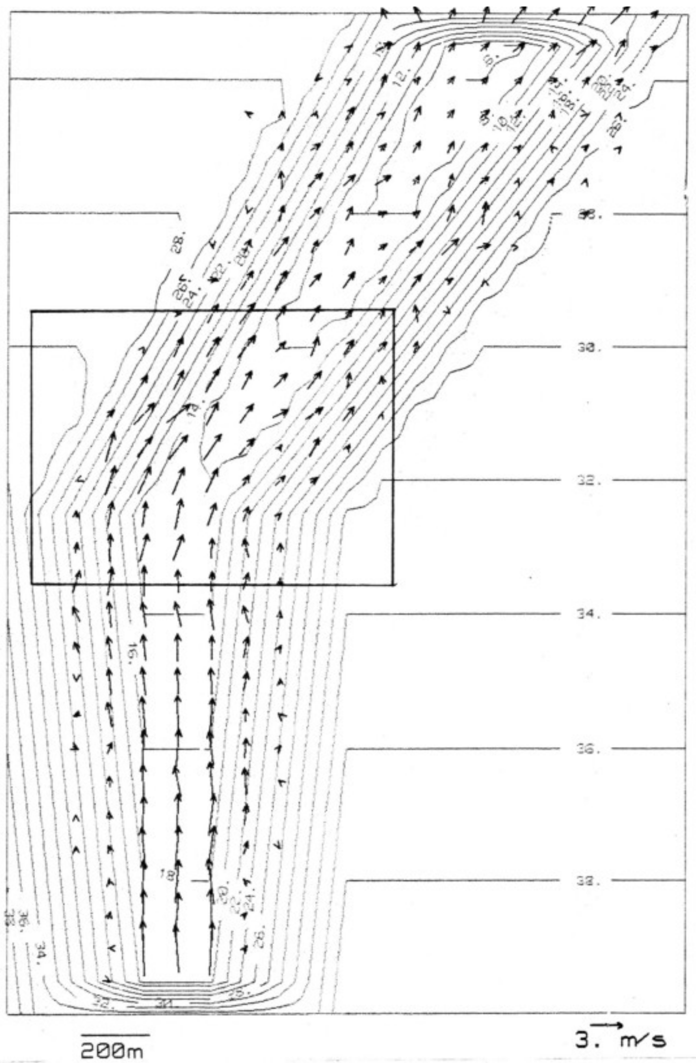

Figure 21: Contour map of bent channel shown in Figure 20, and flow pattern resulting after simulated time of one day has elapsed. Arrows indicate flow velocities. Box indicates area enlarged in Figure 22. Contours are in meters.

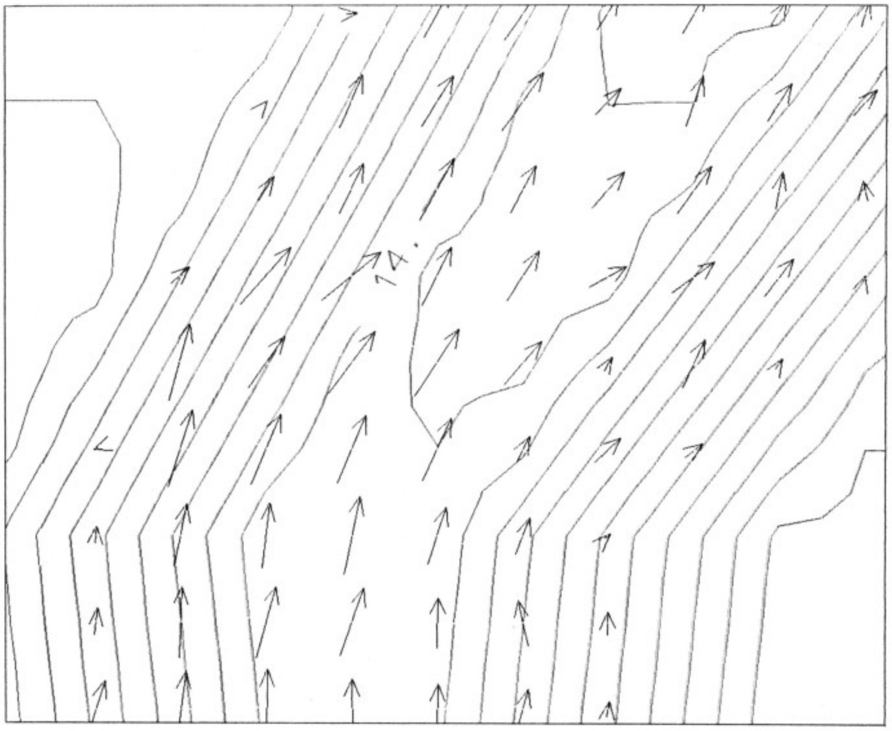

Figure 22: Enlargement of Figure 21 showing asymmetric distribution of flow velocities near bend.

Because SEDSIM represents flow in two horizontal dimensions, SEDSIM is unable to represent the three-dimensional spiral or helical flow that actually takes place in river meanders. Therefore, when erosion and deposition are introduced, SEDSIM's prediction of the rate of erosion on the outside of bends and deposition inside will not be accurate. However, the pattern of erosion and deposition in river bends is not caused exclusively by spiral flow. Erosion and deposition are also affected because shear stress is higher on the outside of a bend than on the inside. SEDSIM, of course, simulates differences in shear stress, and therefore SEDSIM can simulate lateral erosion and deposition, but at rates that are less than actual rates. In Chapter III the channel-bend experiment is repeated to demonstrate how asymmetry in channels results at a bend, even though SEDSIM does not simulate spiral flow.

Basin-circulation experiment

SEDSIM is able to simulate water circulation in a basin. SEDSIM may have limited use in this context because only horizontal circulation is simulated and Coriolis' forces are ignored, but SEDSIM's performance illustrates that flow can be simulated both in open channels, and in semi-closed basins. While potential flow has been used to simulate flow in evaporite basins (Harbaugh and Bonham-Carter, 1970). methods that employ purely potential flow cannot produce closed circulation patterns. Flow as represented in SEDSIM, however, could be used in an evaporite simulation model in which closed circulation patterns are present.

A simulation experiment to demonstrate circulation was carried out in a partially closed rectangular basin whose dimensions are 1.5 km by 2 km. The circulatory motions are induced by a stream flowing into the basin, with excess fluid flowing out of the basin through an opening located opposite to the stream's mouth, as shown in Figure 23.

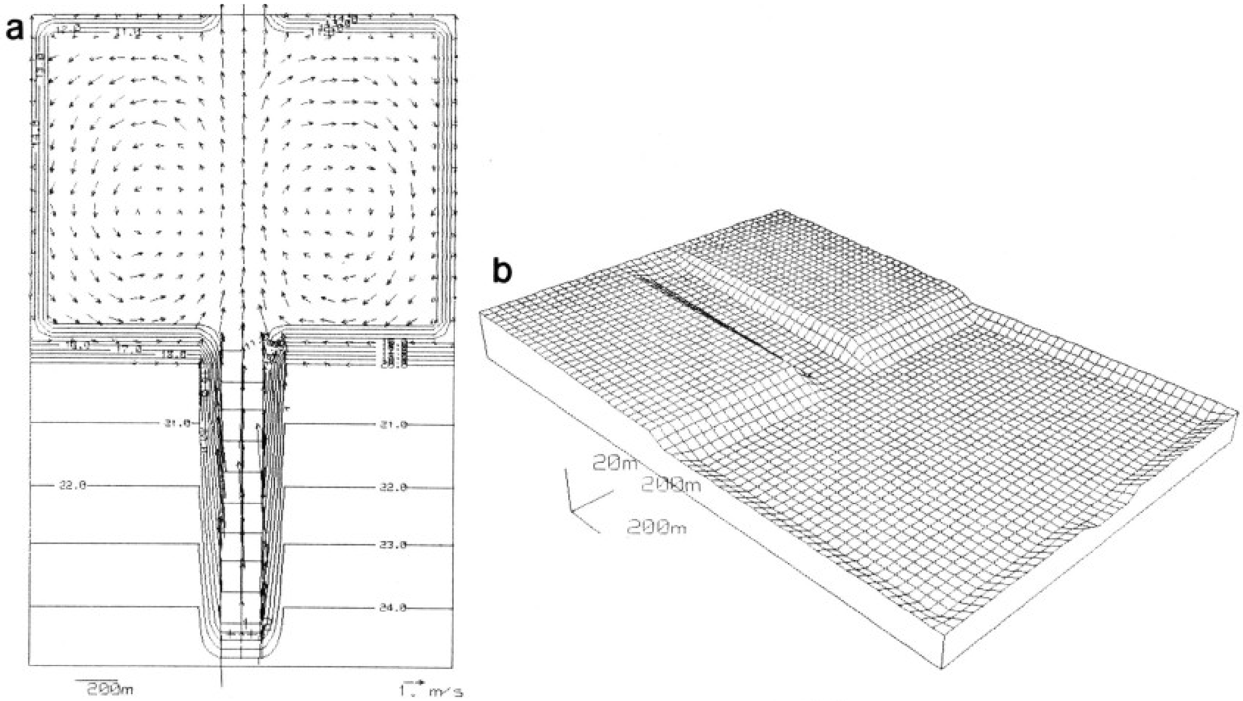

Figure 23: (a) Contour map of topographic surface used in experiment illustrating SEDSIM's capability of simulating circulation in basin. Topography involves channel entering rectangular basin. Fluid sources are placed at upper end of channel. Flow exits basin through opening opposite to channel's mouth. (b) Fishnet diagram of topographic surface displayed as contour map in Figure 23a.

Closed circulatory patterns would be impossible to represent if SEDSIM did not take fluid momentum into account. The experimental results shown in Figure 23, illustrate the benefits of incorporating momentum into the flow model, namely the feasibility of simulating circulation.

Turbidity-current experiment

Unsteady Flow can be illustrated by a simulation experiment in which a large amount of fluid is released, and is not replaced during the experiment. A practical application involves simulation of subaqueous turbidity currents, whose density is appreciably higher than the surrounding water. The experiment involves a steep surface adjacent to a surface that slopes so gently that it is nearly horizontal (Figure 24), representing a continental slope and rise. The flow parameters were set so that the subaqueous flow has a density of 1.5, thus representing a turbidity current of high density.

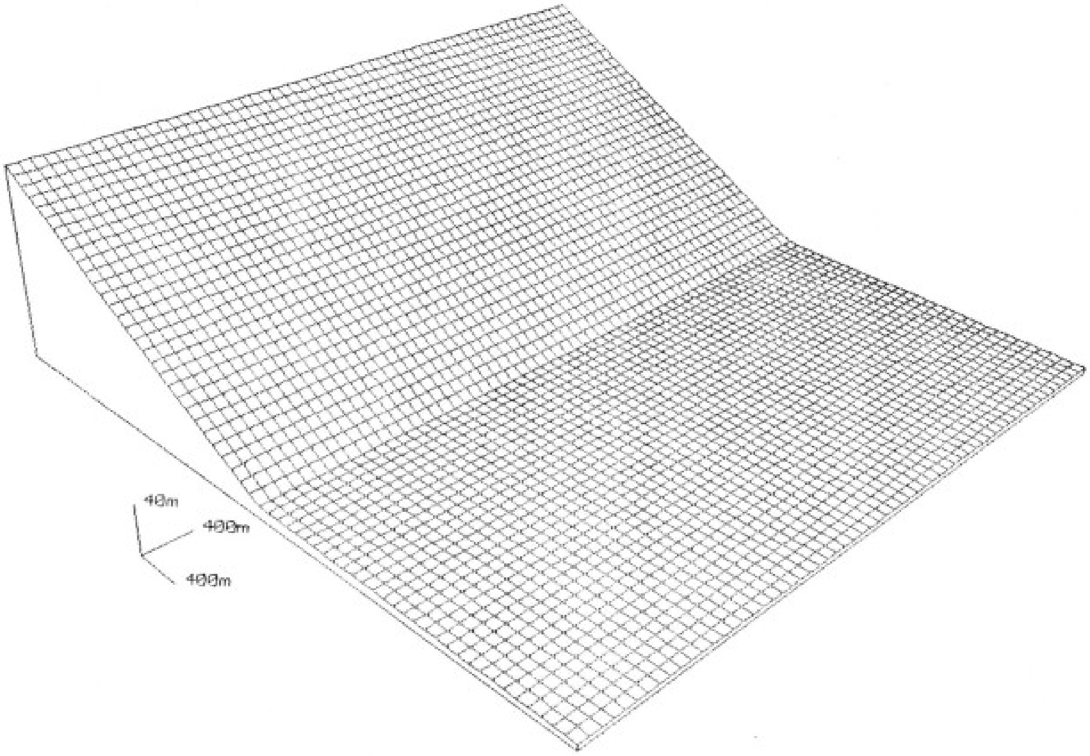

Figure 24: Fishnet display of submerged slopes used as starting condition for experiment involving high-density turbidity flow.

The results of the experiment are shown in Figures 25a through 25e. In Figures 25a and 25b, the flow rushes down the slope and reaches the bottom of the steep slope, whereas in Figures 25c through 25f the flow slows down and spreads out when it reaches the nearly horizontal surface. The flow's behavior is that of a turbidity current as it debouches upon a gentle slope after flowing rapidly down a steep slope.

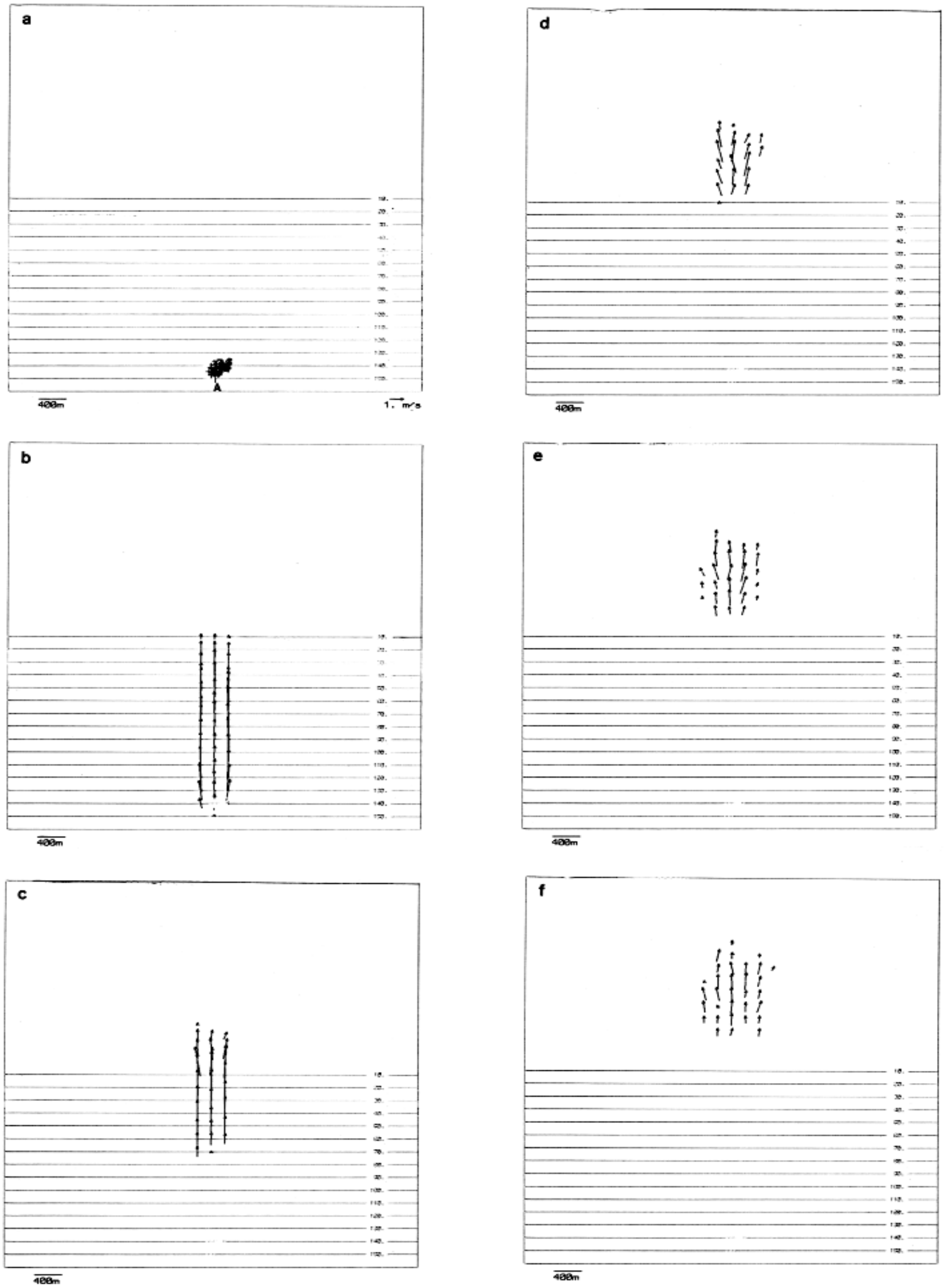

Figure 25: Series of contour maps and flow patterns showing single high density turbidity current. Arrows are proportional to velocity. Flow is released on steep slope at point "A". Successive Figures (a through f) show progress of flow at intervals of one minute simulated time. Flow slows and spreads after reaching surface with gentle slope. Contours represent elevation in meters above arbitrary datum.

Because the topography in the experiment is featureless, except for the two slope angles, and neither erosion or deposition have been allowed to occur, the flow moves in a relatively uniform path down the slope. Chapter III describes an equivalent experiment in which the flow causes erosion and deposition to occur, yielding very different results.

ASSESSING THE PERFORMANCE OF THE FLOW MODEL

The flow model described in this chapter is adequate for simulating flow on an arbitrary topographic surface. The main limitation of the flow model is that it is essentially two-dimensional, providing only the flow's horizontal velocity and depth. Although the velocity profile can be arbitrarily chosen, only a profile in which the velocity is constant with depth is practical.

The model's parameters are not independent from flow conditions and should ideally be calibrated for the range of conditions that are likely to be met in each particular simulation experiment. The flow model should also be used with caution when the flow is surrounded by a medium that can affect the flow’s characteristics, as is the case with turbidity currents and hypopycnal flow.

The numerical method employed is computationally lengthy, but it allows the model to simulate steady or unsteady flow with equal ease over topographic surfaces of arbitrary configuration. These characteristics make it ideal to be used as a basis for sedimentation models in natural environments, as described in the next two chapters.

Chapter III
SIMULATION INVOLVING SEDIMENT OF A SINGLE PARTICLE SIZE

The "fluid element" representation of flow described in Chapter II can be extended to simulate sediment erosion, transport, and deposition. The main challenge in extending SEDSIM to simulate erosion, transport, and deposition of sediment lies in defining how much sediment can be transported under given hydraulic conditions. There is no complete theory that quantitatively relates flow conditions to rates of erosion, transport, or deposition of a particular sediment type. However, semi empirical formulas can be used to create a generalized, flexible simulation model.

SEDIMENT CONTINUITY EQUATION

Topographic changes caused by water flowing over a topographic surface are closely related to changes in the flow's sediment content. Erosion causes the topographic elevation to decrease locally, and the sediment content of the flow is increased by the amount of sediment eroded. The reverse takes place during deposition; the sediment content of the flow decreases, and the topographic elevation is increased by the newly deposited sediment. Thus, sediment is neither created nor destroyed, and the continuity or conservation of matter is represented. Clearly, sedimentary process models must incorporate the principle of continuity if they are to perform realistically. Continuity can be represented by means of an accounting mechanism that ensures that sediment is conserved. The continuity principle also ensures that all sediment that enters the system is either retained within the system, or accounted for as it exits the system's boundaries.

The sediment content in a fluid that transports it can be represented quantitatively by providing one of three possible parameters: (1) the sediment concentration (mass or volume of sediment per unit volume of fluid), (2) the sediment load (concentration times flow depth), or (3) the sediment transport rate (sediment load times sediment velocity). Any of these three parameters can be converted readily to any other.

The continuity principle is described mathematically by an equation that states that the amount of sediment eroded is the same that is incorporated into the flow, and that the amount of sediment deposited is the same that drops from the flow, as follows:

$$(H-Z)\frac{\partial l}{\partial t}+(Q\cdot\nabla)l = -\frac{\partial Z}{\partial t} \qquad (108)$$

where:

l = volumetric sediment concentration
H = free-surface elevation with respect to saea level
Z = topographic elevation with respect to saea level
t = time
Q = horizontal flow velocity (defined by Equation 21 in Chapter II)

Volumetric sediment concentration, l, is defined as the volume of "settled" sediment per unit volume of fluid. A value of 0.01 for l, for example, decrees that one cubic meter of water contains an amount of sediment that, when completely settled, occupies a volume of 0.01 cubic meters.

In Lagrangian form Equation (108) becomes:

$$(H-Z)\frac{Dl}{Dt} = -\frac{\partial Z}{\partial t} \qquad (109)$$

where:

D = derivative alomg the direction of the flow

Equations (108) and (109) imply that the sediment moves at the same velocity as the flow. This is not wholly true in actual flows. The total sediment load consists of bed load and suspended load. The bed load is composed of particles that move in a thin layer immediately above a stream's bed by rolling, saltation (jumping), and traction (dragging). The suspended load, however, consists of particles that are held in suspension by turbulence. The bed load moves slower than the flow, whereas the suspended load moves at approximately the same speed as the flow. The lower speed of the bed load in actual flows can be corrected by proportionally reducing the model's bed load content. The correction takes place automatically if the model is calibrated using sediment transport rate data.

Although sediment cannot be created nor "lost", it can be brought into the system being simulated, and retained within the system, or it can be carried beyond the system's boundaries. Boundary conditions are treated later in this chapter (subsection “Initial and Boundary Conditions).

SEDIMENT TRANSPORT EQUATION

The continuity equation ensures that sediment is conserved, but does not prescribe how hydraulic conditions affect the amount of sediment that is transferred between a stream and the bed over which it flows. The load of sediment at a given point in a flow depends upon the stream’s load upstream, and upon modifications of the load that are governed by (1) flow conditions (which include depth, velocity, bed slope, slope of the water surface, and sediment load), and (2) the type of material available for transport at the bed. In the version of the simulation model described in this chapter (the single-sediment-type model), the type of sediment available for transport is of a single, uniform grain size.

Variations in sediment load can be expressed mathematically in general form as:

$$(H-Z)\frac{Dl}{Dt} = f(Q, \nabla H, \nabla Z,\ l,\ F) \qquad (110)$$

where:

f = load variaion function

F = array of coefficients defining sediment properties

N_f = number of coefficients

Equation (110) incorporates parameters that affect sediment load in a two-dimensional flow model, although function f requires a definition which can be obtained by reviewing some of the commonly used formulas that describe sediment load.

Some of these formulas define only the threshold conditions for sediment movement, without quantitatively specifying the sediment load. Other formulas apply only to a fraction of the total load, such as to the bed load only, or only to the suspended load. Yet other commonly used formulas define sediment load under equilibrium conditions in which neither erosion nor deposition occur. SEDSIM incorporates a general formula (Equation 122) that specifies the total transport rate for sediment under equilibrium, and also the rates of erosion or deposition when flow conditions change. It is desirable, however, that SEDSIM's formulation be more or less compatible with generally accepted methods by which sediment load or transport rate are represented quantitatively, as described next.

Review of formulas to calculate threshold of sediment movement:

Shields' criterion (Shields, 1936) is a commonly used formula that defines the threshold conditions for sediment transport. Shields' criterion assumes that the beginning of motion of bed material is a function of the dimensionless numbers F* (Shields' parameter), and R* (the "particle Reynolds number", which is similar to the Reynolds number), defined as:

$$F_o = \tau_c / (\gamma_s - \gamma) d \qquad (111)$$

$$R_o = v_o \; d / \nu \qquad (112)$$

where:

τ_c = critical boundary shear stress

γ_s = specific weight of sediment particles

γ = specific weight of water

d = sediment particle diameter

v_o = shear velocity = $\sqrt{\tau_0 / \gamma}$

ν = kinematic viscosity

Shields (1936) determined a relationship between F* and R* that defines incipient motion. A graph of F* as a function of R* for incipient motion is shown in Figure 26.

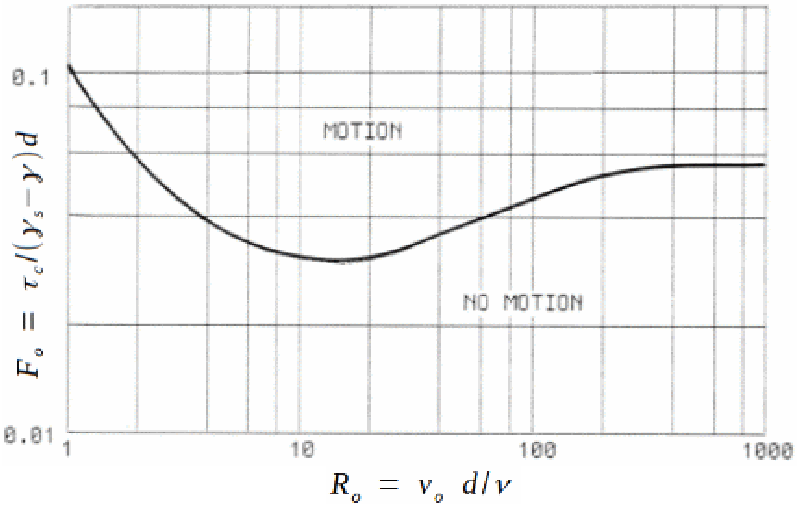

Figure 26: Shileds's diagram showing dimensionless shear stress F (vertical axis) as function of particle Reynolds number R* (horizontal axis). Points above curve represent conditions under which sediment moves (after Shields, 1936).*

White (1940) also developed a formula that defines conditions for incipient motion. White analyzed the forces acting on a typical single sediment grain, and concluded that the critical shear stress that regulates incipient motion can be expressed as:

$$\tau_\psi = (\pi/6) \; r \;\; \rho \;\; d \;\; (s_s - 1) \;\; \tan(\phi) \qquad (113)$$

where:

r = packing factor $0 \leq r \leq 1$ (proportion of "prominent grains")
ρ = fluid density
s_s = sediment particle relative density with respect to water
ϕ = angle of repose

The U. S. Bureau of Reclamation (Lane and Carlson, 1953) provides still another method to calculate maximum allowable shear stresses. for materials that are coarser than about 0.04 inches, or 1 mm, and that are not cohesive, the maximum shear stress, in pounds per square foot, is 0.4 times the grain diameter in inches. The shear stress is higher for finer materials. Figure 27 shows critical shear stress as a function of particle size according to the U.S. Bureau of Reclamation's criterion, as compared with values obtained with Shields' criterion, and with empirical values determined by Du Boys (1879). SEDSIM employs the Bureau of Reclamation's curve for sediment coarser than 0.1 mm. for finer sediment, SEDSIM assumes that maximum shear stress remains constant (Fig. 27).

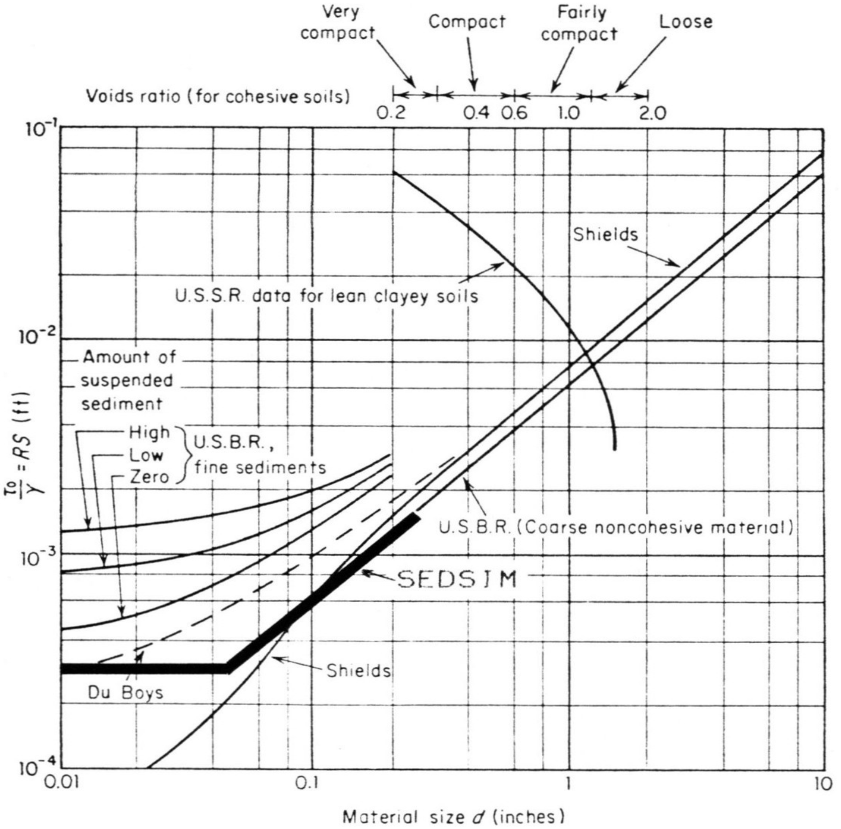

Figure 27: Graph showing maximum shear stress (vertical axis) for cohesive and non-cohesive materials as function of grain size (horizontal axis), according to U. S. Bureau of reclamation (Lane and Carlson. 1953), Du Boys (1879), and Shields (1936). Bold line shows function employed by SEDSIM. Data for lean clayey soils are shown as a function of voids ratio (scale across top of graph). Additional curves on left half of graph show increase in maximum shear stress due to presence of fine suspended material in the flow.

Review of sediment transport formulas:

Du Boys' (1987) equation is one of the oldest and best known formulas that describe bed-load transport rates.

$$Q_s \;=\; k \;\; \tau_0 \;\; \left(\tau_0 - \tau_c\right) \qquad (114)$$

where:

Q_s = bed transport rate
k = transport coefficient
τ_0 = shear stress at the bed

Du Boys' formula, as well as many other bed-load formulas, utilizes excess shear stress (τ_o – τ_c) as the primary factor that determines sediment-transport rate. The value at which shear stress becomes critical (τ_c) was determined empirically by Du Boys (Fig. 27).

Shields (1936) also developed a simple and useful bed-load formula:

$$\frac{Q_s s_s}{Q S} \;=\; 10 \frac{\tau_0 - \tau_c}{\gamma\left(s_s - 1\right) d} \qquad (115)$$

where:

S = slope
γ = specific weight of water

Equation (115) is dimensionally homogeneous and fits experimental data reasonably well.

$$Q_s \;=\; \frac{12.85}{\sqrt{\rho}\,\gamma_s}\left(\tau_0 - \tau_c\right)^{3/2} \qquad (116)$$

where:

ρ = water density
γ_s = specific weight of sediment particles

Meyer-Peter and Muller (1948) assumed that part of the energy of the flow is transformed to heat in transporting sediment. Therefore, transport rate can be estimated from the change in

$$Q_s \;=\; \left(A_2 / A_1\right) \lambda \, p_s \, d^2 \qquad (117)$$

where:

A_1 = ratio of grain area to diameter sqared
A_2 = ratio of grain volume to diameter cubed
λ = average number of grain diameters traveled by saltation
p_s = probability that a particle will be dislodged during one second

kinetic and potential energy along the flow. Their equation reduces to:

Einstein (1942, 1950) developed one of the most complete bed-load formulas:

Einstein provided a method to evaluate λ and p_s, that is not described here.

Suspended load can be calculated using a method that was also developed by Einstein

(1942). Einstein’s formula for suspended load is as follows:

$$Q_s \; = \; 11.6\, v'_o C_a a \left(2.303 \log \left(\frac{30.2 h}{\Delta} \right) I_1 + I_2 \right) \qquad (118)$$

where:

v'_o = share velocity due to grain roughness = $\sqrt{gRS}$
(g=gravity, R=hydraulic radius due to grain roughness, S=slope)
C_a = reference sediment concentration near the bed
(obtained by applying bed-load theory)
a = thickness of bed layer
h = flow depth
Δ = apparent roughness of bed surface
$I_1 \; = \; 0.216 \frac{E^{z-1}}{(1-E)^z} \int_E^1 \left(\frac{1-y}{y} \right)^z dy$
$I_2 \; = \; 0.216 \frac{E^{z-1}}{(1-E)^z} \int_E^1 \left(\frac{1-y}{y} \right)^z \ln(y) dy$
$z \; = \; w/(0.4 v'_o)$
$E \; = \; h/a$

Bagnold (1966) developed formulas for both bed-load and suspended-load transport. Although they were developed mainly for application to marine currents and waves, they are of interest for comparison with other formulas. Bagnold’s bed-load formula states:

$$Q_s \; = \; \frac{E_b C_d \gamma Q^3}{\tan \Phi - \frac{QS}{|Q|}} \qquad (119)$$

where:

E_b = efficiency of bedload transport (=0.21; Richmond and Sallenger, 1984)
C_d = drag coefficient
γ = fluid density
S = local slope
Φ = friction angle
(Q and Q_s are scalars in Bagnold's formulas)

The suspended-load formula developed by Bagnold states:

$$Q_s = \frac{E_s C_d \gamma Q^3 |Q|}{W - QS} \qquad (120)$$

where:

E_b = efficiency of suspended load transport (=0.25; Richmond and Sallenger, 1984)
C_d = drag coefficient
γ = fluid density
W = fall velocity of sediment grains

Yalin (1963) developed a formula for total load based partly on the mechanics of saltation, as follows:

$$\frac{Q_s(s_s - 1)}{v_o d s_s} = 0.635 r \left(1 - \frac{\log_e(1 + ar)}{ar}\right) \qquad (121)$$

where:

v_o = shear velocity
$r = (\tau_0 - \tau_c)/\tau_c$
$a = 2.45 s_s^{-0.4} \sqrt{\frac{\tau_c}{\gamma s_s d}}$

All the transport formulas described above are applicable to a single sediment type. Formulas for sediment transport that involve mixtures of different grain sizes are described briefly in Chapter IV.

Transport formula employed by SEDSIM

The method employed by SEDSIM assumes that sediment transport depends on the balance between (1) the flow's transport capacity, denoted by Λ, which depends solely on hydraulic characteristics, and (2) the effective sediment concentration Λ_e. The effective sediment concentration is the volumetric sediment concentration l divided by a factor f_1, called transportability, that reflects the ease with which the sediment is transported by the flow. If the effective sediment concentration is greater than the transport capacity, deposition occurs at a rate that is proportional to the excess effective concentration. If the sediment concentration is less than the transport capacity, erosion occurs, provided that the critical shear stress is exceeded. SEDSIM also assumes that no erosion can occur in hypopicnal flow, but this case is omitted for clarity in the transport equations. Thus:

$$(H-Z)\frac{Dl}{Dt}= \begin{cases} (\Lambda-\Lambda_e)f_2 & \text{if } \Lambda-l.f_1>0 \text{ and } \tau_0\geqslant f_3 \\ 0 & \text{if } \tau_0\geqslant f_3 \text{ and } \Lambda-l.f_1\leqslant 0 \end{cases} \qquad (122)$$

where:

Λ = transport capacity (defined in Eq. 124, below)

$\Lambda_e=1/f_1$ = effective sediment concentration

f_1 = sediment transportability

f_2 = erosion-deposition coefficient

$f_3=\tau_c$ = threshold shear-stress for sediment concentration

Shear stress along the bottom of the flow is given by

$$\tau_0=c_1|Q|^3\rho \qquad (123)$$

where:

c_1 = bottom friction coefficient defined by Eq. 80

SEDSlM's method for quantifying sediment transport resembles that of Meyer-Peter and Muller (1948) in recognizing that the change in the energy of the flow regulates sediment transport. But SEDSIM assumes that the power dissipated by bottom friction per unit volume of fluid controls transport capacity (rather than the energy loss per unit distance). Therefore

$$\Lambda=c_t\frac{dP}{dV}=c_t\tau_0|Q|^3/h \qquad (124)$$

where:

P = power dissipated by bottom friction

V = volume

c_t = transport coefficient

Applying (106) and (123) we obtain:

$$\Lambda=c_t g\frac{n^2}{h^{4/3}}\rho|Q|^3 \qquad (125)$$

where:

g = gravity

n = Manning's roughness coefficient

Coefficients f_i in Equation (122) depend on sediment particle diameter, density, and shape. A procedure for their calibration is described later. Transport capacity is described in the same units as volumetric sediment concentration l, which is dimensionless. Therefore the dimension of c_t is:

$$[c_t]=[\text{distance}\times\text{time}^3/\text{mass}] \qquad (126)$$

Because equation (122) can be calibrated by adjusting coefficients f_1, f_2, and f_3, the value of c_t may be selected arbitrarily. For convenience c_t can be defined to be 1 ms^3/kg.

Equation (122) has proven to be satisfactory for simulating sedimentary processes because it is readily represented in a computer program, and is accurate enough for good results. Other formulas can be substituted readily for equation (122) in SEDSIM if desired.

Comparison between transport formulas:

If Equation (122) is compared with other equations that represent sediment load and sediment transport, it is necessary to reduce the equations to the same form. For example, Laursen (1956) reduced several sediment-transport equations to make transport rate dependent on flow velocity, depth, and bed roughness. Table 7 shows Laursen's results together with SEDSIM's formula reduced to the same form. SEDSIM’s equation in Table 7 involves the assumption that sedimentary equilibrium exists (neither erosion or deposition occur), thereby permitting the left side of Equation (122) to be zero. After applying (126), and combining constants, the following equation is obtained:

$$Q_s = B\frac{n^2}{h^{1/3}}|Q|^4 \qquad (127)$$

where:

B = constant

Table 7 shows that SEDSIM's formula resembles both Du Boys’ formula as well as the formula of Meyer-Peter and Muller, in that transport rate is proportional to the fourth power of flow velocity. SEDSIM's formula’s main difference from the other formulas presented in Table 7 is that SEDSIM’s formula assumes that the cube root of flow depth (rather than a higher power of flow depth) controls transport rate. SEDSlM’s formula agrees better with experimental results for total load (Colby, 1964) than the bed-load formulas presented in Table 7. Colby's results, displayed in Figure (31), show that for high flow velocities, total sediment-transport rate remains constant or increases slightly with flow depth, rather than decreasing rapidly with depth as bed-load does. Thus, according to Colby's data, SEDSlM's formula, even though it is based on bedload criteria, may be adequate for representing total load.

Table 7: Comparison between reduced forms of bed-load transport formulas and formula employed by SEDSIM.

Author	Formula
Du Boys (1879)	$Q_s = B_1 n^4 \frac{Q^4}{h^{2/3}}$
Meyer-Peter, Muller (1934)	$Q_s = B_2 n^3 \frac{Q^4}{h}$
Shields (1936)	$Q_s = B_3 \frac{n^4}{d} \frac{Q^5}{h^{2/3}}$
Einstein (1950)	$Q_s = B_4 \frac{n^3}{d^{3/2}} \frac{Q^6}{h}$
Tetzlaff (1987) (SEDSIM)	$Q_s = B_5 n^2 \frac{Q^4}{h^{1/3}}$

where:
Q_s = sediment discharge rate
B = constant
n = Manning's roughness coefficient
Q = water flow rate
h = flow depth

Initial conditions and boundary conditions:

When a simulation run is begun, the initial flow conditions must be prescribed (Chapter II, equations 83 and 84), as well as the initial conditions for sediment load. Initial sediment load can be prescribed by defining a function l_0 that assigns an initial sediment concentration at ever point where flow occurs:

$$l(x, y, t_0) = l_0(x, y) \qquad (128)$$

Initial topography must of course be prescribed too. Boundary conditions in the single-particle-size model involve not only flow boundary conditions provided by Equations (85) through (88), but also sediment content of the flow at the sources and at the edges. The sediment sources coincide with the flow sources and provide input of sediment throughout the simulation, as prescribed by the following equation:

$$l(x_{si}, y_{si}, t) = l_{si}(t) \qquad (129)$$

where:
l_{si} = sediment concentration at source s_i

Boundary conditions at the edges for the flow-only model described in Chapter II have been defined so that the flow can freely exit the simulation's geographic domain (Equation 87). If flow occurs at the edges and erosion is permitted, any except the most cohesive of sedimentary materials would be rapidly eroded because a "water-fall effect" would ensue, in which flow velocity and erosion magnify each other (Figure 28a). On the other hand, if the boundaries are closed to outflow, water would quickly accumulate to form "lakes", and there would be excessive deposition near the edges (Figure 28b). Figure 28c shows the boundary condition adopted for SEDSIM. While flow may exit the domain of the simulation, neither erosion nor deposition are permitted to occur on the line that represents the simulated area's edges. Erosion and deposition are permitted immediately inside the edges. When these conditions are applied, there is generally only a narrow "band" adjacent to the edges in which outflow at the boundaries significantly affects sedimentation, and deposits tend to "wedge out" toward the edge. The sedimentation boundary conditions employed by SEDSIM are represented mathematically by:

$$\frac{\partial Z(x_e, y_e)}{\partial t} = 0 \tag{130}$$

where:

x_e, y_e = points on the edge of the simulated area

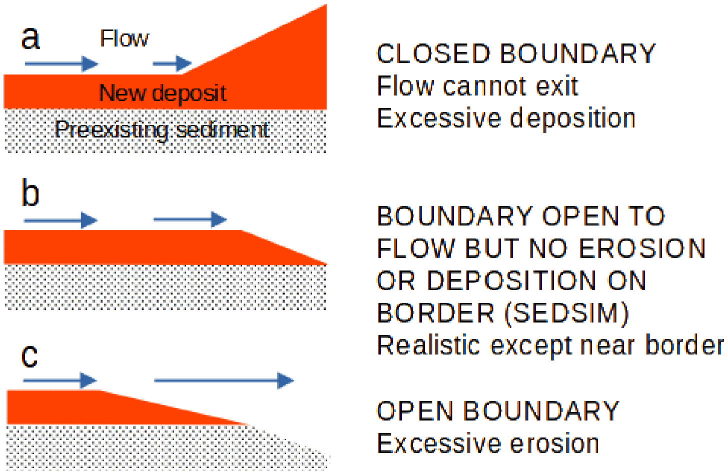

Figure 28: Diagrams showing alternative procedures for representing relationships at boundaries of simulation model: (a) Closed boundary prevents flow, and causes excessive deposition near boundary. (b) Boundary permits flow of both water and sediment across boundary, but erosion and deposition are prohibited on edge of simulated area (procedure employed by SEDSIM). (c) Open boundary, allowing flow and unlimited erosion, usually resulting in erosion and flow velocity causing each other to increase, and cutting sharply into sedimentary deposits inside simulated area.

The boundary conditions assumed still have some effect on sedimentation, because they restrict the thickness of deposits that form immediately inside the boundaries. Similarly, if we perform experiments on a sand table, we cannot completely eliminate the limitations imposed at the edges of the sand table.

NUMERICAL APPROXIMATION OF THE SEDIMENT-CONTINUITY AND SEDIMENT-TRANSPORT EQUATIONS

The concentration of sediment contained in a moving volume of fluid at time t is equal to the initial concentration (Equation 128), plus the net gain or loss of sediment between time zero and time t (integration of Equation 122). Thus it is appropriate to represent sediment concentration as a property of an elemental volume of fluid that can be updated at discrete time intervals by a numerical approximation of Equation (122).

Sediment-continuity equation

The sediment continuity equation (109) is approximated numerically as follows:

$$\frac{Z_{i,j,t+1}-Z_{i,j,t}}{\Delta t} = -h_{i,j}\sum_{k}\frac{l_{k,t+1}-l_{k,t}}{\Delta t} \qquad (131)$$

where:

Z = topographic elevation

i, j = row and column of node nearest to element k

t = time increment number

Δt = time increment duration

h = topographic elevation

k = fluid element number

$\sum_{k}$ = summation over k, $1 \leqslant k \leqslant L$

L = number of elements near node (i, j)

Equation (131) can be used to update topographic elevation at every time increment, as follows:

$$Z_{i,j,t+1} = Z_{i,j,t} - L h_e \sum_{k} \Delta l_k \qquad (132)$$

where:

h_e = fluid element depth = V_e / A (Eq. 95)

Sediment-transport equation

Equation (122) and the boundary condition imposed by Equation (130) can be approximated as follows:

$$h_e \frac{l_{k,t+1}-l_{k,t}}{\delta T} = \begin{array}{ll} (\Lambda_{i,j}-l_k/f_1)f_2 & \text{if } \Lambda_{i,j}-l_k/f_1>0 \text{ and } \tau_{i,j} \geqslant f_3 \text{ and } (i \neq 1, j \neq 1, i \neq N, J \neq M) \\ 0 & \text{otherwise} \end{array} \qquad (133)$$

where:

N, M = number of rows and columns of grid nodes

$\tau_{i,j} \wedge \Lambda_{i,j}$ are defined as in Eqs. (123) and (125) but replacing Q by $Q_{i,j}$ and h by $h_{i,j}$

At every time increment. the sediment concentration of each fluid element is updated as follows:

$$l_{k,t+1} = l_{k,t} + C\frac{\Delta t}{h_e} \qquad (134)$$

where:

C = right side of Eq. (133)

An intuitive explanation of the numerical method embodied in equations (132) and (134) is shown in Figure 29.

The sediment provided as input to the simulation's geographic domain at the sources is given simply as the initial sediment concentration of the fluid elements that enter the area per each increment of time.

COMPUTER PROGRAM FOR SINGLE SEDIMENT-TYPE MODEL

Computer program SEDCYC2 incorporates the algebraic expressions described above (Equations 132 and 134) into the flow simulation program (SEDCYC1) described in Chapter II. The flow chart for SEDCYC2 is identical to that of SEDCYCI (Figure ll), but the tasks performed by some of the subroutines and main program in SEDCYC2 are more complicated because they incorporate procedures and variables that simulate erosion, transport, and deposition of sediment. The data file (Table 8) that provides input to SEDCYC2 is also longer than that for SEDCYC1 (Table 4), because sediment characterisitics and concentration of sediment supplied as input at the sources must be supplied to SEDCYC2.

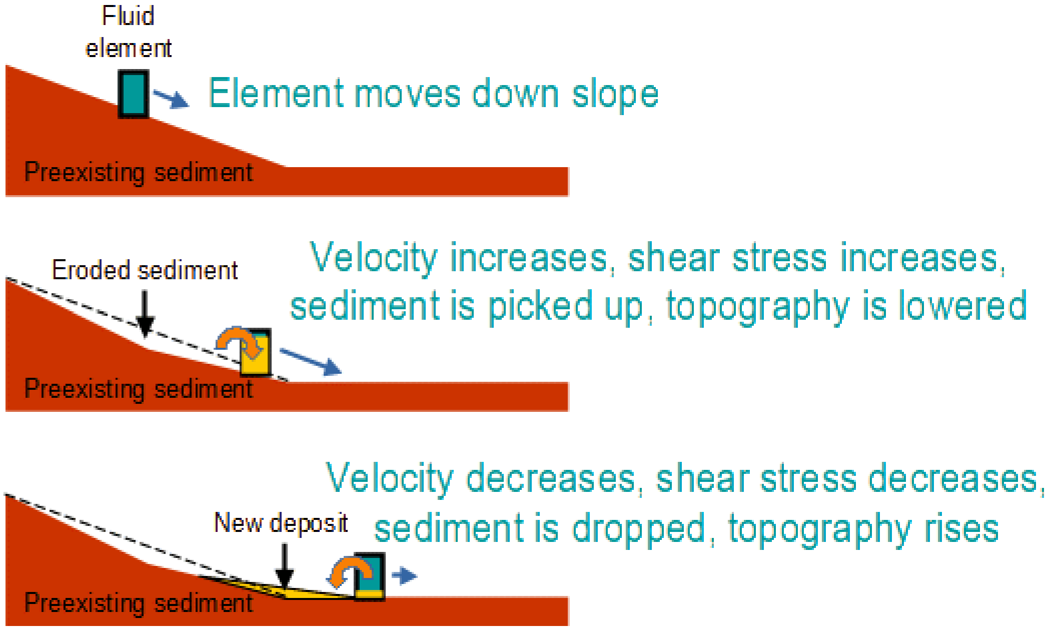
Fluid element
Element moves down slope
Preexisting sediment
Eroded sediment
Velocity increases, shear stress increases, sediment is picked up, topography is lowered
Preexisting sediment
Velocity decreases, shear stress decreases, sediment is dropped, topography rises
New deposit
Preexisting sediment

Figure 29: Diagram illustrating mechanics of sediment transport in SEDSIM: (a) fluid element moves down slope by gravity. (b) when velocity is such that critical conditions of sediment movement are exceeded, sediment starts to be eroded and transported, so that topographic elevation is reduced. (c) when velocity decreases, reduced transport capacity causes sediment to progressively drop out of flow, resulting in deposition.

Table 8: Sample Input data file for program SEDCYC2.

```
TITLE: SINGLE—SEDIMENT EROSION AND DEPOSITION ON INCLINE
RUN PARAMETERS:
START TIM=0.00E+00 Y
END TIH =0.IOE+O0 Y
DISPL INT=0.IOE+00 Y
TIM INCR1=0.50E+0I S
TIM FACTI=0.10E+04
TIM INCR2=0.IOE+00 Y
TIM IDLE =0.00E+00 Y
TIM fACT2=0.IOE+0I
GENERAL PHYSICAL PARAMETERS:
fLOW DENS= I000. KG/H3
SEA DENS = 1027. KG/H3
LAT fRICT= I00. NS/H2
ROUGHNESS= 0.0400
EL VOLUME=0.IOE+05 H3
CURR(X.Y)=0.00E+000.00E+00M/S
SEDIMENT PARAMETERS:
SI
DIAMETER = .50E—0I M
DENSITY = 2700. KG/M3
BAS DECAY= 0.200
COHESION = .60E+00 ~
SOURCES:
INTERVAL = .50E—04 Y
SOURCE5= I
X(N) Y(M) XV(H/S) YV(fl/5) SI(M3)
I000. 2675. -0.5 -1.5 .80E+04
TOPOGRAPHY:
GRID SIDE= 100.0 H
NROWS = 5
NCOLS = 5
GRID NODES ELEVATION (SURFACE) (H)
50.0 50.0 50.0 50.0 50.0
45.0 45.0 45.0 45.0 45.0
40.0 40.0 40.0 40.0 40.0
35.0 35.0 35.0 35.0 35.0
30.0 30.0 30.0 30.0 30.0
ELEMENT POSITIONS AND VELOCITIE5:
of ELEM= 0
X(H) Y(H) XV(M/S) YV(M/S) SI(M3)
I31
```

Program Cycles

Almost all of the additional tasks carried out by SEDCYC2 are performed by subroutine NEWELM. for each fluid element and for each time increment, NEWELM calculates transport capacity. If concentration divided by sediment transportability is greater than transport capacity, deposition occurs. If it is less, erosion occurs, provided that critical shear stress is equaled or exceeded (Equations 133 and 134). These steps are imbedded into the same program loops that are used to update flow parameters during each time increment or program cycle.

At each display interval specified in the data file, subroutine WRITGU writes the complete topographic grid on the graphics file, because topography changes progressively through time.

Graphic Output

Graphic output involves program SEDSHO2, which is substantially more complicated than SEDSHO1 because it is necessary to update the topographic contour map during each display cycle.

An important addition to SEDSHO2 consists of the capability of drawing cross sections. The cross sections show both topography and the age of deposits of sediment that lie beneath the topographic surface. The actual drawing of the cross section is handled by subroutine CRSSEC. To construct a cross section, the user interacts with SEDSHO2. SEDSHO2 asks the user for a point and an azimuth direction that define the trace of the cross section. At each display increment, CRSSEC successively draws the topogrpahic surface in the cross section. If the current topographic elevation is higher than the topographic elevation drawn on the previous display, the area in between the old and the new topographic elevation lines is shaded with a color to identify the age of the newly formed deposit. If the new elevation is lower than the old one, the area that was occupied by the eroded deposit is erased.

Techniques For Extrapolating Sedimentation in Time

It would be impossible to simulate a span of time that is of "geologic time" magnitude if the simulation operates continuously, utilizing time increments of only a few seconds. Yet, time increments of only a few seconds are necessary for flow calculations, if flow is to be accurately simulated. Clearly the demands relating to geologic time on one hand, and effective simulation of flow on the other hand, are in conflict. It is vital to devise procedures that economize on the vast amount of arithmetic that should otherwise be involved.

One simple technique for economizing is to assume that the effects of flow can be sped up, so that erosion, transport, and deposition of sediment is greatly accelerated, thus "speeding up" geologic time. We can speed up the sedimentary processes by increasing the transport coefficient, ct. Unfortunately, excessively high values of ct lead to unrealistic results, and therefore we cannot simply increase parameters that regulate processes and expect suitable results.

An alternative involves extrapolating the effects of processes, by operating on a "compute-an -coast" basis. In natural environments, steady flow ordinarily modifies deposits of sediment slowly and steadily. Therefore. it is possible to simulate sedimentary processes for a short period (a few days), and then extrapolate the effect for a much longer time, as for example, a year. SEDSIM can "remember" a specific topographic grid, then operate for a few days of simulated] time and produce 5 new topographic grid that is compared with the previous grid. The differences between the two grids can be magnified by a given factor, representing an extrapolation over a much longer interval of time. for example. if during a simulated time of one day, SEDSIM erodes 1 mm. of sediment at a given location, a year's equivalent erosion would be

365 mm. Such a scheme can be carried only so far and is not universally applicable. After a certain amount of erosion and deposition have taken place, the flow pattern must be recalculated. Attempts to extrapolate too long may result in unrealistic topographic "holes and mounds" being formed because the flow is improperly controlled, and does not respond to changes in topography. The geographic vicinity of the "sources", where fluid and sediment are supplied, is particularly susceptible to the development of unrealistic topographic features because erosion and deposition tend to be relatively rapid there, where the flow and topographic surface may be far from equilibrium status, particularly early in a simulation run. The "compute—and—coast" scheme for extrapolation described above cannot be applied when the flow is highly unsteady, as for example in a turbidity current or in a river flood, because the flow varies continually. Fortunately, most natural processes involving unsteady flow are of short duration, and are separated by long periods of inactivity. For example, turbidity currents flowing through a submarine canyon may last a few hours and yet recur only every 50 years or so on average . A river's annual flood may last only a few days, and it may not be necessary to simulate flow between floods because most of the erosion, transport, and deposition of sediment occurs during floods. SEDSIM can simulate an individual event involving unsteady flow, and then proceed with simulation of the next unsteady flow event. ignoring the time between. Thus. spans of geologic time can be represented effectively when unsteady flow is involved by a "compute-and-wait" technique without extrapolating the processes during the waiting intervals.

VERIFICATION OF SEDCYC2

Program SEDCYC2 has been tested with various sedimentation experiments. SEDCYC2 can be used much as a sand table, starting with an initial topographic form with a specified homogeneous sediment present, and then supplying sources of water and sediment, and observing what happens over a specified span of time. Before SEDCYC2 can be utilized for such experiments. the parameters that control sedimentary processes in SEDCYC2 must be calibrated.

Estimating SEDCYC2's coefficients

Coefficient f_1 in Equation (122) governs sediment transportability, or in other words, the amount of sediment that can be carried in the flow under equilibrium conditions, in which there is neither erosion nor deposition. Fortunately, a wealth of experimental data that deal with sediment loads in equilibrium are available for calibrating f1. One possible method for calibrating f1 is similar to that described in Chapter II for calibration of the flow coefficients. We can use the value for f_1 that best fits either a set of data or an empirical function. we need more than a single value for f_1, however, because we must also specify how f_1 varies with a sediment's characteristics, including grain size, grain shape. and grain density. These characteristics can be summarized in terms of a particle's fall velocity in water. As a first approximation. coefficient f_1 is assumed to be inversely proportional to particle fall velocity:

$$f_1 = c_f / W \qquad (135)$$

where:

c_f = constant of proportionality
W = particle fall velocity

Under the condition specified by Equation (135). it is necessary to find only a single value of cf to calibrate f1 for any sediment whose fall velocity is known.

Most data for calibration relate sediment transport to hydraulic parameters of the flow, and to grain size, rather than to grain fall velocity. Therefore, it is necessary to convert sizes to fall velocities. By equating weight and drag, fall velocity can be found by the following formula:

$$W=\sqrt{\frac{\gamma_s-\gamma}{\gamma}\frac{4}{3}\frac{D}{C_d}} \qquad (136)$$

where:

C_d = drag coefficient

Empirical values of the drag coefficient, Cd, as a function of Reynolds number for spheres, disks, and ellipsoids are graphed in Figure 30. SEDSIM estimates fall velocity by using drag coefficient values that are indicated with the bold line in Figure 30. In the range of Reynolds numbers under which drag coefficient remains constant at 0.55, Equation (136) yields the fall velocity. In the range in which the drag coefficient is represented by an inclined straight line in the log-log graph (Fig. 30), the following expression provides the fall velocity:

$$W=\left(\frac{\gamma_s-\gamma}{\gamma}g\frac{4}{90}\right)^{4/5}v^{3/5}d^{7/5} \qquad (137)$$

where:

v = kinematic viscosity of water

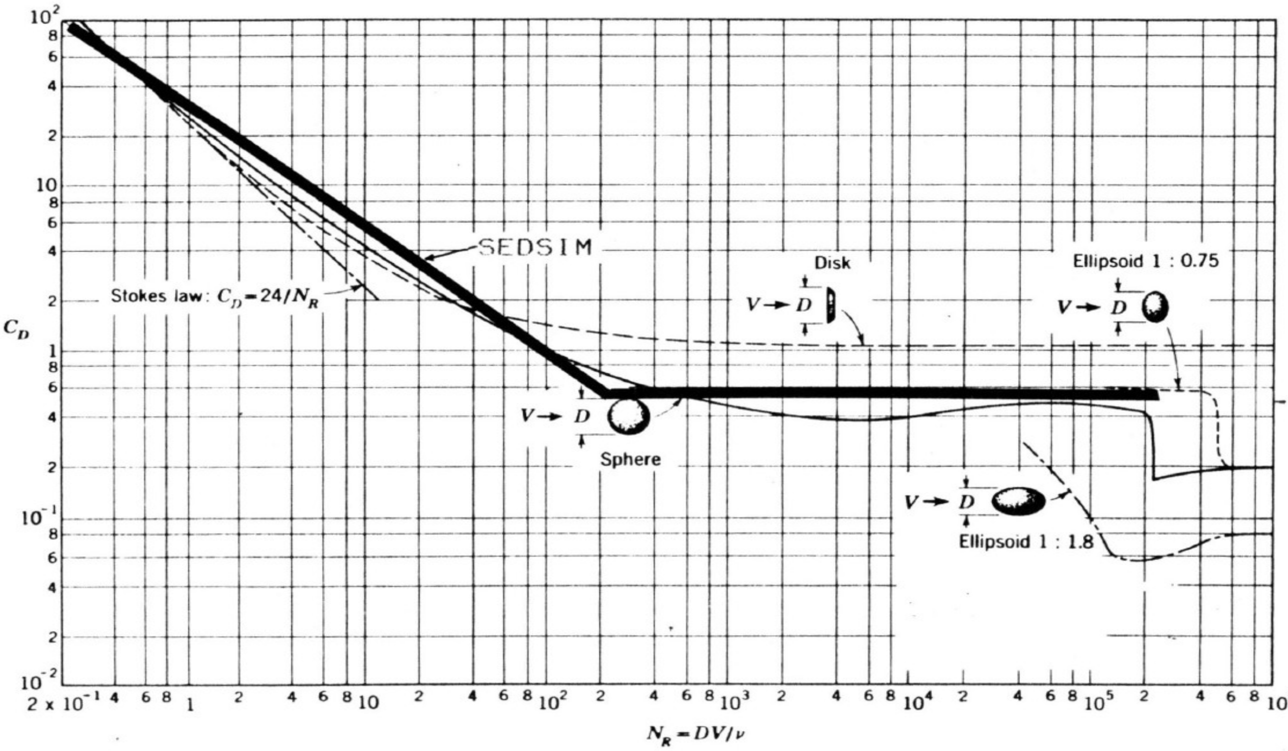

Figure 30: Curves showing drag coefficients (vertical axis) as function of Reynolds number (horizontal axis) for disks, spheres and ellipsoids (after Prandtl, 1930). Bold line indicates drag-coefficient function employed by SEDSIM to calculate fail velocity of sedimentary particles through water.

Equations (136) and (137) can be combined into the following formula for estimating particle fall velocities in water at 15° Celsius:

$$w = min(1895\, r_\gamma^{4/5} d^{7/5}, 4.88\, r_\gamma^{1/2} d^{1/2}) \qquad (138)$$

where:

$$r_\gamma = \frac{\gamma_s - \gamma}{\gamma}$$

Given equations (135) and (138). it is possible to find a value for cf that best agrees with empirical data of sediment load or transport rate_for various types of sediment in equilibrium. A data set for transport rates of sands was provided by Colby (1964), and ls illustrated in Figure (31). A value for c_f of 1.18 x10^{-6} s/m best fits the observed data for sands.

Coefficient f_2 governs the rate at which sediment is transferred between the flow and the deposits at the base of the flow when erosion or deposition take place. If f_2 is large, the transfer rate is high, and if f_2 is infinite, the transfer is instantaneous. It is difficult to calibrate f_2 because of the lack of data, but values for f_2 do not significantly affect SEDSIM's behavior. Most formulas that estimate sediment load or transport rate. either assume that the load instantaneously adjusts to changing hydraulic conditions, or do not specify the rate of adjustment.

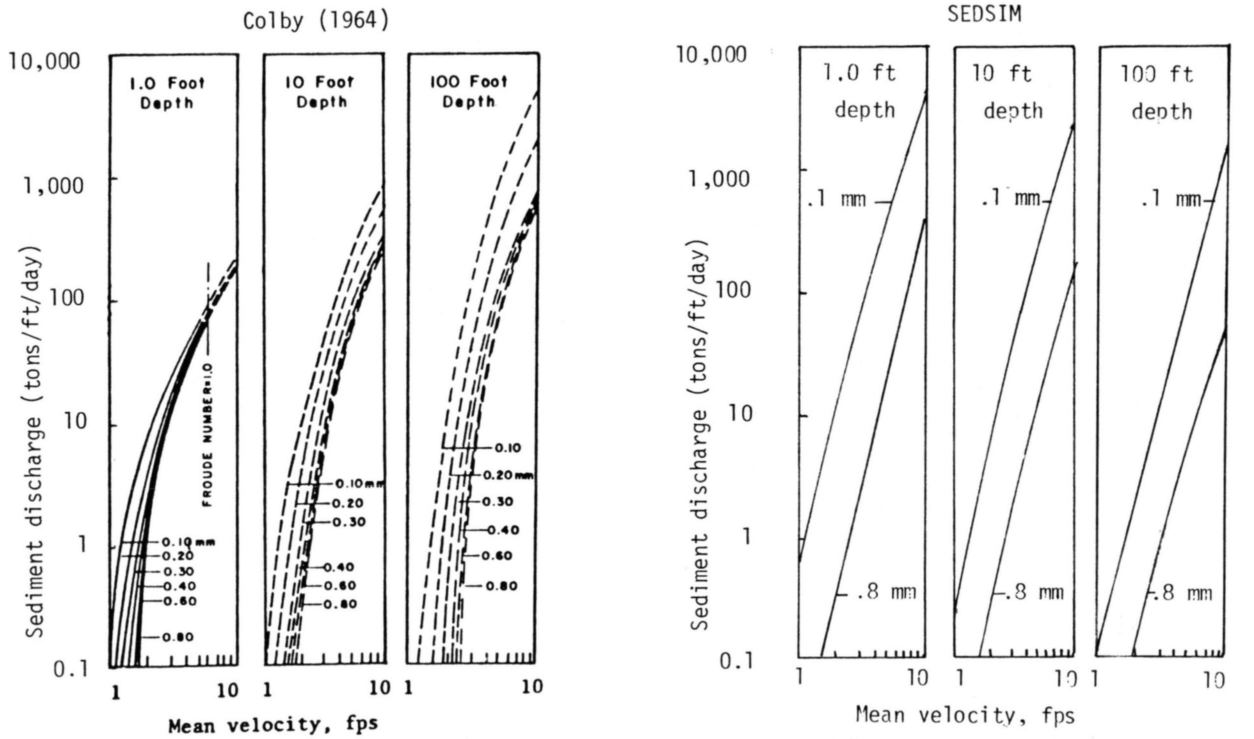

Figure 31: (a) Graphs showing relation of discharge of sands (vertical axis) to mean velocity (horizontal axis) for six median sizes of bed sands and three depths of flow, (after Colby, I964). (b) Graph at same scale as (a) showing sand discharges predicted by SEDSIM.

It is reasonable to use the same value of f_2 for erosion than for deposition. During deposition, we can assume that f_2 depends on the time it takes the sediment to settle out of the flow, the time being closely related to fall velocity. During erosion. it is also reasonable to assume that fine sediment, with a lower fall velocity. takes longer to achieve equilibrium. For lack of better data, and because f_2 must have the same units as velocity, we assume that f_2 is equal to the fall velocity W. In other words, if flow that is in equilibrium with the sediment it carries suddenly came to rest, the concentration would initially diminish at the same rate that would occur if the sediment is uniformly distributed throughout the flow.

Coefficient f_3 is the critical shear stress, which SED SIM calculates using a modified version of the Bureau of Reclamation's method (Lane and Carlson, l953), described later.

The single-sediment version of SEDSIM, SEDCYC2, calibrated with the procedure described above, was verified using data for sediment discharge in natural environments. Two data sets published by Vanoni et al (1960) and shown in Figure 32 were used for the verification. Figure 32 shows results of actual measurements of flow rate and sediment discharge for two major rivers. The measurements are com- pared with values predicted by various sediment discharge formulas. The experiments involved an initial topographic configuration similar to that shown in Figure 17. The flow rate at the sources placed at the upper end of the channel was set, and the sediment discharge near the lower end of the channel was recorded. Values predicted by

SEDSIM are represented as crosses in Figure 32.

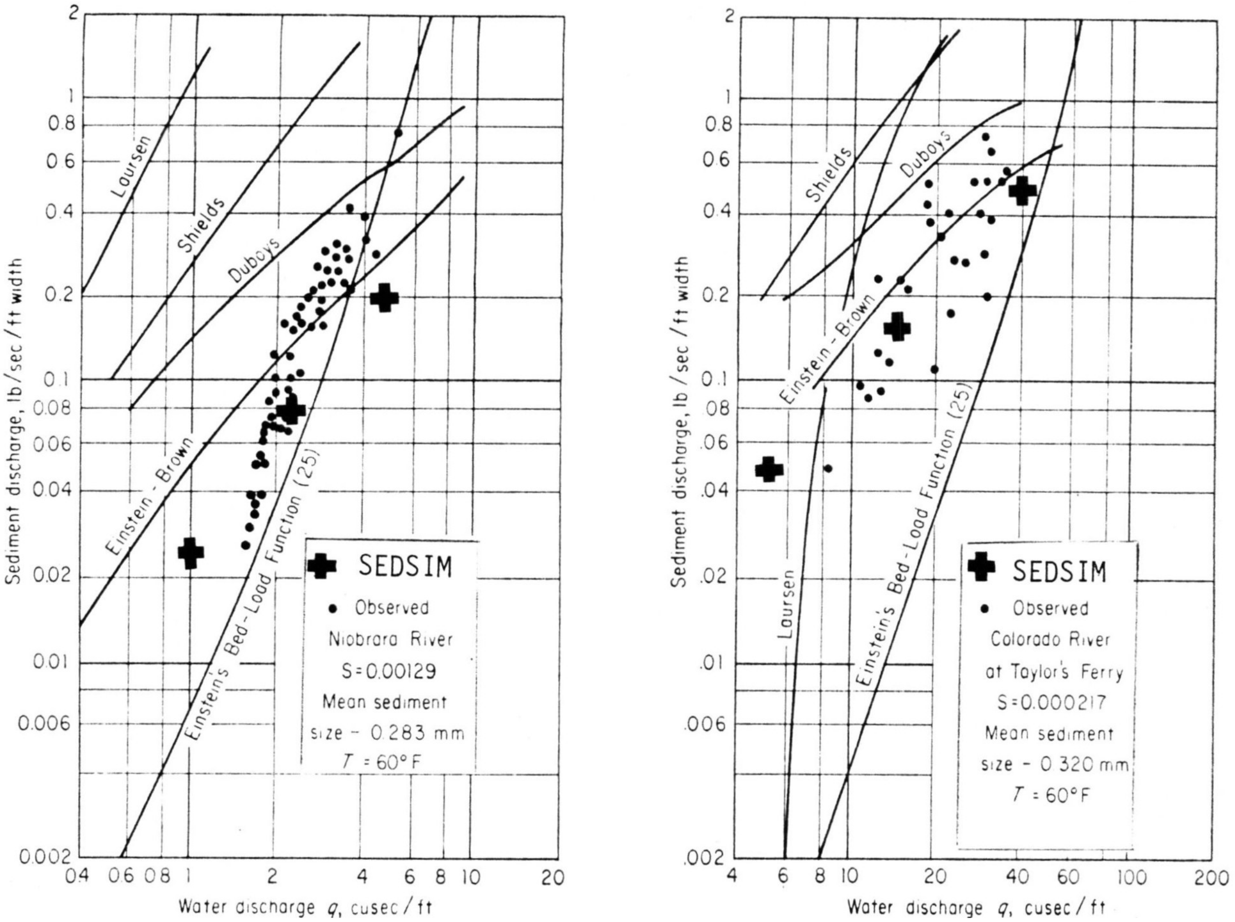

Figure 32: Sediment-rating curves showing sediment discharge (vertical axis) as function of water discharge (horizontal axis). according to various authors. Dots indicate values observed in natural streams (Adapted from Vanoni et al., 1960). Crosses indicate values predicted by SEDSIM using straight channel similar to that shown in Figure 20.

Channel-Bend Experiment

The initial topographic configuration used for the flow—only experiment that involves a channel containing a bend (Figs. 2l and 22), was used again to determine SEDCYC2's response when erosion and sedimentation are represented. in the experiment involving sedimentation. It was assumed that the basin contained only loose, homogeneous fine sand. Then, a flow rate was assumed that caused slight over bank flooding adjacent to the channel. The experiment involved a simulated period of one year.

After 0.2 years (Figs. 33, 34. and 35), some erosion has occurred in the channel, causing it to develop under water sand dunes (Fig. 33). Because the average "wavelength" between dunes is only a small multiple of a grid cell's size, we cannot determine whether or not the model is realistic in simulating the dune's wavelength in accordance with flow conditions. However, if we analyze flow conditions represented by numerical output from SEDCYC2, we find that from a qualitative standpoint, the processes that generate the sand dunes in sub—critical flow are represented in SEDSIM. Depth decreases, and flow velocity increases on the upstream faces of dunes, causing erosion there. However, on the downstream faces of dunes, flow velocity decreases and deposition occurs. To determine whether the rates at which these processes operate at the dune faces are realistic will require experiments with a much finer grid.

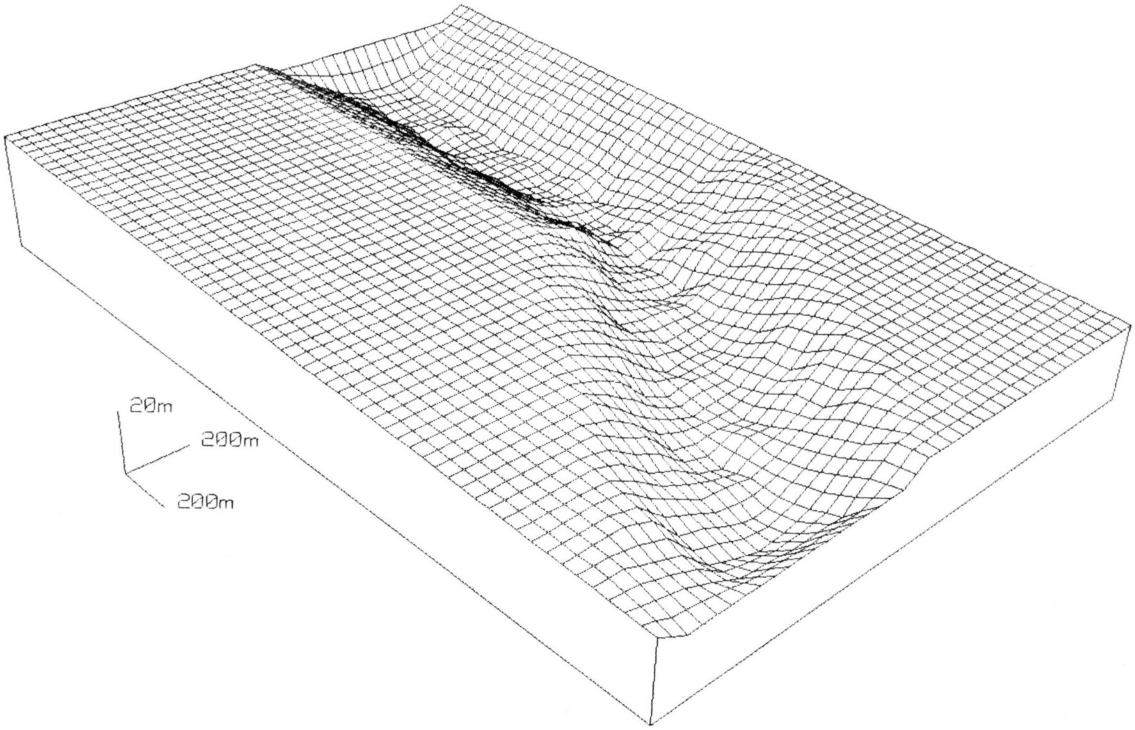

Figure 33: Fishnet diagram showing topographic surface of bent channel after a simulated time of one year.

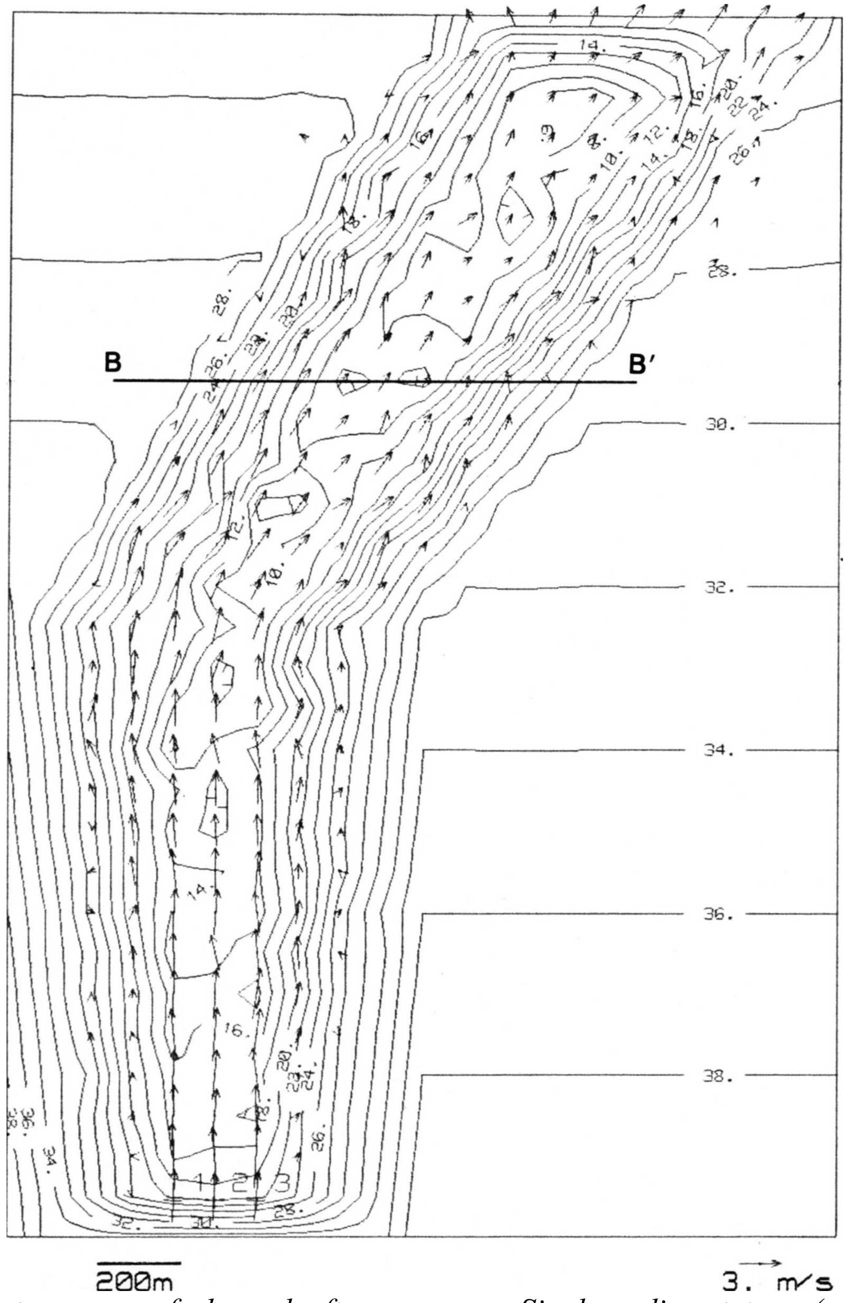

Figure 34: Contour map of channel after one year. Single sediment type (medium sand) is assumed to form channel and to be transported by stream Section B-B is showing in Figure 35. Contours are in meters.

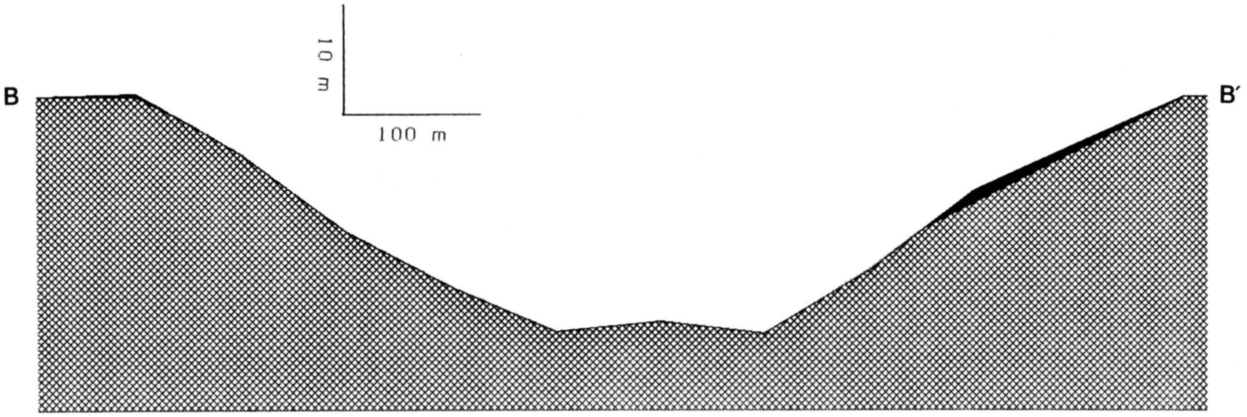

Figure 35: Part of section B-B' (Figure 34) showing asymmetric channel starting to develop. Point bar has formed on inside of bend (right), and levee has formed on outside (left).

After a simulated time of one year (Figs. 36, 37. and 38), substantial erosion has occurred near the source of fluid, in the upper part of the channel, and the channel bottom has become increasingly irregular. The channel's cross section has also changed, and levees have formed where overbank flooding has occurred. The enlarged part of section B-B' (Fig. 38) reveals the depositional details of the levees as well as deposition on the alluvial plain beyond the levees.

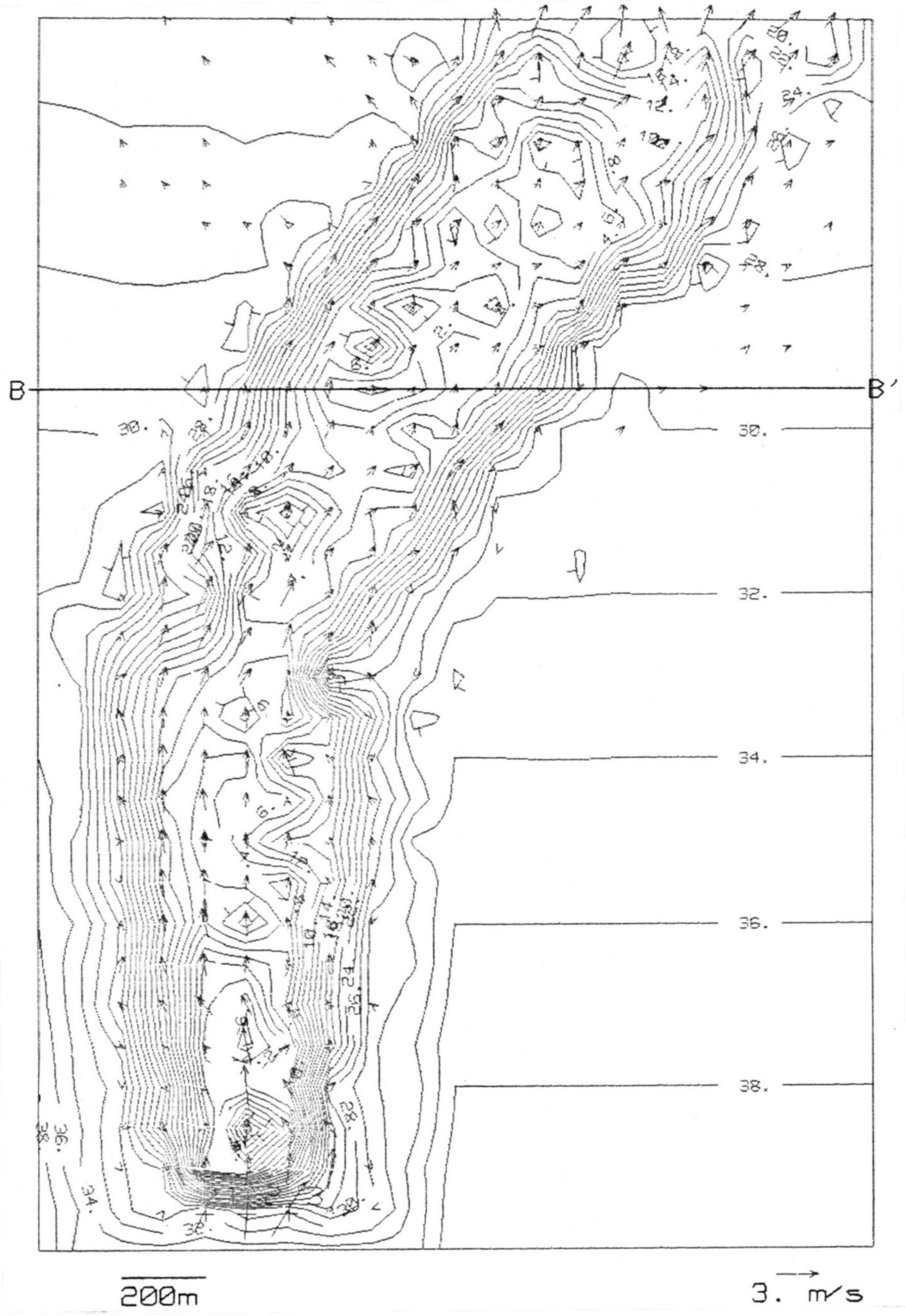

Figure 36: Contour map of bent channel after five years have elapsed in simulation experiment. Extensive erosion has occurred near sources of fluid at upsrteam end of channel, and channel floor has become irregular.

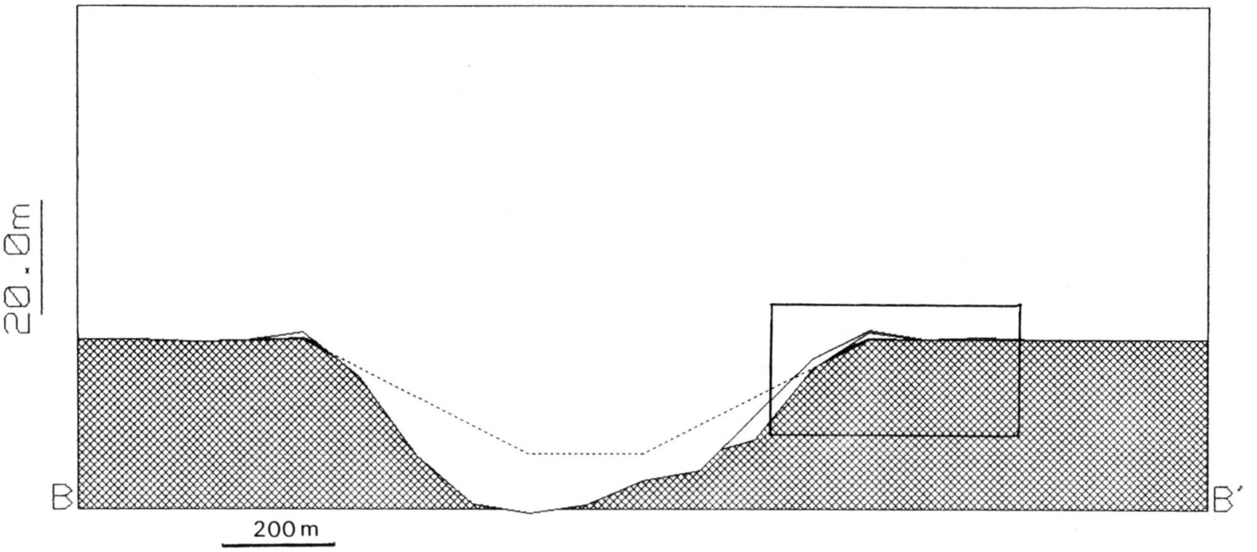

Figure 37: Section B-B' (Figure 36) after simulated time of five years. Dotted line shows original shape of channel. Point bar on right has continued to develop. Levees have formed on both banks. Box outlines portion enlarged in Figure 38.

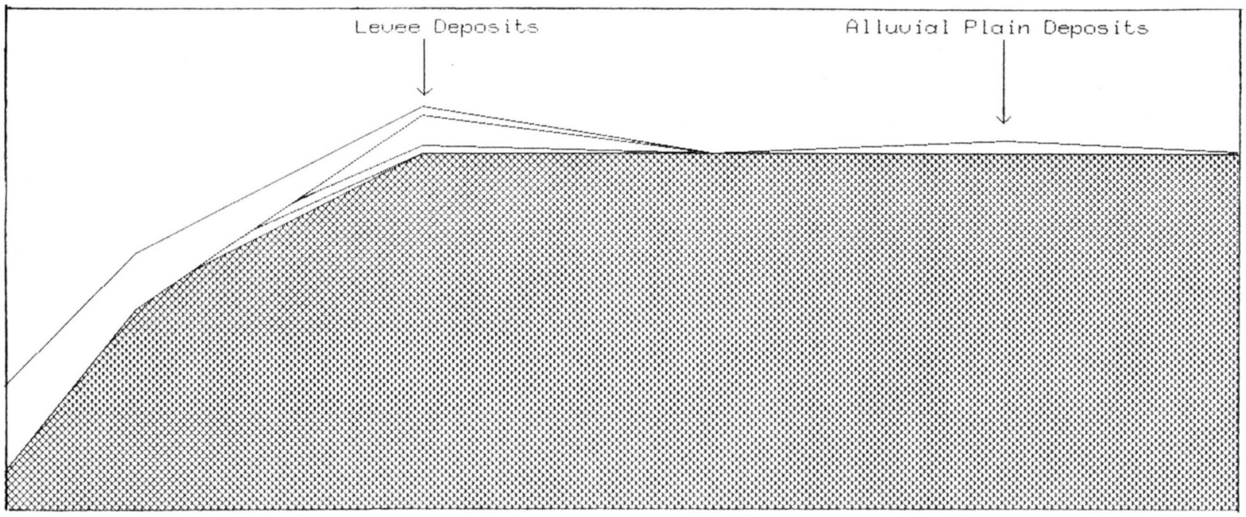

Figure 38: Enlargement of part of section B-B, showing details of levee deposits. Alluvial plain deposits have form ed beyond levee.

Alluvial-Fan Experiments

SEDSIM can simulate deposition of alluvial fans efficiently because a relatively small proportion of fluid with respect to sediment is involved. Reducing the number of fluid elements has the advantage of reducing computing time.

Two experiments in which alluvial Fans were created are described below. The initial topogrpahic form for both experiments is a rectangular area of dimensions 2 km by 3 km, that consists of a subaerial surface that slopes gently, except where it is broken by a steep escarpment (Fig. 39).

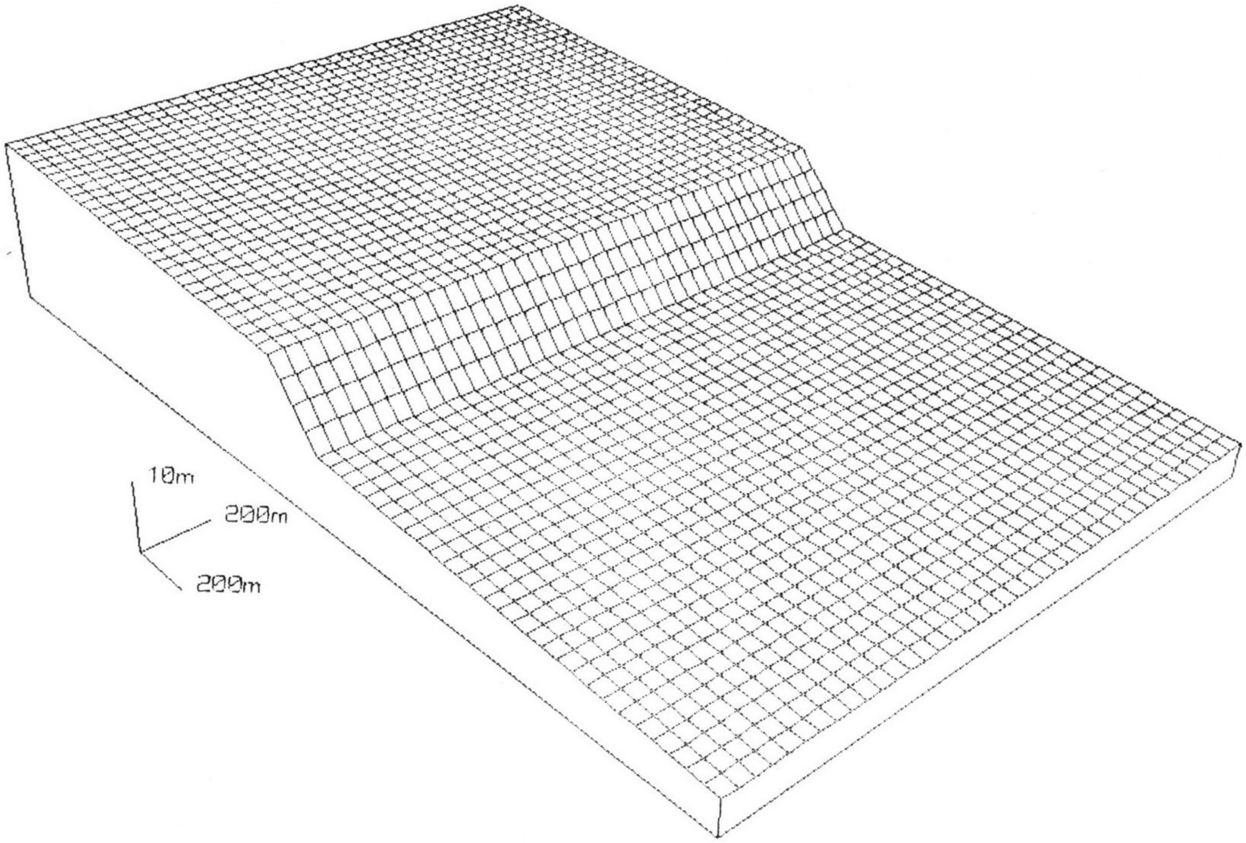

Figure 39: Fishnet diagram showing initial topographic surface for aluvial—fan experiment. Vertical exaggeration is 20.

The sediment present is poorly consolidated sand. In the first simulation experiment (Fig. 40), a stream enters at point 1 and flows over the surface. The fluid source is turned on and off 100 times to represent 100 unsteady flows, as might be produced by a flood each year for 100 years. The results are shown in Figures 41 and 42.

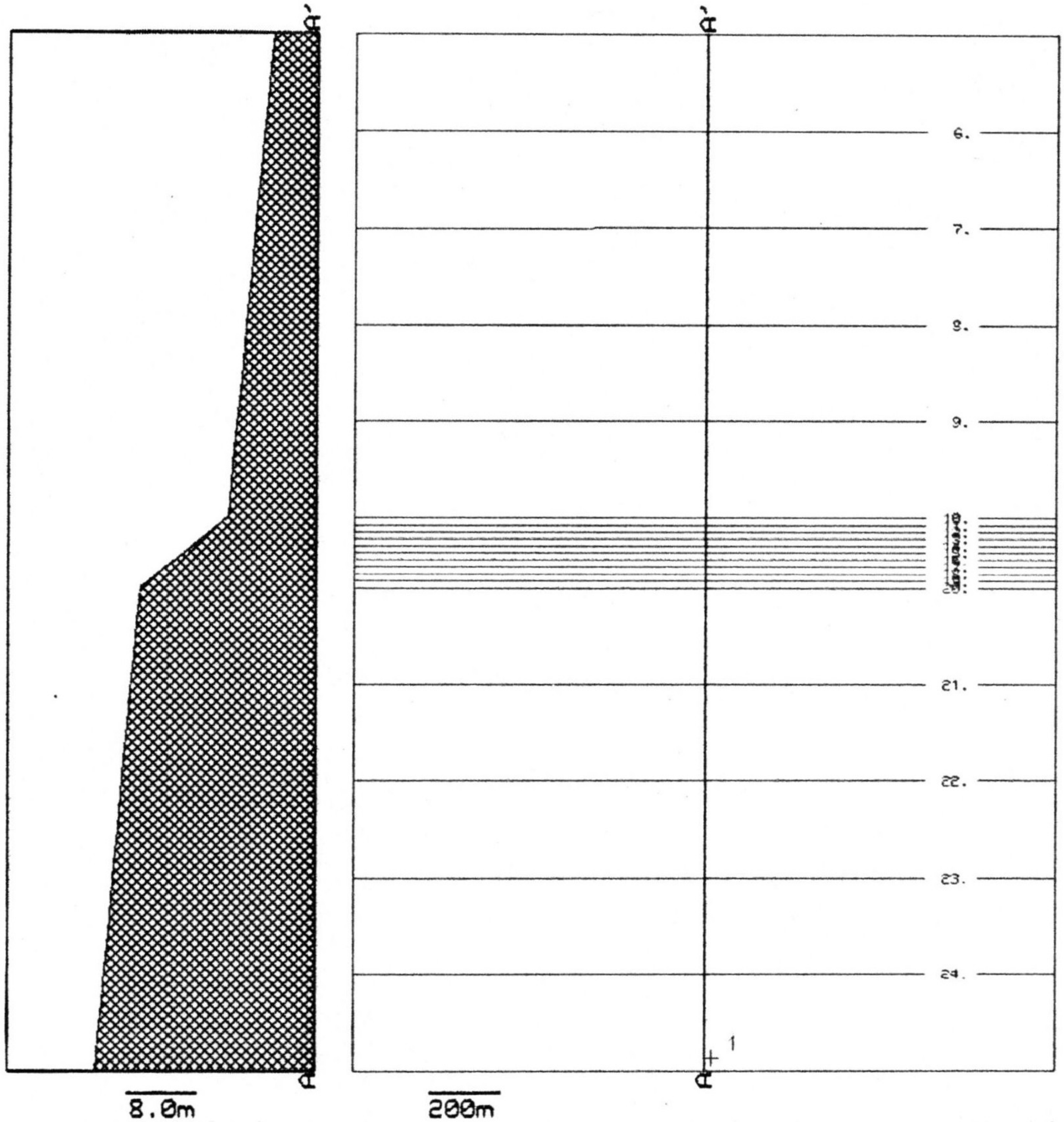

Figure 40: Section and contour map of initial topographic surface for aIluviaI-fan experiment. Single fluid source is placed at point l. Contours in are in meters.

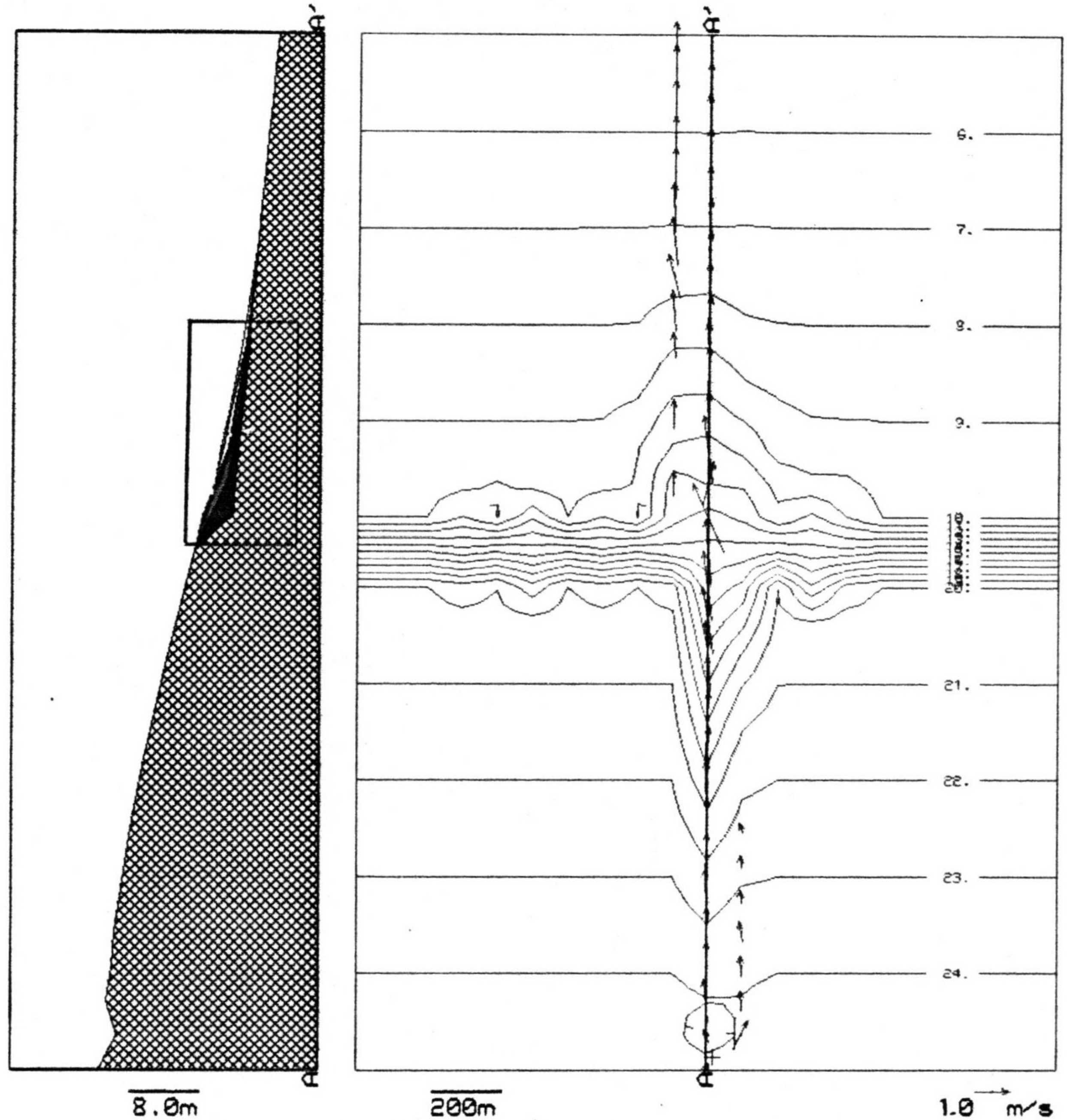

Figure 41: Section A-A' showing features after have elapsed. Layers of sediment in alluvial fan A-A' are enlarged in Figure 42.

The second experiment is similar, except that the flow comes from two separate sources. The resulting "snapshots" of the system (Fig. 43) show that two main valleys developed on the steep slope, with corresponding alluvial fans formed where the slope decreases. There are also small valleys near the main valleys. One of the small valleys (marked X in Figs. 43c and 43d) was traversed by a stream at the 40-year point in the simulated time (Fig. 43c), but the valley was abandoned later by the stream (by 100 years time, Fig. 43f) in response to changes in the drainage network upstream, which caused the stream to be diverted.

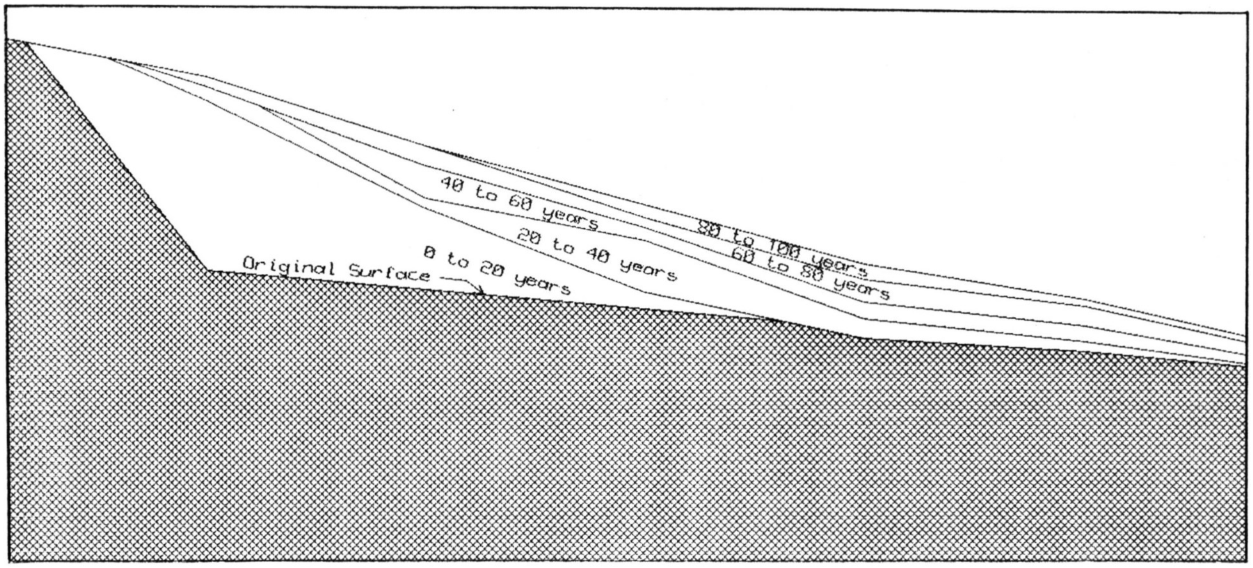

Figure 42: Enlarged portion of section A-A' of Figure 41, using time lines plotted every 20 years, revealing that other deposits have been truncated and overlapped by younger deposits.

Fishnet diagrams for 20- and 100—year time points are shown in Figures 44a and 44b. Cross-sections (Figures 45 and 46) show the sediment in place when the simulation began with cross hatching, whereas the newly formed deposits are shown with colors. Furthermore, the new deposits are marked with time—lines every 20 years, thus clarifying the succession of deposits with respect to their age. The longitudinal section in Figures 45a and 45b shows that the longitudinal profile of the valley and fan approximate an exponential curve, in general accord with a stream's equilibrium profile. The enlarged part of the longitudinal section (Fig. 45b) reveals the details of the new deposits. The transverse cross—sections (Figures 46a and 46b) reveal that the areas of maximum deposition have shifted laterally.

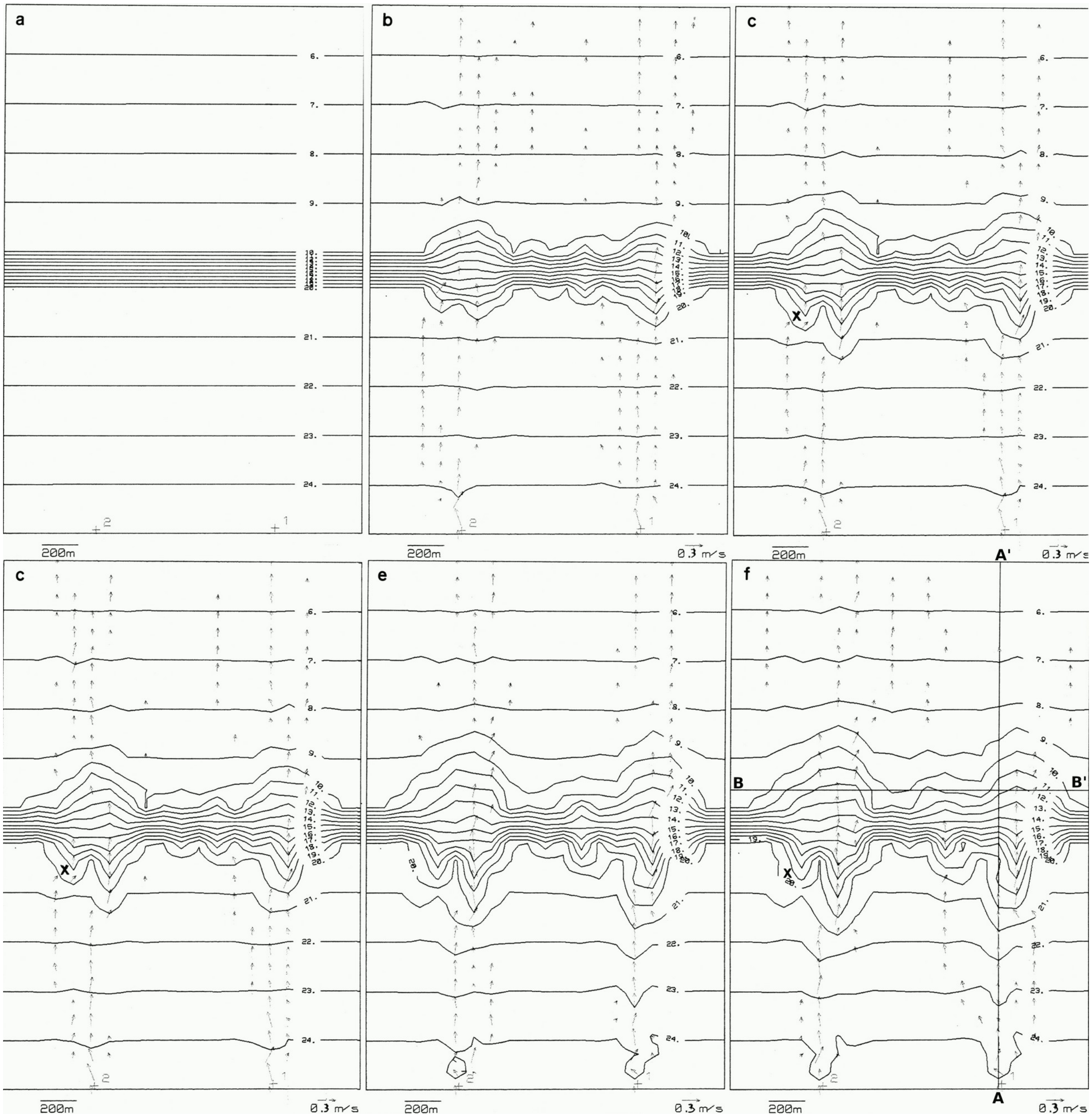

Figure 43: Succession of contour maps and vector plots (a through F) showing changes in topographic configuration and f ow pattern in alluvial—fan simulation experiment involving two separate sources of fluid. State of system is displayed every 20 years. Gorges are eroded on escarpment. some of them are abandoned later by channel. Contours are in meters.

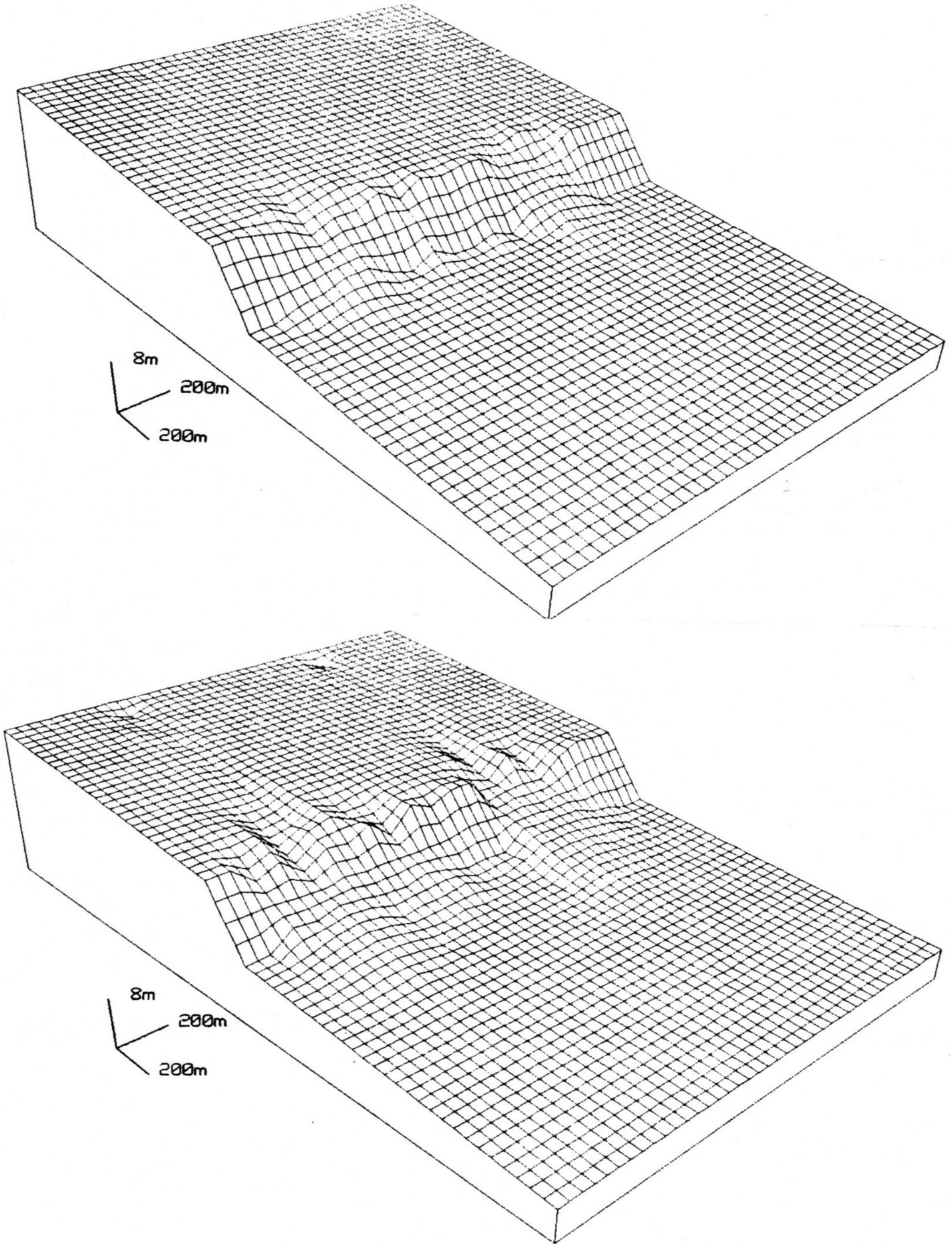

Figure 44: Fishnet diagram showing alluvial fans formed (a) after 20 years, and (b) after 100 years.

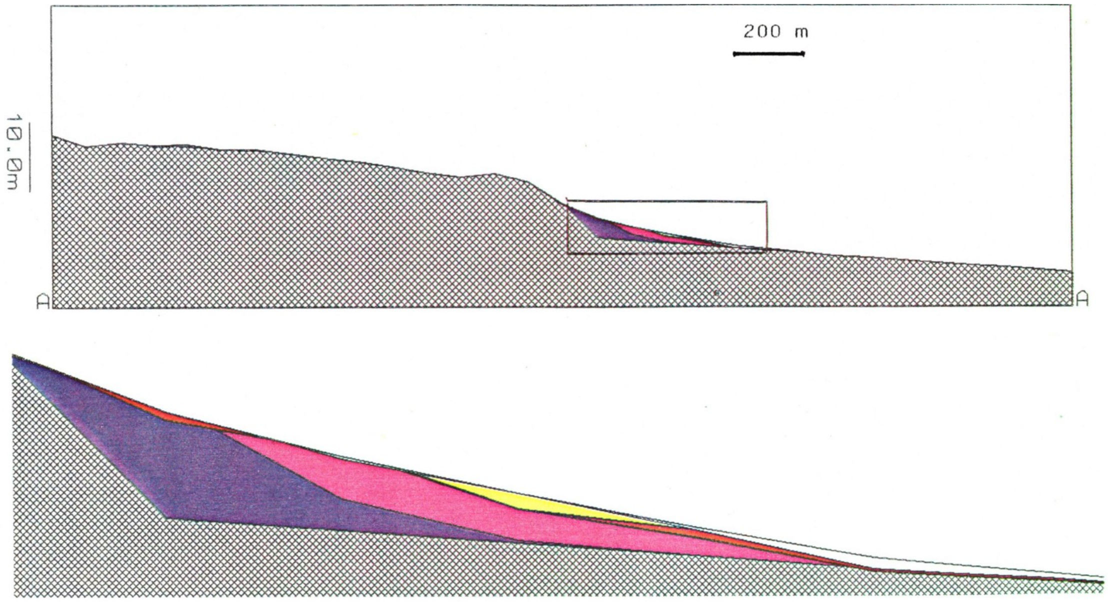

Figure 45: (a) North-south section A-A' through easternmost fan in Figure 43f, revealing irregular profile produced by erosion of substrate, and smoother profile approximating an exponential equilibrium curve formed where fan has been deposited. (b) Enlarged frame showing deposits every 20 years. Older deposits are present near escarpment, whereas younger deposits extend farther out.

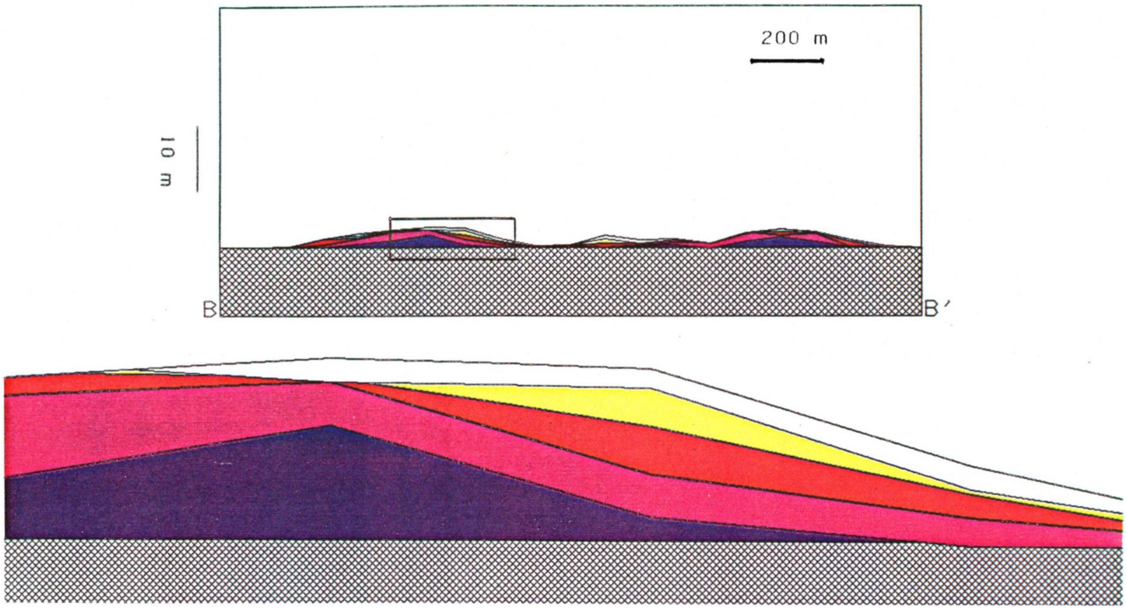

Figure 46: (a) Section B-8' through alluvial fans shown in Figure 43f. Colors represent relative ages at 20 year intervals. (b) Enlarged frame reveals that area of maximum deposition has shifted laterally.

In spite of the simple form of the initial topographic surface, both the flow pattern and the topography at the end of the simulation experiment are irregular. These irregularities have been produced even though SEDSIM contains no components that are deliberately random. Such behavior is realistic, because natural flows and their deposits exhibit similar characteristics. The seemingly random behavior is discussed in Chapter VI.

Turbidity Current Experiment

An experiment involving simulated turbidity currents ,similar to the experiment described previously, was performed using the single sediment model. The earlier turbidity—flow experiment incorporated unsteady flow. but neither erosion nor deposition were allowed to occur. In the first run of the new experiment, shown in Figure 47, the sediment initially present is medium sand. The turbidity current was initiated by releasing 2000 cubic meters of fluid at the location shown in Figure 47a. The fluid is of high density, containing 1,000 kg of fine sand per cubic meter of fluid. The fluid glided down the slope. its progress being shown in Figures 47b through 47f.

The turbid flow is less regular than in the earlier. flow—only experiment, because the flow causes both erosion and deposition along its path. The flow itself is affected by changes in the topography, Flow and topography being mutually interdependent. The flow slows at the bottom of the steep slope (Fig. 47c), where deposition has formed a fan.

A second turbidity experiment involves 20 successive flows. Each new flow was released when the previous flow had been completed. The output shows that a deep canyon and a fan have been formed, and is displayed in Figures 48a through 48f, that represent the topographic configuration at successive intervals, separated from each other by four intervening flows. A perspective diagram of the resulting configuration of the deposits is shown in Figure 49.

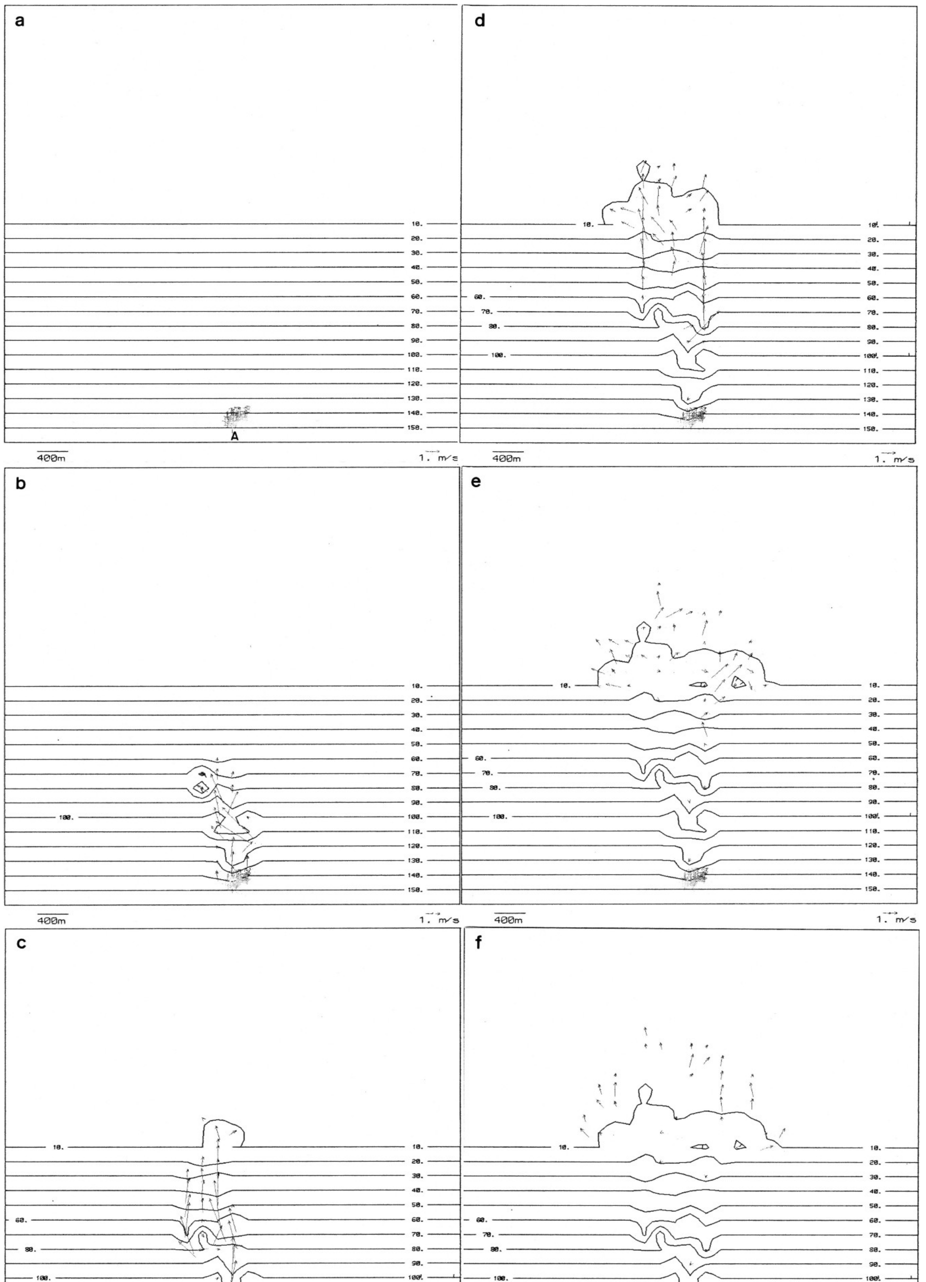

Figure 47: Succession of contour maps and arrow plots (A through F) showing single turbidity current in loose fine sand displayed at intervals of one minute of simulated time. Erosion and deposition occur while flow is in progress, causing flow to be less regular than flow shown in Figure 25. Flow spreads rapidly after reaching base of steep slope, where depositional fan has formed. Contours are in meters.

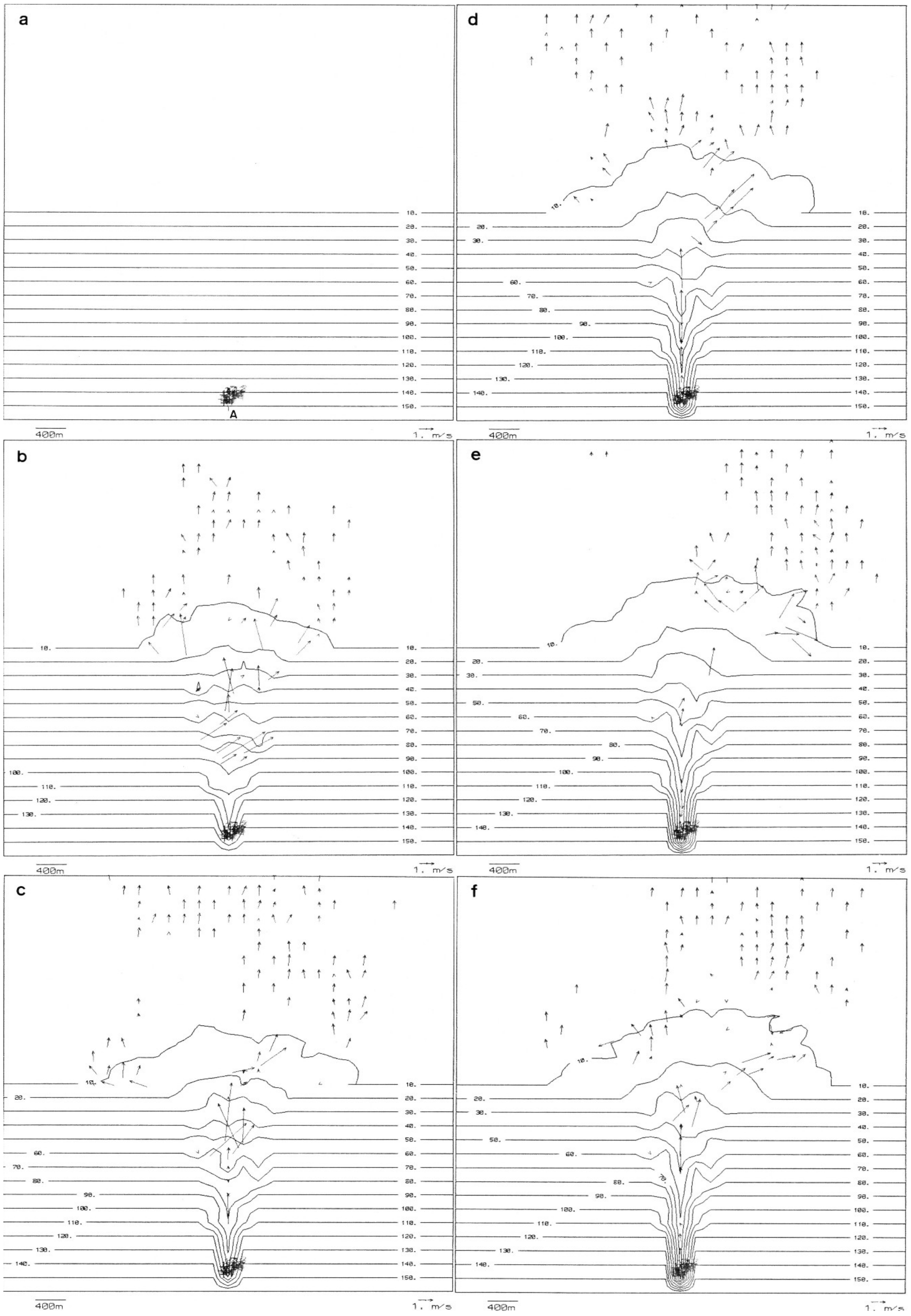

Figure 48: Succession of contour maps and _arrow plots (A through F) showing effect of 20 turbidity currents in loose fine sand creating canyon and fan. Displays are shown every four such events. Canyon is deeper and fan is larger than those produced by single current shown in Figure 47. Contours are in meters.

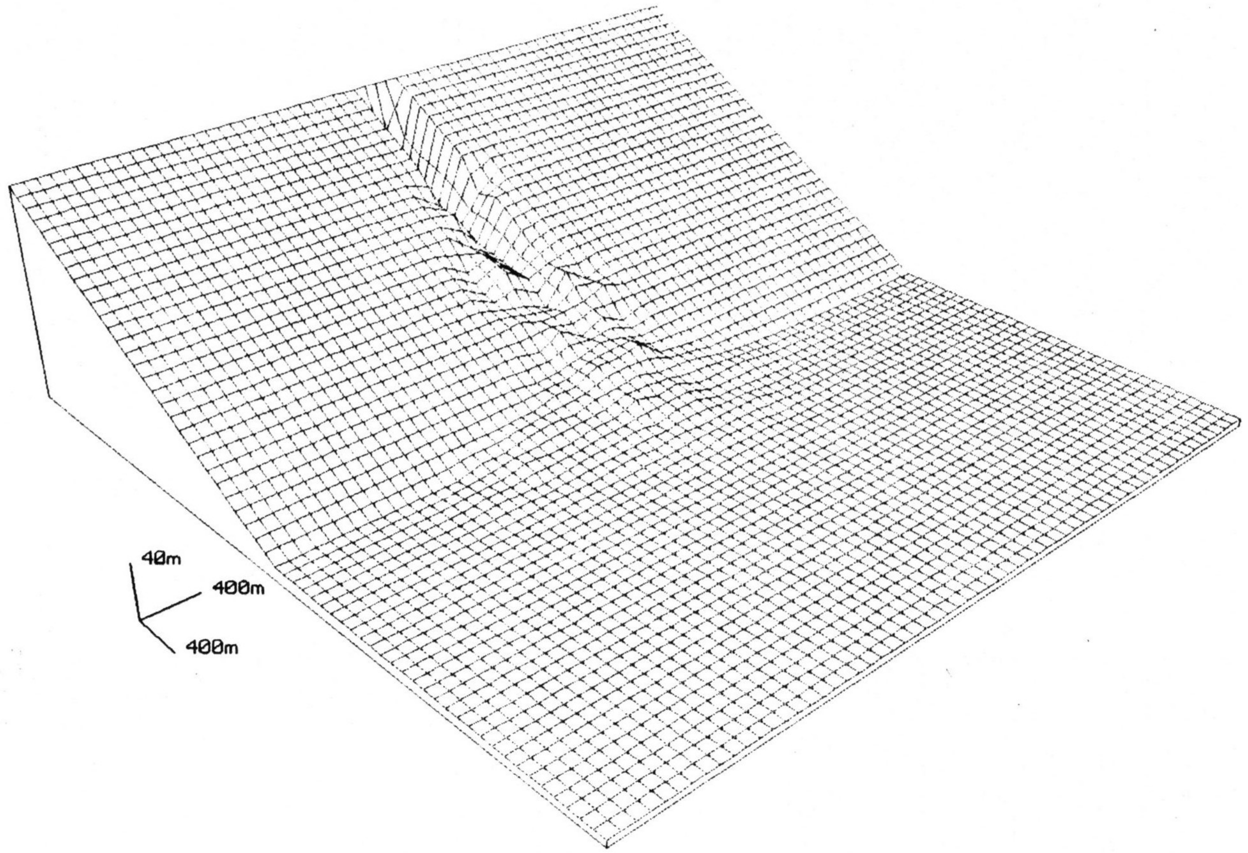

Figure 49: Fishnet diagram of final state of experiment involving canyon and fan, corresponding to topographic map of Figure 48f.

Delta Experiment

An experiment was devised to test SEDSlM's performance in simulating a large delta. The initial state of the system being simulated is depicted by Figure 50. The single sediment type is assumed to be loose medium sand and a single steady source of fluid containing sand was located slightly inland from the shore.

Although most rivers that flow into ocean are less dense than sea water, most of the sediment is distributed by currents that are more dense than sea water (Bea and Bernard. 1973) . Therefore, in this experiment the flow was assumed to be denser than sea water. The simulation experiment extended for 1,000 years, and result are shown in Figure 51. During that period, the shoreline prograded about 10 km toward the sea, creating deposits that are roughly sigmoidal in cross section near the shore (Fig 52). offshore, erosion and deposition have created an irregular sequence of deposits. Channels and gullies have been carved by high density flow, as commonly occurs in actual deltas (Matthews and Shepard, 1963). Simulated deposits appear to thin towards the sea more rapidly than actual deltaic deposits, probably because a single sediment type is represented and deposition of progressively finer sediments, as the flow slows, is not represented. Chapter V describes a more realistic simulation of a delta in which there are multiple types of sediment.

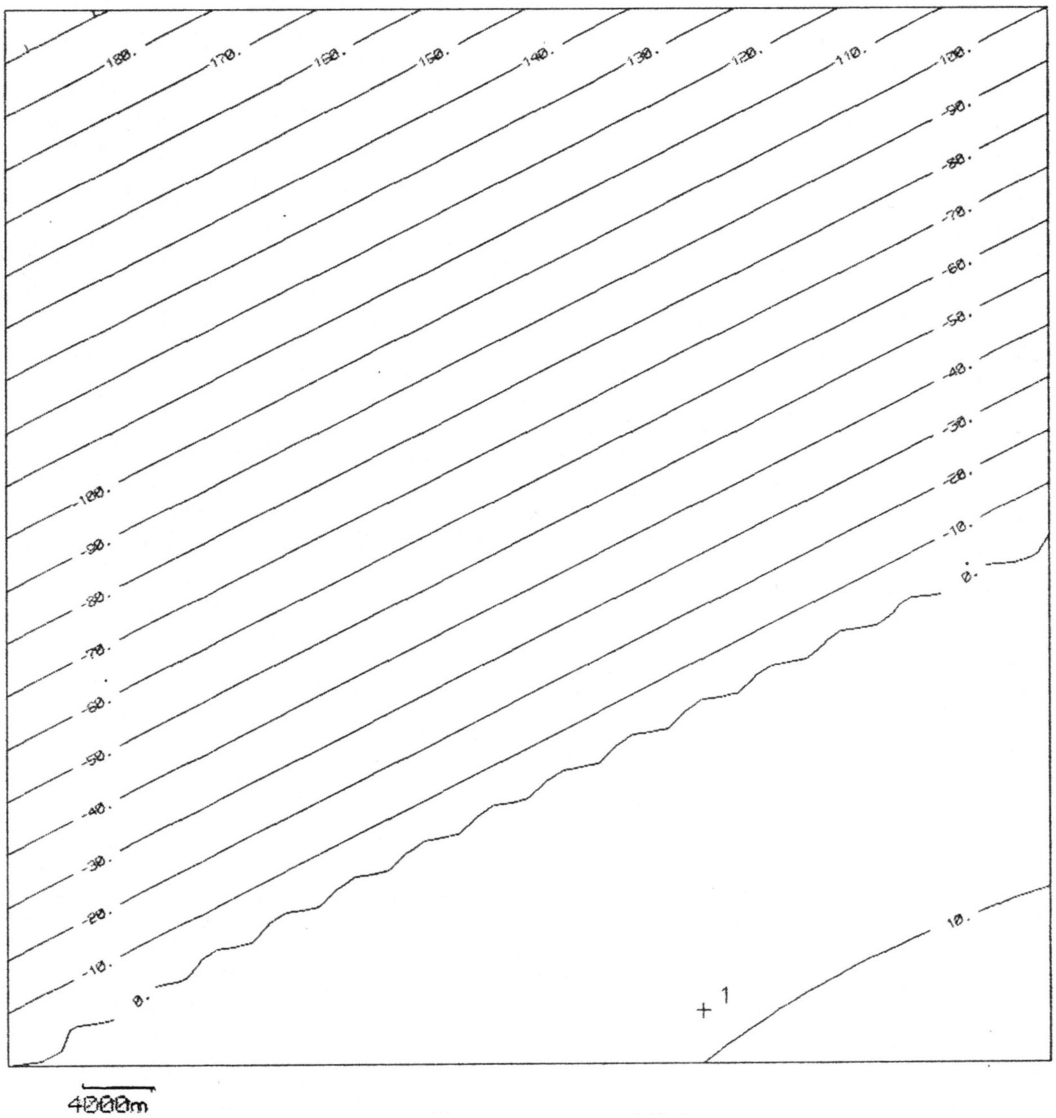

Figure 50: Contour map showing initial topography for single-sediment delta experiment. Shoreline is marked by "0" contour. Onshore area slopes gently at rate of 0.5 m per km, whereas submerged basin slopes toward northwest at 5 m per km. Contours are in meters.

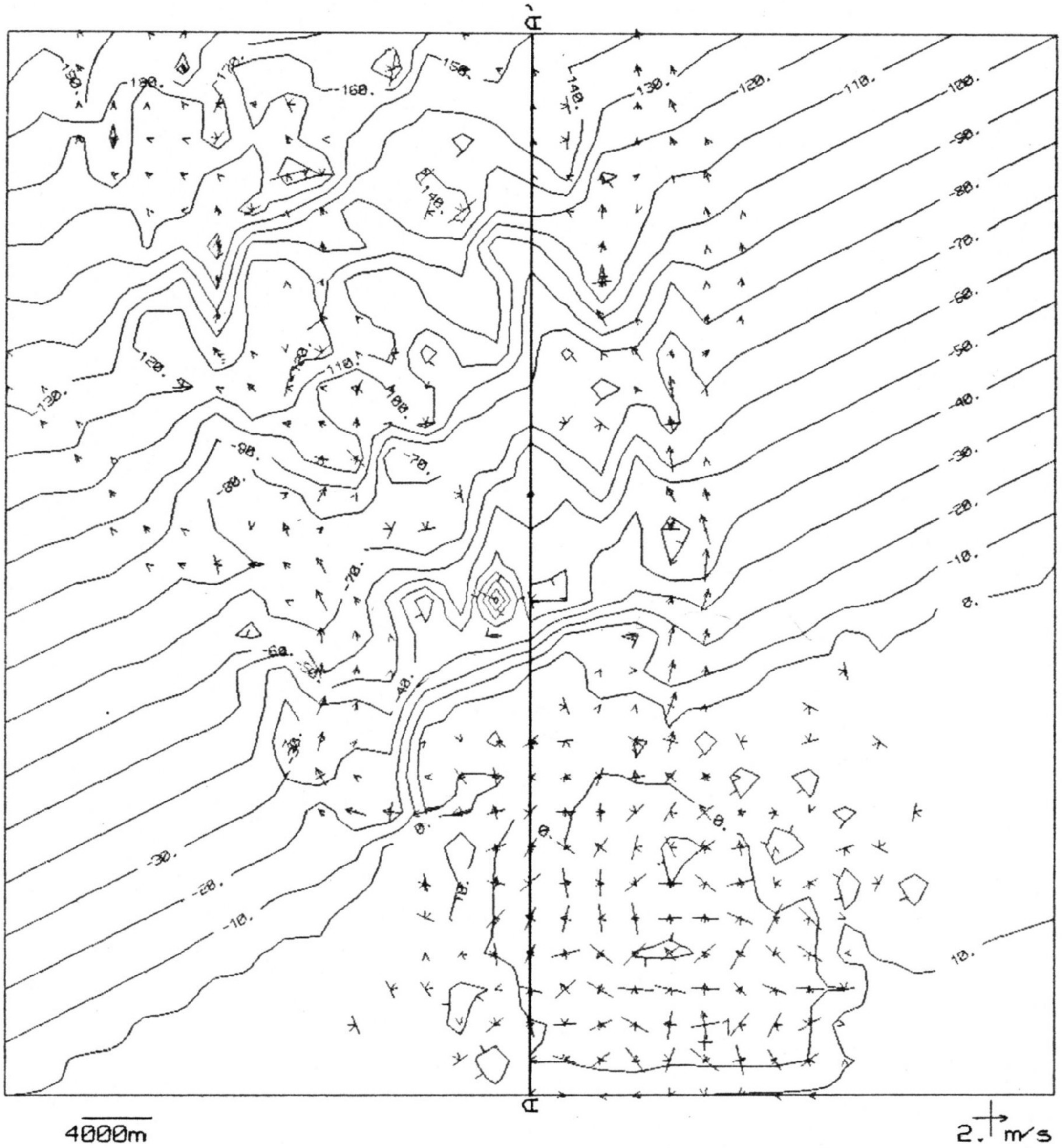

Figure 51: Contour map of simulated delta after a period of 10,000 years.

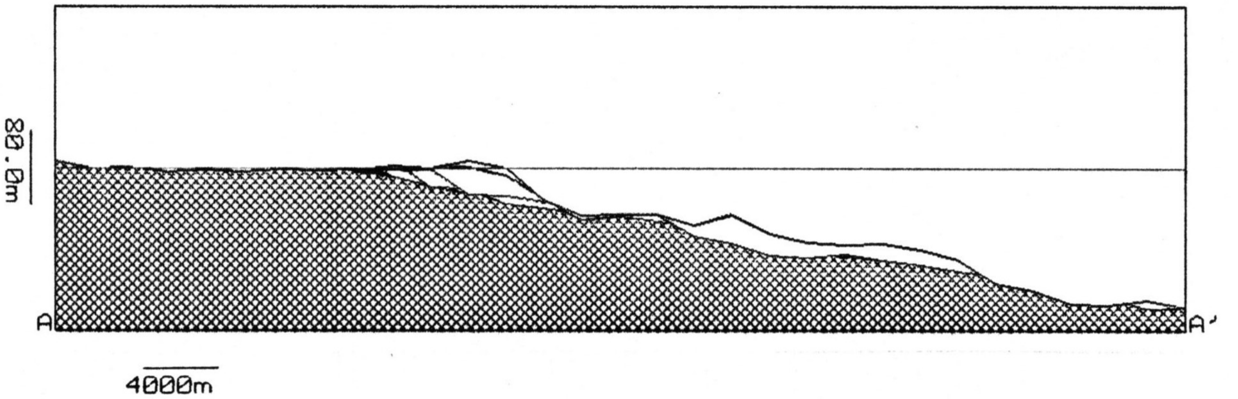

Figure 52: Section A-A' through simulated deltaic deposits

ASSESSING THE PERFORMANCE OF THE SINGLE-SEDIMENT MODEL

The single-sediment model described in this chapter is an extension of the two-dimensional flow model described in Chapter ll. The restriction to two dimensions affects the simulation of sedimentary processes in which vertical variations in velocity are important. Thus SEDSIM cannot simulate subaqueous ripples, or any sedimentary feature whose vertical dimension is significantly smaller than the flow depth. However. SEDSIM can simulate the formation of large underwater dunes that are caused by large-scale changes in flow velocity and depth. Even though SEDSIM does not reproduce the spiral flow that takes place in channel bends. It can still simulate erosion and deposition in channel bends, as well as lateral shifting of channels. because it does reproduce variations in shear stress that occur across channels. further testing is needed to determine if the rates at which these processes occur in nature are accurately represented by SEDSIM.

SEDSIM's performance possibly could be improved by improving its sediment-transport formula. Because transport mechanisms are not thoroughly understood, it is difficult to devise an appropriate sediment-transport formula that is general enough to be suitable over a wide range of conditions. The use of a transport formula that treats bed load and suspended load separately would probably increase the accuracy of SEDSIM's sediment transport rate calculations, but would also significantly increase computer time, because the computer program must evaluate the transport formula for every fluid element at every time increment.

In general. the single-sediment model adequately reproduces major sedimentary processes in channels, alluvial fans, turbidity currents, and deltas. In most natural environments, however, more than one sediment particle size is present, and thus lt ls necessary to extend SEDSIM so as to incorporate several sediment types a task described in Chapter IV.

Chapter IV
MULTIPLE-SEDIMENT SIMULATION MODEL

Chapter III described the extension of the flow model to incorporate a single, uniform sediment type. The present chapter deals with a further extension that permits simulation of sedimentation with multiple types of clastic sediment. The different types are specified in terms of grain characteristics, such as size, shape. and density. This expanded capability opens a wide range of geological applications, but it also poses two new difficulties. as follows:

1. Different sediment types carried in a flow are not independent of each other, because the capacity of the flow to transport each sediment type is affected by the presence of all other sediment types carried by the flow. The interaction between sediment types in the flow is poorly understood, and difficult to predict.
2. A multi-sediment model must account for variations in the types of sediment that have been deposited. furthermore, the accounting involves the distribution of the types in three-dimensional space. Although the accounting procedure is simple, it requires a large proportion of the computer's resources that are devoted to the simulation.

MATHEMATICAL MODEL

The mathematical theory developed here for the multi-sediment model is valid for any number of types of sediment, but the present computer program accommodates a maximum of four types. The limit of four is a compromise between realism in dealing with a spectrum of types of elastic sediment, and the computing resources required. Another advantage of a limit of four components is that a mixture of any proportion of the components can be represented unambiguously with a single color, thus facilitating graphic representation.

The first step in defining the multi-sediment model is to define the function that describes the composition of the deposits in the subsurface (i.e., their sedimentary facies in three dimensions):

$$\kappa_{(x,y,z)}=K_s \qquad (139)$$

where:

κ = function assigning a sediment type to every point underneath the surface

K_s = sediment type

(x,y,z) = point underneath the surface, $z \leqslant Z$

Each sediment type is represented by an integer because it is assumed that the number of sediment types is finite, rather than a continuous gradation, and that only a single type can be represented at any point in the three-dimensional volume forming the "subsurface". Thus, at a very detailed level, SEDSIM does not represent sediment mixtures, because mixtures are defined only when a volume of sediment is considered. The computer program (SEDCYC3) represents a single sediment type at each cell endowed in a three-dimensional network of cells. Thus, a mixture of types of sediment can be defined only by aggregating various cells together, as described later. The representation is justified because at any point in an actual deposit, only a single grain of sediment can be present.

Continuity Equation for Multiple Sediment Types

The continuity equation for multiple sediment types is an extension of the continuity equation for a single sediment (Equation 108). The extension of the continuity equation specifies that the volume of material represented by net change in topographic elevation is equal to the net change in the load of all sediment types:

$$(H-Z)\frac{\sum_{\kappa} Dl_{Ks}}{Dt}=\frac{-\partial Z}{\partial t} \qquad (140)$$

where:

H = free surface elevation with respect to sea level

Z = topographic elevation with respect to sea level

$\sum_{\kappa}$ = summation over the number of sediment types

l_{K_s} = volumetric sediment concentration of type K_s

K_s = sediment type

$t = time$

It is also necessary to specify that only the sediment type that is at the water-sediment interface can be eroded, and that the sediment type being deposited necessarily becomes the sediment type at the water-sediment interface. These relationships can be expressed in a single statement:

$$\frac{Dl_{Ks}}{Dt}\neq 0 \quad \Rightarrow \quad \kappa(x,y,Z)=K_s \qquad (141)$$

Multi-sediment Transport Equation

The general form of the sediment-transport equation for several sediment types is the following:

$$(H-Z)\frac{Dl_{Ks}}{Dt}=f(\vec{q},\nabla h,\nabla Z,L,F,K_s,\kappa(Z)) \qquad (142)$$

where:

L = vector defining sediment concentration of each type: $(l_1,l_{,2},...l_{Ns})$

F = matrix of coefficients defining sediment types: $\begin{bmatrix} f_{1,1} & f_{1,2} & \cdots & f_{1,Nf} \\ f_{2,1} & f_{2,2} & \cdots & f_{2,Nf} \\ \vdots & \vdots & \ddots & \vdots \\ f_{Ns,1} & f_{Ns,2} & \cdots & f_{Ns,Nf} \end{bmatrix}$

N_f = number of coefficients that define each sediment type

N_s = number of sediment types

As in the single-sediment model, the general form of the sediment-transport equation does not define how much sediment is transported until function f is defined. To define f, it is convenient to revise existing methods of quantifying sediment transport for sediment mixtures

$$Q_s = (A_2/A_1)r\,v_o d \qquad (143)$$

where:

A_1 = ratio of grain area to diameter sqared

A_2 = ratio of grain volume to diameter cubed

r = relative excess shear stress = $\frac{\tau_0-\tau_c}{\tau_c}$

τ_0 = bottom shear stress

τ_c = critical shear stress

v_o = shear velocity

d = sediment particle diameter

Review of sediment-transport formulas

Two of the most useful formulas for determining transport rate of a sediment mixture were provided by Kalinske (1947), and Laursen (1958).

Kalinske (1947) developed a simple formula for determining sediment transport rate for a sediment mixture that is similar to Einstein's (Eq. 117):

When Kalinske's formula is applied to a mixture of several particle-size fractions, the transport rate for each fraction is given by Equation (143), and then the result is weighted by a "coverage factor". The coverage factor represents the proportion of the water-sediment interface that is covered by sediment grains of a specific size, and is proportional to p_i/d_i where p_i is the proportion by weight of sediment fraction i. and d_i is the particle diameter of that fraction.

Laursen (1958) also provided a multi sediment type formula:

$$\bar{c} = \sum_i p_i \left(\frac{d_i}{h}\right)^{7/6} \left(\frac{\tau'_0}{\tau_c} - 1\right) f\left(\frac{v_o}{W}\right) \qquad (144)$$

where:

$\bar{c}$ = mean concentration of suspended load in percentage by weight
p_i = proportion by weight of fraction of size d_i
τ'_0 = shear stress due to grain resistance alone = $v^2 d_i^{1/3} / (30 h^{1/3})$
W = particle fall velocity
f = function determined experimentally (Fig. 53)

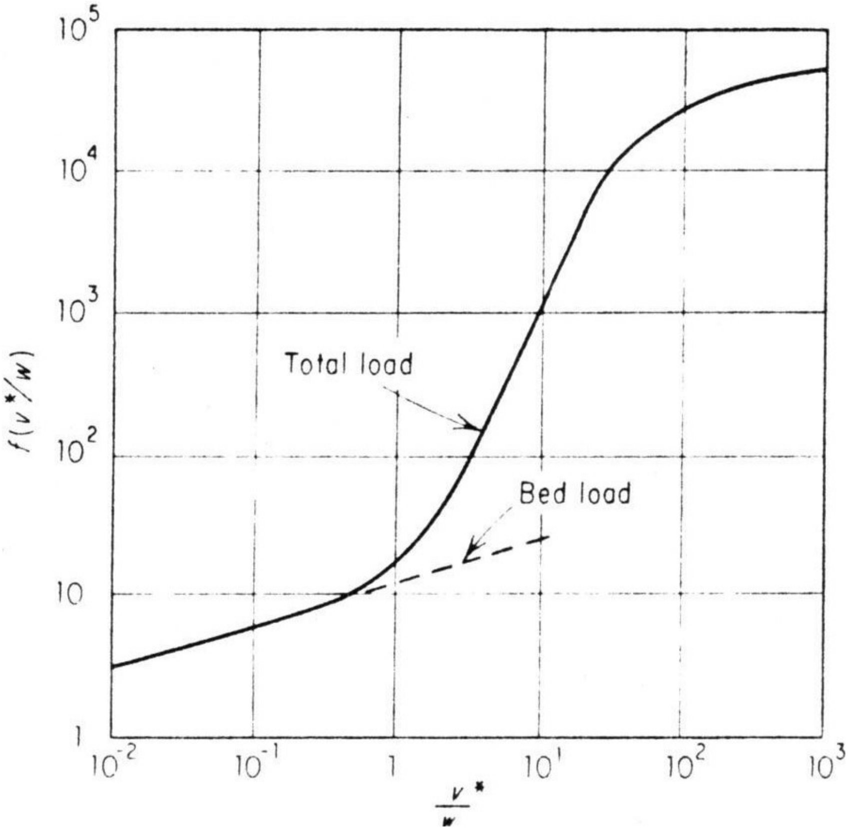

Figure 53: Graph after Laursen (1958), which provides an empirical value of "sediment-load" function f (vertical axis) for each value of quotient between shear velocity and particle fall velocity (horizontal axis). Values of f are used to solve for sediment concentration in bed load or suspended load, utilizing Equation (143).

Kalinske's and Laursen’s formulas are simple to apply because the interaction between sediment types is determined by a single parameter (i.e.. the coverage factor or the proportion by weight of each sediment type). The formula used by SEDSIM, described fully in the next section of the present chapter, makes use of a similar approach. But to maintain compatibility with the single-sediment formula. SEDSIM's formula assumes that the main parameter determining total transport rate is power dissipated by bottom friction per unit volume of fluid (P), rather than relative excess shear stress (r).

Other authors provide methods of estimating sediment transport for the components of a sediment mixture. Which are more accurate, but are lengthier than the two methods described above. Einstein (1950), for example, provides a method by which his single-sediment formula (Equation 117) can be applied to each component in a mixture of different types of clastlic sediment by applying corrections for the interaction between particles belonging to different size fractions. But the corrections involve lengthy calculations. Other procedures in dealing with multiple sediment types are provided by Colby and Hembree (I955). and by Bagnold (1957). The methods of Einstein. Colby and Hembree, and Bagnold could be incorporated into SEDSIM, but they would make the computer program extremely slow because they involve lengthy operations. Since the sediment-transport formula used by SEDSIM needs to be evaluated at every time increment for every fluid element, it should be simple in order to economize computer effort.

Although there are different methods of estimating sediment transport rates of a mixture of sediments, the methods all agree, in that the transport rate of each sediment type depends on the proportion and the characteristics of the other types of clastic sediment present in the flow. In other words, whether erosion or deposition occurs under given hydraulic conditions depends not only upon the total sediment load, but also on the composition of the sediment in the load.

Transport formula Employed by SEDSIM

The formula employed by SEDSIM for transport of multiple sediment types resembles the single-sediment formula (Eq. 122) because it shares the assumption that erosion and deposition depend on the balance between the flow's transport capacity, (Eq. 122) and the "effective sediment concentration", which was defined in Chapter III for one sediment type (A_e in Equation 122). To compare the effect of different sediment mixtures on a flow’s capability to transport them, it is necessary to define the effective sediment concentration for specific sediment mixtures. A_{em}. In SEDSIM we assume that A_{em} is the sum of the values of A_e of each component, as defined by Equation (122). Therefore:

$$\Lambda_{em} = \sum_{Ks} l_{Ks} / f_{1,Ks} \qquad (145)$$

where:

Λ_{em} = effective sediment concentration of mixture

l_{Ks} = sediment concentration of each type

$f_{1,Ks}$ = transportability of each type (as defined in Chapter III)

As in the single-sediment model, transport capacity is defined by Equation (I24). The equivalent of the single-sediment transport equation (Eq. 122) in the multi-sediment model then can be expressed by Equations (146) and (147) :

Let $R=(\Lambda-\Lambda_{em})f_{2,Ks}$ (146)

where:

$f_{2,Ks}$ = erosion-deposition rate coefficient for sediment type K_s

$$(H-Z)\frac{Dl_{Ks}}{Dt}= \begin{cases} R \text{ if } (R>0 \text{ and } \tau_0 \geqslant f_{3,Ks} \text{ and } \kappa(x,y,Z)=K_s) \\ \quad \text{or } R<0 \text{ and } (K_s=1 \text{ or } l_{Ks-1}=0) \\ 0 \qquad \text{otherwise} \end{cases} \qquad (147)$$

where:

K_s = sediment type

K_s-1 = next coarser sediment type

Equation (147) specifies that when the effective load is less than transport capacity, material is eroded if the threshold conditions for moving the exposed sediment are exceeded (as in the single-sediment model. the transport equation is modified to prohibit erosion in hypopycnal flow). When the effective load exceeds transport capacity, deposition occurs, and coarser sediments (i.e. with higher fall velocities), are deposited first. Erosion and deposition rates are proportional to the difference between effective load and transport capacity.

Equation (147), which regulates erosion, transport, and deposition, has two important advantages: First, it is compatible with the single-sediment transport equation (Eq. 122). If only one sediment type is used in Equation (I47), or if all sediment types are the same, Equation (I22) and (147) are identical. Second, if we accept that the effective sediment concentration of a sediment mixture is the sum of the effective concentration of its components (Equation 145), it is unnecessary to calibrate other sediment parameters for the multi-sediment model.

Initial conditions and Boundary Conditions

Initial conditions for the multi-sediment model are similar to those for the single-sediment model (Eq. 128), except that sediment concentrations for all sediment types must now be provided. as follows:

$$l_{Ks}(x,y,t_0)=l_{Ks,0}(x,y) \qquad 1\leqslant K_s\leqslant N_s \qquad (148)$$

Also, the type of sediment existing at every point beneath the surface must be prescribed at the start of a simulation experiment:

$$\kappa(x,y,z,t_0)=\kappa_0(x,y,z) \qquad (149)$$

Boundary conditions require that if sources of fluid and sediment are being supplied, the concentration of each sediment type must be defined at each source:

$$l_{Ks}(x_{si},y_{si},t)=l_{Ks,si}(t) \qquad (150)$$

The "Basement"

In many experiments, we can assume that sedimentary deposits rest upon homogeneous material which has no lower bound, and can be regarded as "basement". The basement can be eroded, however, thus yielding one or more types of sediment. In the context of this model, the basement is not necessarily a competent rock, because it could be composed of loose material. although by definition it is homogeneous and extends downward without limit.

The definition of "basement" as presented above has many advantages. Because the basement is homogeneous, it is unnecessary to retain information about its composition, and the only information to be retained involves the shape or configuration of its surface. Since the sediment-type function K must be defined everywhere beneath the surface, it is arbitrarily assumed to be 0 within the basement. But the computer procedure that evaluates K can identify sediment-type "0" much faster than the other sediment types, simply by noticing that the point to be evaluated is below the basement surface. Therefore not only does this procedure reduce storage requirements, it also reduces computation time.

If the basement is to be included in SEDSIM, Equation (I47) must be expanded to incorporate the possibility of the basement being eroded, as follows:

Let $R=(\Lambda-\Lambda_{em})f_{2,Ks}$ (151)

where:

$f_{2,Ks}$ = erosion-deposition rate coefficient for sediment type K_s

$$(H-Z)\frac{Dl_{Ks}}{Dt}= \begin{array}{l} R_0 f_{4,Ks}\text{ , if } R_0>0 \text{ and } \tau_0\leqslant J_{3,0} \text{ and } \kappa(x,y,Z)=0 \\ \\ \text{defined by Equation (147) otherwise} \end{array} \qquad (152)$$

where:

$f_{2,0}$ = basement erosion coefficient

$f_{3,0}$ = threshold shear stress for basement erosion

$f_{4,Ks}$ = proportion of sedimment type K_s into which the basement decays, $1\leqslant K_s\leqslant N_s$

NUMERICAL METHOD FOR MULTI-SEDIMENT MODEL

Representation of fluid flow is unchanged with the incorporation of multiple types of sediment. Therefore Equations (94), (98), and (99), which were introduced in Chapter II and used again in Chapter Ill, remain valid in the multi—sediment model. The equations describing sedimentary processes, however, are different, and are discussed next.

Subsurface Sediment Type

First, function K, which assigns a specific sediment type to every point in the subsurface, must be expressed in a form convenient for discrete approximation. The basement's top surface, as the topographic surface, is represented by a grid with square cells. κ can be prescribed by a set of three-dimensional cells that forms the volume between the basement and the topographic surface. Each cell can be assigned a sediment type, represented by a positive integer, while points beneath the basement's top are assigned sediment type "0" (i.e., basement).

There are many possible configurations for three-dimensional grids. SEDSIM uses one of the simplest three-dimensional grids, in which the cells are square prisms that are stacked in columns between the basement-top grid and the topographic grid (fig. 54). The three-dimensional sediment cells have the same horizontal dimensions as the cells in the basement-top and topographic grids, but are displaced by half a cell in both the *x* and *y* directions (Fig. 54). Therefore the corners of topographic cells, where hydraulic parameters are calculated, are directly underneath the centers of sediment cells, where erosion and deposition take place. The vertical dimension of each sediment-containing cell in the three-dimensional grid is fixed, except for the uppermost cell in a column, which may be thinner to accommodate the specific topographic elevation defined by the corresponding topographic grid point.

Sediment Continuity

When multiple sediment types are represented, every fluid element must have values that represent the concentration of each sediment type that it contains. Thus we must provide the sediment concentration for each type Ks. For fluid element k, and for each time t, which can be written as 1 $_{k,Ks,t}$' . The multi-sediment continuity equation (140), can be approximated in finite-difference form as follows:

$$\frac{Z_{i,j,t+1}-Z_{i,j,t}}{\Delta t}=-h_{i,j,t}\frac{\sum_{k}\sum_{Ks} l_{k,Ks,t+1}-l_{k,Ks,t}}{\Delta t} \qquad (153)$$

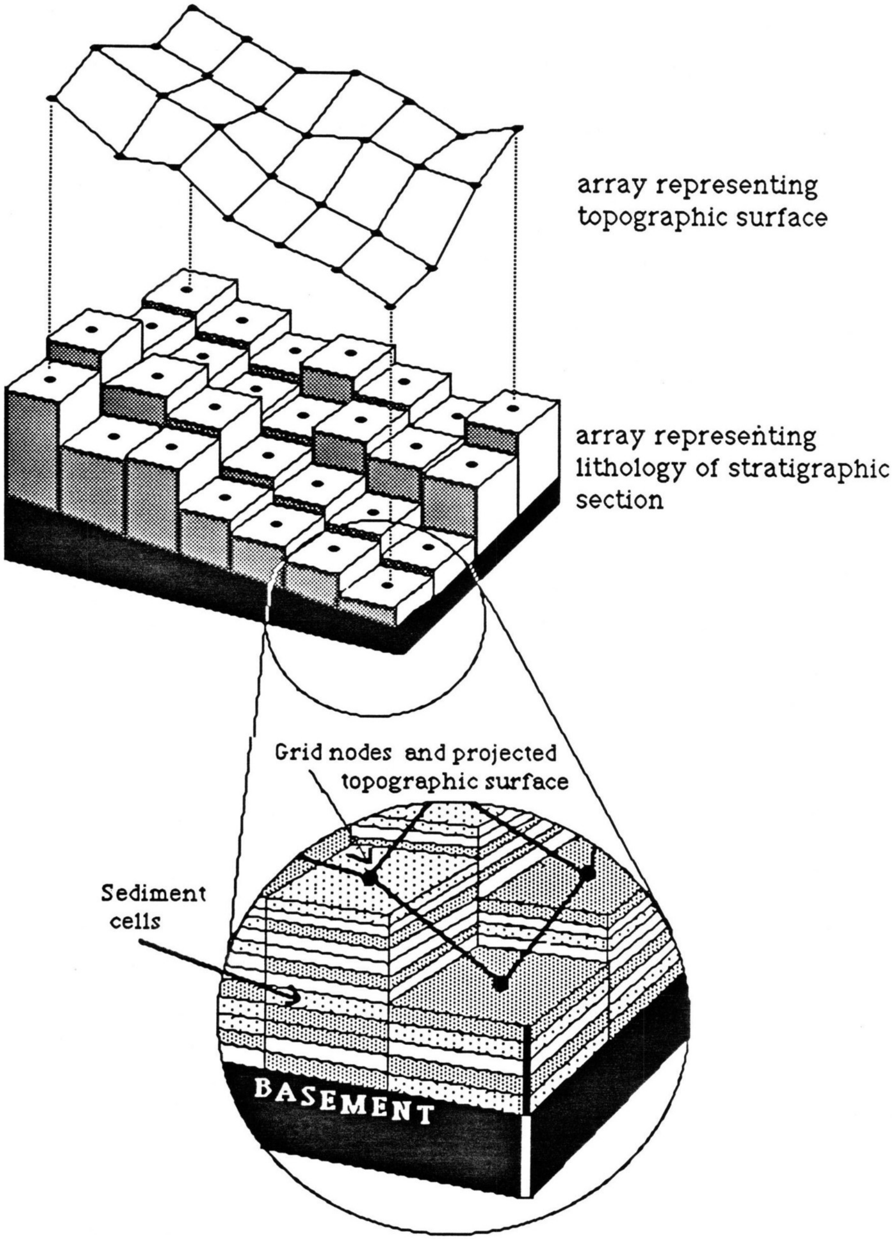

Figure 54: Schematic block diagram showing how SEDSIM records distribution of types of sediment in three dimensions.

Variables in Equations (153) through (159) are defined as in the single-sediment model unless otherwise stated.

Sediment Transport

To approximate the sediment transport equations (Equations l47 and l52) with algebraic expressions, it is convenient to define the following terms first:

(1) D(Ks, iJ.z) is the thickness of sediment type Ks contained above level z underneath the topographic surface at grid point (i, J).

(2) DI(t.i.j) is the depth below the surface of the highest point whose threshold for erosion (f3'KS) is greater than I at grid point (l,J).

(3) Λ (i, jz) is the effective sediment concentration that would be contributed to a single fluid element if all the sediment (or basement) above level z at grid point (i,J) was eroded, as follows:

$$\Lambda_c(i,j,z)=\sum_{Ks}\left(\frac{D(K_s,i,j,z)}{h_e f_{1,Ks}}+\frac{D(0,i,j,z)}{h_e f_{1,Ks}}\right) \qquad (154)$$

The inverse of Λ_C will be noted as Λ_c^{-1}(i ,j,l). and represents the thickness that must be eroded to contribute an effective sediment concentration l to a single fluid element.

(4) C is defined to simplify notation as follows:

$$C=\left(\Lambda-\sum_{Ks} l_{k,Ks,t}/f_{1,Ks}\right)f_{2,Ks} \qquad (155)$$

where:

$$\Lambda = |Q_{i,j}|^3 c_1 c_t$$

Now it is possible to define Equations (156) through (I59). which provide the expressions used by SEDSIM to approximate the sediment transport equations. Equations (156) through (159) are applied at every time increment t to every fluid element k, and to every sediment type Ks.

If C>0, and if the fluid element is not near a grid point on the edge of the grid (i.e. if 1<i<M, 1<j<N), then erosion occurs, and the following equation applies:

$$l_{k,Ks,t-1}=l_{k,Ks,t}+D\left(K_s,i,j,min\left(\Lambda_c^{-1}(i,j,C,\Delta t,h_e),D_\tau(\tau_{i,j},i,j)\right)\right)/h_e \qquad (156)$$

If C<O and the fluid element is not near grid point on the edge of the grid point on the edge of the grid, then deposition occurs, and the following equation applies:

$$l_{k,Ks,t-1}=l_{k,Ks,t}-min\left(l_{k,Ks,t},max\left(\left(\sum_{K=1}^{Ks} l_{k,K,t}\right)-C\Delta t/h_e,0\right)\right) \qquad (157)$$

When deposition occurs, it is also necessary to specify the sediment type that fills each new cell, as follows:

$$\kappa_{i,j,n_z} = K_s \quad \text{if} \quad \begin{array}{c} \left(K_s = 1 \text{ or } z_b + n_z + z_c > h_e\left(\sum_{K=1}^{Ks-1} l_{k,K,t}\right) - C\Delta t\right) \\ \text{and} \\ z_b + n_z + z_c > h_e\left(\sum_{K=1}^{Ks} l_{k,K,t}\right) - C\Delta t \end{array} \qquad (158)$$

where:

κ_{i,j,n_z} = sediment type at cell (i, j, n_z)
n_z = sediment cell number above basement
z_b = elevation of basement top
z_c = vertical dimension of one sediment cell

If C=0, (or if the grid point nearest κ is on the edge of the grid and if the fluid element is not near a grid) then no change occurs:

$$l_{K,Ks,t+1} = l_{K,Ks,t} \qquad (159)$$

COMPUTER PROGRAM SEDCYC3

The computer program which incorporates up to four sediment types is called SEDCYC3. Its main difference with respect to predecessor SEDCYC2 described in Chapter III, is that SEDCYC3 maintains an account representing the three-dimensional composition of deposits beneath the topographic surface, thus requiring much more additional computer memory.

The use of a "basement" grid reduces memory requirements as previously described. A second reduction in memory requirements is accomplished by representing each of the four sediment types by two bits of information, rather than an integer or a character, a procedure known as "packing". Here, packing allows the composition of 16 sediment cells to be represented in the same memory space of 32 bits that would be required to represent a single cell if integers were used. Packing however. causes execution time to increase. Memory requirements can be reduced further when running SEDCYC3 by defining the "basement" in such a way that the sediment-type grid is kept as small as possible, encompassing only sediment that is "active" (i.e., that may be eroded or deposited) during a simulation run.

Program Cycles

The flow chart for SEDCYC3 is similar to that for SEDCYC2 (Figure 11), except that SEDCYC3 incorporates procedures that deal with multi-sediment processes. Also, the input data file for SEDCYC3 is longer than the one for SEDCYC2. The example input data file in Table 9 shows that SEDCYC3 incorporates much more information than needed by the single-sediment model (Table 8). The multiple-sediment file contains a grid for the basement top, as well as a grid for the topographic surface. It also contains the three-dimensional "sediment-type" grid that describes the sediment distribution in the subsurface. As the previous versions of the program, SEDCYC3 produces two output files: (1) a formatted output file that is in the same format as the input file, and can be used to continue a simulation run, and (2) a graphics file, to be processed by the display programs.

The algorithms in SEDCYC3 that handle several sediment types are almost entirely contained in subroutine NEWELM. Therefore the version of NEWELM used by SEDCYC3 is considerably longer than the version used by SEDCYC2. At each time increment, and for every fluid element, NEWELM calculates the transport capacity and the effective sediment concentration. NEWELM also identifies the sediment composition at the cells that that are beneath the water-sediment interface. Then it decides whether erosion, deposition, or no change is to occur, the program then performs one of the following actions:

(1) If erosion is to occur, Equation (156) applies. Then the elevation of the topographic grid is lowered and the sediment concentration of each sediment type that is supplied by erosion of the basement is increased accordingly in the flow (Equation 153). The uppermost sediment cells in each column where erosion occurs transfer their content to the flow. If erosion affects the basement. the basement grid is lowered accordingly.

(2) If deposition occurs, then Equations (157) and (158) apply. Each sediment type carried by the flow is deposited. from coarsest to finest, until deposition balances the excess sediment concentration that the flow had carried (Equation 157). Deposition lowers the concentration of transported sediment by increasing the topographic elevation accordingly (Equation 153), and by adding new sediment to cells. thus representing newly formed deposits (Equation 158).

(3) If neither erosion or deposition occur. then of course no changes in the sediment load or the topographic elevation take place (Equation 159).

Table 9: Sample input data file for program SEDCYC3.

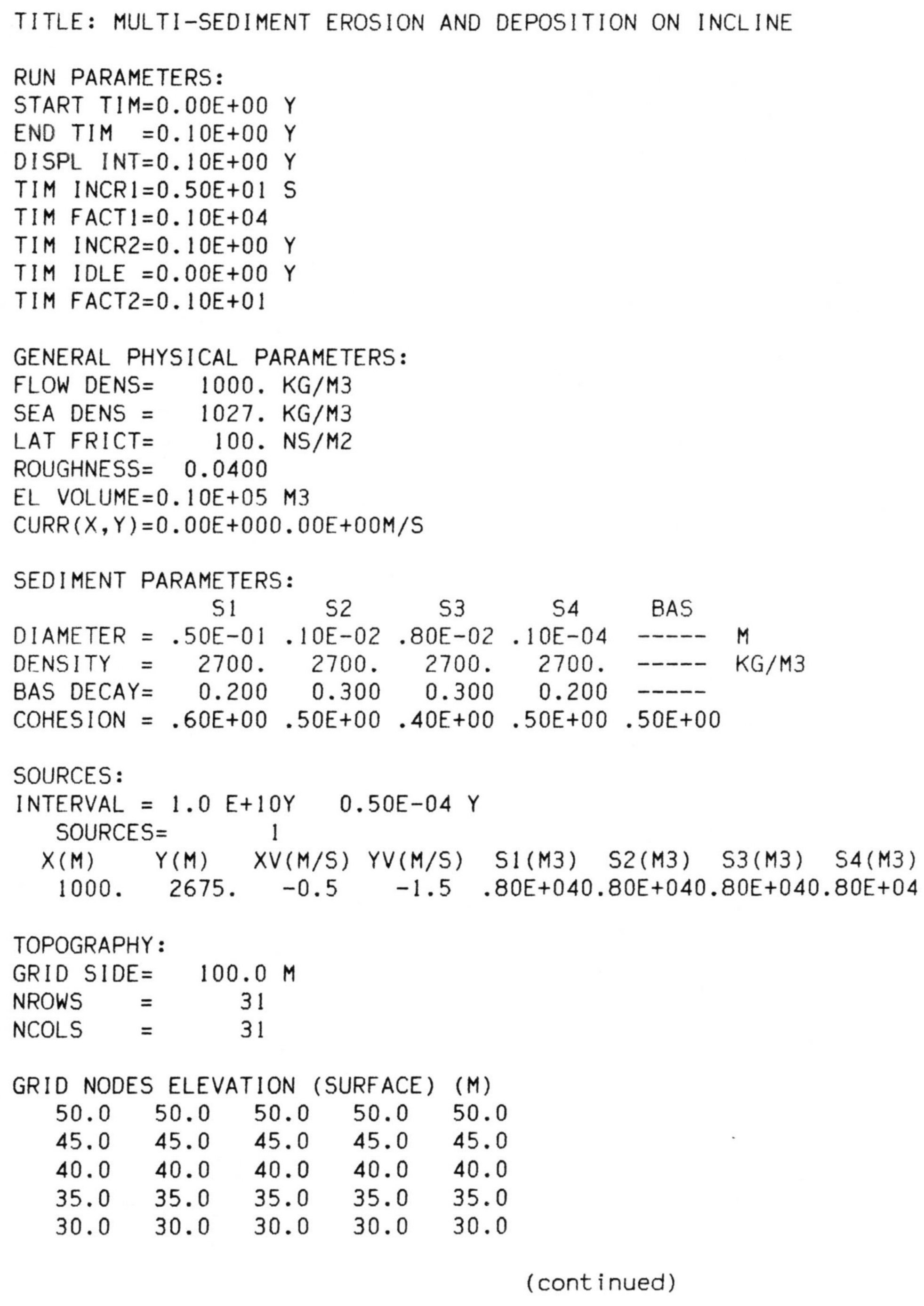

```
TITLE: MULTI-SEDIMENT EROSION AND DEPOSITION ON INCLINE

RUN PARAMETERS:
START TIM=0.00E+00 Y
END TIM  =0.10E+00 Y
DISPL INT=0.10E+00 Y
TIM INCR1=0.50E+01 S
TIM FACT1=0.10E+04
TIM INCR2=0.10E+00 Y
TIM IDLE =0.00E+00 Y
TIM FACT2=0.10E+01

GENERAL PHYSICAL PARAMETERS:
FLOW DENS=   1000. KG/M3
SEA DENS =   1027. KG/M3
LAT FRICT=    100. NS/M2
ROUGHNESS=  0.0400
EL VOLUME=0.10E+05 M3
CURR(X,Y)=0.00E+000.00E+00M/S

SEDIMENT PARAMETERS:
               S1       S2       S3       S4      BAS
DIAMETER = .50E-01 .10E-02 .80E-02 .10E-04  -----   M
DENSITY  =   2700.   2700.   2700.   2700.  -----   KG/M3
BAS DECAY=   0.200   0.300   0.300   0.200  -----
COHESION = .60E+00 .50E+00 .40E+00 .50E+00 .50E+00

SOURCES:
INTERVAL = 1.0 E+10Y   0.50E-04 Y
   SOURCES=        1
  X(M)     Y(M)   XV(M/S) YV(M/S)  S1(M3)  S2(M3)  S3(M3)  S4(M3)
   1000.   2675.    -0.5    -1.5  .80E+040.80E+040.80E+040.80E+04

TOPOGRAPHY:
GRID SIDE=   100.0 M
NROWS    =       31
NCOLS    =       31

GRID NODES ELEVATION (SURFACE) (M)
   50.0   50.0   50.0   50.0   50.0
   45.0   45.0   45.0   45.0   45.0
   40.0   40.0   40.0   40.0   40.0
   35.0   35.0   35.0   35.0   35.0
   30.0   30.0   30.0   30.0   30.0

                                        (continued)
```

TABLE 9 (continued)

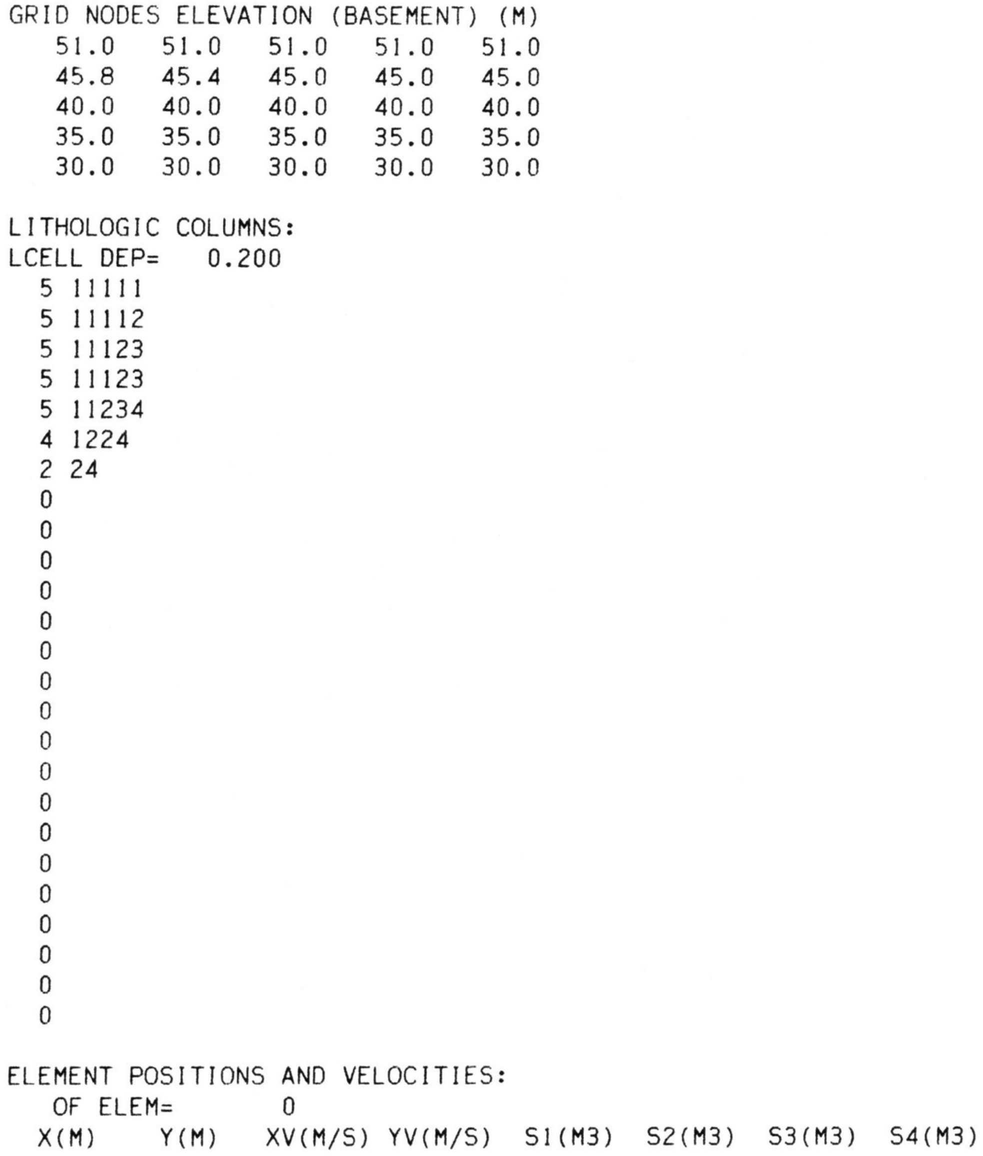

```
 GRID NODES ELEVATION (BASEMENT) (M)
    51.0    51.0    51.0    51.0    51.0
    45.8    45.4    45.0    45.0    45.0
    40.0    40.0    40.0    40.0    40.0
    35.0    35.0    35.0    35.0    35.0
    30.0    30.0    30.0    30.0    30.0

 LITHOLOGIC COLUMNS:
 LCELL DEP=   0.200
   5 11111
   5 11112
   5 11123
   5 11123
   5 11234
   4 1224
   2 24
   0
   0
   0
   0
   0
   0
   0
   0
   0
   0
   0
   0
   0
   0
   0
   0
   0
   0

 ELEMENT POSITIONS AND VELOCITIES:
    OF ELEM=       0
   X(M)    Y(M)   XV(M/S) YV(M/S)  S1(M3)  S2(M3)  S3(M3)  S4(M3)
```

Graphic Output

The graphics program for the multi-sediment model is called SEDSHO3. SEDSHO3 operates similarly to the single-sediment model's SEDSHO2 in that successions of maps or fishnet diagrams can be produced. However, when SEDSHO3 provides a section, two drawings are produced. The upper drawing indicates the relative age of the deposits, while the lower drawing indicates the sediment types (i.e. the sedimentary facies).

Because cells that represent sediment types may be small, and each cell contains only one type of sediment, representation of sediment types in graphic sections involves defining a mixture of sediment, which requires an average of their proportions within a group of adjacent cells (Fig. 55). The group of cells used to define sediment composition extends vertically between two consecutive time lines, while its horizontal extension is a fixed distance determined by the user. A time line represents the water-sediment interface at a specific moment in time; SEDSHO3 draws time lines at intervals that are also determined by the user. Thus, layers within the sediment-type section have the same shape as those in the relative age section (see Chapter III). But the colors of each layer in the sediment-type section vary laterally in response to changes in composition within a bed of uniform age. Each group of adjacent sediment cells is represented in the section as a panel. whose color is a blending or average of the types of sediment in cells spanned by the panel. SEDSHO3 uses proportions of the three coarsest components, and then matches them to intensities of the three additive primary colors (red, green, and blue). The resulting color unambiguously represents a four-component mixture (Fig. 56). the fourth component being automatically represented as black (the absence of color).

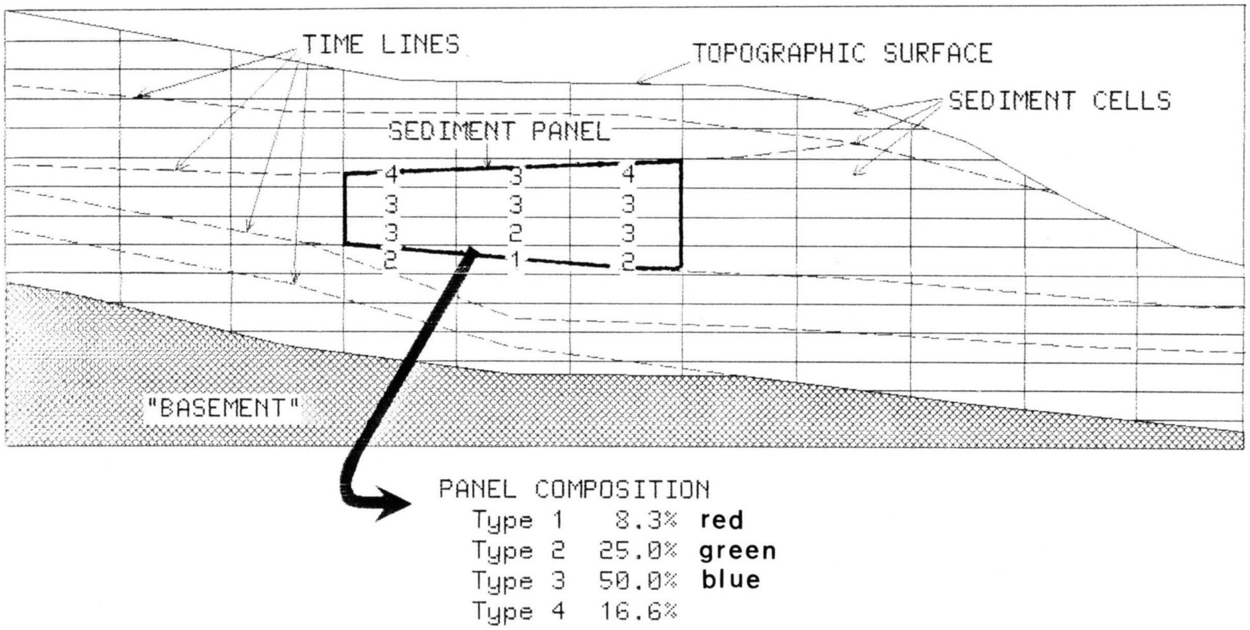

Figure 55: Section showing how SEDSHO3 computes average sediment composition of group of adjacent and represents mixture with single color.

The mapping routines incorporated in SEDSHO3 provide the possibility of drawing facies maps, which represent the sediment composition of a layer of constant thickness underneath the surface at any time. Facies maps are constructed by using a "blending" procedure similar to the one used for sediment-type sections. Figures 107 and 108 in Chapter V are examples of facies maps.

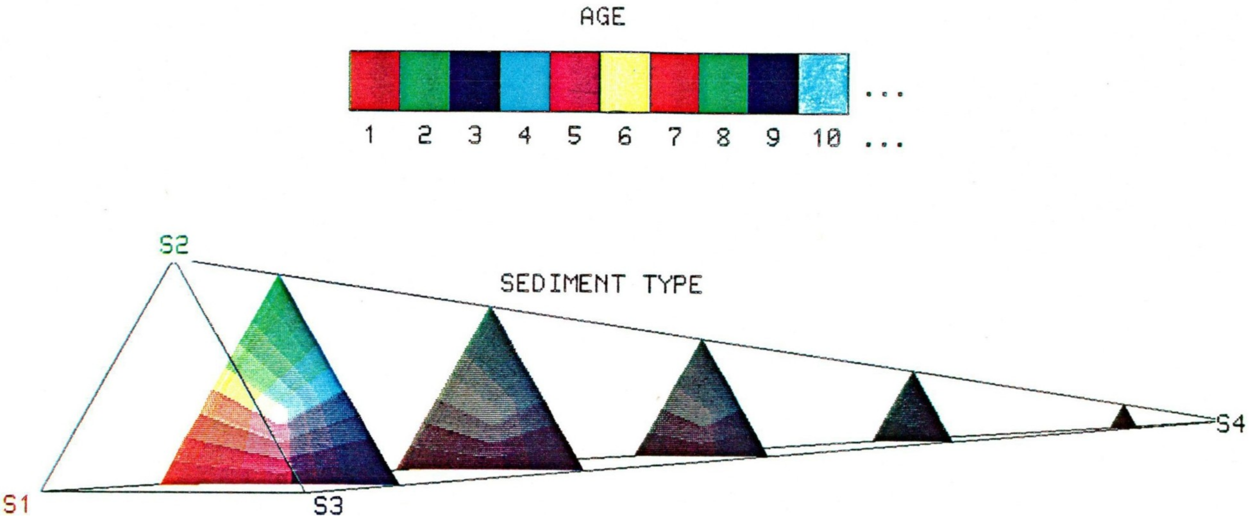

Figure 56: (a) Diagram showing sequence of ten colors that define relative ages of sedimentary deposits shown in sections. Successive ages are represented by repetition of sequence of colors. (b) Tetrahedral diagram that represents composition of sediments as shown in sections and in sedimentary facies maps. Colors at vertices (red, green, blue, and black) represent pure sediment types, while additive color mixtures represent corresponding mixtures of sediment types.

VERIFICATION OF SEDCYC3

The multi-sediment model can simulate clastic sedimentary environments in which four types types of sediment (and their mixtures) are sufficient.

Four examples are described next.

Experiment Involving Deposition of Alluvial Fans and Lake Sediments

Lacustrine and alluvial-fan deposition can be simulated by SEDSIM in a single experiment. The example in Figures 57 through 59 illustrates SEDSlM’s simulation of several sedimentary environments. The initial conditions for the experiment assume an asymmetric V-shaped valley (Fig.57) with sources of fluid and sediment on both sides of the valley, as might be present in a rift valley. Figure 58 shows the state of the simulated system after 1,000 years simulated time. Alluvial fans formed at the base of the slopes have closed the outflow through the main valley, thereby forming small lakes in which fine sediment has accumulated. The section through one of the alluvial fans (Fig. 59) shows that the lower part of each fan is actually a small lacustrine delta.

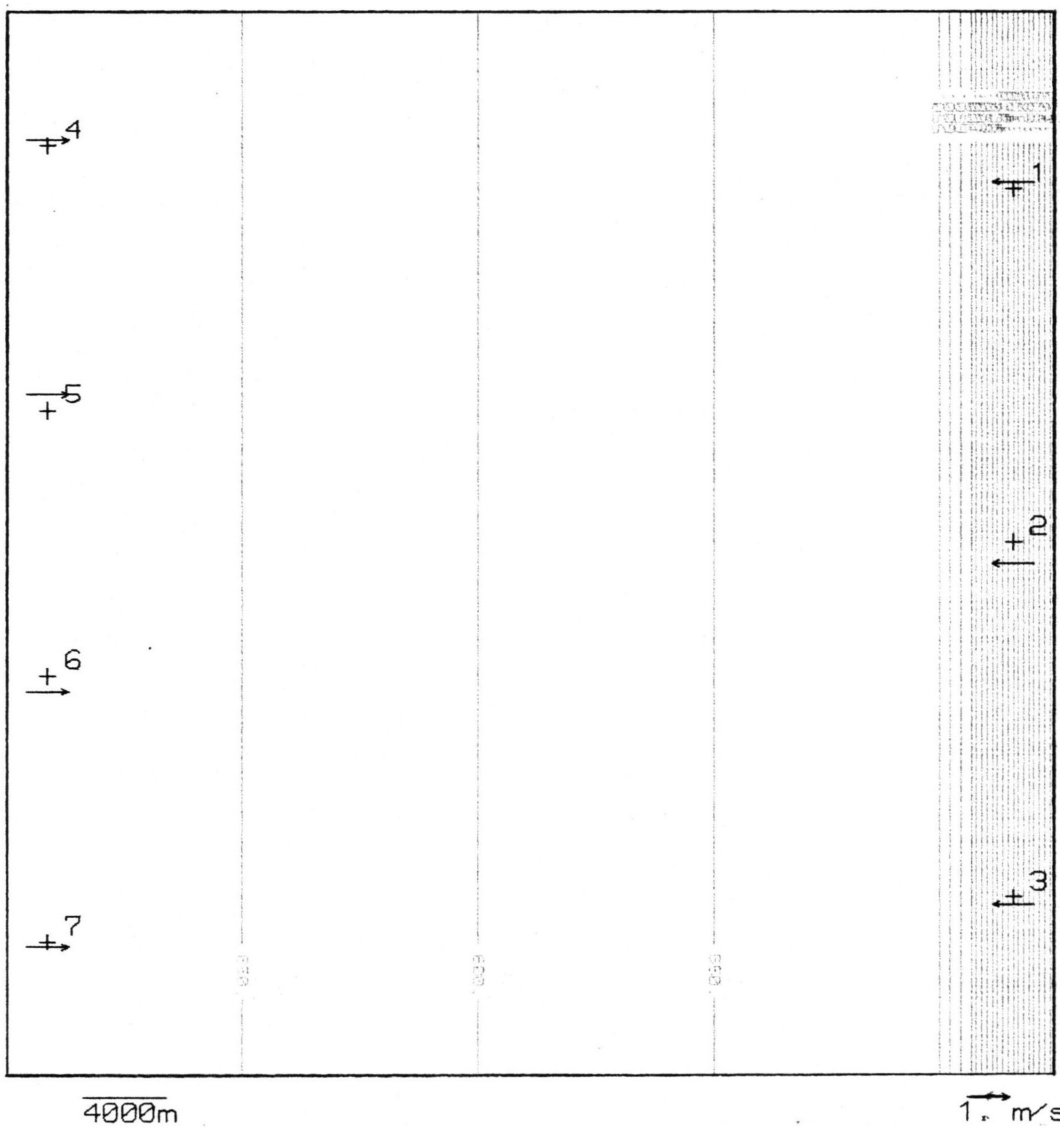

Figure 57: Contour map showing initial topography of area in which development of deposits in asymmetric valley has been simulated. Location of sources of water and sediment are indicated by numbers 1 through 7

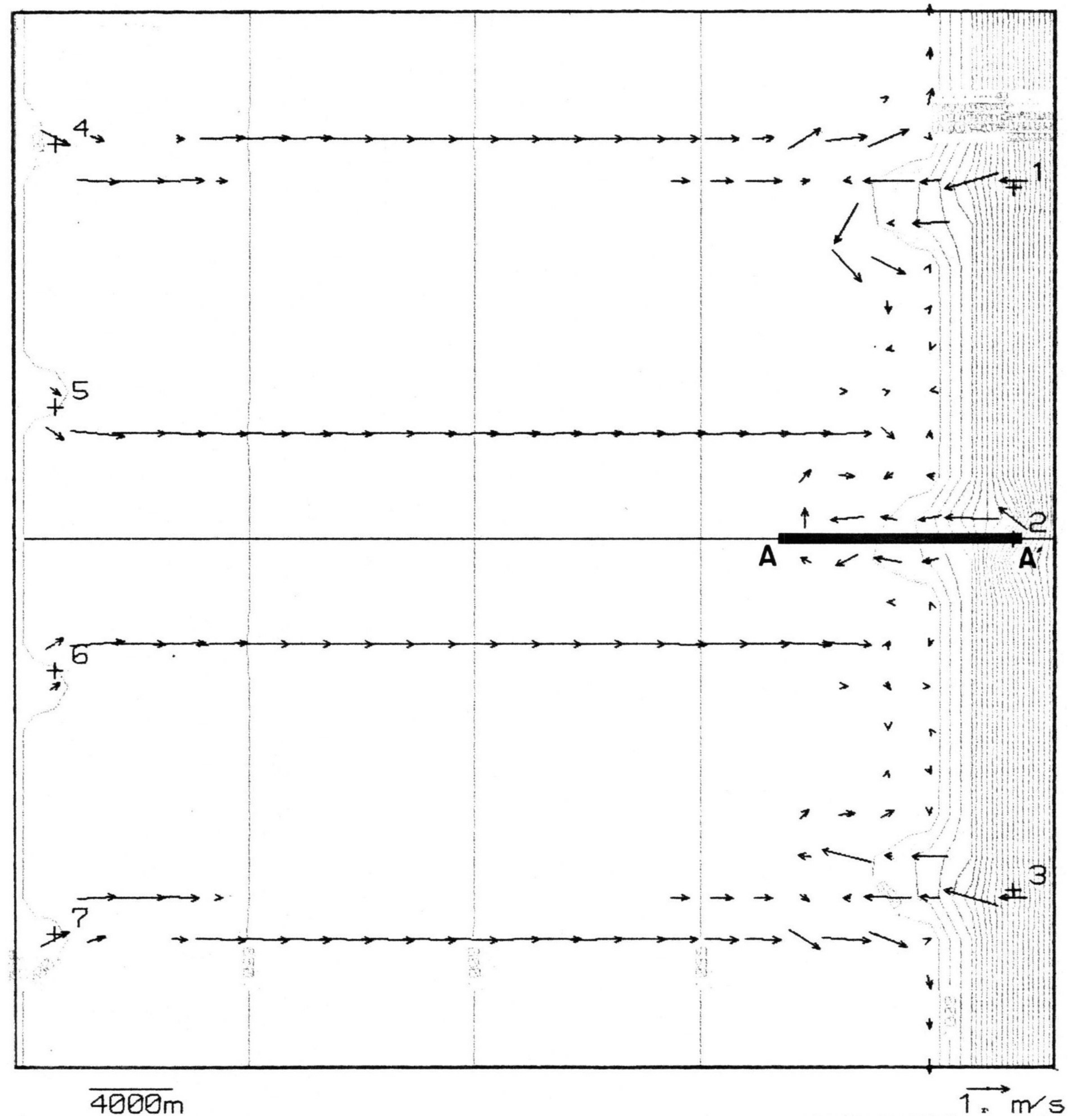

Figure 58: Topographic map showing simulated valley after 1,000 years. Alluvial fans have formed deposited near valley floor, and lakes have formed in basins between fans.Section A-A' is displayed in Figure 59.

Three different processes are represented in simplified form in this experiment: fluvial erosion, alluvial—fan deposition, and deltaic deposition. The experiment illustrates SEDSIM's capability of representing the interaction between flow and sedimentation. The formation of lakes and the development of small deltas within the lakes can be represented only by a model that is capable of simulating both flow and sedimentation over specific topographic surfaces, under various alternative hydraulic conditions. SEDSIM's ability to perform realistically when initial conditions have significantly changed, makes it useful for interpreting the processes that created actual deposits.

Experiments Involving Braided Streams

Braided streams involve a small proportion of fluid relative to the proportion of sediment transported. This enhances SEDSIM’s ability to simulate braided streams, because relatively few fluid elements are involved in the flow calculations, and computer processing effort is reduced. Scott (I986) simulated braided streams with SEDSIM, with the purpose of reproducing sedimentary features in the Ivishak formation, which forms one of the reservoirs in the Prudhoe Bay Oil field in Alaska. A description of some of his results follows.

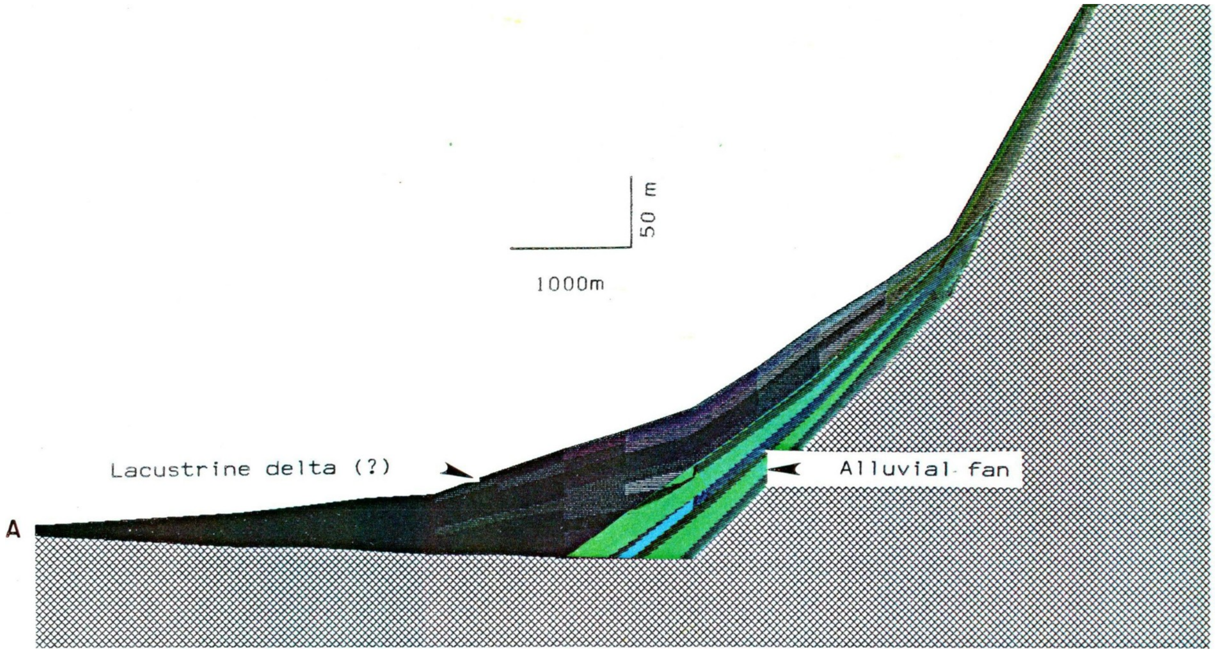

Figure 59: Section A-A’ through fan shown in Figure 58 revealing changes in particle size of deposits. Clay has been deposited in distal part of deposit, corresponding to possible lacustrine delta.

The topography, assumed at the beginning of Scott's experiments (Figures 60 and 61), consists of a surface 3 km wide by 5 km long, that slopes with segments representing three gradients that decrease downstream. The uppermost segment is 1.5 km long and has a 4.6 percent slope, the middle segment is 2 km long and slopes at 3.0 percent, and the lower segment is 1.5 km long and slopes at 1.4 percent. Sources of water and sediment were placed at the locations shown by crosses in Figure 60. During simulation runs, sources are activated in "pulses", at frequencies ranging from several times a day to several times a year. During each pulse. a combined volume of 80,000 to 120,000 cubic meters of water, containing 100 to 1,000 cubic meters of sediment is released. The four sediment types (gravel, sand, silt, and clay) are represented in varying proportions. Gravel constitutes the smallest proportion of sediment supplied, and clay the highest. Simulated time ranges from 10 to 500 years.

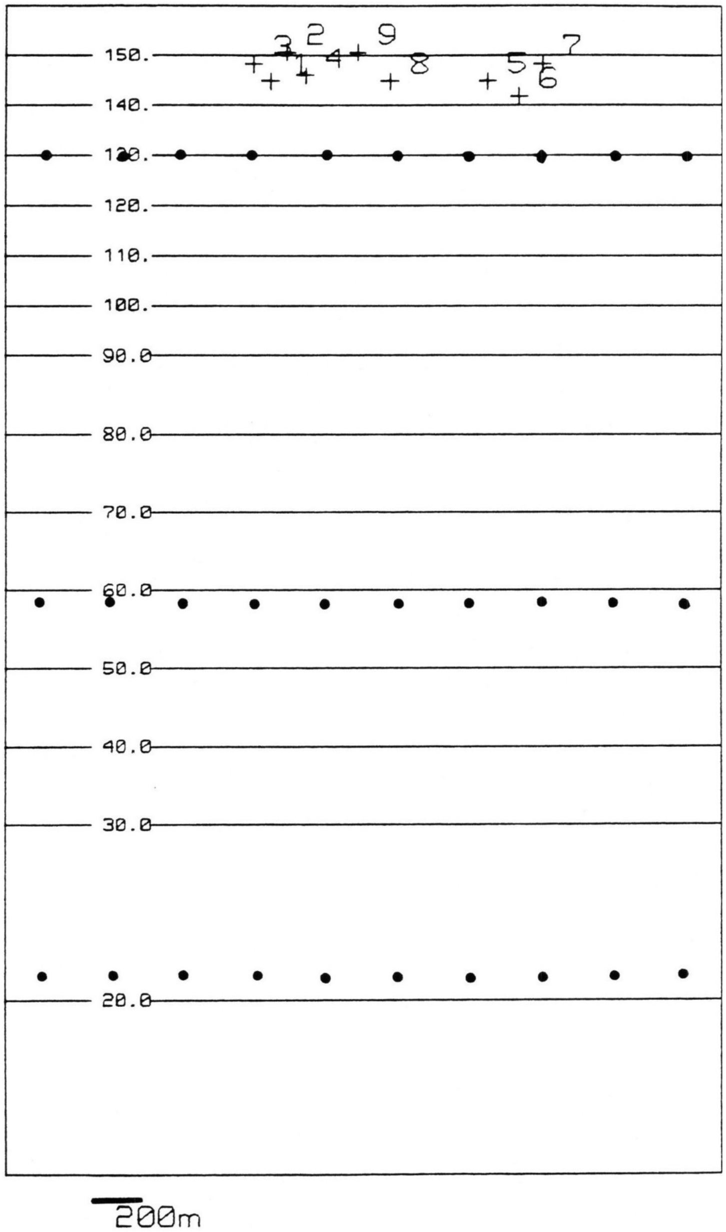

Figure 60: Initial topographic contour map of experiment involving braided streams. Slope progressively steepens toward north. Contours are in meters. Sources of water and sediment are indicated by crosses, while bold dots indicate locations where flow, slope, and sediment content were measured in sensitivity analysis.

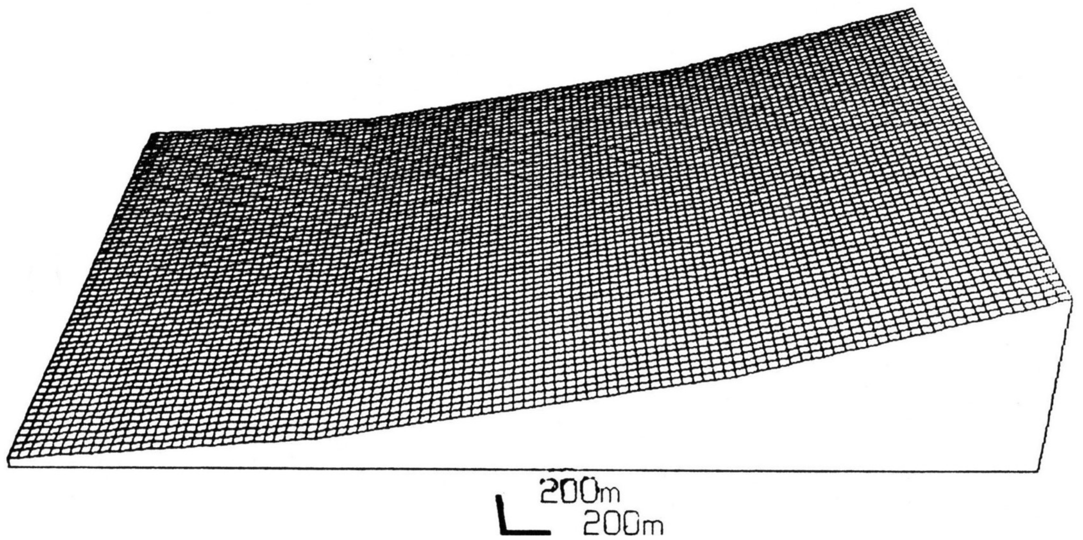

Figure 61: Fishnet diagram corresponding to Figure 60

The development of river bars is clearly seen in Scott's first simulation experiment, displayed in Figure 62. The experiment involved 20 years simulated time. One display is shown every five years. After the first five years, elongated bars developed as a consequence of channel braiding and shifting. The bars continued to change in shape and location with time, but their general characteristics, such as average length, width, and thickness, did not change significantly. The system can be regarded as being in equilibrium from a geomorphic or fluvial standpoint.

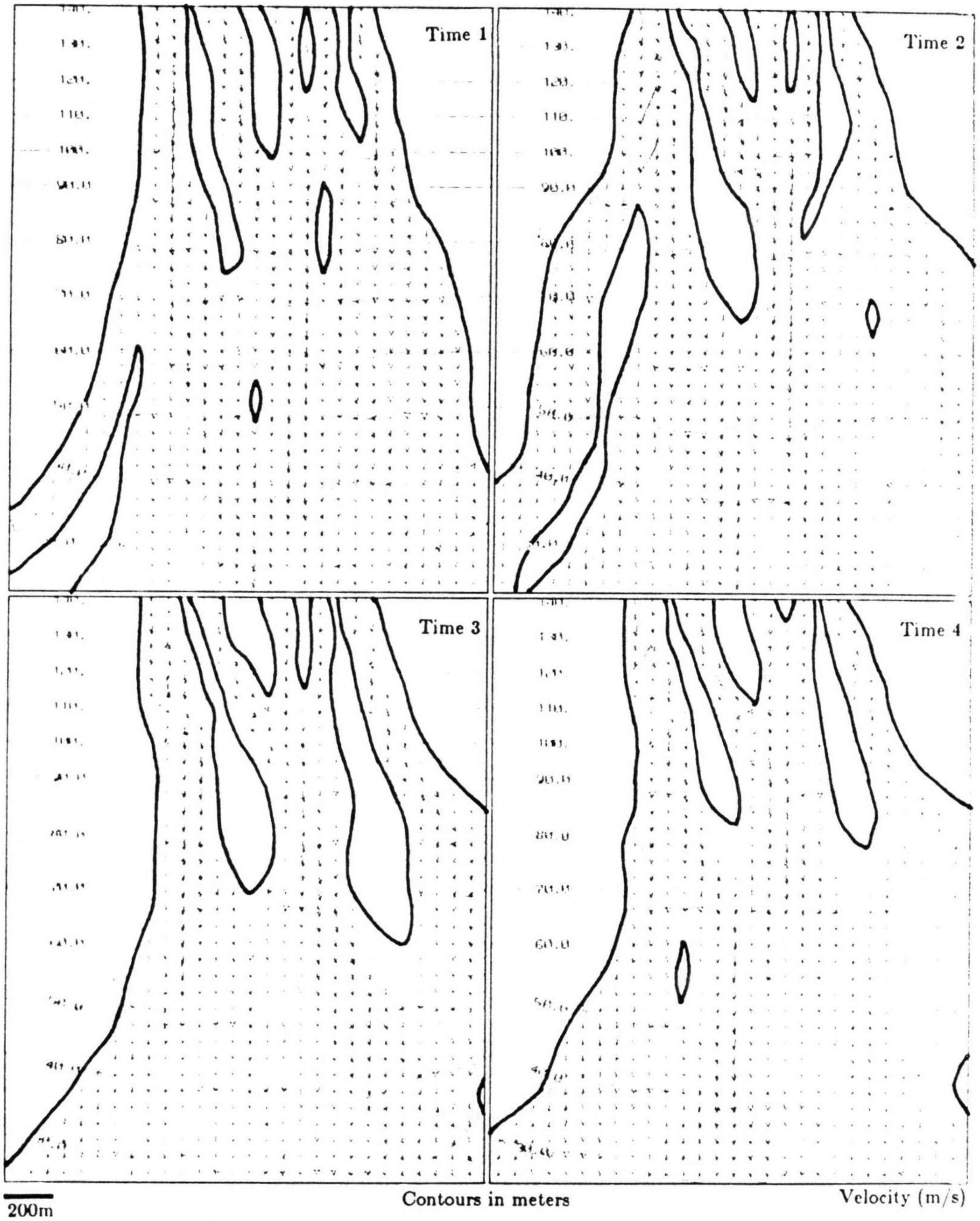

Figure 62: Contour maps and flow patterns in braided steams involving simulation of bars. maps represent one-year intervals.

A second simulation experiment, involving a relatively high proportion of gravel and sand, is shown in Figures 63a and 64. four channels, separated by gravel bars, developed early in the simulation experiment (Time 1, in Figure 64). The areas occupied by the channels in the cross section have been labeled "l" through "4" The channels in areas 1 and 3 rapidly filled with sand, while gravel fill predominated in the channel that occupied area 2. In area 4, however, the corresponding channel shows little filling.

A third experiment involved a higher proportion of finer materials compared with the first and second experiments. A contour map of the topography produced by the third experiment is displayed in Figure 63b, while figures 65a and 65b show sediment-type cross sections through the deposits. Figure 65a shows the development of an overbank deposit as the channel shifted to the left of the cross section. The formation of an abandoned-channel deposit is illustrated in Figure 65b. The bed of the channel on the right side of the cross section consisted of sand until Time 3. but silt was deposited during the reduced flow in Time 4. Higher flow rates through the channel resumed at Time 5, causing deposition of sand, thus preserving the abandoned- channel deposit.

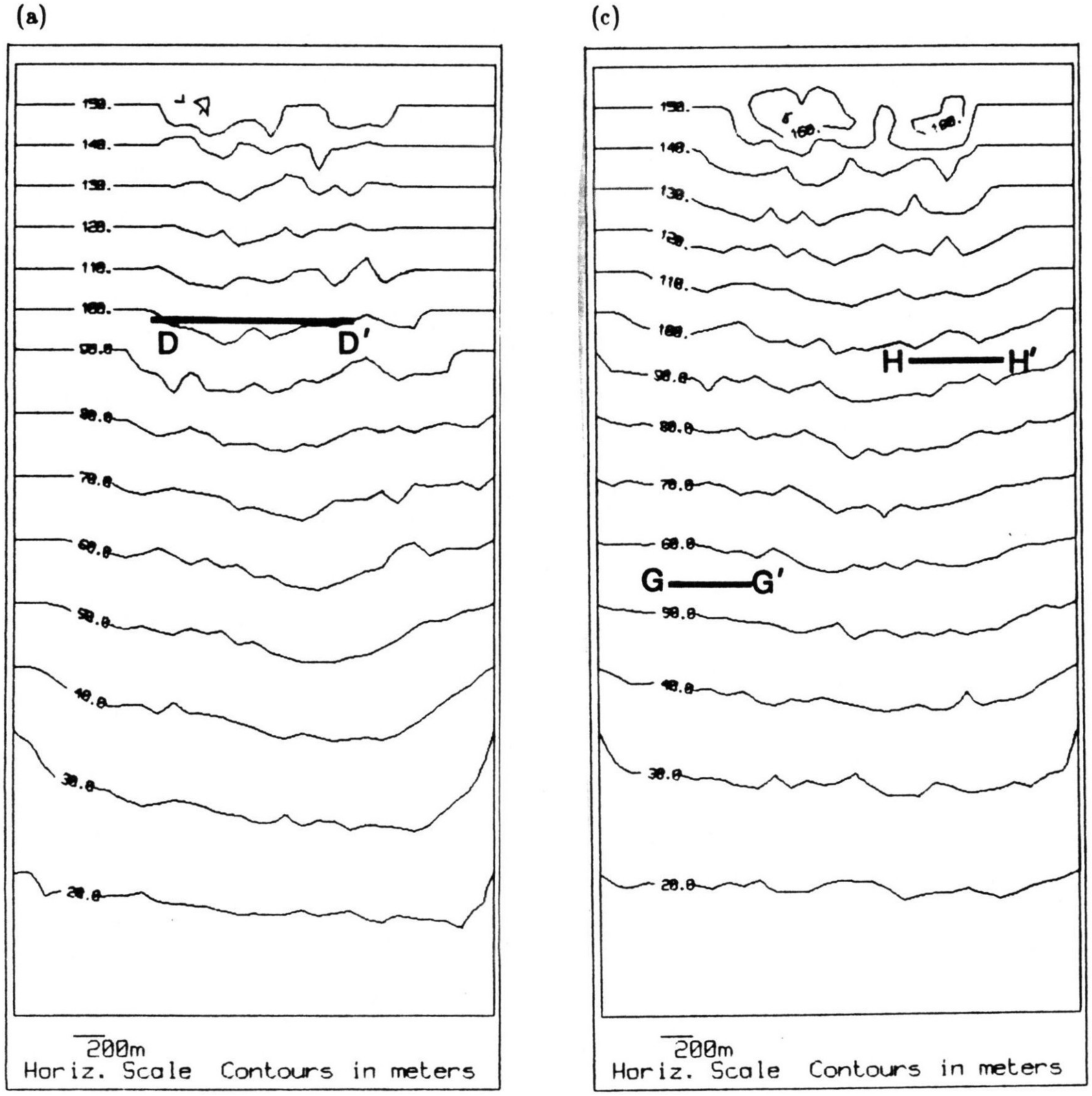

Figure 63: Topographic contour maps of stream deposits produced in two braided-stream simulation experiments: (a) Experiment to show formation of bars and channels. Section D-D' is shown in Figure 64. (b) Experiment to show overbank deposits and abandoned—channel deposits. Sections G-G' and H-H' shown in Figure 64.

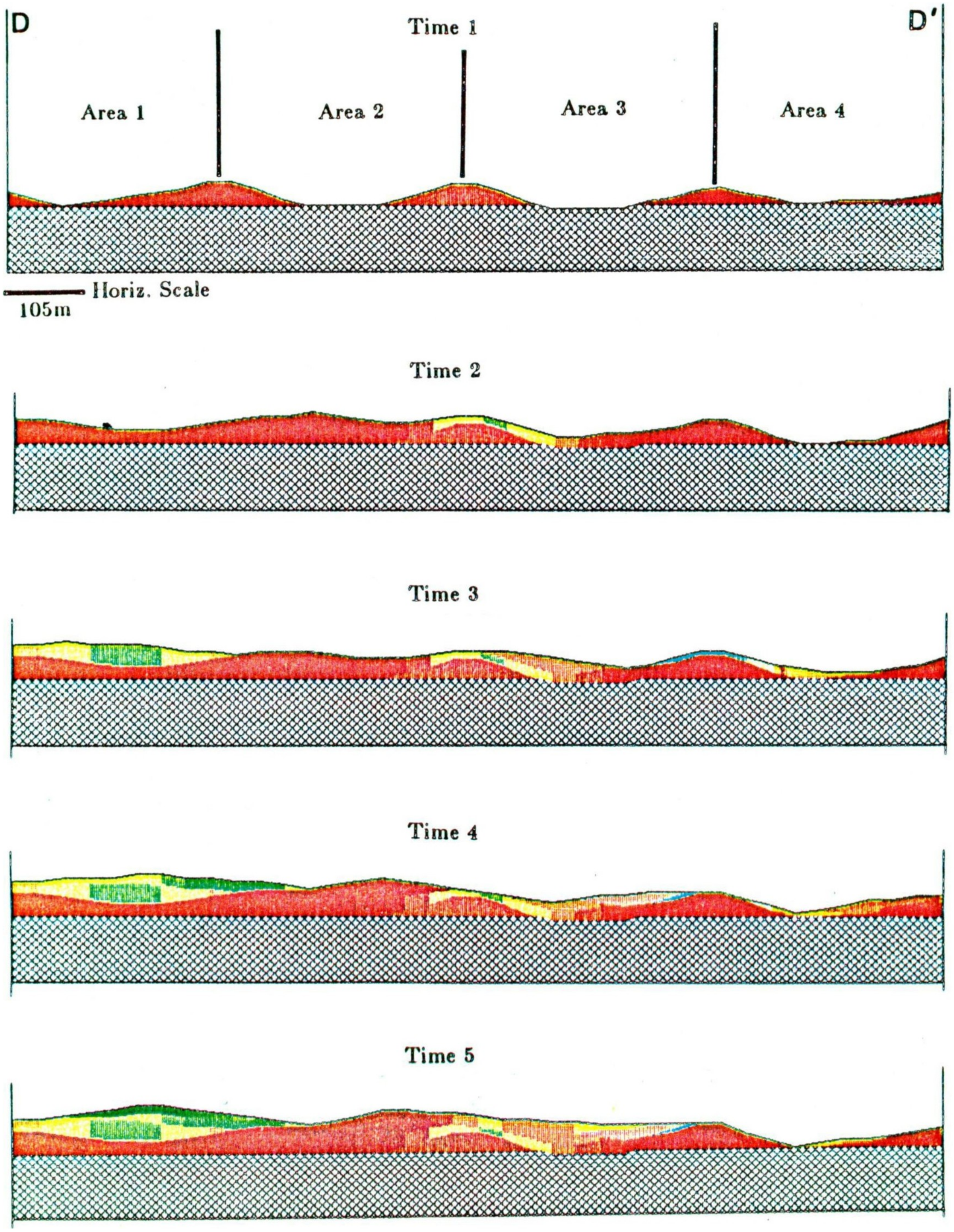

Figure 64: Sections showing types of deposits produced by braided streams. Sediments are gravel, sand, silt, and clay. Figure 56 provides key to composition of deposits. Vertical exaggeration = 10. Location of section shown in Figure 63a.

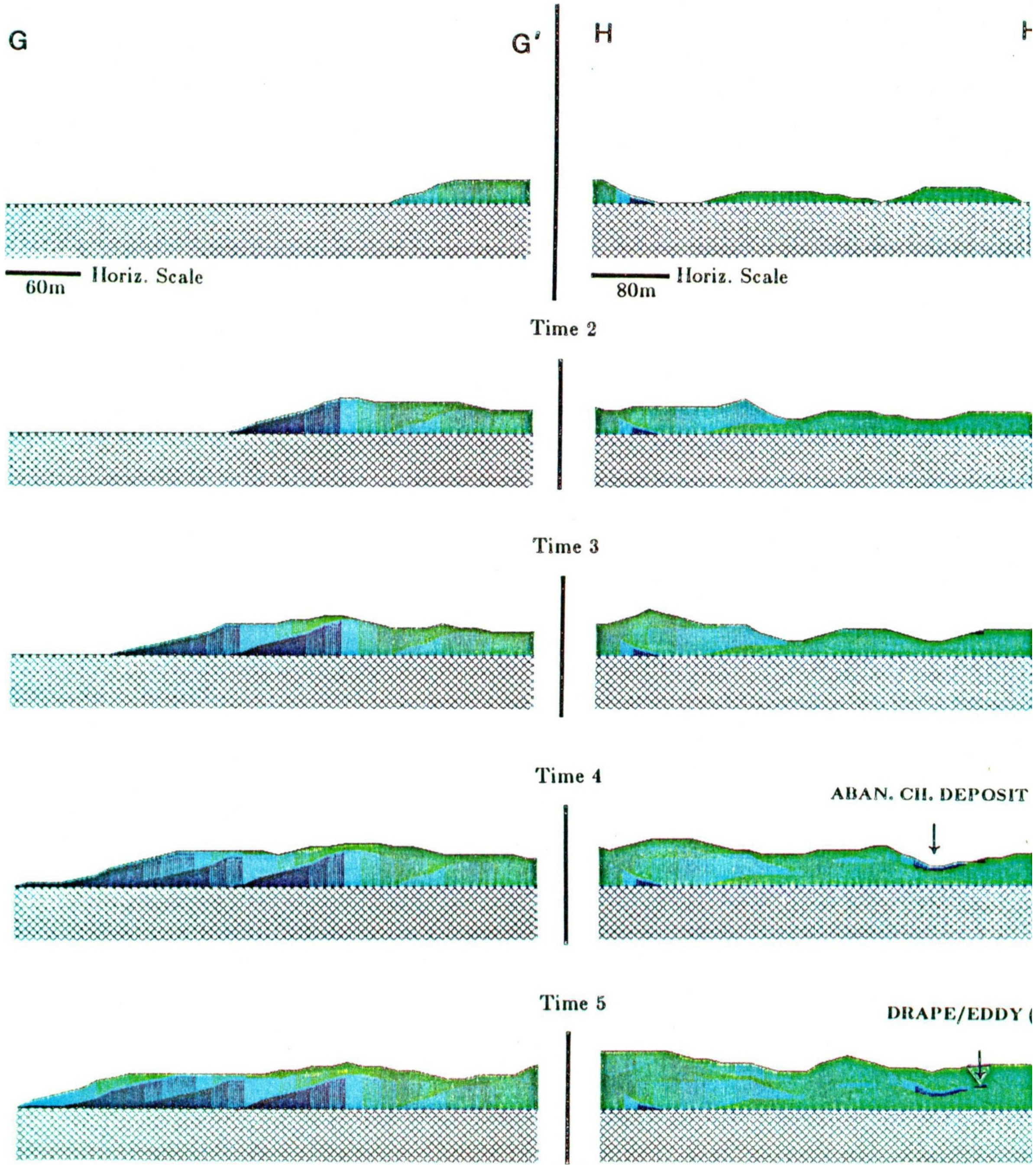

Figure 65:Sections showing overbank deposits and abandoned-channel deposits produced by braided streams. Vertical exaggeration = 30: (a) Example of developing overbank deposit. Location of section shown in Figure 63a (b) . Example of abandoned-channel deposit and possible drape deposit. Location of section is shown in Figure 63b.

Sensitivity tests:

Scott (1986) also performed quantitative sensitivity tests in braided-stream environments by measuring the response of the braided-stream system to changes in the input parameters at various points in the simulated area. Measurement points are shown by bold dots in Figure 60. The initial test involved a "base case" experiment with parameters listed in Table 10a. SEDCYC3 was allowed to run until the flow and sediment-transport parameters were reasonably stable. Then the experimental run was repeated several times. Each time a different input parameter was increased by 50 percent with respect to its value in the base case. while other input parameters remained unchanged. Table 10b shows the stream's response to the changes in input, as manifested by changes in the other parameters (i.e. the response parameters), such as flow velocity. depth, sediment discharge, and slope.

Table 10: a) List of four different variables (velocity, depth, sediment discharge, and slope) that were evaluated in "base case" experiment. Numbers underneath variable names indicate their value in "base case" experiment. for example, flow velocity in "base case" experiment is 0.140 m/s, depth is 0.107 m, and so on. b) List of input variables that were increased by 50 percent with respect to base case, including flow rate, initial slope. basement erosion factor, sediment transportability, and sediment input, and resulting percent change in base case parameters velocity, depth, sediment discharge, and slope. Table ls to be read by finding row corresponding to variable that was increased by 50 percent on leftmost column of table. Then column corresponding to variable whose change needs to be evaluated is found across top of table. Number at intersection of row and column is percent change. for example, when initial slope was increases by 50 percent, depth increases by 9 percent with respect to base case. (Adapted from Scott. 1987). a) fluvial parameter for base case.

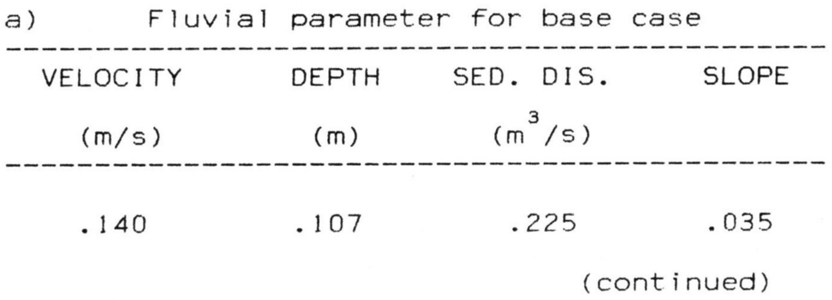

a) Fluvial parameter for base case

VELOCITY (m/s)	DEPTH (m)	SED. DIS. (m^3/s)	SLOPE
.140	.107	.225	.035

(continued)

TABLE 10 (continued)

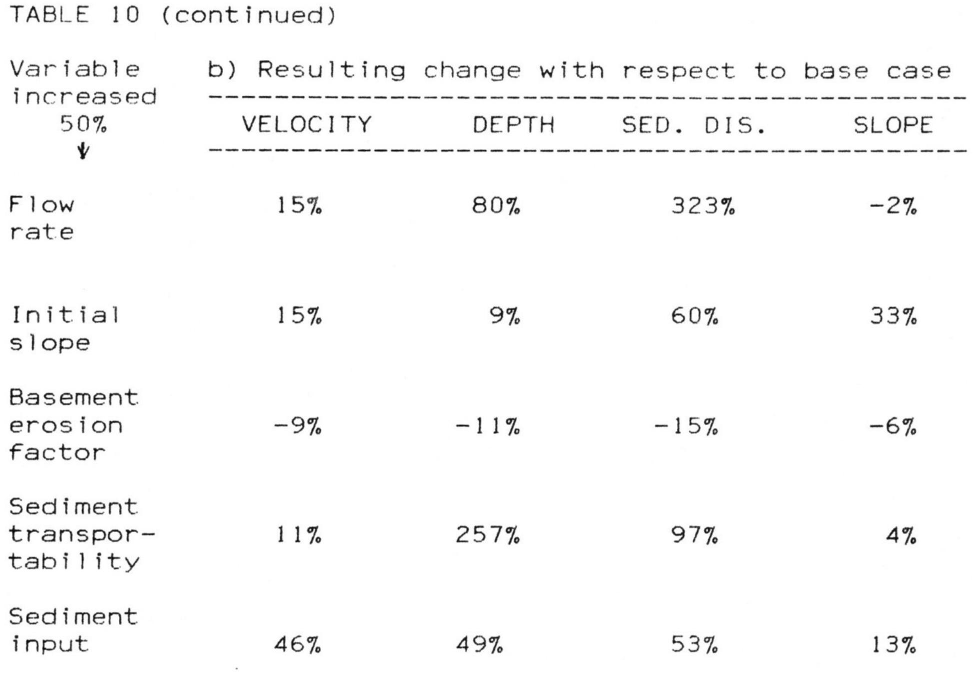

Variable increased 50% ↓	b) Resulting change with respect to base case			
	VELOCITY	DEPTH	SED. DIS.	SLOPE
Flow rate	15%	80%	323%	-2%
Initial slope	15%	9%	60%	33%
Basement erosion factor	-9%	-11%	-15%	-6%
Sediment transportability	11%	257%	97%	4%
Sediment input	46%	49%	53%	13%

The changes in response parameters are difficult to predict analytically because of the complicated interaction between flow and sedimentation. Increasing the flow rate, for example, immediately increases both velocity and depth of flow in a fixed channel. However, if the channels are permitted to change in response to erosion and deposition, the increase in flow also permits more sediment to be carried. A consequence is that erosion is greater near the sources, and channels become narrower, further increasing velocity and depth. Some of the responses of a braided-stream system to changes in input conditions might be predicted from formulas. but the details of the migration of channels and changes in the channel's cross sections could not be forecast readily, so that simulation experiments are very helpful in understanding the response posed by changes in the input parameters.

Changes in the initial slope on a braided-stream environment also have consequences that are difficult to predict without a simulation model. for example, if slope is increased 50 percent, velocity increases, but depth also increases due to narrowing 0f the channels, and sediment discharge increases slightly. Increased deposition down-stream partially compensates the initial increase in slope.

The effects of resistance to erosion and sediment transportability have also been studied by Scott. An increase in the coefficient of basement erosion has much the same effect as an increase in sediment input, because basement erosion provides more sediment to the flow. Therefore velocity, depth, and sediment discharge decrease. while slope does not change significantly. However. an increase in sediment transportability has much the same effect as a decrease in sediment input, the flow's sediment content becoming depleted. The fact that sediment discharge may decrease when sediment input increases, is a consequence of increased deposition upstream and an overall decrease in velocity.

Scott's experiments document SEDSlM's use in treating a specific form of sedimentary environment as a dynamic system. Studies in fluvial geomorphology often provide a way to predict the response of a single variable to changes in input parameters, when all other variables are assumed to remain constant. SEDSIM. however. provides a way to predict a braided river's response, allowing the entire system to adjust to changes in input conditions.

Turbidity-Current Experiments

An experiment similar to the experiments involving turbidity currents illustrated in Chapters II and III, was repeated with the multi-sediment model, where sand and silt were assumed to be present. Figures 66. 67, and 68 show the result after a single flow has occurred, including a longitudinal section through the deposits formed. The flow deposited coarse material in the upper part of the fan and finer material in the lower part, at a greater distance from the source.

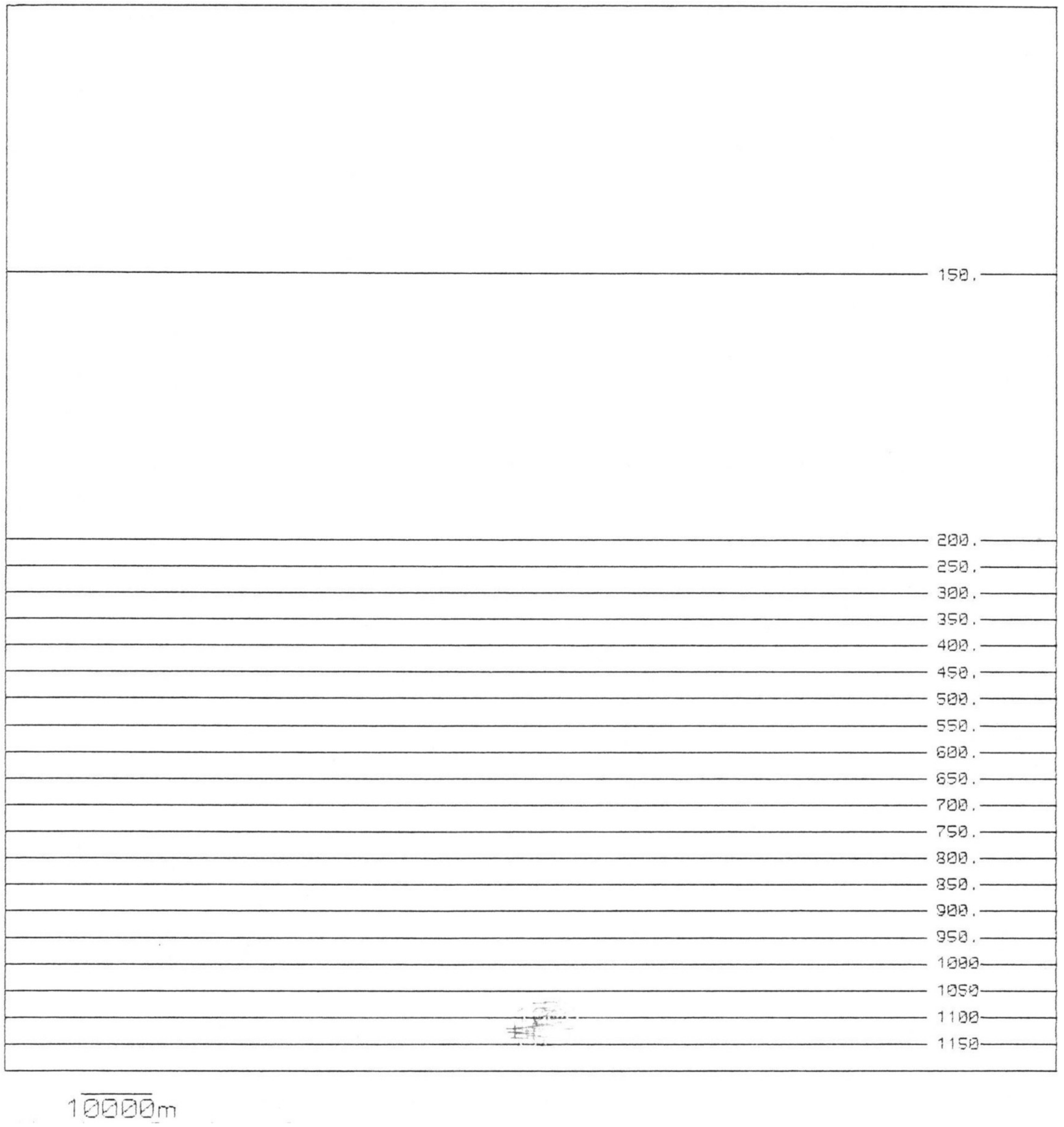

Figure 66: Contour map of initial topographic configuration used in turbidity-current experiments involving four sediment types (fine gravel, sand, silt, and clay). Contours are in meters.

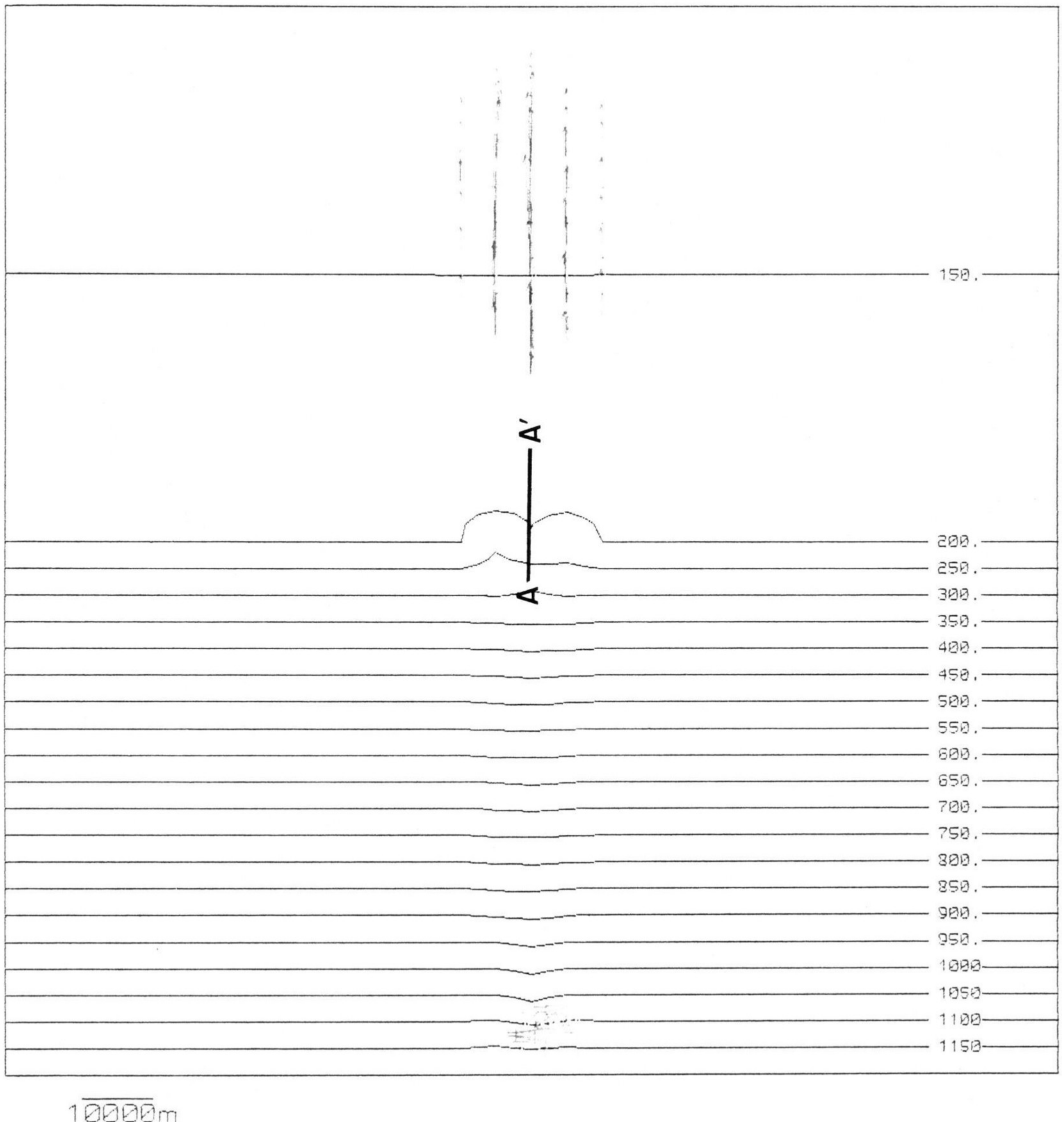

Figure 67: Contour map of topographic configuration after flow of single turbidity current.

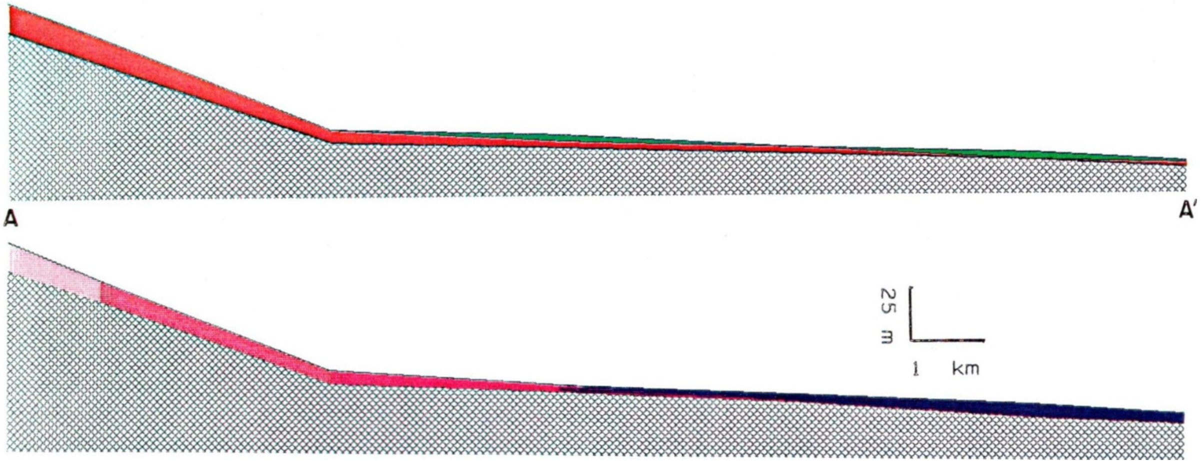

Figure 68: Section of deposits produced by single turbidity current: (a) Relative age of deposits. revealing that distal deposits formed relatively late. (b) Sediment composition indicating that deposits become progressively finer toward distal end.

The turbidity experiment was then repeated with 20 turbidity currents, with results shown in Figures 69, 70, and 71. Figure 69 reveals a deep canyon and large fan, similar to features produced by the turbidity current experiment performed with the single-sediment model. Figures 70 and 71 show the alternation of coarse and fine sediments that are typical of sequences of turbidity current deposits.

Delta Experiments

Deltaic deposits are of strong interest because they provide favorable conditions for oil generation and entrapment. Simulation of deltaic deposits could have useful practical applications in petroleum exploration. However, deltas are challenging sedimentary environments to simulate because flow conditions on the subaerial portions of a delta are different from those in the submerged portions.

A series of experiments was performed with the purpose of estimating SEDSIM's capability to simulate major deltas. Figure 72 shows the initial topography used in these experiments. Within the region simulated, the initial topography consists of a narrow area onshore (at the northern edge of the region), and a sloping submerged platform that extends 120 km offshore, reaching a maximum depth of 250 m.

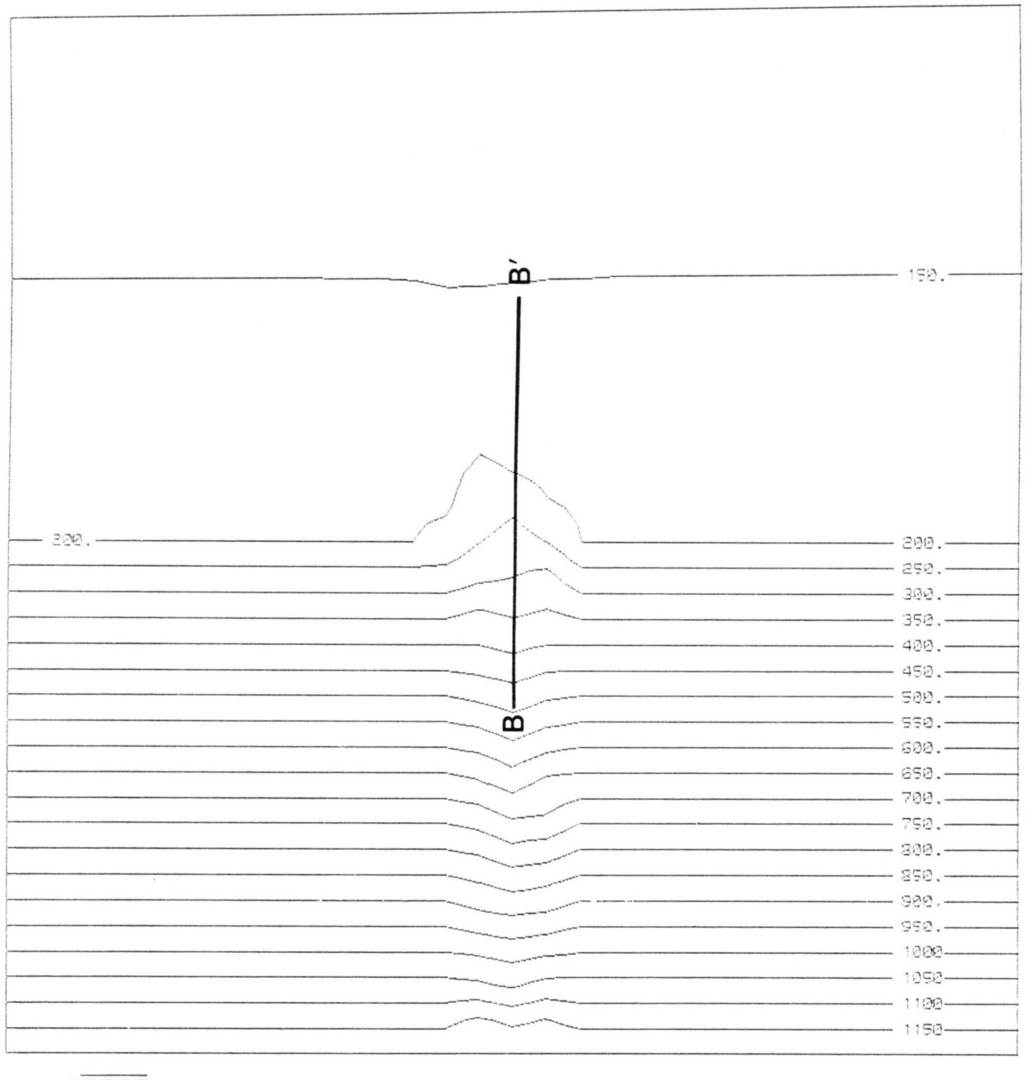

Figure 69: Contour map of topographic configuration after flow of 20 turbidity currents.

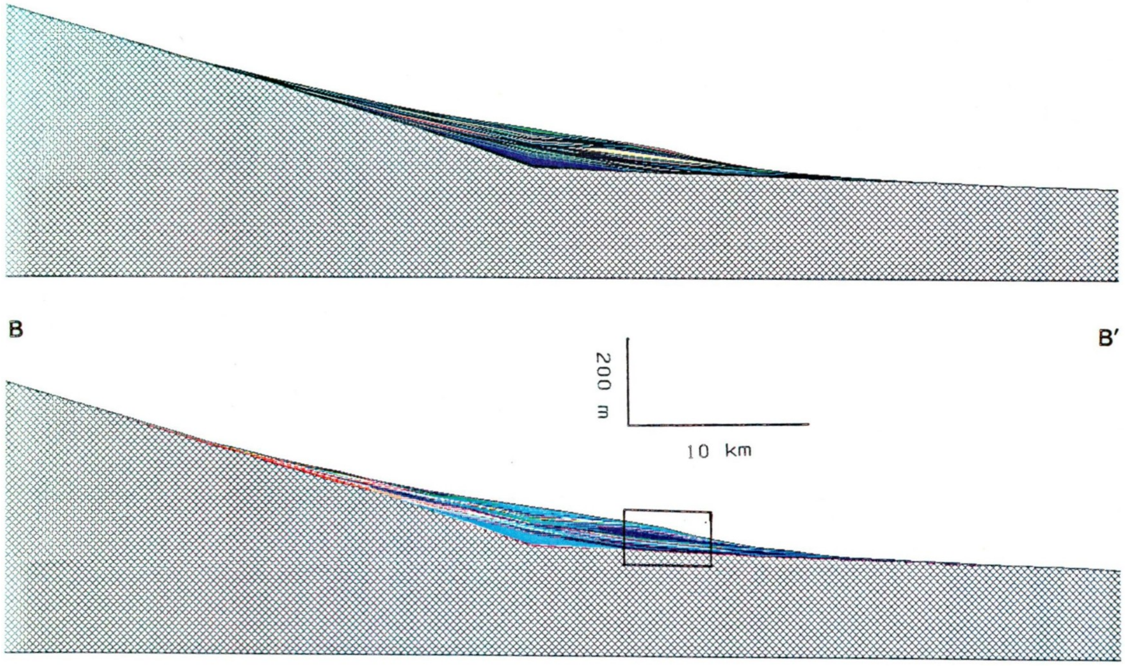

Figure 70: Sections through deposits produced by 20 turbidity currents: (a) Relative age. (b) Sediment composition (box outlines enlarged segment shown in Figure 71)

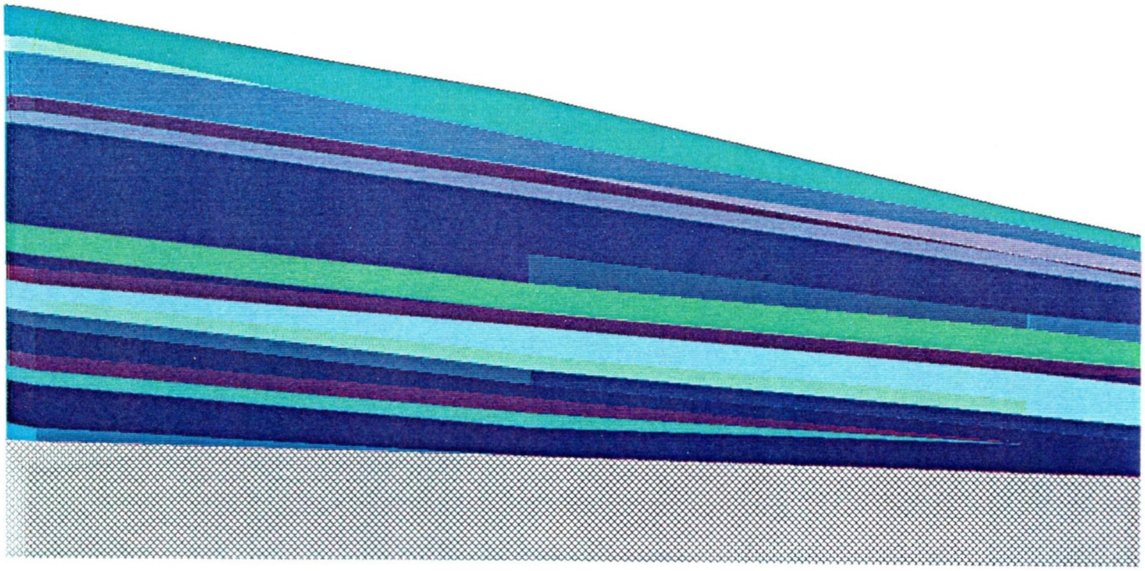

Figure 71: Enlarged section of Figure 70 showing composition of deposits formed by multiple turbidity currents, revealing alternation of coarse and fine material.

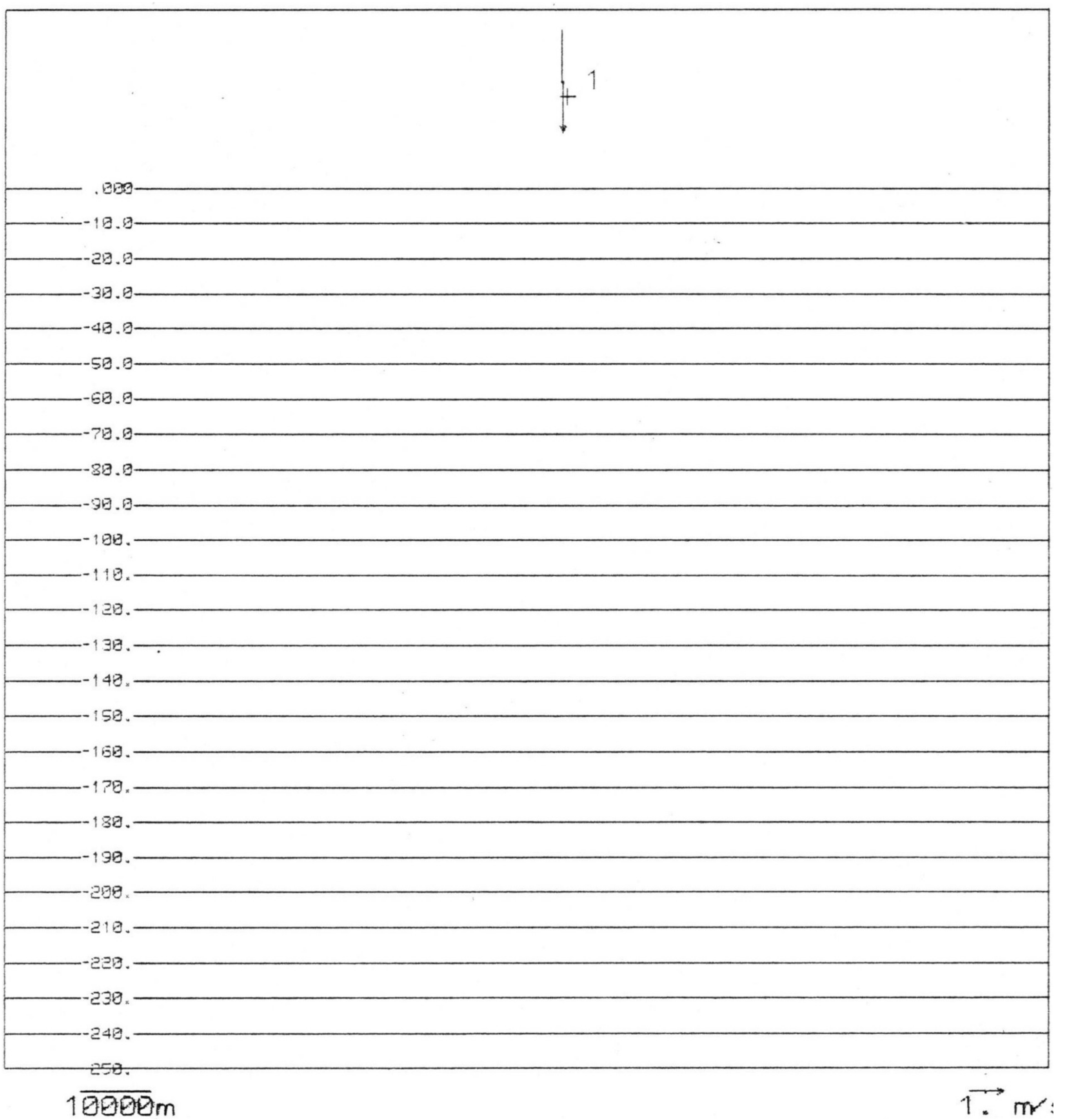

Figure 72: Contour map of initial topography in which formation of large delta is simulated. four types of sediment (medium sand, fine sand, silt, and clay) are supplied by river. Single, steady source of fluid and sediment representing river mouth is located at point "1". Contours are in meters.

All simulation runs spanned 10,000 years of simulated time. The sections that represent age employ a different color for every 100 year interval (Figure 56). The four sediment types used in the experiments are medium sand, fine sand, silt, and clay. Sections that represent sediment composition show the pure sediment types in red, green. Blue, and black, respectively, while mixtures of sediment are represented by color combinations, as shown in Figure 56.

A single source, representing a river, is located onshore. The source in these examples is steady and supplies 7500 cubic meters of water per second. In the first experiment, the sediment concentration at the source is 0.002, or approximately 30,000 kilograms per second. The sediment supplied as input consists of 15 percent medium sand, 22 percent fine sand, 28 percent silt. and 35 percent clay. The topographic configuration after 10,000 years is shown in Figures 73 and 74. Over the 10,000 years, the shoreline prograded about 25 km, with several channels forming onshore.

Sections through the deposits

Sections through simulated deltaic deposits show variations in composition from onshore to offshore. Figures 75, 76, 77. and 78 show north-south sections that are perpendicular to the shore, or parallel to the direction of progradation. The upstream parts of the channels were cut and filled several times during the depositional sequence revealed by the section. Deposition (in contrast to erosion) predominates offshore, with materials becoming progressively finer with distance from shore. The gross form of beds viewed in sections perpendicular to shore is sigmoidal, and there is large variation in composition vertically, even though the sediment/fluid source remained steady throughout the experiment. The variation in composition was caused largely by lateral migration of deltaic lobes. and the continuous shift of local areas of maximum deposition.

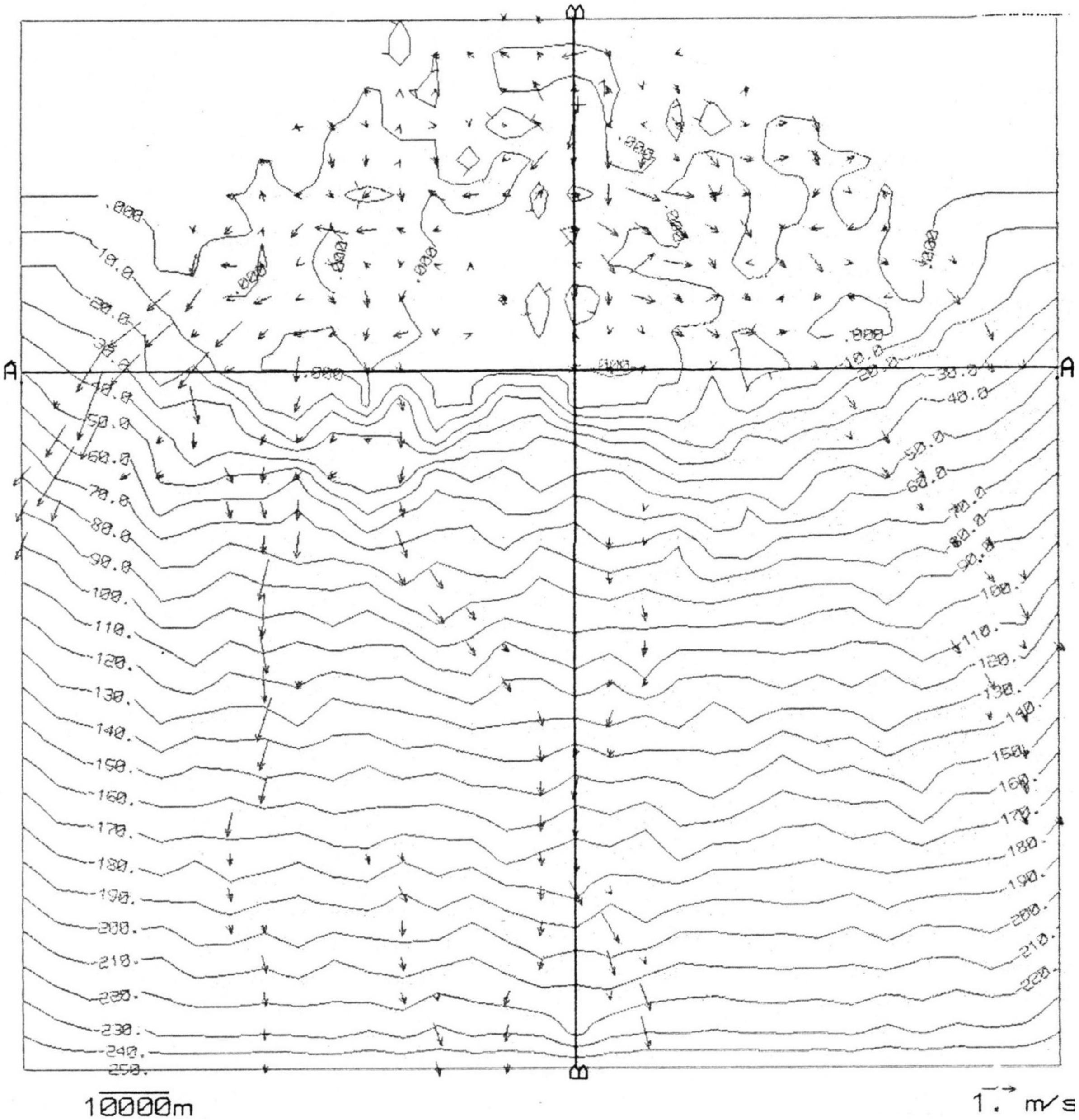

Figure 73: Topographic map of deltaic deposits after 10,000 years. Sections are shown in Figures 75 through 82.

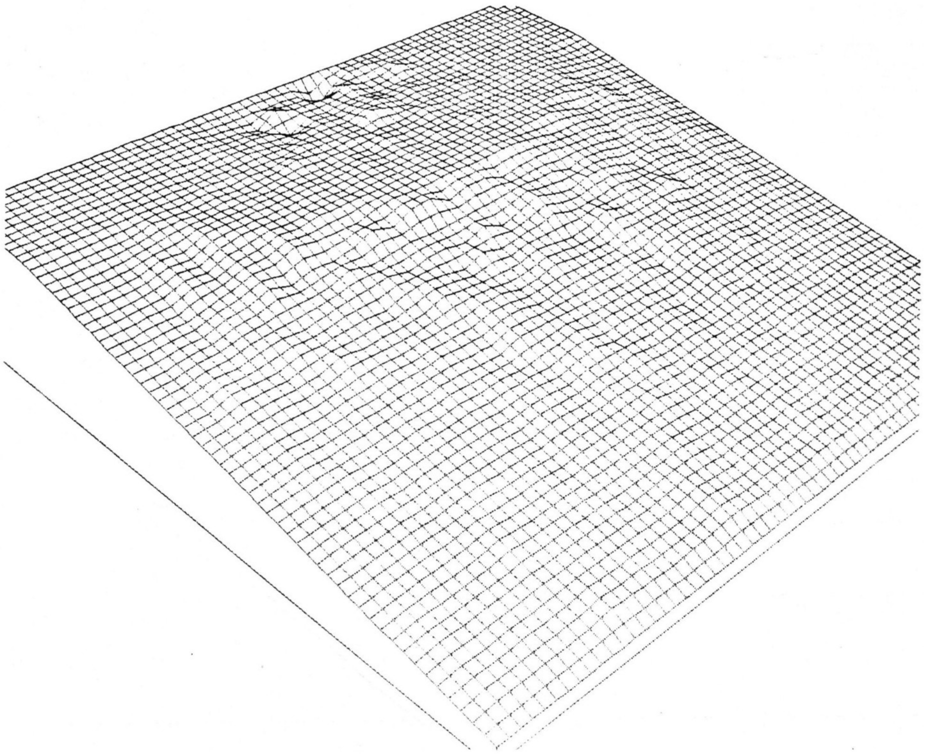

Figure 74: Fishnet diagram of topographic surface shown Figure 73.

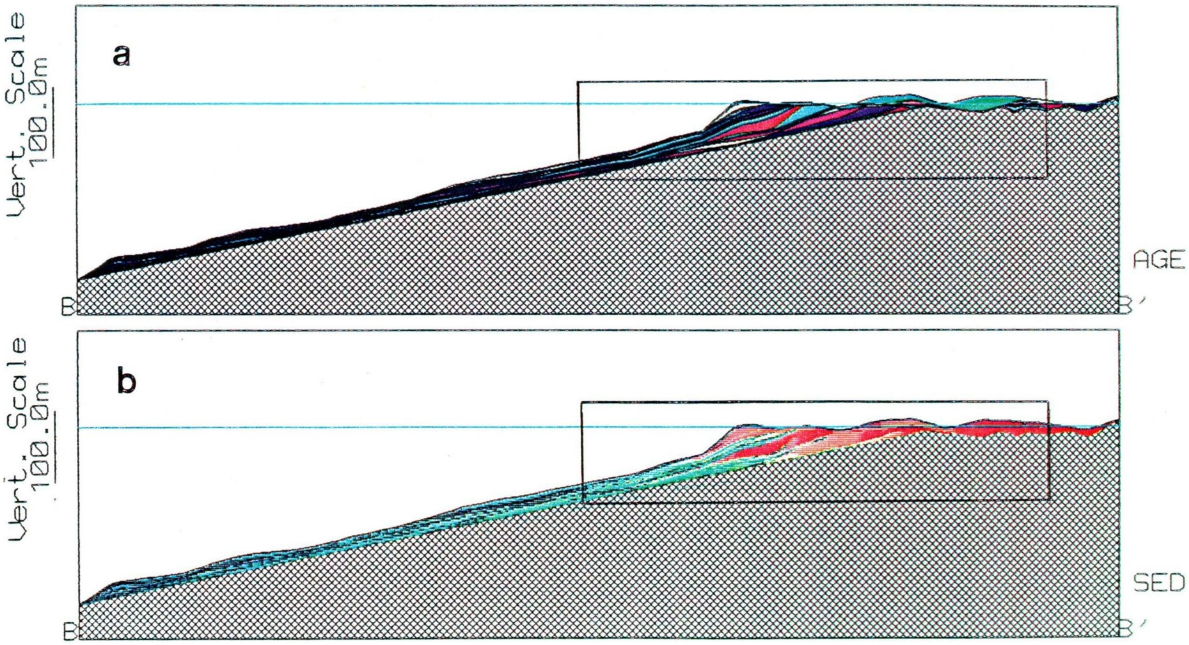

Figure 75: North—south section B—B' through deposits shown in Figures 73, and 74. Section ls 150 km long, and trace is shown in Figure 73: (a) Relative ages of deposits are shown by repetitive cycles 0f colors whose sequence in single cycle is shown in Figure 56a. (b) Sediment composition denoted by combinations of colors that represent four sediment types (medium sand, fine sand, silt, and clay) as defined I Figure 56b. Boxes outline enlarged portions shown in Figures 76 and 77.

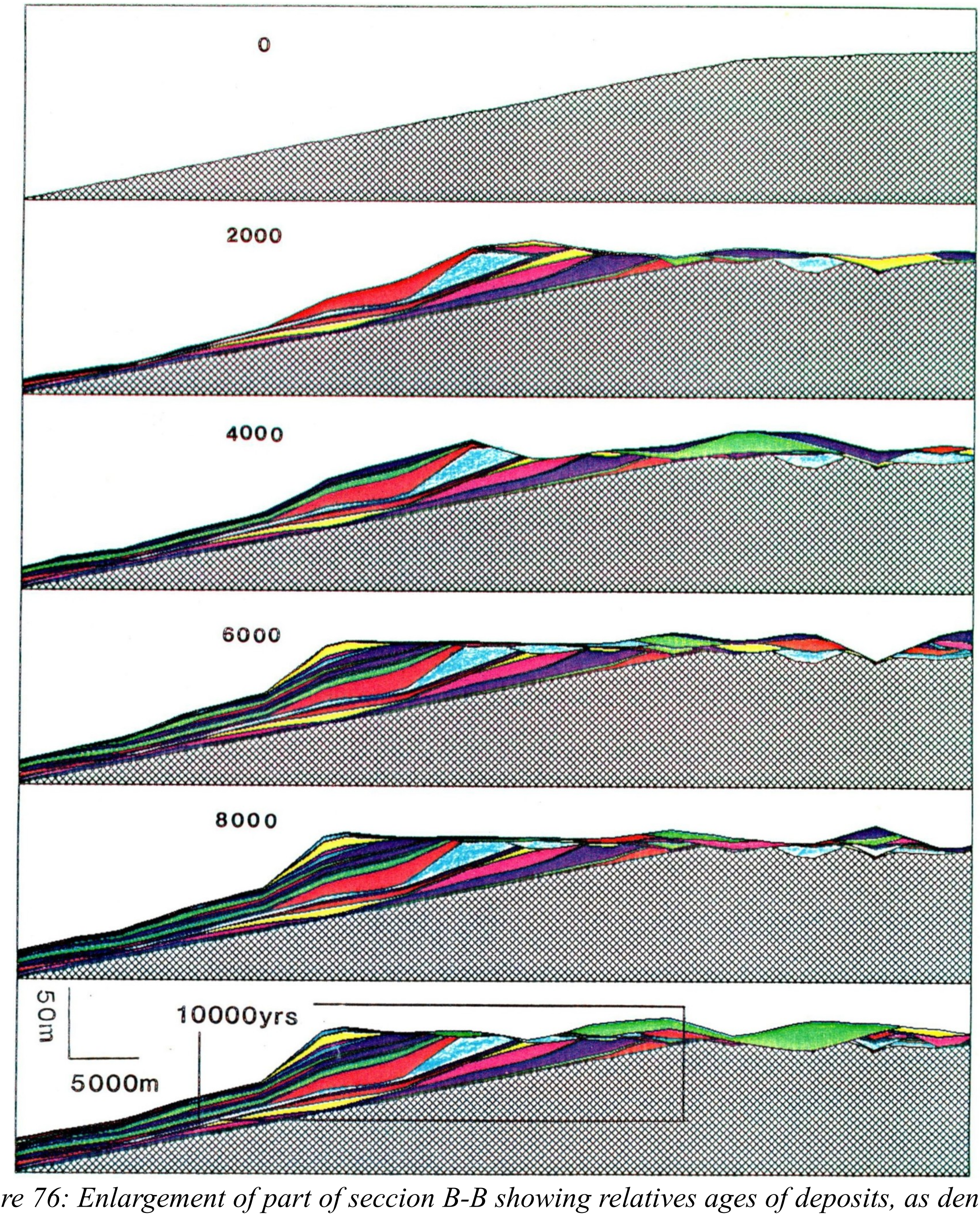

Figure 76: Enlargement of part of seccion B-B showing relatives ages of deposits, as denoted by colors (Fig. 56a). Box outlines further enlargement shown in Figure 78a.

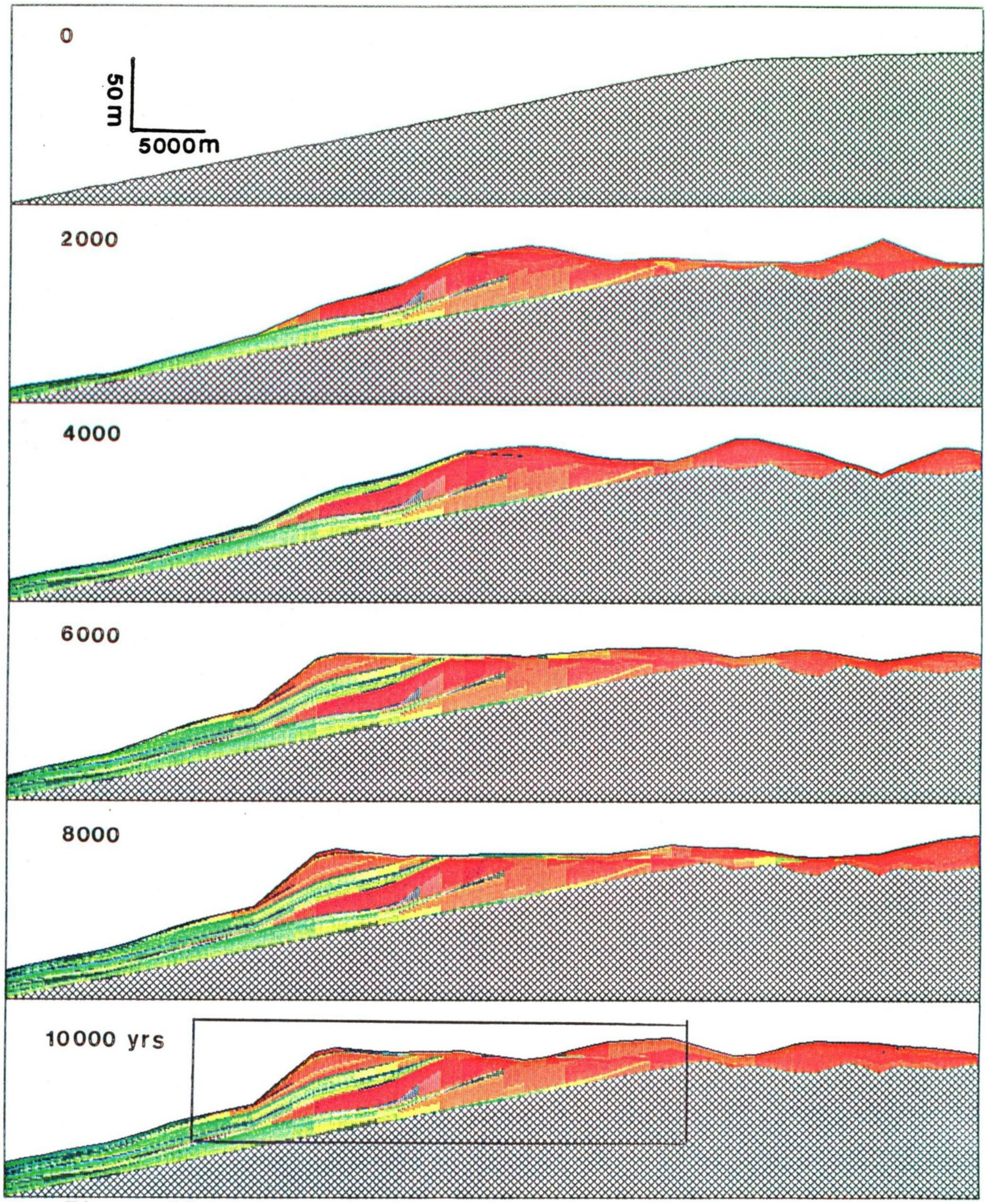

Figure 77: Enlarged portion of section B-B showing composition of deposits, as denoted by colors (Fig. 56b). Box outlines further enlargement shown in Figure 78b.

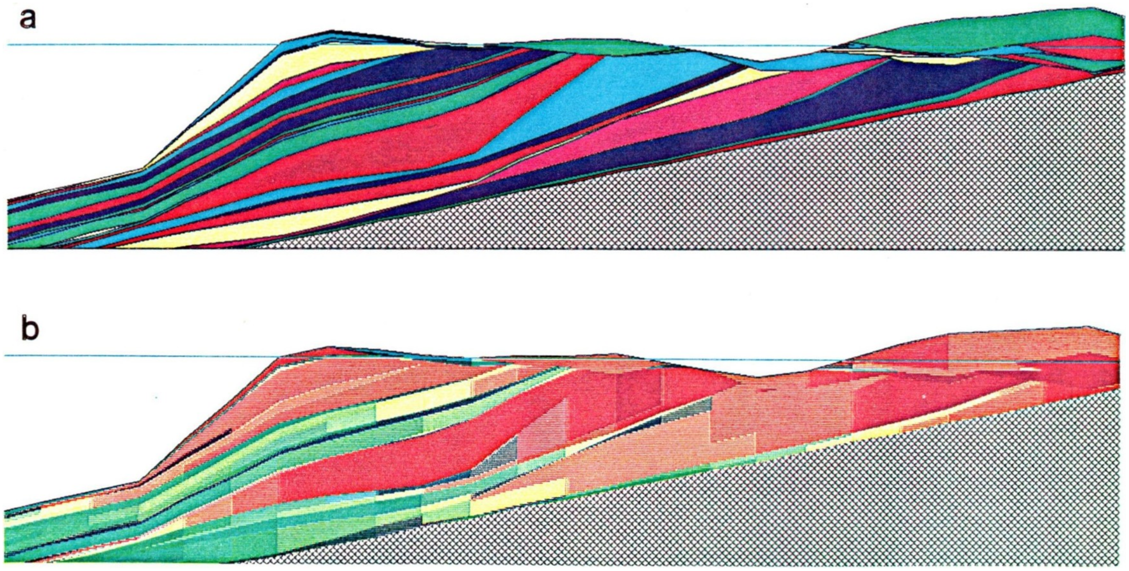

Figure 78: Further enlargement of part of section B-B', shown in Figures 75, 76, and 77: (a) Relative ages of beds reveal channels formed in upper part of deposits, with beds of sigmoidal shape having been deposited farther from shore. (b) Sediment composition indicated by colors. Sediment within deposits of equivalent age becomes progressively finer with distance from shore.

The gross form of beds viewed in sections perpendicular to shore can be termed "oblique progradational", adhering to the terminology 0f Sangree and Widmier (1977), and Mitchum (1977). An oblique progradational pattern consists of beds that terminate by toplap (truncation) updip. Such a pattern is present typically in fan-shaped units that contain numerous channel deposits on or near the shore. and is produced in an environment in which there are strong fluvial currents, a high sediment supply, and constant sea level. The simulated deposits reproduce the geometrical features in response to the paleoenvironmental conditions. Toplap is produced because SEDSIM's earlier deposits formed near the shore are subsequently eroded and truncated by strong fluvial currents. The degree to which beds are truncated would probably be lessened or be absent if compaction, isostatic compensation, and sea-level rise were incorporated in the simulation model. These processes permit the nearshore deposits to be buried and therefore partly or wholly protected from subsequent erosion.

Sections parallel to shore (and thus perpendicular to the direction of progradation) show lateral variations of the sedimentary features. Figures 79, 80, 81, and 82 display transverse (east-west) sections through the deltaic deposits. Lateral shifting of the coarsest deposits (red) occurs as sedimentation progresses. The undulated bed formed by shifting lobes are commonly shown in seismic record sections that are perpendicular to the direction of progradation of deltaic deposits.

Changing sediment composition

Changes in the input variables used in the delta simulation experiment (such as slope, flow rate, sediment content. and sediment composition) can significantly alter the aspect of the resulting deposits. A thorough sensitivity analysis has not been undertaken, but the effects of changes in sediment composition and flow rate were studied. Figures 83 and 84 are sections resulting from a revision of the previous simulation experiment shown in Figures 74 through 82. The first of two subsequent experiments assumes a lesser proportion of sand. and a lower flow rate (Fig. 83). The second experiment assumes a higher proportion of sand and a higher flow rate (fig. 84). Figure 77 shows the section through the deposits produced by the original experiment. A comparison with the two modified experiments reveals the geographic distribution of sediments in the deposits differs, sand being transported farther offshore in the experiment shown in Figure 84. Also the slope of the prodelta deposits decreases as the flow rate and content of coarse sediment increase.

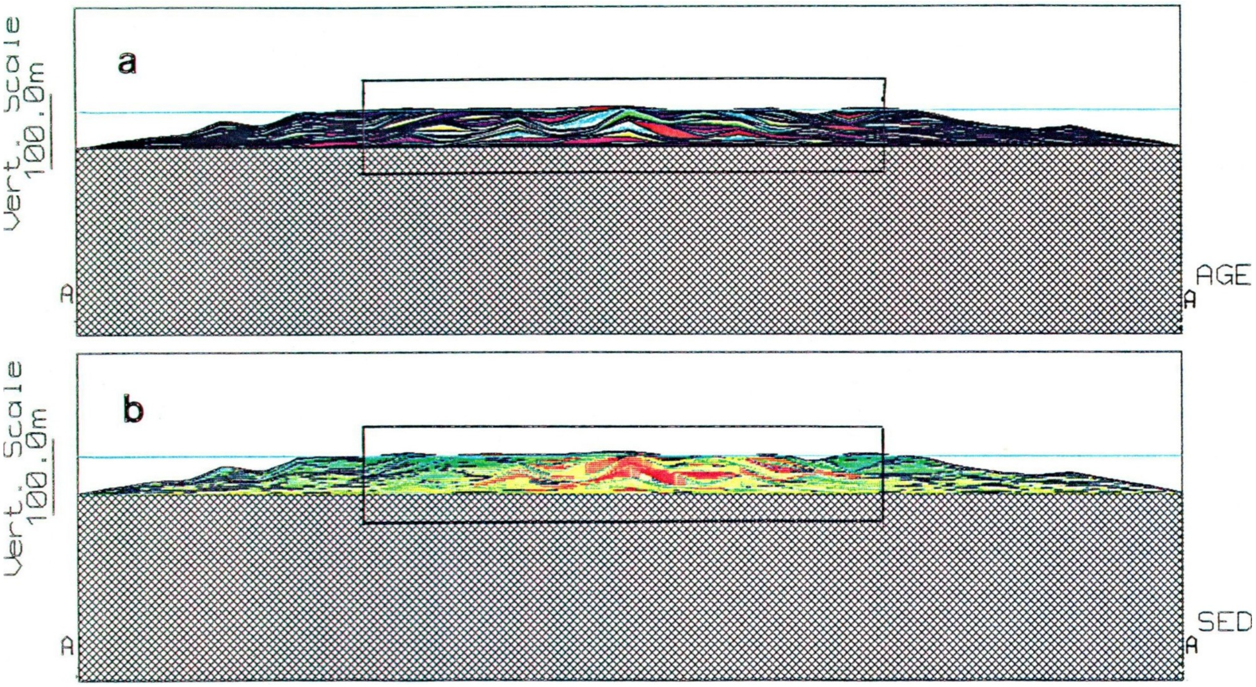

Figure 79: East-west section A-A', parallel to shoreline and perpendicular to section BB', that represents 10.000 years deposition. Trace of section is shown in Figure 73: (a) Relative ages. (b) Sediment composition. Figure 56 provides color code. Boxes show enlarged portions displayed in Figures 80 and 81.

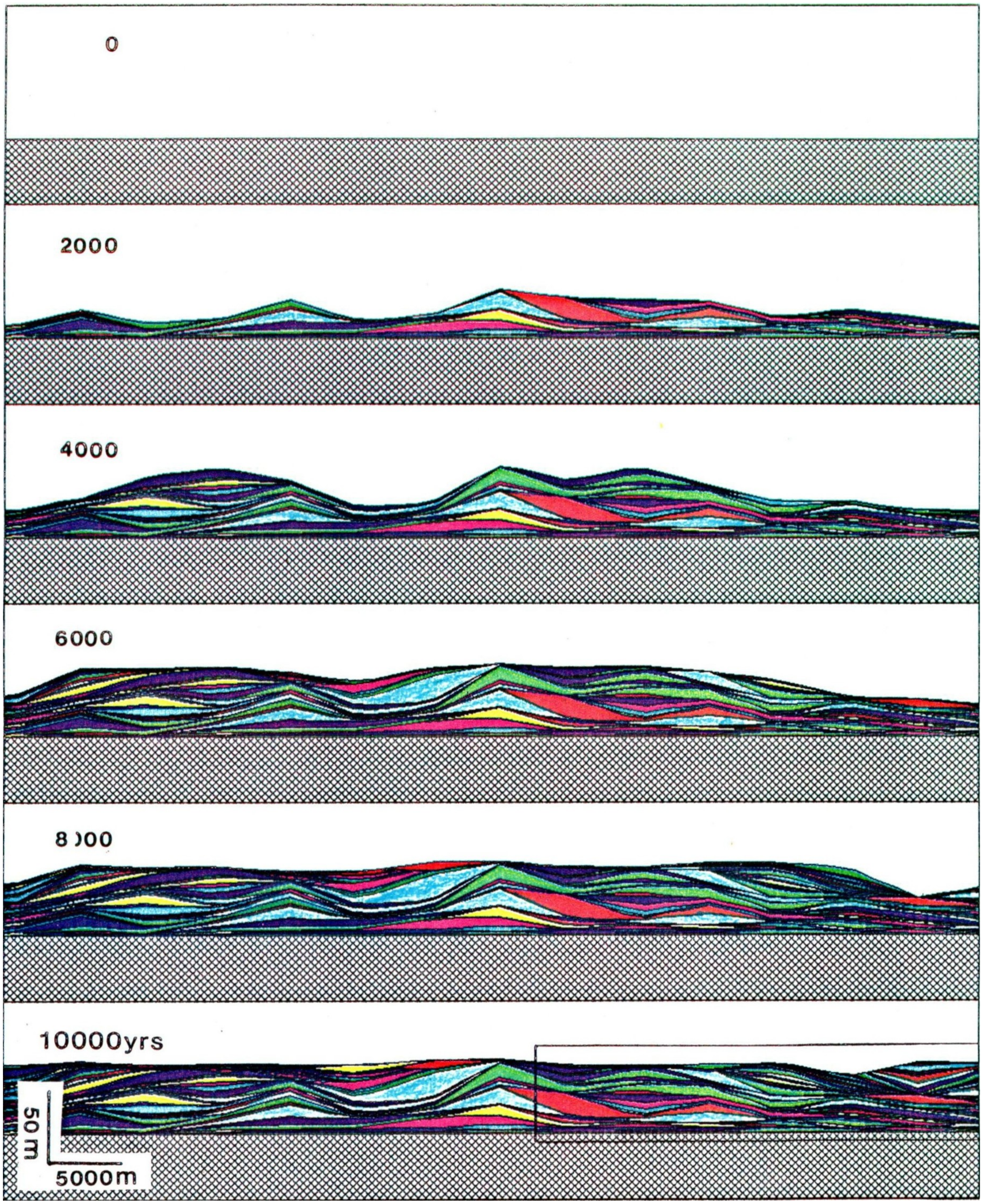

Figure 80: Enlargement of part f section A-A ' showing relative ages of deposits formed at increments of 2,000 years. Box outlines further enlargement shown in Figure 82a.

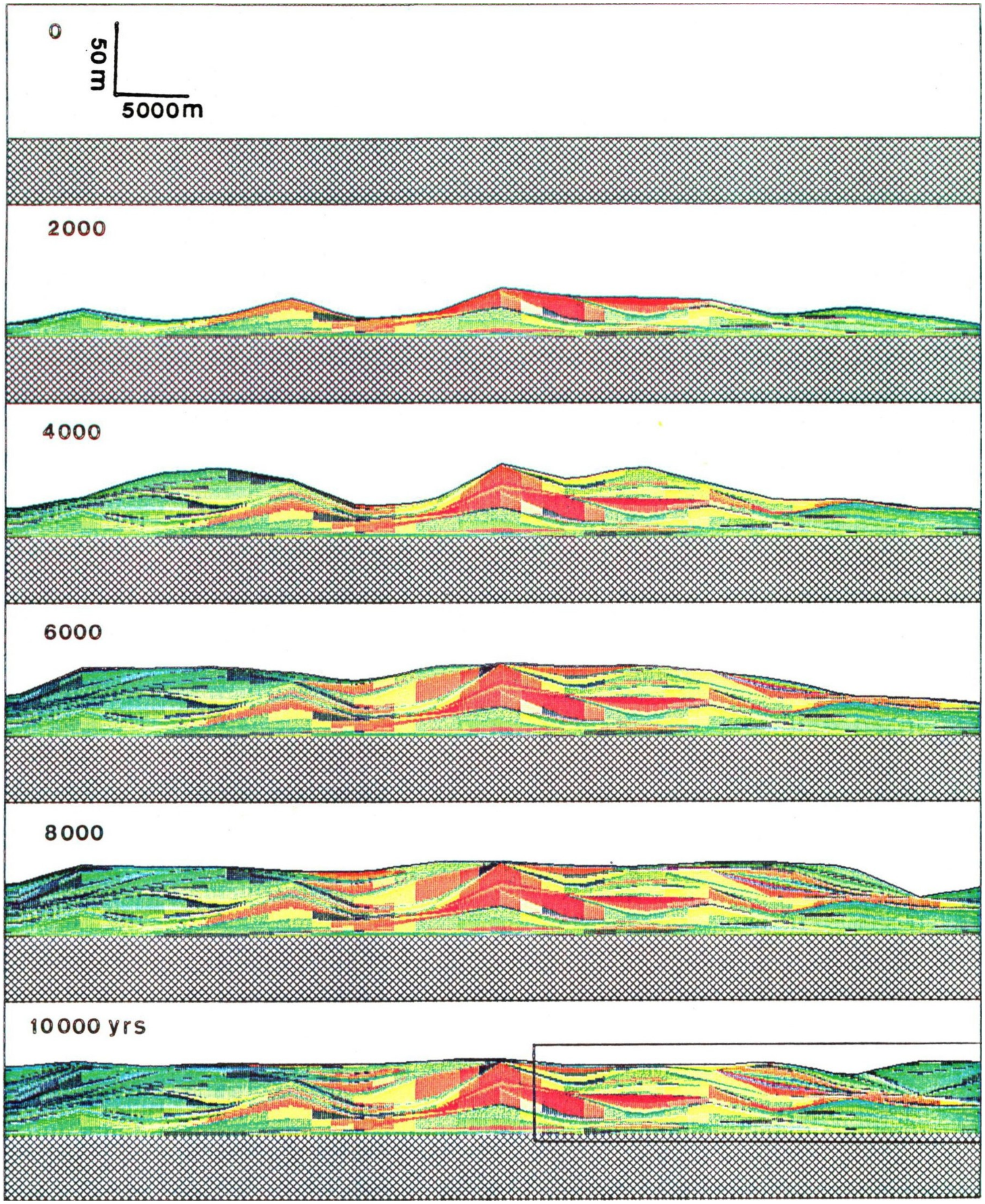

Figure 81: Enlarged portion of section A-A showing composition of deposits as denoted by colors in Figure 56b. Box outlines further enlargement shown in Figure 82b.

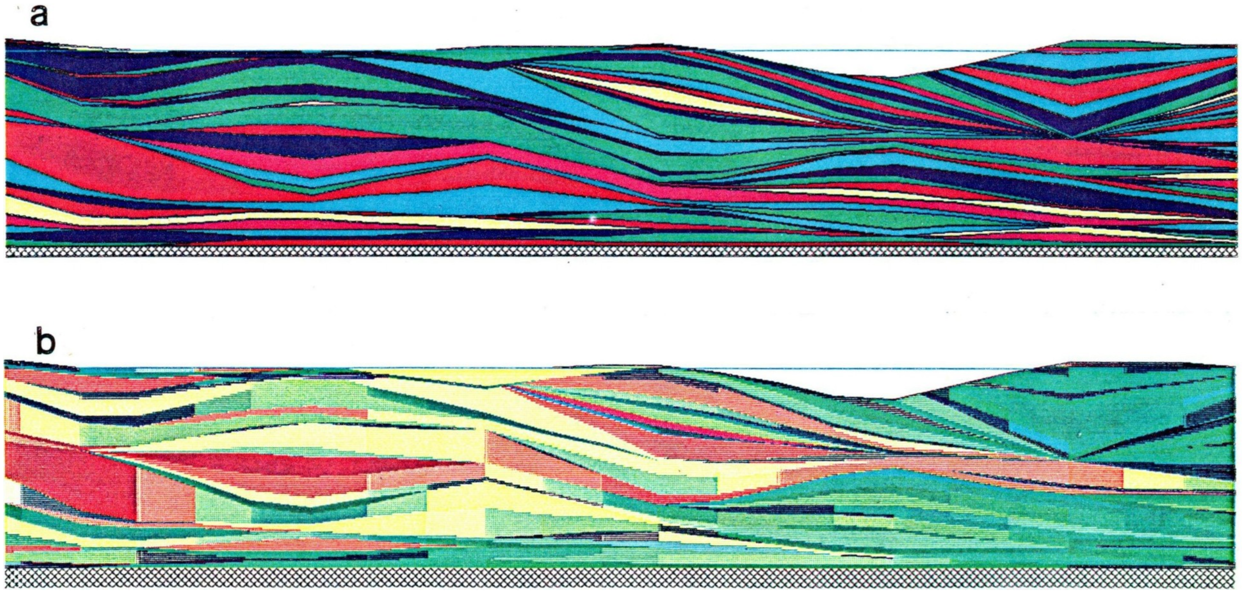

Figure 82: Further enlargement of part of section B-B', shown in Figures 79, 80, and 81: (a) Relative ages” (b) Sediment composition, revealing thick lenses of coarse sediment corresponding to deltaic lobes that shift from side.

The experiment involving finer sediments (Fig. 83) has been affected by a a pronounced "source effect" which manifests itself in the form of a deep erosional depression near the source. Onshore channelization is also prominent in the experiment shown in Figure B3. Both the excessive erosion near the source, as well as the numerous channels (Figure 83), are caused by a low content of coarse sediment in the flow. which therefore has had increased capacity to erode the pre-existing deposits. Such channels are common in natural environments in which the flow is depleted of coarse sediment. The depression near the source, however, would not be present in an actual delta. Similarly, the "mound" near the source in Figure 84, would not appear in an actual delta. These artificial features are caused by a sediment load at the source that is either much lower or much higher, than the load that would be carried by an actual river under similar hydraulic conditions. An actual river adjusts its sediment load throughout its length before reaching the delta. in SEDSIM. the user must provide a sediment input rate that is neither too high\nor too low for the given hydraulic conditions. Otherwise erosion or deposition occurs at the sources. and the flow adjusts its load only after it has traveled some distance downstream.

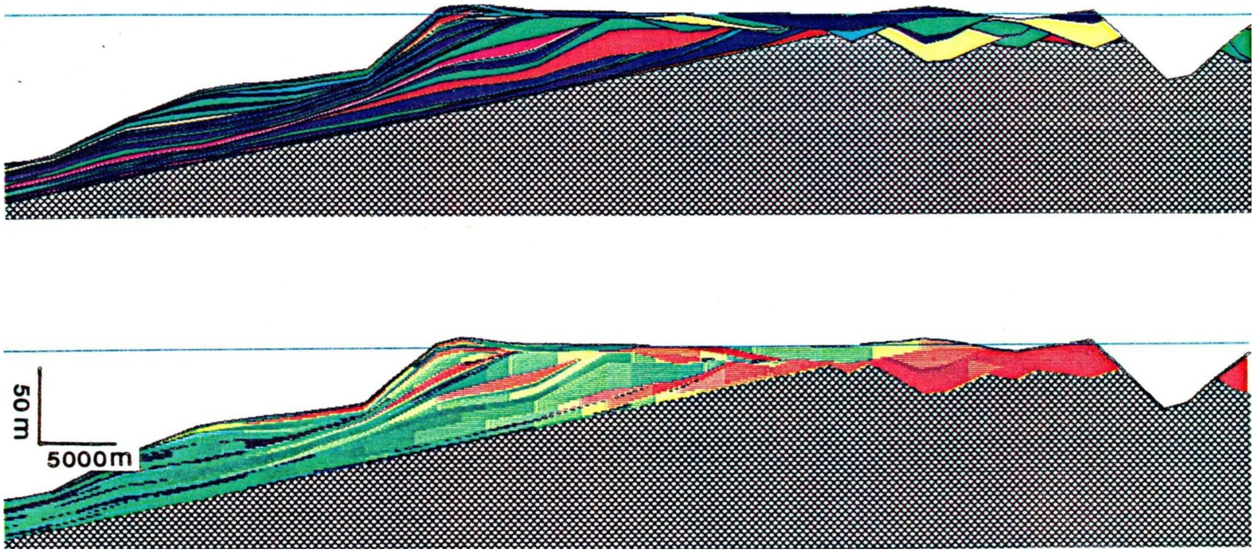

Figure 83: Longitudinal section through deltaic deposits produced by simulation experiment involving lower proportion of coarse sediments than experiment shown in Figures 76 and 77.

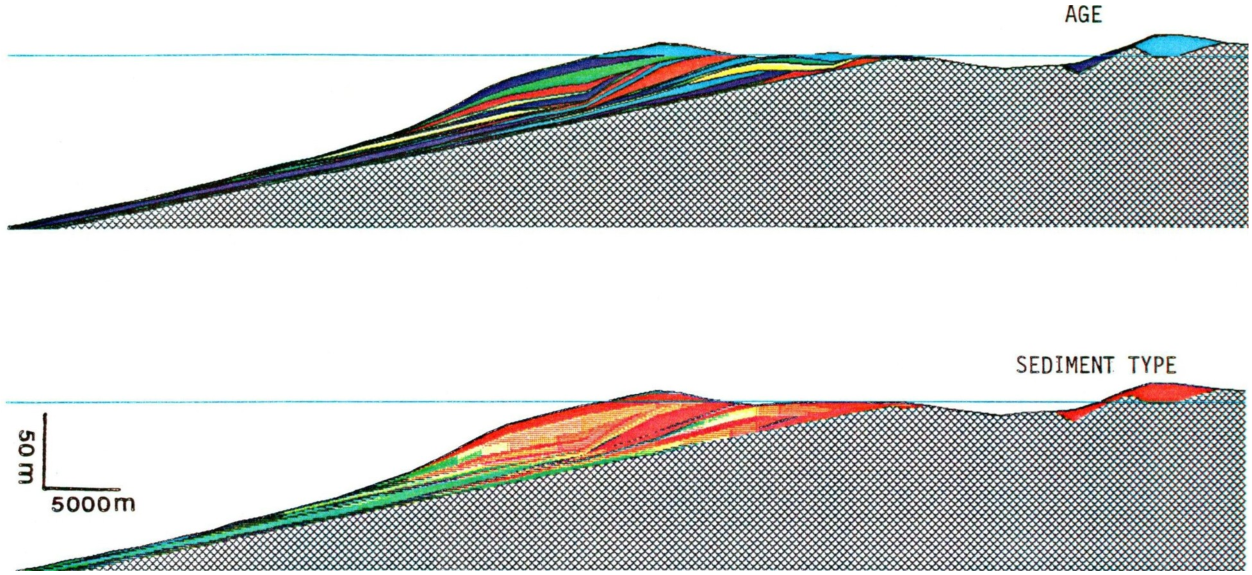

Figure 84: Longitudinal section through deitaic deposits produced by simulation experiment involving higher proportion of coarse sediment than experiment shown Figures 76 and 77.

The experiments involving deltas show that SEDSIM is able to simulate various characteristics of deltaic deposits in response to flow conditions and sediment characteristics. Other experiments involving deltas are feasible. Chapter V describes experiments with the objective of simulating an actual deltaic sedimentary sequence of Tertiary age in Louisiana.

ASSESSING THE PERFORMANCE OF THE MULTl-SEDIMENT MODEL

The simulation experiments described above show that SEDSIM is able to reproduce sedimentary features in systems involving four sediment types. The general form of the con figuration of simulated deposits, as well as the distribution of sediment types within them, generally agree with the configuration of actual sedimentary deposits. Dimensions of the simulated deposits also seem to agree with those produced by actual sedimentary processes. However, further testing of SEDSlM's performance in producing simulated deposits that compare well with actual deposits is needed for thorough evaluation.

Perhaps the most useful characteristic of SEDSIM is that it is able to simulate clastic sedimentary processes under conditions that change progressively over relatively long periods of time. Thus. SEDSIM should be useful in predicting the geographic or spatial characteristics of ancient sedimentary sequences, a capability that is treated in the next chapter.

Chapter V
APPLICATIONS TO PETROLEUM EXPLORATION

The preceding chapters describe experiments with SEDSIM under hypothetical conditions. This chapter describes SEDSIM's application in interpreting two actual sedimentary environments. The First involves an ancient submarine canyon, Simpson Canyon. that was carved in Cretaceous sediments and refilled with Cretaceous and Early Tertiary sediments. Simpson Canyon is located in the northern part of the National Petroleum Reserve in Alaska, and is known almost entirely from information provided by seismic sections.

The second example is a deltaic sequence of Tertiary age in the Golden Meadow oil and gas field, in coastal Louisiana. The Golden Meadow field has been extensively drilled, and well logs provide the primary information, enabling SED5lM's performance in simulating sequences of sedimentary deposits to be compared with actual sequences interpreted from well logs.

SIMPSON CANYON, ALASKA

The National Petroleum Reserve in Alaska (NPRA) is located in northern Alaska and extends over an area whose boundaries are irregular but are roughly 500 miles by 300 miles in extent (Fig. 85).

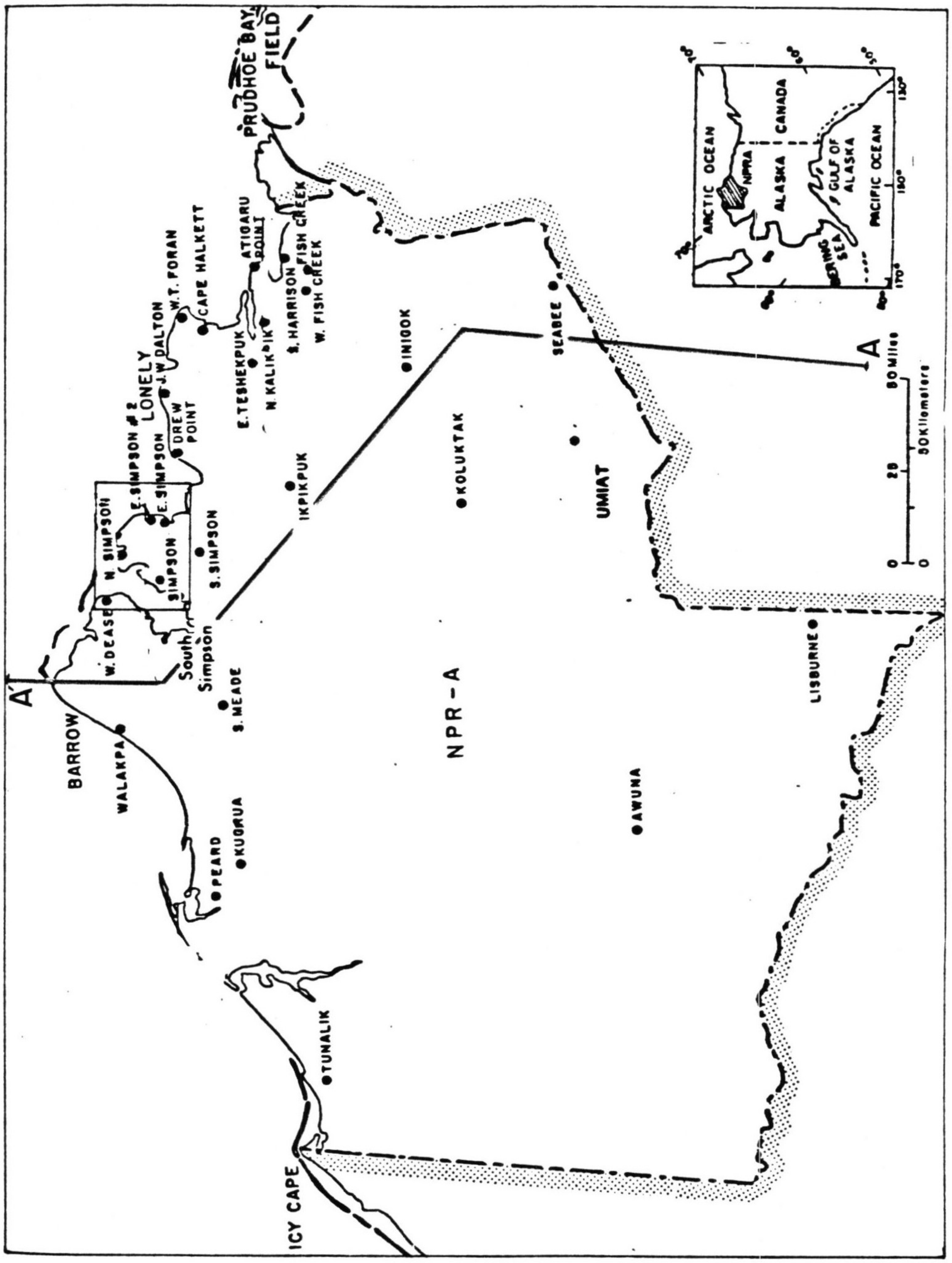

Figure 85: Location map of Cape Simpson in northern part of National Petroleum Reserve in Alaska. Trace shows location of section displayed in Figure 86. Adapted from Robinson (1984).

Process simulation is potentially useful in the northern part of the NPRA for three principal reasons: First, there is a high degree of geologic interest attached to the sedimentary features observed in seismic sections, which include the ancient and now-filled submarine canyon, Simpson Canyon. Second, the northern part of the NPRA has undergone little tectonic activity since deposition, except for slight regional tilting (Fig. 86), permitting simulation of the sedimentary features without the complications of extensive structural deformation. Third, there is a large amount of modern seismic data, and some well data, that are publicly available (Fig. 87), although public data are lacking in the Arctic Ocean, offshore from the NPRA. Thus, process modeling can be useful for inferring the properties of sedimentary deposits that lie beneath the Arctic Ocean, where data are not publicly available.

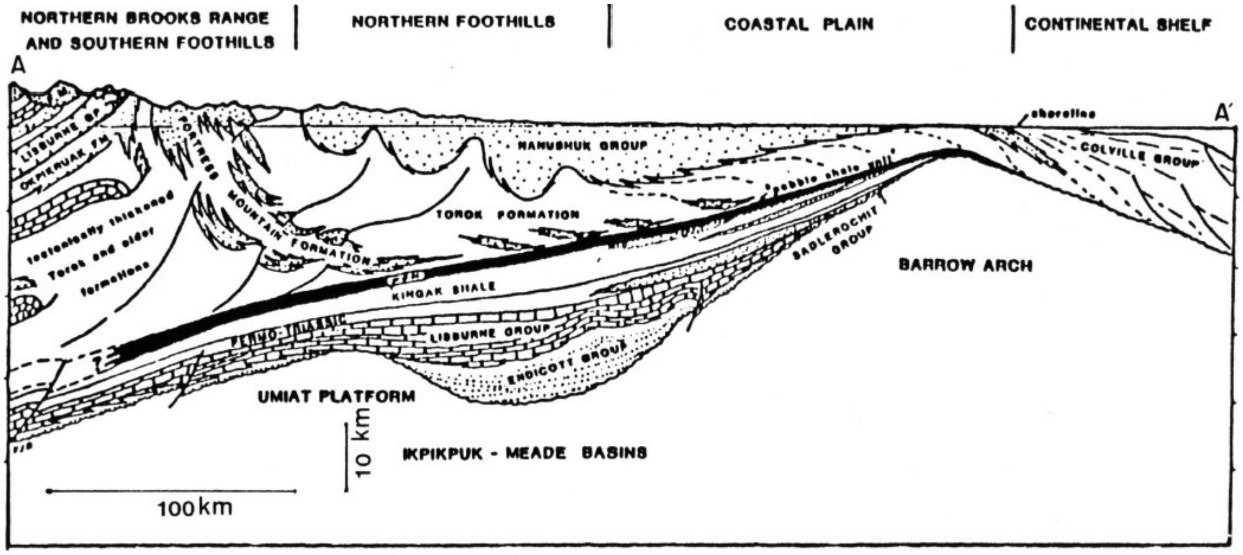

Figure 86: North-south geologic section through National Petroleum Reserve in Alaska. Trace shown in Figure 85. From Bird (1981).

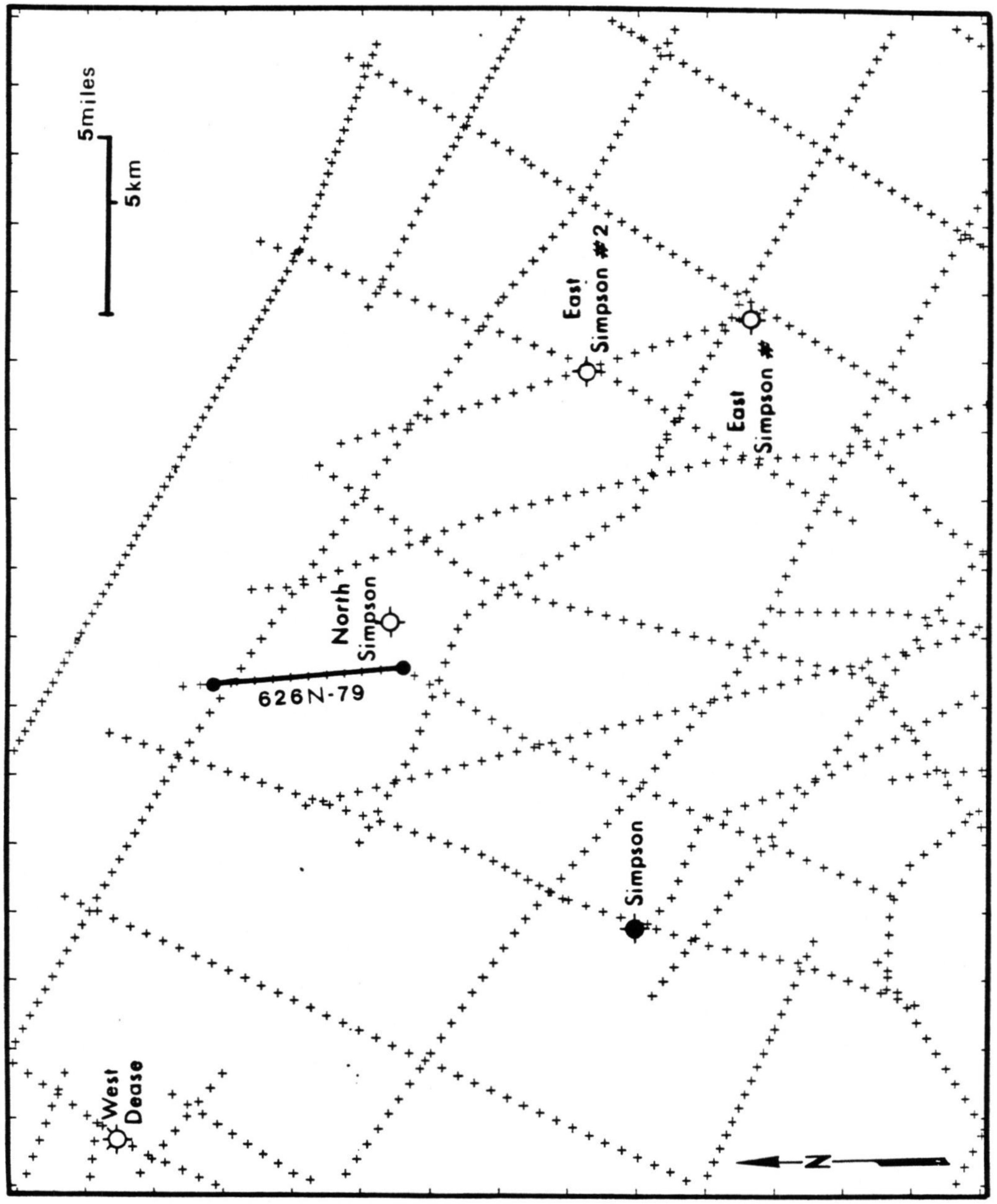

Figure 87: Traces of seismic lines and data points used in producing maps of Simpson Canyon, Seismic section 626N-79 is shown in Figure 88. Location of inset in Figure 85.

Before SEDSIM can be used to predict the properties of sedimentary deposits beyond an area in which information is available, the input parameters must be carefully adjusted to reproduce sedimentary deposits that are in reasonable accord with those in areas where data are available. At Cape Simpson, the seismic data available onshore are critically important because they provide information about the canyon, permitting the process simulation model's parameters to be adjusted so as to reproduce the canyon's onshore features with reasonable fidelity. and in turn, to predict sedimentary features beyond the canyon's mouth, that now lie offshore beneath the Arctic Ocean.

While Simpson Canyon is entirely buried, seismic surveys how that it is approximately 25 miles long, 10 miles wide, and over 4,000 feet deep. Simpson Canyon was previously mapped (Tetzlaff, 1984), employing information obtained in reflection seismic surveys. Computer mapping procedures were used to reproduce the topography of the canyon at successive stages that facilitate interpretation of its history which involved three successive cycles of carving and refilling. Oil seeps on Cape Simpson may be related to the presence of Simpson Canyon and its fill. The oil may have migrated either through the canyon fill or through older Cretaceous rocks in which the canyon is carved, the migrating oil being diverted by the boundaries of the fill to the present seeps. It is possible that deposits near the base of the canyon fill may create suitable oil reservoirs. And deposits beyond the mouth of the canyon may also constitute prospective reservoirs. Both prospects need to be evaluated by future drilling.

Geologic and Geophysical Data at Cape Simpson

Seismic data in the area of Cape Simpson consist of about 350 line-miles of reflection seismic sections (fig. 87), recorded and processed by Tetratech Inc. for the U.S. Navy and the Geological Survey from 1974 through 1981. Most of the sections are unmigrated time sections, with six-fold multiplicity. The average density of seismic lines in the vicinity of Simpson Canyon is about 500 linear miles of seismic lines per 1,000 square miles of land area. Geophysical data north of Cape Simpson in the Arctic Ocean are not publicly available, and therefore were not used in this study. Information within the boundaries of the NPRA is publicly available, and may be obtained for the cost of reproduction of the seismic sections.

Logs from a few exploration wells drilled on Cape Simon complement the seismic sections. A set of synthetic seismogbrams, produced by the National Oceanic and Atmospheric Administration (NOAA) for all wells in which sonic logs have been recorded. permit seismic sections to be tied to wells, and provide transformation from reflection time to depth for all seismic sections, so that the horizons can be mapped in terms of elevation with respect to sea level, rather than in terms of seismic reflection time.

A small amount of information was provided by rotary cores and sidewall cores obtained for several intervals in wells drilled by the U.S. Government at Cape Simpson. Some of the cores were studied in the core library in Anchorage, Alaska, maintained by the U.S. Geological Survey (USGS). The USG5 has published descriptions of cores and cuttings from most wells in the NPRA (Collins, 1958, 1959, 1961; Robinson and Collins, 1959; Robinson, 1959, 1964), and these were employed in interpreting paleogeographic conditions.

Geologic Setting of Simpson Canyon

Simpson Canyon is both carved in and filled with silt stones and graywackes that form part of the Brookian sequence (Carter and others, 1977). The beginning of deposition of the Brookian sequence is marked by two events that strongly influenced the paleogeography of the North Slope in the Cretaceous and Tertiary, namely (1) uplift of the Brooks Range and (2), rifting of the Arctic Ocean. One consequence was a change from northern to southern sources of sediment. The "pebble shale" (Fig. 86) is usually considered to be the earliest deposit in the Brookian sequence (Morgridge and Smith, 1962).

The "pebble shale" is a dark gray sandy shale. 300 to 600 feet thick, with occasional chert granules. It is believed to be the main hydrocarbon source rock in the Prudhoe Bay, Umiat, and Point Barrow Fields, all in the North Slope (Rickwood, 1970). Thick wedges of sediment derived from a southerly source were deposited upon the "pebble shale", filling the Colville trough (Fig. 86) and migrating progressively toward the northeast. The Torok formation and Nanushuk Group (Fig. 86) were deposited unconformably on the "pebble shale". The Torok formation and Nanushuk Group are two stratigraphic units that partially intergrade laterally, and range from Albian to Cenomanian in age (Bird and Andrews, 1979; May, 1979; May and Stein. 1979). The units are probably of deltaic origin, and appear in the seismic sections as sets of sigmoidal surfaces that prograde towards the northeast. The Torok represents the bottomset and foreset beds of the delta, whereas the Nanushuk represents the topset beds (Fig. 86).

The Nanushuk is covered by the Colville Group of Late Cretaceous age, which consists mostly of marine shales. In the northeastern NPRA, deposition of the Colville Group continued into the Tertiary. The Colville Group constitutes the fill of Simpson Canyon.

Three different surfaces can be mapped within Simpson Canyon. The lowest and oldest erosion surface (Figs. 88 through 90) has several smaller tributary canyons. It is possible. however, that some of these "tributaries" actually may be slump deposits. The bottom of the canyon is relatively flat by comparison with ordinary shaped canyons, perhaps because erosion lowered the canyon's floor to the base of the Torok formation. below which further erosion was limited by the relatively resistant qualities Of the "pebble shale". Alternatively, it is possible that the flatness of the canyon's floor is not related to the presence of the "pebble shale", and may be due to the adjustment of the canyon's floor to the "base level" determined by the surface extending beyond the canyon's mouth. as suggested by simulation experiments described below.

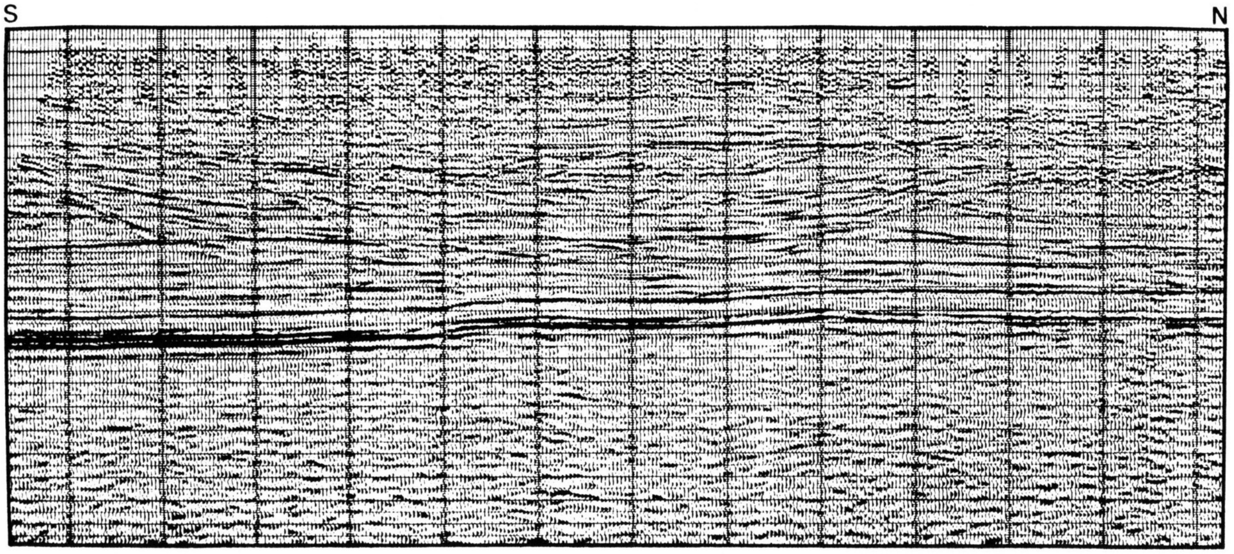

Figure 88a: Part of seismic section 626N-79 whose trace is shown in Figure 87. Interpretation is outlined in Figure 88b.

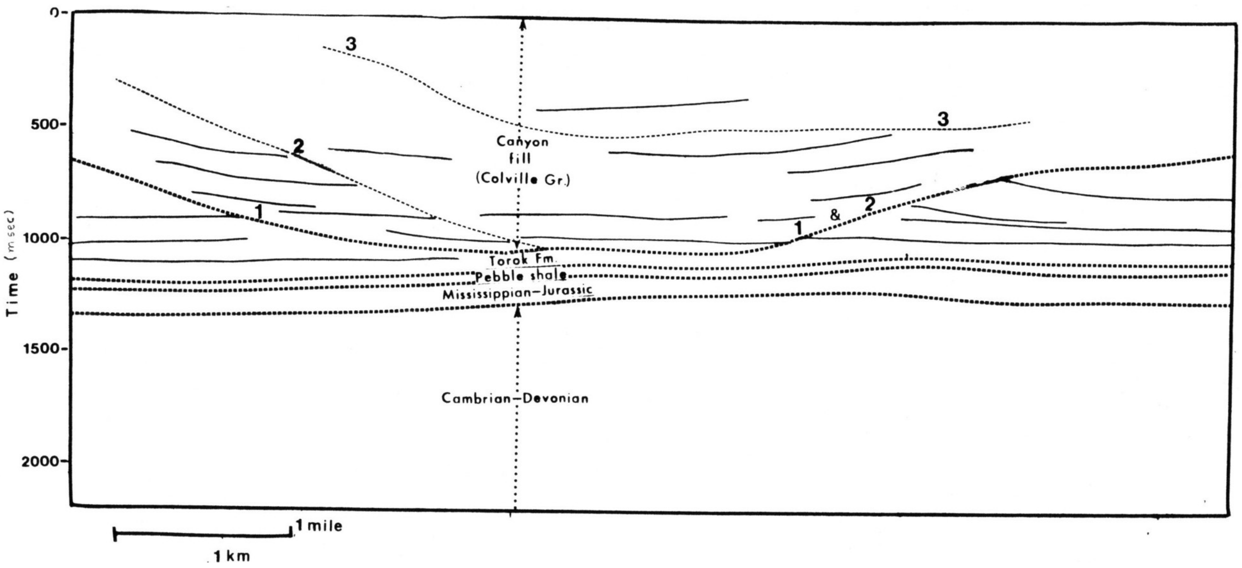

Figure 88b: Outline of interpreted in seismic section displayed in Figure 88a, including three former erosion surfaces.

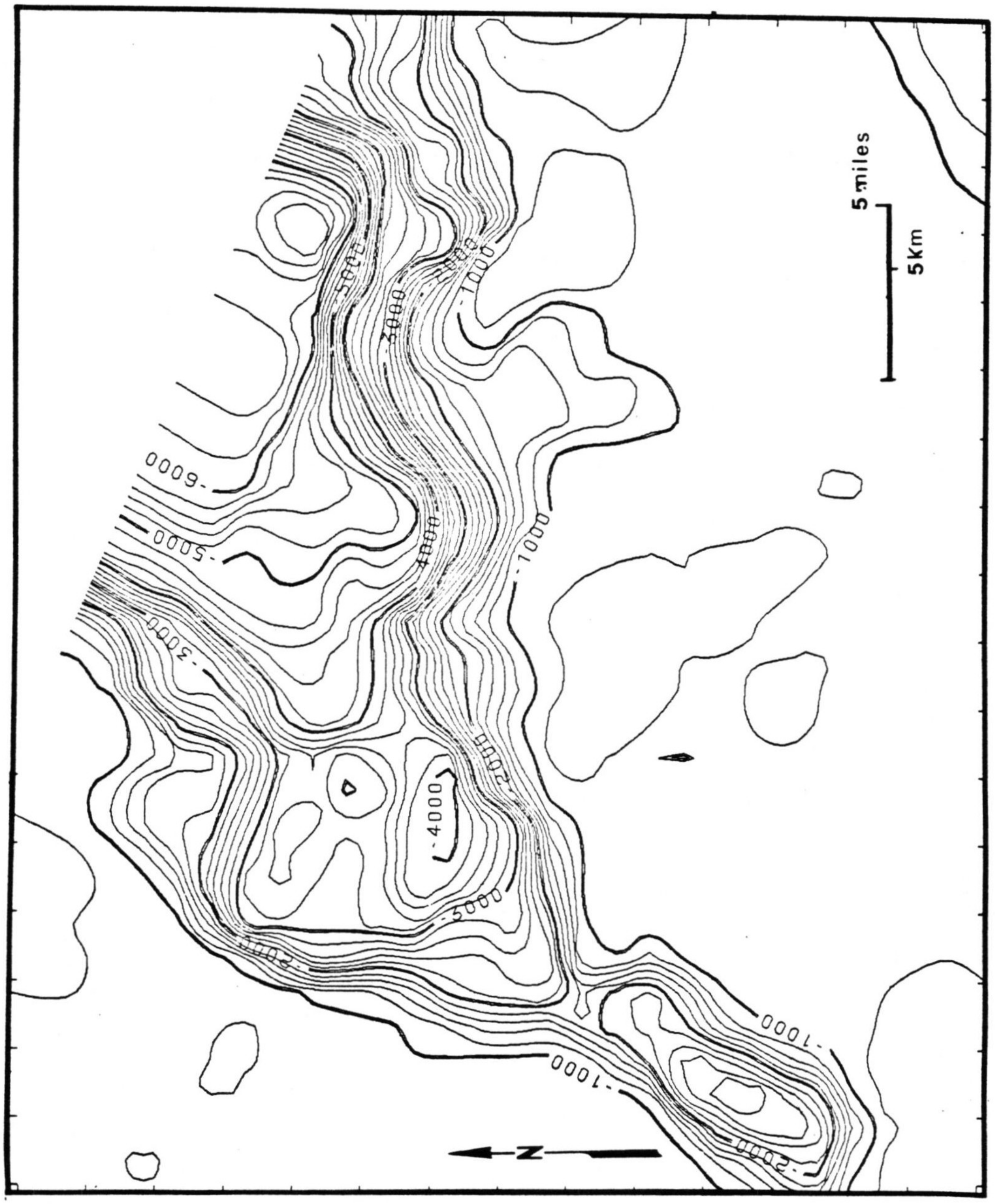

Figure 89: Contour map of structure of Simpson Canyon's lower erosion surfaces as define in Figure 88. Contour are in feet below present day sea level. Map is based solely on seismic information, and data are lacking in northeast corner of area. Simulation experiment has been employed to predict features north of the canyon's mouth, beyond area where seismic or well data are available.

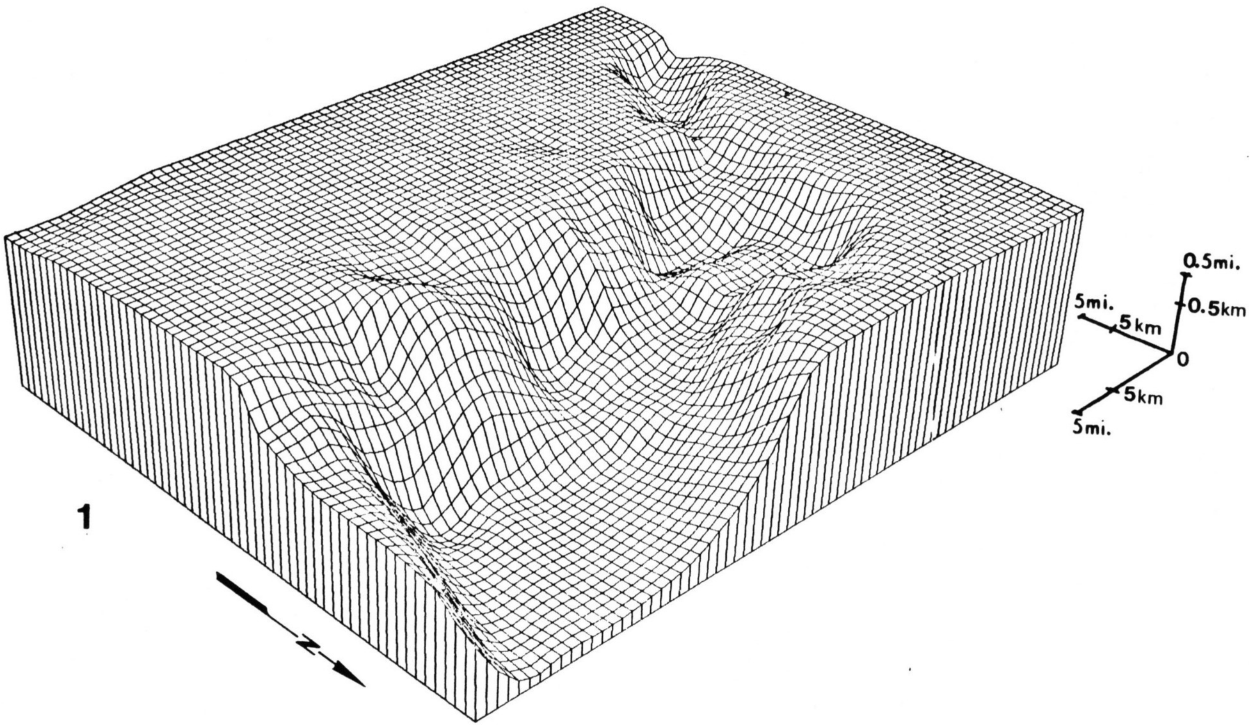

Figure 90: Fishnet diagram showing lowermost erosion surface (Horizon 1) of Simpson Canyon, based solely on seismic information.

Simulation Experiments

The development of Simpson Canyon was simulated with the single-sediment model described in Chapter III. The propose was to simulate the carving o the canyon, and the deposition of the fan that may extend beyond the canyon's mouth. Materials forming the fan may consist of material partly of wholly eroded from the canyon.

Paleotopographic conditions at Cape Simpson were inferred from seismic section near the canyon. The inclination of the paleotopographic surface and thickness of the deltaic deposits into which the canyon is carved were inferred from three-dimensional topographic reconstructions on the canyon (Figure 91) at different stages based on specific seismic reflecting horizons in the Torok Formation and Nanushuk Group. The topography initially assumed for the first set of experimental simulation runs is shown in Figure 92 y 93. The topographic surface consist of a gentle slope broken by a step scarp.

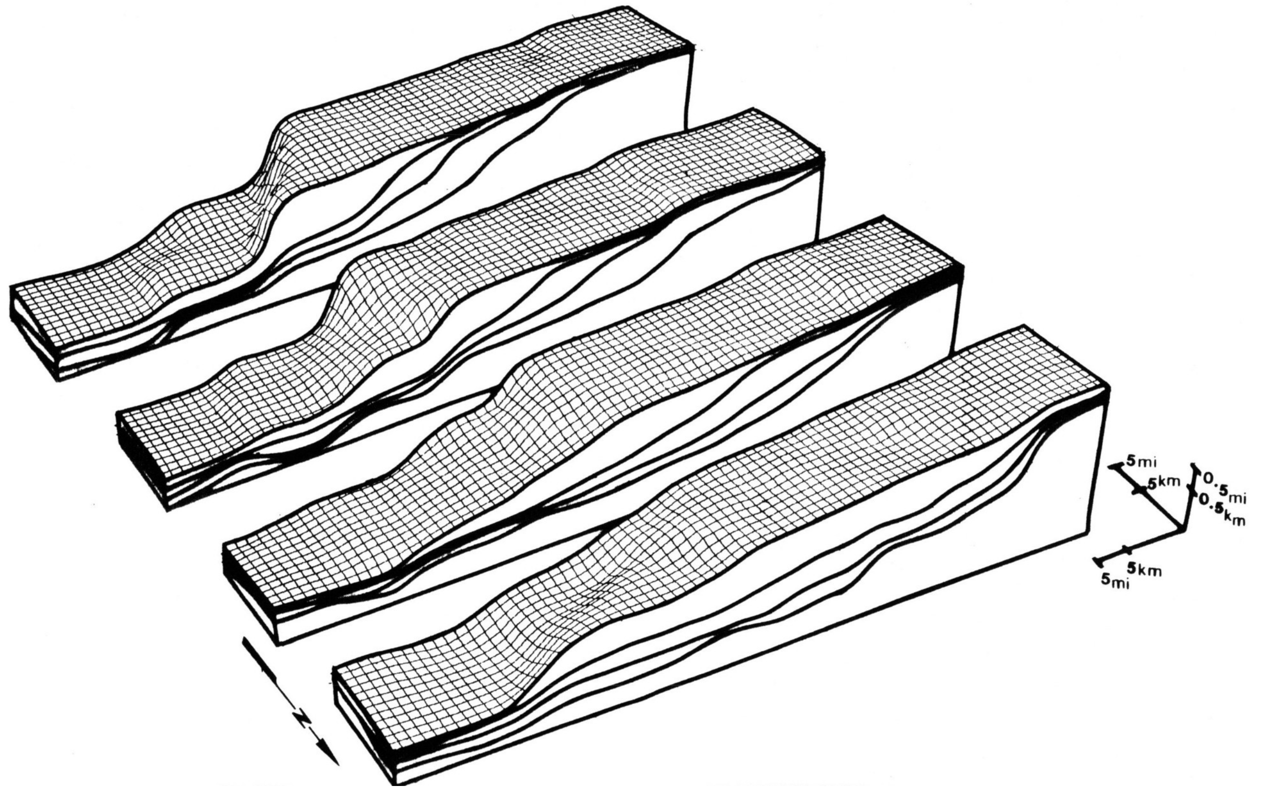

Figure 91: Three-dimensional block diagram showing paleotopographic reconstruction of deltaic deposits in vicinity of Simpson Canyon based on seismic sections. Four paleotopographic surfaces that are shown were not affected by canyon erosion, and provide information on configuration of sedimentary deposits before canyon was cut.

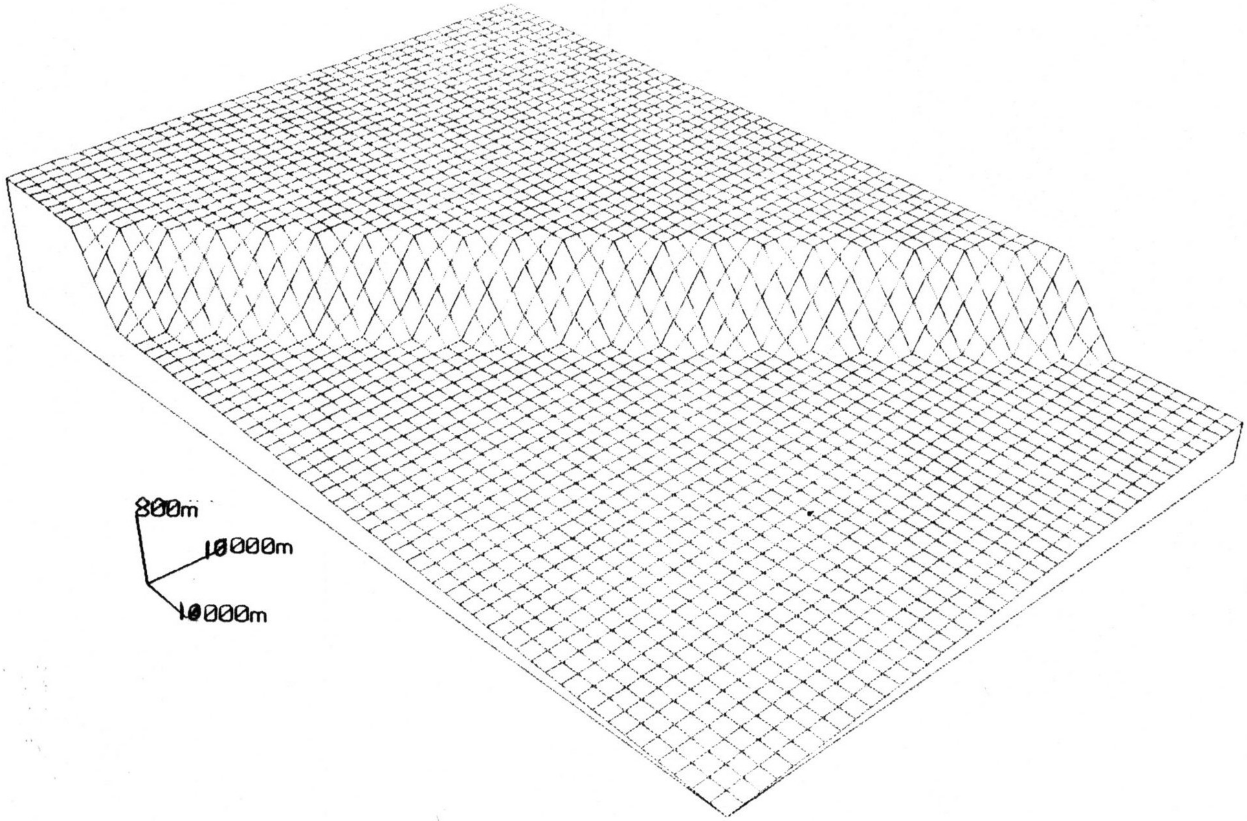

Figure 92: Fishnet diagram showing initial topographic configuration of simulation experiment whose objective has been to reconstruct Simpson Canyon.

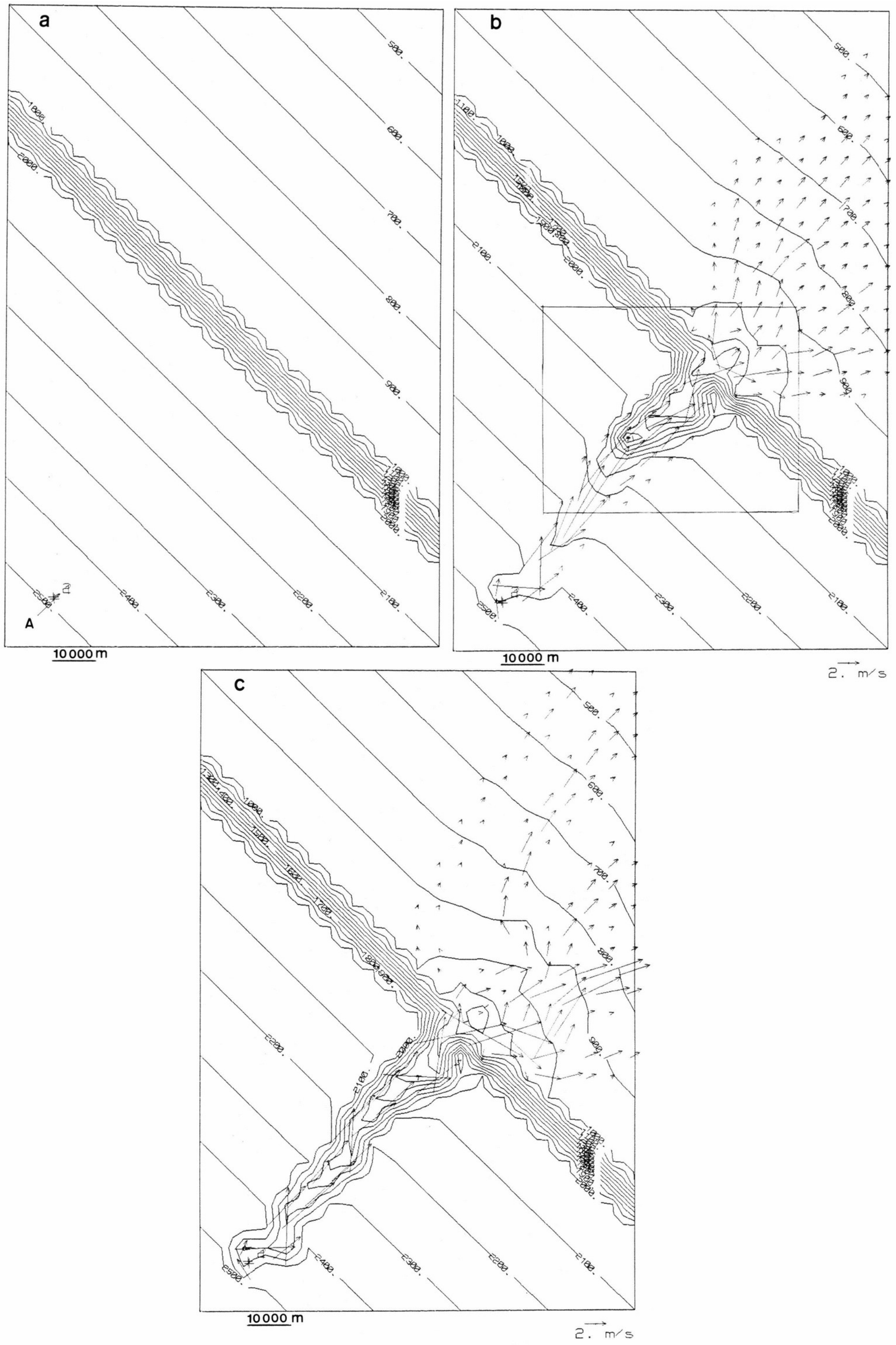

Figure 93: Topographic contour maps showing simulated reconstruction of Simpson Canyon. Contours are in meters. Area is assumed to be submerged. Topography representing deltaic deposits consists of gentle slope broken by steeper slope. Source A represents river mouth. "Best match" is found at 20,000 years, perhaps implying that paleogeographic conditions changed afterwards, preserving form of canyon by filling it. (a) Initial state, (b) at 20,000 years (area outlined can be compared to Figure 89), (c) at 60,000 years.

Due to its depth of more than 1,000 m below the depositional plain of the ancient continental shelf that surrounded it., Simpson Canyon could not have been incised solely by subaerial erosion following a drop in sea level because the maximum decline in sea level was much less than 1,000 m in the Cretaceous and Cenozoic (Vail et al.,1977). Uplift of the Barrow arch (Fig. 86) may have steepened the topographic gradient, causing the output from a river flowing into the ancient Arctic Ocean to be concentrated near the head of the canyon, progressively causing it to deepen and also causing turbidity currents to flow down the edge of the deltaic deposits. The river's flow rate and sediment input may also have been increased by climatic variations at the end of the Cretaceous. Whether uplift or climatic change was responsible, it is likely that Simpson Canyon was incised by submarine turbidity currents. Therefore, the simulation experiment involving the reconstruction of Simpson Canyon incorporated the assumption that turbidity currents carved the canyon.

Well logs and cores document that the Torok Formation and Nanushuk Group, into which the canyon is cut, consist mainly of silt with some clay and fine sand. Cores from the only well that penetrates the canyon fill (the North Simpson well in Figure 87), show that a similar material filled the canyon. Therefore, the simulation experiments involved the assumption that the sediment into which the canyon was cut as well as the sediment with which it was filled, consisted of loosely consolidated silt.

In the simulation experiment, in addition to specifying the sediment type, it was also necessary to specify the frequency, sediment concentration, and volume of the turbidity flows. Selecting the frequency of turbidity flows is difficult because the effect of frequent turbidity flows over a short period, may be nearly identical to the effect of infrequent flows over a longer period. Thus, there is large uncertainty as to the overall duration of the canyon-carving processes that formed Simpson Canyon, but the geometric form of the canyon and its deposits can be simulated with some confidence, in spite of the uncertainty.

A number of simulation runs were performed to establish he volumes and the sediment concentrations that produced a simulated canyon that best matched Simpson Canyon in both form and size. Using the hypothetical paleogeographic conditions described above, SEDSIM was not very sensitive to the initial sediment concentration. probably because sediment concentration adjusts automatically to conditions of flow. Adjustments in flow volume, however, proved to be much more important. The closest match between the simulated and the observed canyon is shown in Figures 93a through 930, which spans 40,000 years of simulated time. The specific simulation shown involves the assumption that a turbidity flow recurred every twenty years, each flow having an initial volume of 500 million cubic meters of water containing silt in suspension, with the suspended silt forming 20 per cent of the flow by weight. The best accord between the simulated canyon and the actual canyon as interpreted from seismic sections is obtained at 20,000 years simulated time (Fig. 93b). Therefore about 1,000 flows with the specifications stated above could have carved Simpson Canyon.

Conclusions

Thus, the canyon's history can be reconstructed by employing the simulation model that best matches the canyon as reconstructed from seismic sections (Figs. 89 and 90). The simulation model suggests that the canyon was carved as the channel migrated backward from the edge of preexisting deltaic deposits. After about 20,000 years (depending on the frequency of the turbidity currents). erosion ceased. Otherwise, continued erosion would have elongated the canyon further, and it would assume the form shown in Figure 93c. Perhaps the canyon-forming processes were halted by changes in environmental conditions, such as a rise in sea level accompanied by a decrease in sediment supply.

In places the floor of the simulated canyon is relatively flat, even though a resistant basement was not assumed in the experiment. The flat floor appears to have formed in response to control exerted by "base level", namely the level Of the sea floor beyond the mouth of the canyon. The canyon floor and the canyon mouth could have been expected to have formed a smooth profile as viewed in longitudinal section. Thus, the simulation experiment suggests that the "pebble shale" that underlies the actual canyon may simply coincide with the canyon floor, and that base level controlled the elevation of the canyon floor.

The simulation experiment provides a prediction about the shape and areal extent of the depositional fan formed beyond the mouth of the canyon. Figure 93b shows a relatively thin fan that slopes at low angles and spreads over a large area. The thinness of the simulated fan suggests that there is probably little oil and gas potential in the actual fan.

GOLDEN MEADOW OIL AND GAS FIELD, LOUISIANA

Golden Meadow oil and gas field is situated in southern Louisiana, in Lafourche Parish. Township 19 south, Range 21 east (Figs. 94 and 95), within Louisiana's onshore Gulf Coast oil producing region (Landes, 1970). The Gulf Coast onshore region comprises roughly the southern half of the state and is characterized by a thick sequence of Tertiary deltaic deposits that dip southward toward the Gulf of Mexico. The deltaic deposits include a shale sequence deposited offshore that is overlain by interbedded sand and shale that probably represent a near-shore environment (Jones et al., 1954). Oil and gas reservoir rocks in the Gulf Coast district range in age from Upper Cretaceous in the north to Pliocene in the south. The southern part of the district, in which Golden Meadow is located, has been the most productive area in the state (Limes and Stipe, 1959). At Golden Meadow, hydrocarbons are produced from shallow Miocene and Pliocene units.

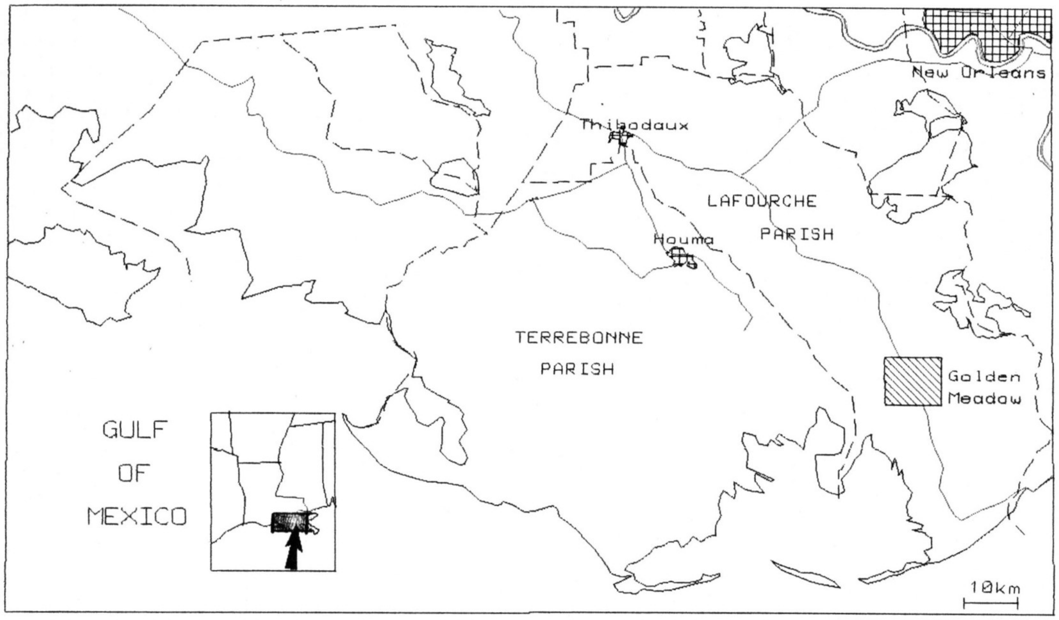

Figure 94: Index map showing location of Golden Meadow oil and gas Field.

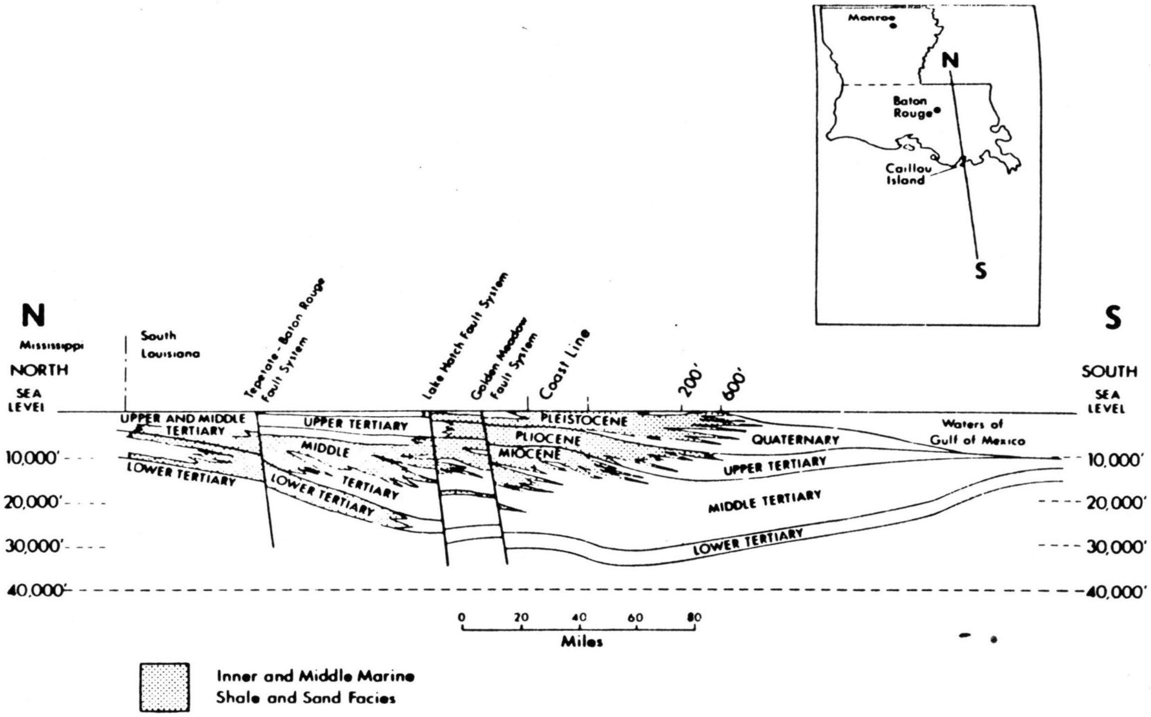

Figure 95: Schematic regional section through Louisiana, onshore and offshore, showing configuration of sedimentary sequence in Gulf Coast. From Jones (1954).

Well Data

Many wells have been drilled at Golden Meadow, 55 of which were available for this study (Fig. 96). All of the available wells reach depths greater than 9,000 feet. While faulting affects the stratigraphic sequence penetrated by the wells. it is possible to correlate well logs across the faults when persistent and easily recognizable units are present. One such unit is the "8,900 foot sand" (Fig. 97), named because it occurs at depths of about 8.900 feet, and can be identified in all the wells that reach that depth. The "8,900 foot sand" is not productive, but was used in this study because it can be easily recognized, thus facilitating comparison with the deposits simulated by SEDSIM.

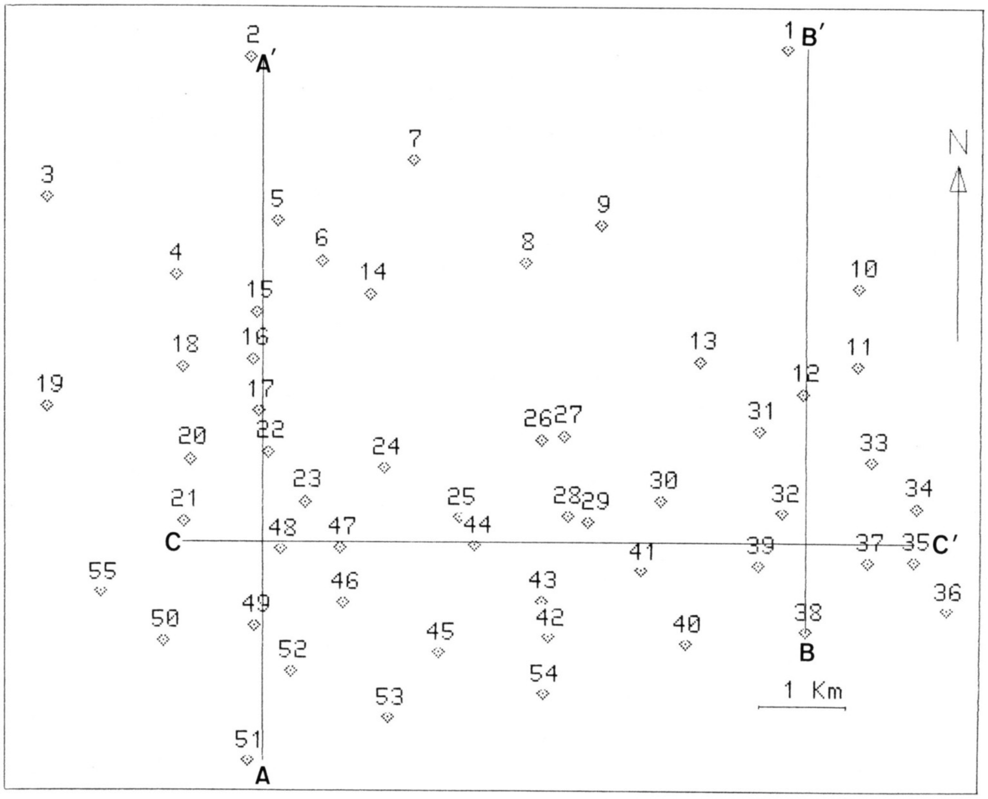

Figure 96: Map showing location of wells in Golden Meadow field used in this study.

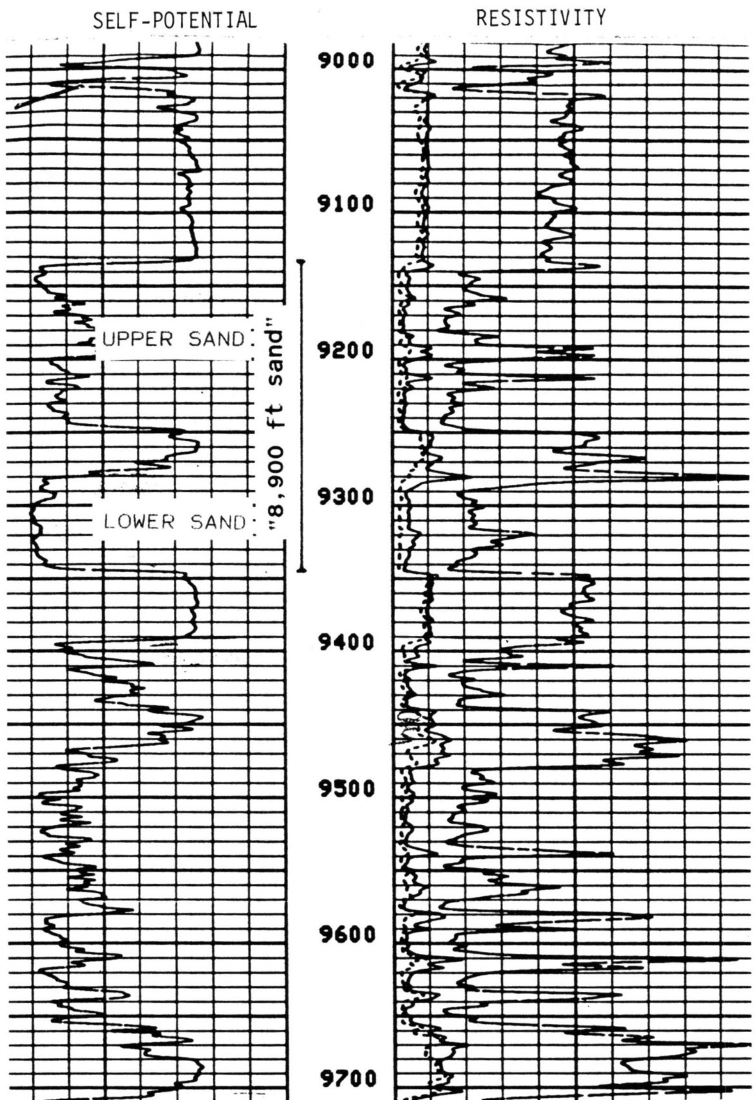

Figure 97: Segment of petrophysical log of well "22" in Golden Meadow field. showing upper and lower sand units that form "8,900 foot" sand.

Geologic Setting

Wells drilled at Golden Meadow reveal a monotonous sequence of fine sands interbedded with silts and clays. The finer sediments often have a high organic content. A few wells have reached depths of up to 20,000 feet, and show that sands are present mostly in the upper 10,000 feet. The upper. sandy part of the sequence is Miocene or younger in age. The "8.9O0 foot sand" lies within the fleming Group of Miocene and Pliocene age.

The sedimentary sequence at Golden Meadow Field was affected by post depositional faults. some of which may be related to salt piercement domes (Halbouty, 1979). Growth faults also may be present. but are not very important at the level of the "8,9O0 foot sand". Although the presence of faults inhibits direct comparison between structural reconstructions and features simulated by SEDSIH, stratigraphic reconstructions from well logs can be compared readily with simulated deposits, provided that growth faults have not significantly altered deposition patterns. Even if growth faulting has been important, the general characteristics of the sedimentary sequence in the vicinity of the"8,9O0 foot sand", such as the proportion of sand and the areal extent of individual sand lenses, can be simulated by SEDSIM.

Features simulated by SEDSIM can be compared with actual geologic features based on stratigraphic well-log correlations (Figs. 98 and 99). Well logs (Figs. 97, 98. and 99) show that the "8,900 foot sand" actually consists of an upper and a lower sand separated by clay. Both sands tend to thin southward, away from the ancient shore. Although the "8,90O foot sand" persists throughout the Golden Meadow area, its thickness and sand content vary considerably. Part of the sequence containing the "8,90O foot sand" was simulated using SEDSIM, with the purpose of test ing SEDSlM's predictions of the areal distribution of sand thickness and sand content. If applied to producing sand units, SEDSIM used in combination with structural information, might suggest locations for additional exploitation wells.

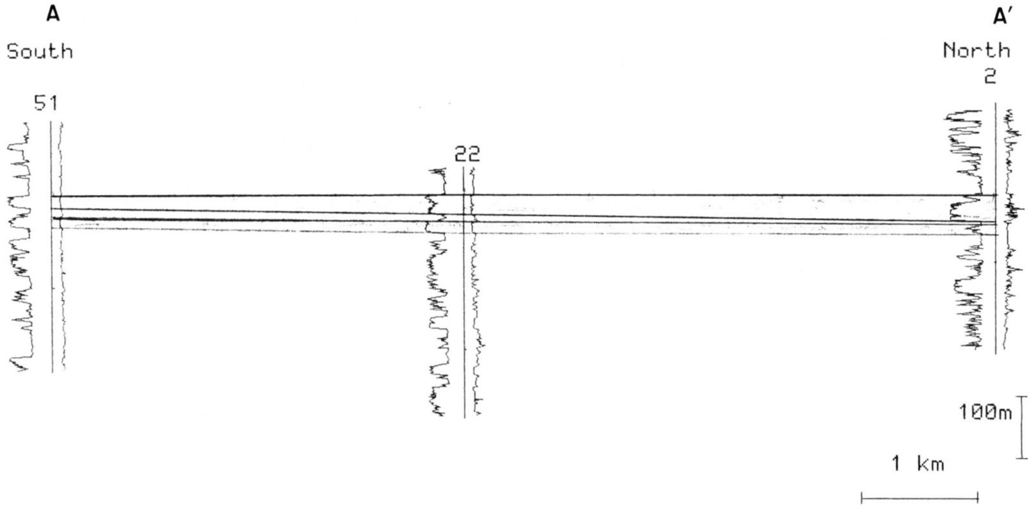

Figure 98: North-south section A-A'. showing stratigraphic correlation of top of "8,900 foot sand", based on logs of three wells, and used together with section B-B' (Figure 99) to adjust simulation model to reconstruct observed sedimentary sequence. Trace is shown in Figure 96.

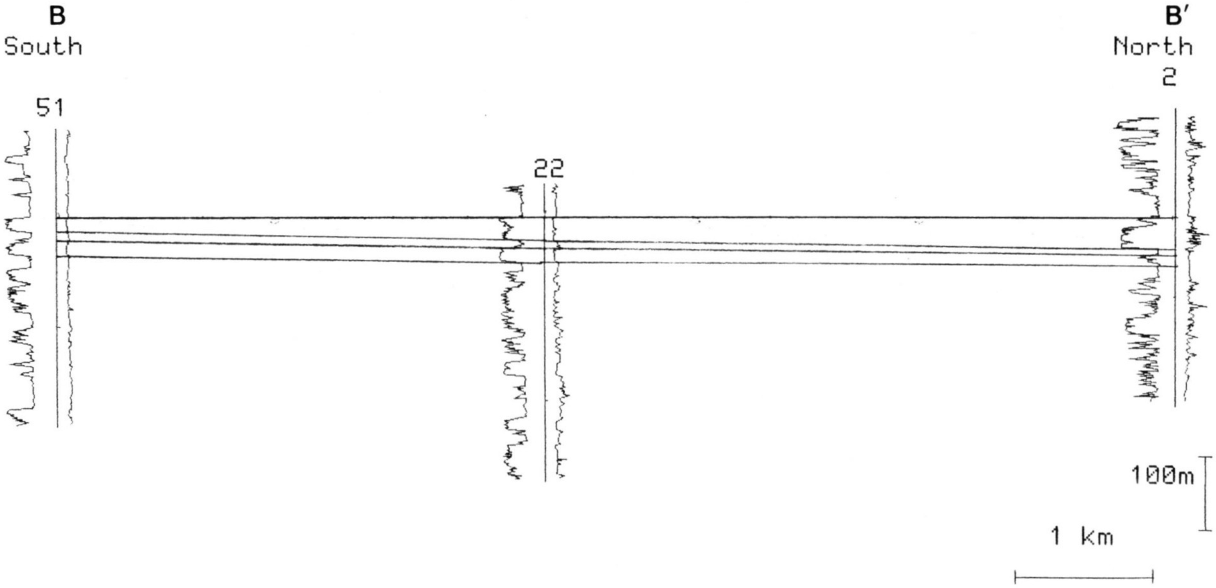

Figure 99: North-south section B-B', showing stratigraphic correlation for top of "8,900 foot sand" based on logs of three wells, and used together with section A-A' (Figure 98). to adjust simulation model to reconstruct observed sedimentary sequence. Trace is shown in Figure 96.

Simulation Experiments at Golden Meadow

Simulation experiments involving reconstruction of beds in the Golden Meadow area were performed to evaluate SEDSlM's ability to predict the shape and areal extent of sand bodies. The simulated stratigraphic interval extends from about 200 feet below. to 100 feet above. the "8.9O0 foot sand". Because Golden Meadow has been extensively drilled, it is possible to adjust the simulation parameters utilizing only a few wells, and then compare SEDS1M's predictions by utilizing information from the remaining wells. The information from only six wells in two north-south sections (sections A-A' and B-B' in figures 96, 98, and 99) was used to adjust the model. The remaining wells were used to verify SEDS1M's predictions after adjusting input parameters with these six wells.

Although the multi-sediment model was used, only two sediment types, sand and clay, were assumed to be present, thereby increasing computation speed. The area simulated is square, 65 km on a side, or about seven times larger in linear dimensions than the Golden Meadow field. The reason for using such a large simulated area is that it may permit us to establish the geographic location of the Golden Meadow field within the ancient deltaic deposits (i.e. whether Golden Meadow's deposits formed onshore, offshore, or on or between major depositional lobes, etc.), while at the same time ensuring that the simulated deposits representing Golden Meadow field's sequence of beds formed far enough from the edges of the simulated area to avoid artificial thinning of the simulated deposits due to boundary conditions.

The initial topography in the Golden Meadow experiments was assumed to be similar to that of the Gulf of Mexico, involving a very gentle slope onshore, and a slope of 5 m per km offshore (fig. 100). A steady fluid/sediment source representing the ancient Mississippi River was placed onshore. The experimental runs involved 50.000 years simulated time. Sand-to-clay ratios, as well as ratios of sediment discharge to water discharge, were obtained from data for the modern Mississippi River (Table 11) as a first approximation, hopefully avoiding unrealistic "source effects", such as those described in Chapter IV. Experience in simulating deltas described in Chapter IV was also used to estimate input parameters that govern the time-extrapolation techniques employed.

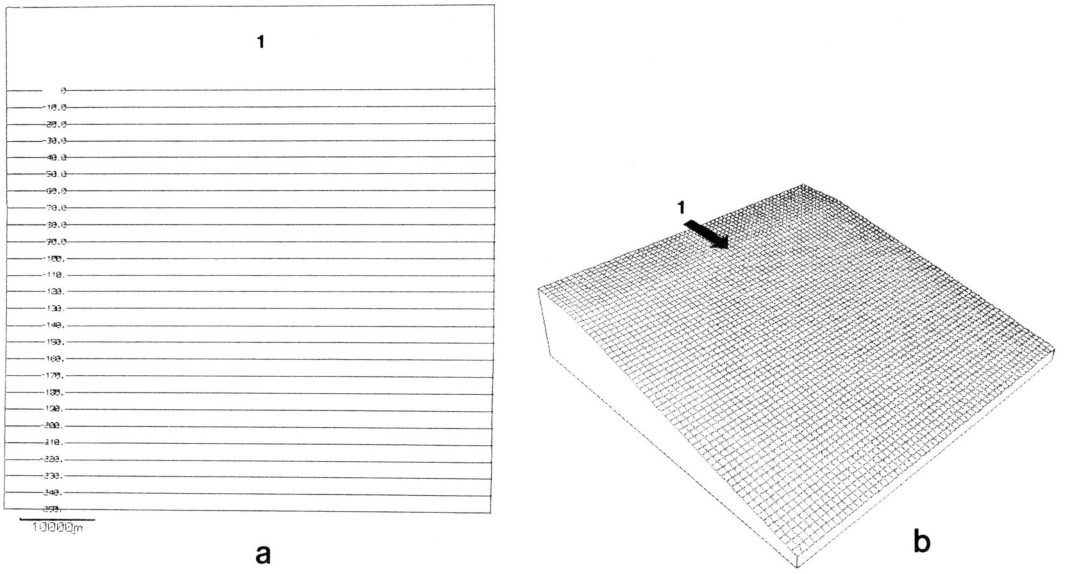

Figure 100: (a) Contour map and (b) fishnet diagram showing initial topography in simulation experiments designed to reproduce deposits of "8,900 foot sand" at Golden Meadow Field.

Table 11: Measured sediment discharge of various particle sizes (in columns) versus rates for water discharge (rows) in modern Mississippi delta. Particle diameters defining boundaries between sediment fractions are given in small boxes. Gravel, sand and coarse silt are grouped into single "coarse" category, while clay was represented as "fine" sediment type in SEDS1M's experiments to simulate sedimentation at Golden Meadow. Table compiled using information from Trowbridge (1930), Saxena (1976), and Perlmutter, personal communication (1987).

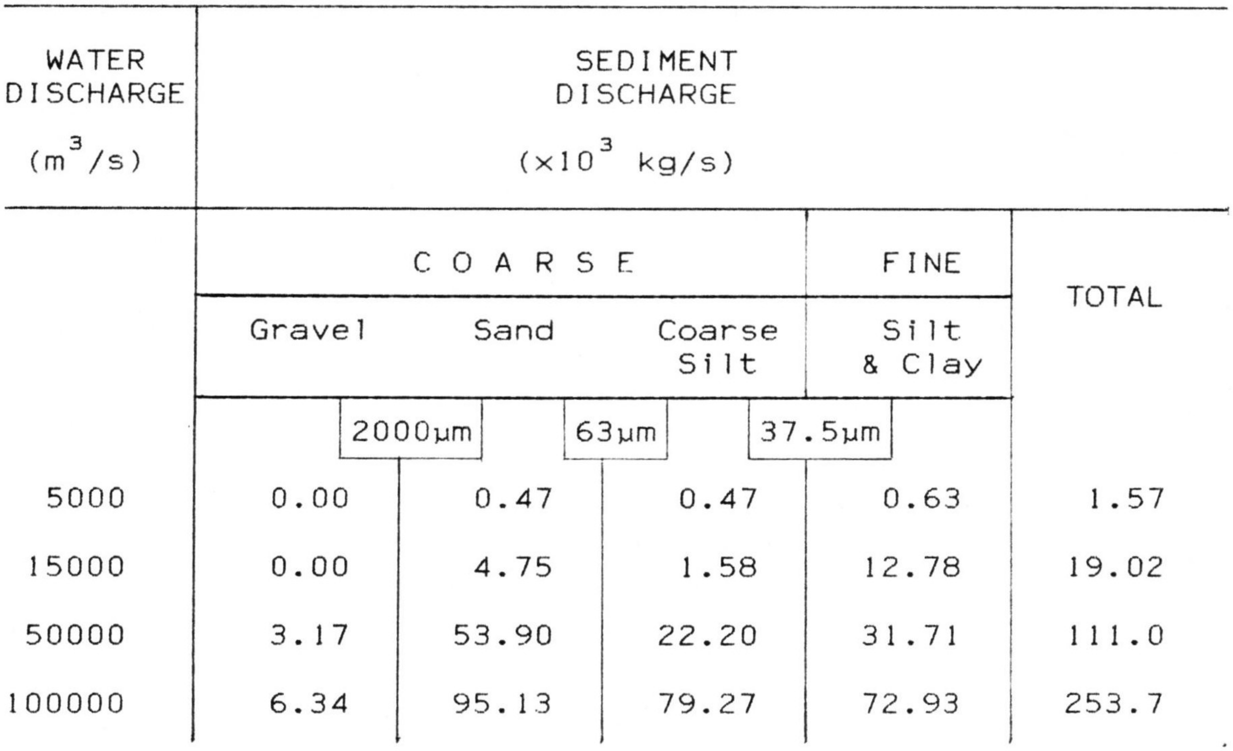

WATER DISCHARGE (m^3/s)	SEDIMENT DISCHARGE ($\times 10^3$ kg/s)				
	COARSE			FINE	TOTAL
	Gravel	Sand	Coarse Silt	Silt & Clay	
	2000µm	63µm	37.5µm		
5000	0.00	0.47	0.47	0.63	1.57
15000	0.00	4.75	1.58	12.78	19.02
50000	3.17	53.90	22.20	31.71	111.0
100000	6.34	95.13	79.27	72.93	253.7

After the initial paleotopography and the proportions of sediment with respect to flow rates had been selected, the main variable that still needed adjustment was the flow rate itself. Various water-discharge rates were employed, accompanied by rates of sediment discharge inferred from data for the modern Mississippi River (Trowbridge. 1930;Saxena, 1976; and Perlmutter, personal communication. 1987) before a reasonable match between the simulated deposits and the actual deposits was obtained. The initial experimental run (Fig. 101) involved a discharge of 5,000 cubic meters of water per second, which is about one third the discharge of the Mississippi River at normal stage today. The simulated river's volumetric sediment concentration was assumed to be 0.00025, which corresponds to a sediment discharge of about 1.570 kilograms per second. The sediment was assumed to consist of 40 percent clay (corresponding to "fine" sediment in Table ll), and 60 percent sand ("coarse" sediment in Table 11). The result obtained in the first experiment yielded a sequence containing more clay than the sequence observed in well logs in the stratigraphic interval of interest. The flow was then progressively increased to 50,000 cubic meters per second. The total sediment concentration increased to 0.0018, corresponding to a sediment discharge of 111,000 kg per second, which accords with values for the modern

Mississippi River (Trowbridge. 1930; Saxena, 1976; Perlmutter. personal communication, 1987).

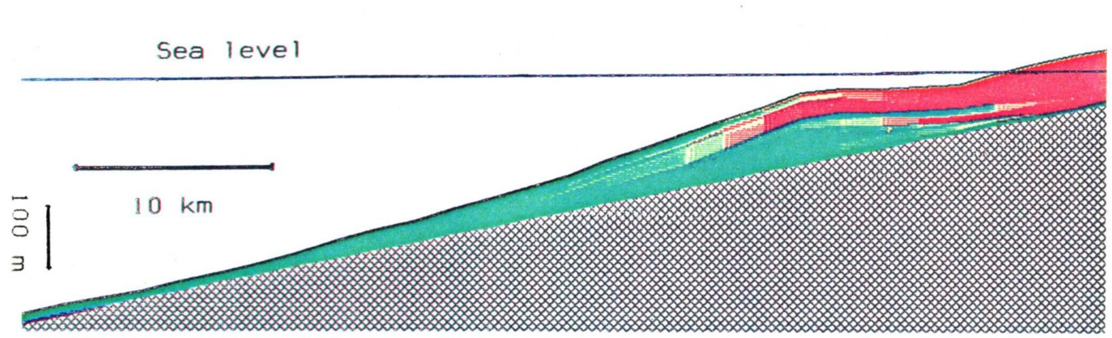

Figure 101: Section perpendicular to shoreline through simulated deltaic deposit formed by initial run using 5,000 cubic meters per second of water, and 1,570 kilograms per second of sediment composed of 60 percent sand and 40 percent clay. Simulated elapsed time is 50,000 years. Simulation has deposited more fine sediments than actual sequence observed in well logs.

The study involved ten simulation experiments. The results of each experiment were compared with the sequence shown by sections A-A' and B-B', with the objective of selecting the simulated sequence that best matches the actual sequence as inferred from well logs. The quality of each match was judged subjectively rather than quantitatively, due to the complexity of the variables involved in the comparison, which included proportion of sand in the simulated interval, thickness and shape of individual sand and clay lenses. and areal variations in sand content.

One of the best matching simulated deposits is shown in figure 102. It involved a flow rate of 7,000 cubic meters per second, and a total sediment concentration of 0.0005 or a sediment discharge of 5,000 kg per second. Although the proportion of coarse and fine sediments approximately matches the actual deposits, the sand lenses in the simulated sequence have very limited extent along the direction of progradation. Therefore the flow rate was increased to 10,000cubic meters per seconds without changing the sediment input (thus reducing sediment concentration to 0.00037) In an attempt to cause the coarse sediments to be carried farther out into the basin. The increased flow rate yelded the expected results, producing amuch better fit with the well-long sections then the previous experiments. A longitudinal section of the deposits thus produced is shown in Figure 103.

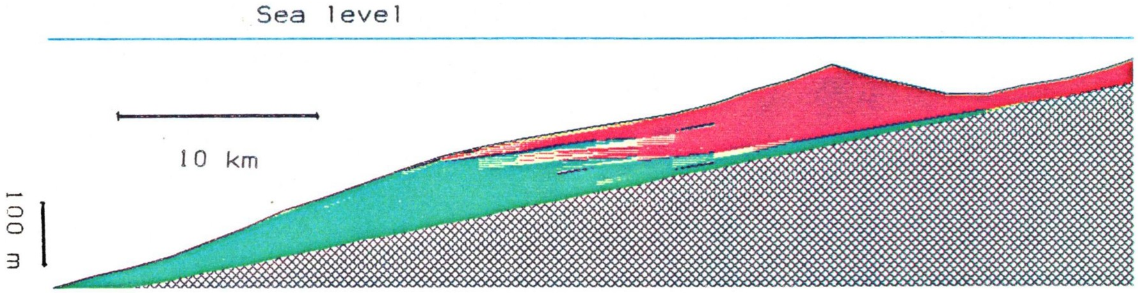

Figure 102: Section through simulated deltaic deposit after 50,000 years have elapsed, using water discharge of 7,500 cubic meters per second, and sediment discharge of 5,000 kilograms per second. Section shows that sand beds pinch out rapidly moving away from shore.

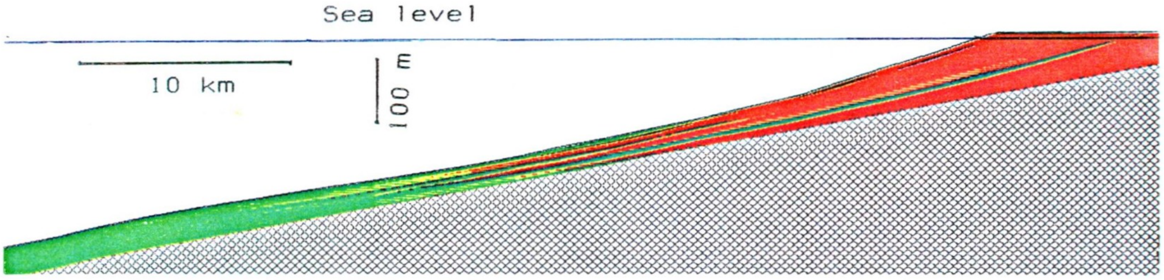

Figure 103: Section through simulated deltaic deposit that best fits actual deposits as observed in well logs. Experiment involves 10,000 cubic meters per second of water, and 5,000 kilograms per second of sediment.

Because the area simulated was much larger than the Golden Meadow field, the location of the Golden Meadow field within the overall simulated area had to be shifted about to obtain a god match between actual ad simulated area and simulated deposits, wich were then compared with the stratigraphic reconstructions based on logs of actual wells shown in sections A-A' and B-B' (Figs. 98 and 99).

Several sections and maps of the "best fitting" simulation experiment are displayed in Figures 104 through 111. Although these simulated deposits represent the best fit in the range of conditions tested. The thicknesses of sand and clay beds are systematically thinner than the actual deposits, although expansion of the vertical scale of the simulated deposits by a factor of two further improves the match. The discrepancy in overall thickness may be due to the fact that SEDSIM does not (in its present stage of development) incorporate either isostatic compensation or compaction of sediments due to load. both of which would tend to allow increased thicknesses of sediment to accumulate.

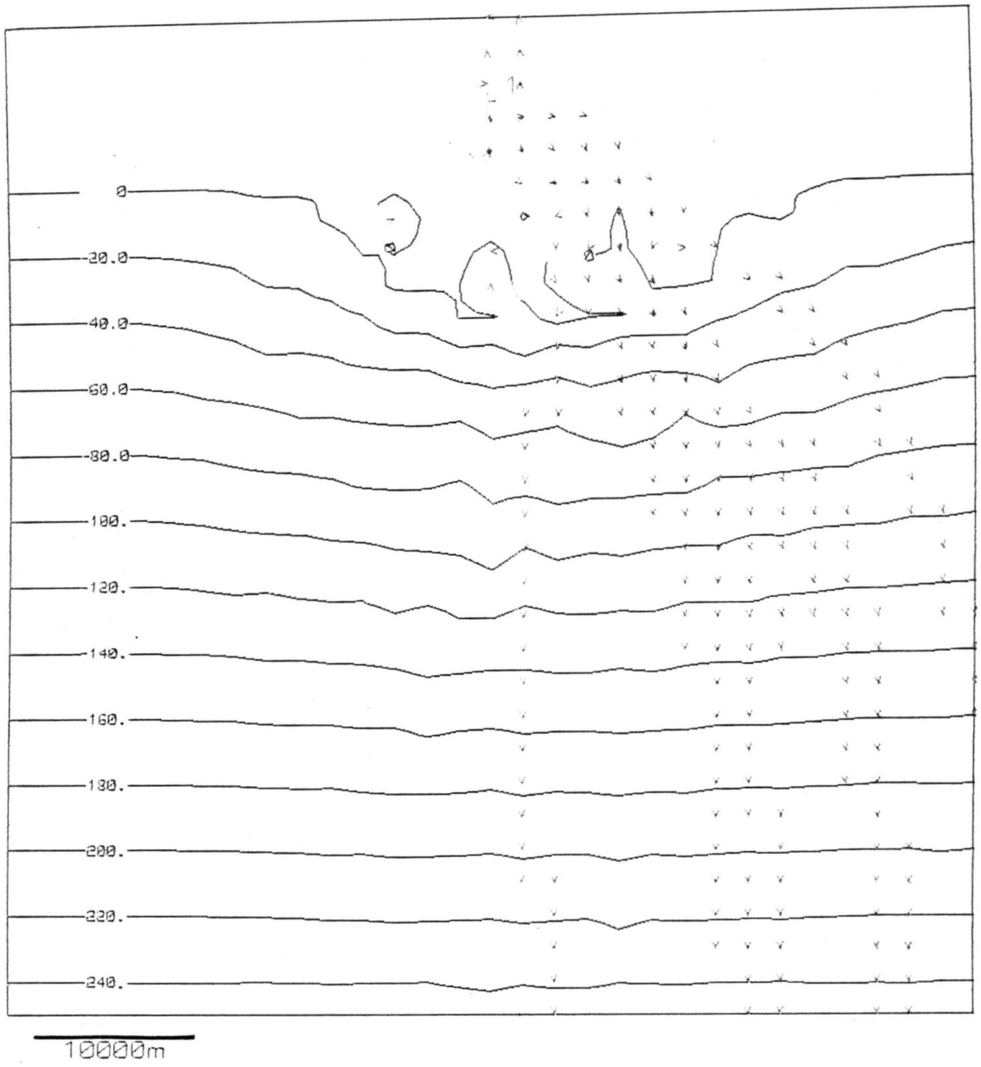

Figure 104: Contour map showing deposit produced by “best fit” model after 50,000 years simulated time.

Figure 104 shows a topographic contour map of the "best matching" deltaic deposits after 50,000 years of simulated time have elapsed. The map shows that the shoreline has prograded a distance of about 30 km. Three different lobes can be identified. Sections through the simulated deposits can be compared to the well-log sections A-A' and B-B' (Figures 98 and 99). Figures 105 and 106 show the well-log sections superimposed on the corresponding sections of the simulated deposits. Two more intermediate wells were added to each section to show that SEDSIM could predict their characteristics.

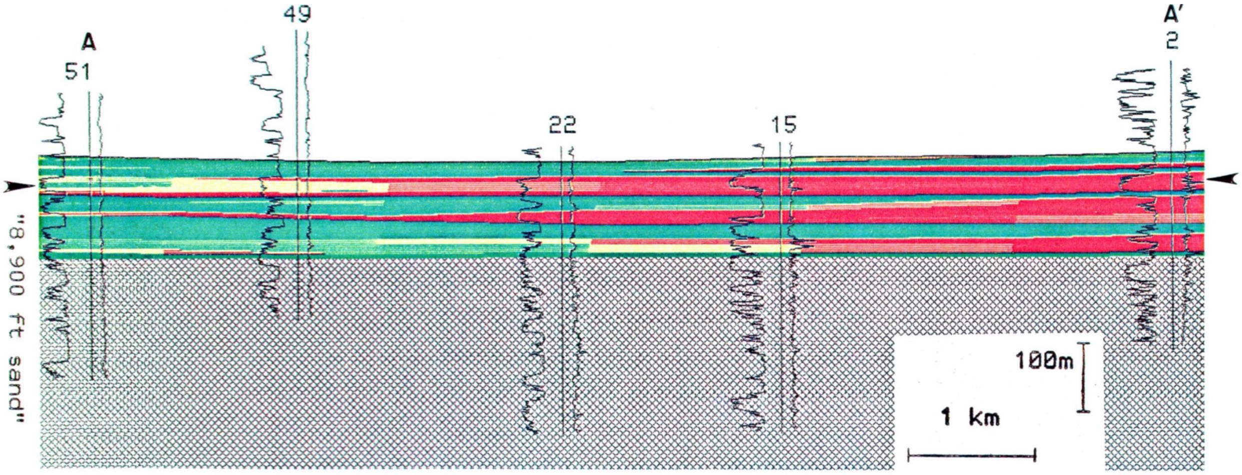

Figure 105: Hell logs from section A-A' (trace shown in Fig- ure 96) superimposed on corresponding section through simulated deposits. Logs from wells "49" and "15" were not used to adjust the model's input parameters, and thus illustrate SEDSIM's ability to predict configuration of sedimentary sequence between existing wells.

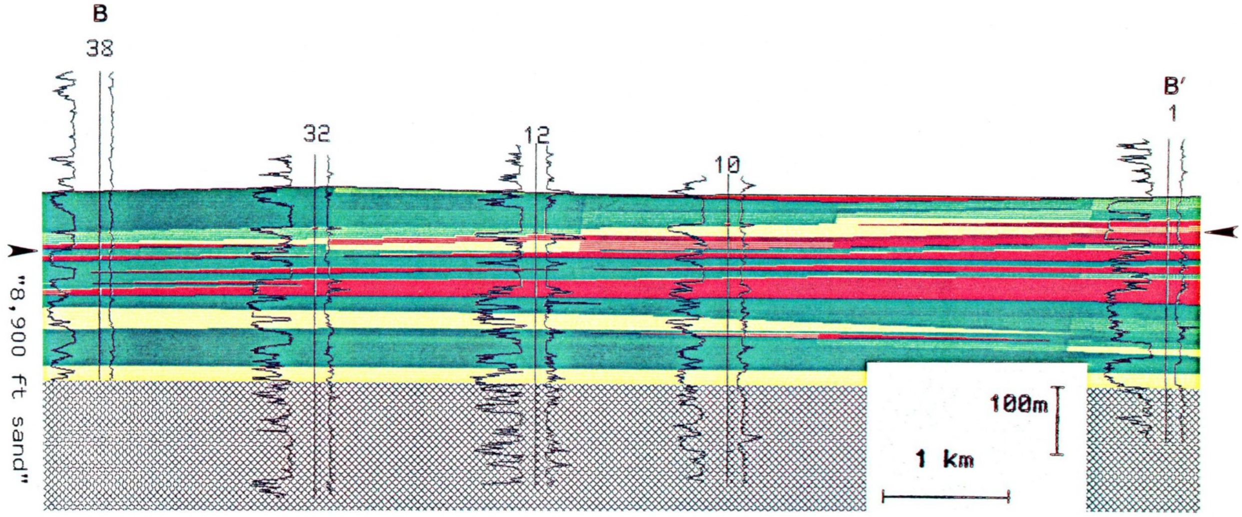

Figure 106: Neil logs from section B-B' (trace shown in Figure 96) superimposed on corresponding section through simulated deposits. Logs from wells "32" and "10" were not used to adjust the model's input parameters.

The simulated deposits obtained can be "explored" by intersecting them with cross sections and by producing facies maps drawn by SEDSHO3, the graphics display program. The facies maps in Figures 107 and 108 display proportions of sand in an interval of 200 feet below the top of the simulated "8,900 foot sand". The maps show a sand lens (indicated "X" in Figure 108) that is not traversed by any of the two sections used in adjusting the model (sections A-A' and B-8'). An east-west section through the southern part of the simulated deposits (section C-C' in Figure

I09) shows that the simulated "8,9O0 foot sand" is considerably thicker in the south central part of the simulated Golden Meadow field. Correlations based on the six wells used to adjust the model do not necessarily suggest that the actual sands thicken here, and instead may imply that the sands tend to thin southwards. The log of an actual well drilled where SEDSIM "predicts" locally thicker sands (well 44). appears to substantiate SEDSIM's prediction. Figure 110 compares logs from well 44 in detail by superimposing them on an enlarged column of the simulated deposits. Although the match is not exact, the general characteristics of the sedimentary sequence at the site of well 44 are predicted by SEDSIM. Figure 111 displays the sequence predicted by SEDSIM compared with well "35", also showing the correspondence between observed and predicted sequences.

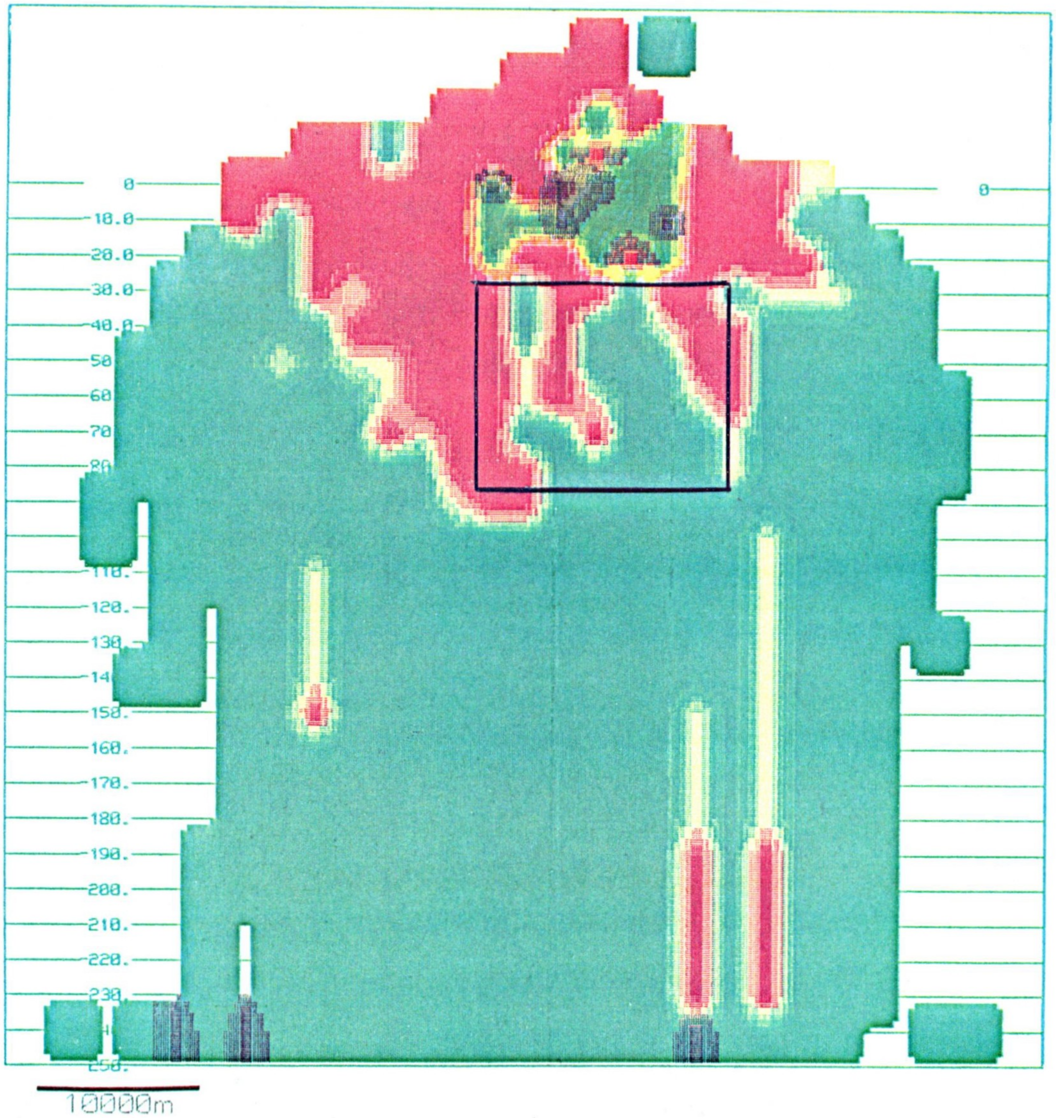

Figure 107: Facies map of simulated Golden Meadow deltaic deposits. Map shows total sand proportion in 30 m interval underneath top of "8,900 foot sand". Red indicates sediment containing over 80 percent sand whereas green indicates less than 20 percent sand. intermediate colors (orange, yellow, and yelIow-green) indicate intermediate proportions of sand at intervals of 20 percent. Box outlines area enlarged in Figure 108.

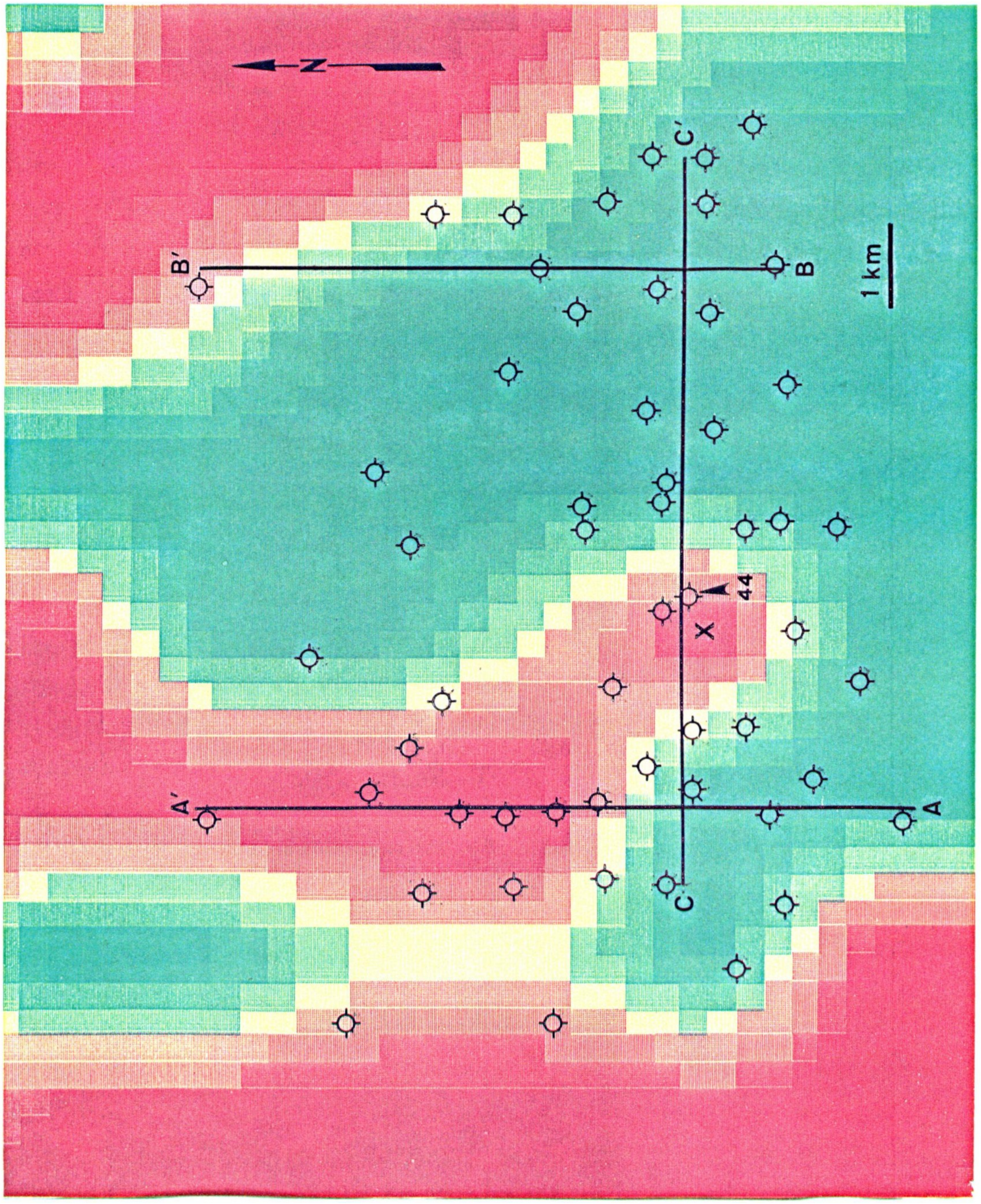

Figure 108: Enlargement of facies map of simulated Golden Meadow deltaic deposits, showing sand lobe that is not penetrated by wells used for calibrating the model's input parameters.

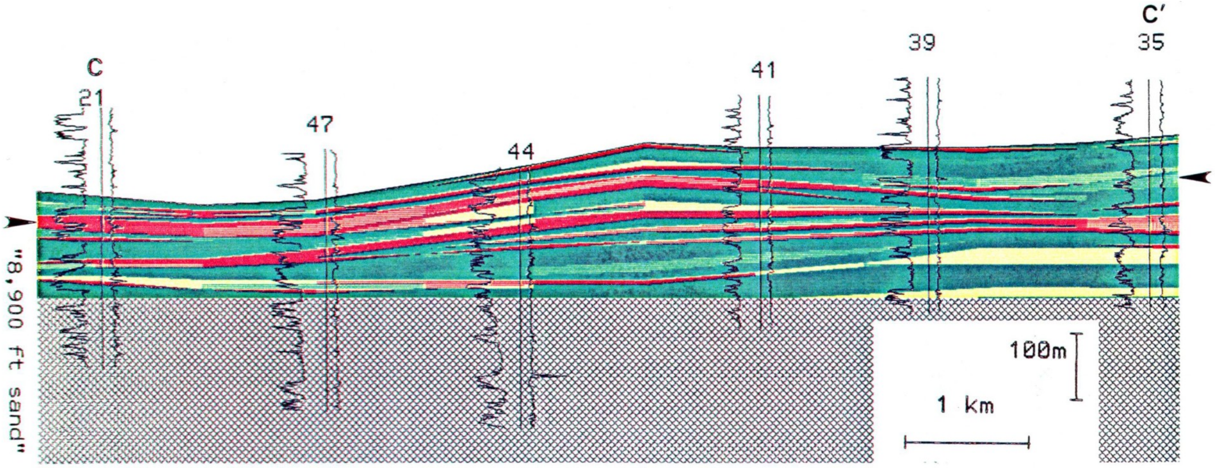

Figure 109: Hell logs forming section C-C' (trace shown ln Figure 96) superimposed on section through simulated deposits. None of well logs shown here were used to adjust model's input parameters. Hell "44" confirms increased thickness of "8,9O0 foot sand" at that locality, as predicted by SEDSIM.

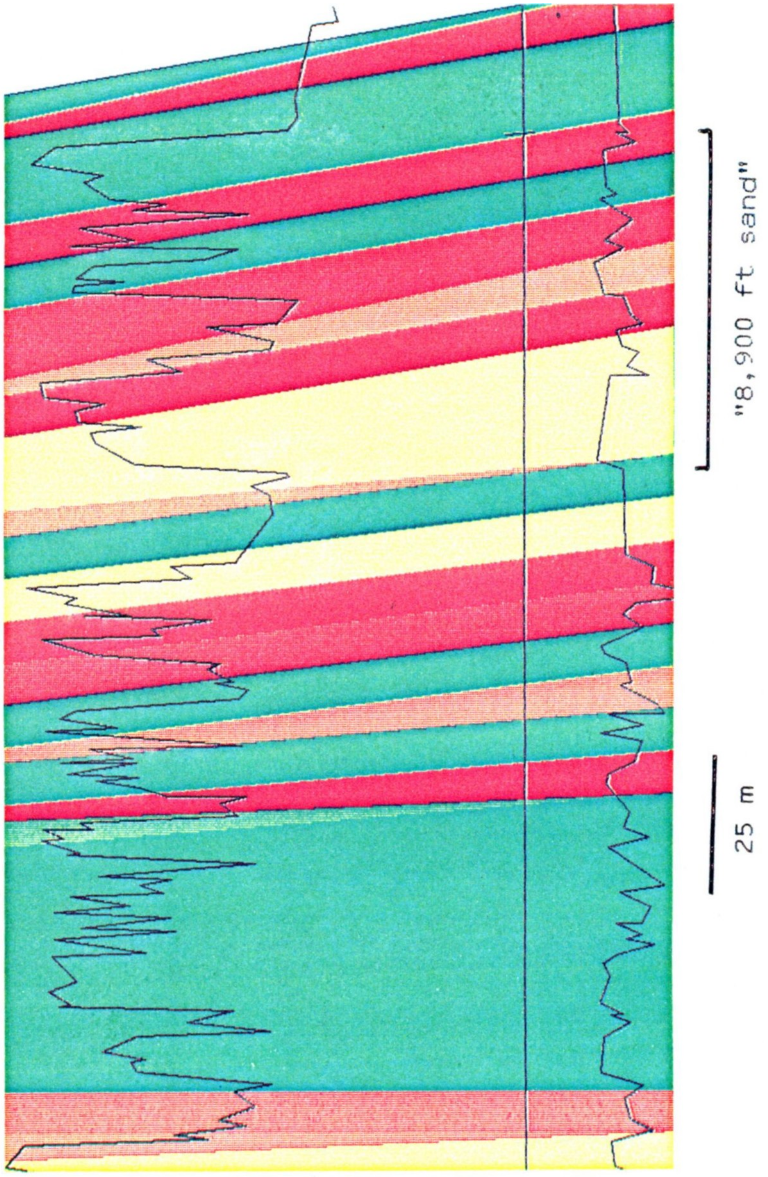

Figure 110: Detailed comparison between simulated sequence and well log 44. Location is shown in Figure 96.

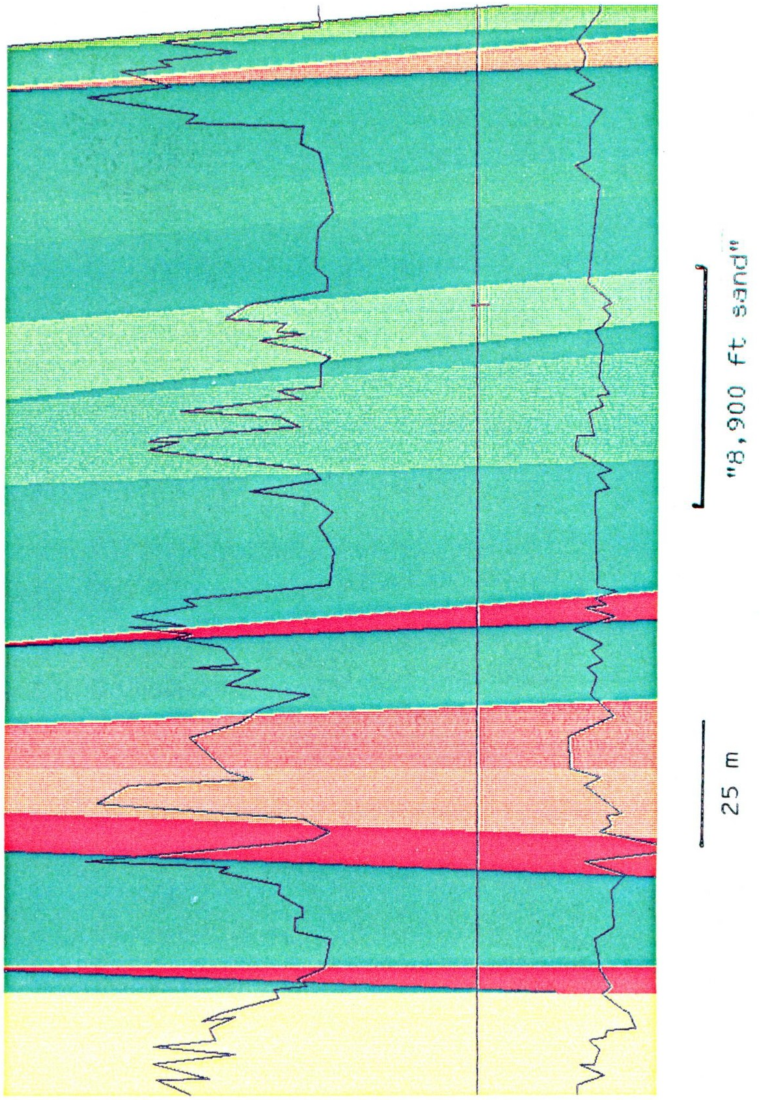

Figure 111: Detailed comparison between simulated sequence and well log 35. Location is shown in Figure 96.

Assessing the Results of the Golden Meadow Experiments

The set of conditions for the simulation experiment that produces the best accord may yield a close approximation to the actual environmental conditions at the "8,900 foot sand" in Golden Meadow during part of Miocene time. Thus. The simulation suggests that the water discharge rate was about 10,000 cubic meters per second. and the sediment discharge was 5,000 kilograms per second.

Conclusions about water and sediment discharge in ancient systems are hard to verify and of little direct use in petroleum exploration or exploitation. but are potentially very useful for paleogeographic studies, which can aid indirectly in exploration and exploitation. SEDSIM has also yielded valuable predictions about the geometry of the sedimentary deposits that has practical application. Also the continuity of sand lenses between wells could be studied with SEDSIM, providing important information in an exploitation situation. Other characteristics of sedimentary deposits predicted by SEDSIM, such as the areal extension of the "8,900 foot sand" beyond the boundaries of the Golden Meadow field, are potentially useful for further exploitation.

Chapter VI
SEDSIM'S LIMITATIONS AND ITS POSSIBILITIES FOR FURTHER DEVELOPMENT

SEDSIM is extremely flexible in permitting Flow and sedimentation to be simulated in a variety of conditions over relatively long periods of time. SEDSIM's flexibility, however, has important limitations that must be considered whenever SEDSIM is used in attempting to reconstruct sedimentary sequences. SEDSIM's limitations can be classified into three main categories:

(1) Knowledge of modeling parameters.

(2) Model's adequacy in representing an actual system.

(3) Computing power.

Knowledge of Modeling Parameters

Even an imaginary laboratory in which sedimentation experiments could be conducted at full scale would still be limited in its ability to predict the configuration of sedimentary deposits formed in the past, because conditions under which ancient deposits were formed can never be fully known. Accurate predictions would require assumptions regarding the model's parameters. such as the location of fluid sources, the composition of sediment carried by flows, and a basin’s ancient geometry. Thus, limitations stemming from a lack of knowledge about modeling parameters cannot be solved directly by SEDSIM. It is possible, however. to use a simulation model to establish ranges for ancient conditions by performing repeated simulation experiments, and then comparing the simulation's results with observations of features of actual sedimentary deposits. Though it is possible that different environmental conditions may produce similar results, geologic constraints may restrict the possibilities so that a reasonable set of assumptions can be employed.

Predictions about the past using "Forward" modeling require some assumptions about the past. It would be ideal, of course, to have a simulation model that could run "back-wards", and reconstruct the past from information about the present. However. it is virtually impossible to devise an intricate process model that could be reversed so as to run "backwards", as discussed below.

Boundary conditions:

Boundary conditions form an important part of the modeling parameters. Boundary conditions constitute a form of limitation arising from the inability to simulate a large system such as the entire earth. Even a sedimentary basin may be too large to simulate as a whole. Thus. Inevitably, boundaries must be established. A physical model, such as a sand table, is so affected by these limitations. In both mathematical and physical models, we must make arbitrary assumptions about how the "outside" world affects the small segment that we have chosen to simulate.

SEDSIM requires assumptions about how processes operate at the edges or geographic boundaries of the system being simulated. Fortunately, we can confine the effects of sedimentation at boundaries to a relatively narrow zone adjacent to the boundaries, but sometimes boundaries affect the entire area represented by the simulation. For example, after a long period of simulated time, it is possible that a state of equilibrium may be reached within a prescribed set of boundaries. In equilibrium, the sediment that moves through a boundary and enters the system at the sources may be equal to that which leaves the system at the edges, and the sedimentary deposits may show little further change. However, if the boundaries of the simulated area were moved so that the area is enlarged, the deposits would continue to form, and the sedimentary sequence in the entire area may be thicker even though the rate of inflow of sediment is unchanged.

When SEDSIM supplies fluid and sediment to a simulated area. it represents an input to the area from the "outside" world. If the flow conditions and the sediment load at a source are not in fluvial equilibrium with the local slope, or with the grain size and fall velocities of the sediments, then "either a steep mound or a deep hole may be formed near the source. Only at some distance downstream will the sedimentary deposits be realistic in form, because the flow must travel for a distance before equilibrium is locally attained.

The Model's Adequacy in Representing an Actual System

Dynamic process models are necessarily simplified versions of actual processes. Hopefully the simplification does not cause the model to perform unrealistically. Usually. however, realism is compromised because of the approximations that are required if the model is to be operated at all. One of the most important approximations in SEDSIM is the reduction of flow to two horizontal dimensions. This simplification makes it possible to represent flow without undue computer resources, but limits some of SEDSIM’s applications. For example. sedimentary features that are affected by vertical movement within a flow, such as ripples of small height with respect to flow depth, cannot be reproduced directly by SEDSIM.

There are other aspects in which SEDSIM provides only a crude approximation of reality. For example. the sediment-transport equations used by SEDSIM are extremely simple so as to minimize computer time. Experimentation is needed to determine whether the use of more accurate and lengthier sediment-transport equations would be Justified.

The "discretization" of a model to represent time as a series of steps and to represent continuous functions as cells of grids, also constitutes an approximation with respect to the actual system. The undesirable effects of such approximations can be reduced by making grid cells smaller and by using shorter time increments, although the price for such reductions is generally a large increase in computing time.

Computing Power

SEDSIM has limitations that arise from limits on the amount of computer power and computer time that can be devoted to SEDS1M’s operation. Most of the simulation experiments with the multi-sediment model involved about 5000 fluid elements. a two-dimensional horizontal 30-column by 30-row grid that contains 900 cells, and a three- dimensional grid containing 31 rows, 31 columns, and 800 layers that represents a total of 768,800 sediment-type cells that contain sediment that has been deposited. How- ever. the memory requirements for the multi-sediment simulation program involve only about 1/2 megabyte of core memory, because measures to minimize memory requirements are employed. Thus. grids can readily be enlarged For greater resolution, but memory requirements will increase rapidly, as will computing time.

Computing time is an important consideration in using SEDSIM. The most complex experiment attempted to date involves simulation of a large delta for an interval of 50,000 years. The experiment required about l2 hours of continuous CPU time on a Gould 32/77 computer. The 32/77 is roughly the equivalent to a VAX 750 computer in performance. The same experiment requires only two hours on a Gould PN9080 computer, the computer presently available for SEDSIM’s development at Stanford.

SEDSIM seems to be more limited by computer speed than by computer memory. Most personal computers. For example, have enough memory to run simple experiments with SEDSIM. but the execution times involved would be prohibitively large, perhaps aggregating weeks. As faster computers are developed, SEDSIM's usefulness will increase. Furthermore, computers that have the capability of performing a number of operations simultaneously (i.e. in parallel) are becoming increasingly available. SEDSIM's code could be rewritten to take advantage of parallel processing, perhaps providing up to a 100-fold increase in processing speed. Under these circumstances. the simulation of a large delta for 50,000 years of geologic time might take only a few minutes. Furthermore. such an increase in speed could be accompanied by graphic output generated while a simulation experiment is in progress. thereby greatly increasing the user's control over the simulation's conditions, permitting alternative parameters to be more efficiently tested during a simulation experiment.

FURTHER DEVELOPMENT OF SEDSIM

Many improvements to SEDSIM are possible, as well as development of other process-simulation models that could interface with SEDSIM, some of which are currently underway at Stanford.

User Interface

When running sedimentation experiments, the user must "interface" with SEDSIM by providing parameters for the simulation and for graphic displays. Thus, while SEDSIM is very general, it also requires information that can be lengthy to keystroke into an input data file. A two- dimensional grid of information representing topography at the start of an experiment, For example, can be tedious to enter manually, and three-dimensional grids containing types of sediments can be even lengthier to enter manually. These tasks would be easier with the use of improved procedures for entering data. For example, a program that "constructs" a grid from contour lines that are entered by means of a digitizing tablet and "mouse" or cursor could provide SEDSIM with the initial topographic grid, as well as the grid representing the structure of the top of the basement. A digitizing tablet and "mouse" could also be used to enter locations of sources where water and sediment enter the area being simulated.

Further possibilities of varying boundary conditions while the model is running could be built into the program. For example, it may be desirable to cause a source of fluid and sediment to fluctuate so as to imitate cyclic variations in flow or sediment input as might be caused by cyclic climatic changes. At present, variations in water or sediment input require to stop the program, change the conditions, and then restart the program.

SEDSIM's output could be made easier to interpret. A program to generate synthetic well logs could linked with SEDSIM, making it feasible to compare SEDSlM's output directly with logs of actual oil wells. Furthermore, synthetic seismic sections could be produced to facilitate comparison with actual seismic sections.

Additional Modeling Capabilities

The mathematical model and computer program described here are able to simulate a large variety of sedimentary environments in which the main transporting agent is water. Within some limitations the model successfully reproduces erosion. transport, and deposition of clastic sediment by flow. But features other than major changes in flow conditions also affect the configuration of sedimentary sequences, both during and after deposition, and some could be linked with SEDSIM, as follows:

Marine currents and wave activity are important in redistributing sediment in littoral areas. The method of simulating flow employed by SEDSIM could be used to simulate waves and currents, but it is not practical to employ it for this purpose because of the large number of fluid elements that would be required. However, it is feasible to develop a separate simulation module that can be linked with SEDSIM that deals with waves and marine currents as they redistribute sediment. Such a module might employ a purely Eulerian procedure, which does not require the use of fluid elements.

The capability of simulating evaporation, and also of simulating infiltration of water into the ground, would be important when modeling sedimentary systems in arid climates. without evaporation or infiltration, lakes or large rivers might form in the simulated system, whereas they might be absent in an actual system. Both evaporation and infiltration can be simulated by providing "sinks" into which fluids disappear, in contrast to "sources", where fluids appear. In a computer program, the "sinks" could be represented by removing a certain number of fluid elements during each time increment at specified geographic locations.

Processes involving organogenic and chemical deposition also can be important in some sedimentary sequences, particularly where the generation of hydrocarbons is represented. Organogenic and chemical processes are extremely complicated, but eventually their simulation could probably be linked with clastic sedimentation processes in SEDSIM.

Folding, faulting, subsidence, uplift. and compaction affect sedimentary sequences by deforming existing sedimentary deposits, as well as influencing deposits of sediment as they are formed. Thus, if tectonic processes and compaction were incorporated in SEDSIM, its behavior should become increasingly realistic.

It should be relatively easy to incorporate crustal subsidence or uplift whose rate is predefined. A "subsidence" grid, equal in expanse and number of cells to the topograhic grid. could define subsidence or uplift rates at every grid point. During each time increment. the column of sediment at each grid point would rise or fall according to the subsidence or uplift rate for that grid point. If every grid point had the same rate of subsidence or uplift, the entire area would rise or subside uniformly. Eustatic changes in sea level could be simulated in this manner. By specifying different rates within an area, tilting, folding, and vertical faulting can be represented. Furthermore, subsidence rates could represent isostatic adjustments that compensate for crustal loading produced by deposition, or unloading produced by erosion.

Incorporating compaction into SEDSIH is more difficult than simulating subsidence or uplift. because the sedimentary column beneath each grid point must be compressed. rather than simply moved up or down as a whole. Thus, cells that contain sediment that vary in height would have to be represented, thereby increasing computer memory requirements and computational effort.

The simulation of fluids migrating through the pores in sediments as compaction takes place would also be an important addition to SEDSIM. Since SEDSIM contains three-dimensional information about the distribution of types of sediment, programs for fluid migration could be adapted to operate interdependently with SEDSlM.

It is possible to envision an extensive suite of simulation modules linked together that represent processes in sedimentary basins, creating a large simulation program (fig. 112). Thus. such program should be able to reproduce sedimentary features that result from complicated interactions or interdependencies that exist between clastic sedimentation and a host of other geologic processes.

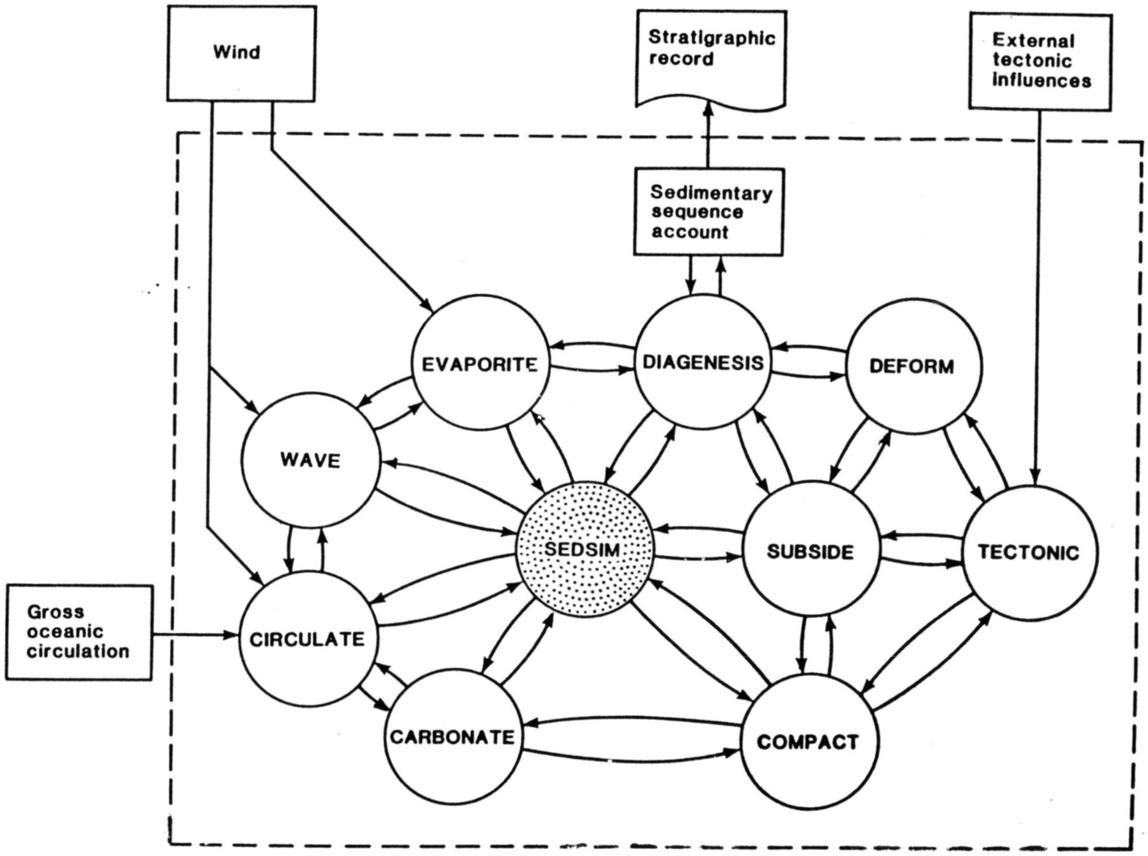

Figure 112: Diagram showing linkage between various modules that could be added to SEDSIM in an enlarged simulation procedure that deals with major processes that create sedimentary basins. Diagram implies central role of simulation procedures that represent processes that erode, transport, and deposit elastic sediments in overall simulation model.

RANDOMNESS AND ENTROPY

SEDSIM illustrates principles of randomness and entropy that are not unique to sedimentary systems. but are of universal importance whenever dynamic processes are considered. first, let us consider "randomness". A phenomenon or system is said to be random when the cause and effect relationships involved in it are not known, or are assumed to be unknown, so that the state of the system cannot be determined with certainty from an earlier state. SEDSIM, for example, does not have any components that are deliberately random, and SEDSIM represents processes deterministically because its behavior is completely determined by initial conditions. Thus a deterministic model of a system can be regarded as a function that links every possible state with subsequent states. The function can be continuous in the sense that "small" variations in the model's state at a given time bring about "small" variations in the model's state at a given later time. An example of such a model is the "single fluid element experiment" illustrated in Figure 13.

Nevertheless, small variations may have major consequences in models that are deterministic in principle. Deterministic mathematical models such as those described by Schuster (1985). operate so that any variation in a given state of the model, no matter how small. leads to a large variation in the model's subsequent behavior. Such models are called "chaotic" (Mayer-Kress, 1985). A chaotic model progresses along a path that is continuous, but the function that links a given state with a subsequent state at a later time is discontinuous at every point. Thus, chaotic models can be represented even by simple deterministic equations (Schuster, 1985). Such models are random for all practical considerations, because the state of the system represented cannot be recorded in complete detail, thereby generating uncertainty about the later states of the system represented by the model.

SEDSIM exhibits such chaotic behavior. Perfect knowledge of the initial state of the system represented is required if we were to consider it to be deterministic. with SEDSIM, the initial state of the actual system, consisting of the paleogeographic conditions at the time the sedimentary processes are deemed to have "started" to operate, is not perfectly known. Therefore the uncertainty in subsequent states cannot be reduced by reducing the uncertainty in the initial state (unless the uncertainty in the initial state was zero). In the example involving turbidity currents shown in Figures 48a through 48f, some small change in initial conditions might have caused the last flow to be diverted to the opposite side of the fan. However, since the initial conditions in the actual system represented by the model are not known in complete detail, they must be treated as probability distributions. A series of experimental runs can be performed using a sample of initial conditions, and the results can be treated as a statistical distribution. Otherwise one might be led to the false conclusion that channel deposits would always form on a particular side of a fan because they might have formed there in a single experiment. Thus, conclusions about the average sizes and shapes of fans and channels produced by SEDSIM would be more reliable than conclusions based on a single experiment.

Entropy and Time's Arrow

When attempting to reconstruct events of the past with a sedimentary process simulation model that runs "forward" in time, one might question whether the model could be run "backwards" by utilizing information about the present to infer the past. In other words "time's arrow" would point backward instead of forward. If such a model existed, it might allow us to begin with the configuration of a sedimentary deposit as it exists today, and then the model would progressively unfold the past history as it moves backward. Unfortunately, such a backward running model that represents sedimentation processes as embodied in SEDSIM cannot be created.

It is true that equations that govern physical phenomena often can be used so that time is reversed. For example, the "single fluid element" experiment, depicted in Figure 13. could be run backwards so that the fluid element would retrace its, path exactly. But the simulation model would have to be very precise if the fluid element is to reach its initial position. If friction is introduced, it becomes increasingly difficult to establish the initial position of the fluid element.

As time advances, information tends to be lost, and cannot be replaced by running the model backwards. Thus, entropy, as loosely defined in this context, can be considered to be the lack of such information. When a process is in operation, entropy progressively increases, and knowledge about the past is progressively lost. The inevitable increase in entropy is "time's arrow" that always points forward, thereby governing the irreversibility of an actual process.

The concept of entropy will not be treated further here, but it is this loss of information that requires a complex process model to operate in the "forward" direction, thereby losing information and creating uncertainty as to whether the initial conditions are correct. A "forward model cannot guarantee that alternative sets of initial conditions do not yield equally plausible results. While it is impossible to reverse a model of a system in which information is lost with time, there is hope because evidence derived independently from simulation experiments may restrict the assumed initial conditions to a manageable number of alternative hypotheses. The simulation’s role is to deduce the consequences that ensue from the assumptions attached to the different hypotheses. If the choice of hypotheses cannot be resolved, at least the merits of various alternatives will be clarified by the simulation experiments.

The difficulties in determining the past with models that work only "forward" is as old as geological science itself. Geologists engage in "forward modeling" as they deduce the consequences of assumptions incorporated in "conceptual" models. SEDSlM's strength is that it provides a means of consistently and quantitatively deducing the consequences of a set of initial assumptions. The user must determine whether the initial assumptions are suitable. SED5IM's principal role is to help, the user rigorously deduce the consequences of alternative assumptions.

REFERENCES

Abraham, G., A.G. van Os, and G.K. Verboom, 1981, Mathematical modeling of flows, and transport of conservative substances: requirements for predictive ability, in Fischer, H.B. (ed), 1981, Transport models for inland and coastal waters, Proceedings of a symposium on predictive ability, Academic Press, 1nc., New York, 542 p.

Bagnold, R.A., 1957, The flow of cohesionless grains in fluids: Phil. Trans. Roy. Soc., London, v. 249, p. 235.

Bagnold, R.A., 1966, An approach to the sediment transport problem from general physics: U.S. Geol.Survey Prof. Paper 422-1, 37 p.

Bates, C.C., 1953, Rational theory of delta formation: Am. Assoc. Petroleum Geol. Bull., v. 37, no. 9, p. 2119-2162.

Bea, R.G., and H.A. Bernard, 1973, Movements of bottom soils in the Mississippi Delta offshore: in offshore Louisiana Oil and Gas Fields: Lafayette Geological Society, 1973, Lafayette, 242 p. Bird, K.J., and J. Andrews, 1979, Subsurface studies of the Nanushuk Group, North Slope, Alaska: in Ahlbrandt, T.S. (ed.), Preliminary geologic. petrologic and paleontologic results of the study of Nanushuk Group rocks, North Slope, Alaska: U.S. Geol. Survey Circ. 794, p. 32- 46.326
Bonham-Carter, G.F., and A.J. Sutherland, 1967, Diffusion and settling of sediments at river mouths: a computer simulation model, Trans. Gulf Coast Assoc. Geol. Soc.. v. 17,p. 326-338.

Bonham-Carter, G.F., and A.J. Sutherland, 1968, Mathematical model and FORTRAN IV program for computer simulation of deltaic sedimentation: Computer Contribution 24, Kansas Geol. Survey, 56 p.

Bridge, J.S., 1975, Computer simulation of sedimentation in meandering streams: Sedimentology, v. 22, pp. 3-43. BUHEWBH, 0-, gt §l., 1980, Principles and capabilities of 3-D, E-M particle simulations: Jour. Computational Physics, v. 38, O. 1-44.

Carter, R.D.. C.G. Mull, K.J. Bird, and R.B. Powers, 1977, The petroleum geology and hydrocarbon potential of the NavalPetroleum Reserve No. 4, North Slope, Alaska: U.S. Geol.Survey Open-file Report 77~475, 61 p.

Cheng, R.T., 1983, Euler-Lagrangian computations in estuarine hydrodinamics: in C. Taylor, J.A. Johnson, and R. Smith (eds.), Proceedings of the Third International Conference on Numerical Methods in Laminar and Turbulent Flow: Pineridge Press, p.341-352 ,Chorafas, D.N.- 1965, Systems and simulation: Academic Press, New York, 503 pp. 327

Colby, B.R. and C.H. Hembree. I955, Computation of total sediment discharge, Niobara river near Cody, Nebraska: U.S. Geol. Survey Water Supply Paper, no. 1357. Colby. B.R., 1964, Practical computations of bed material discharge: Jour. Hydraulics Division, Am. Soc. Civil Engrs., v. 90, n. HY2.

Collins, F.R.. 1958. Test wells, Topagoruk area. Alaska: U.S. Geol. Survey Prof. Paper 305-D. p. 265-3l6.
Collins, F.R., 1959, Test wells, Meade and Kaolak areas, Alaska: U.S. Geol. Survey Prof. Paper 305 F, p. 265-316.

Collins, F.R., 1961, Core tests and test wells, Barrow area. Alaska: U.S. Geol. Survey Prof. Paper 305-K. p. 569-644.

Crutchfield, P.J., gt §i., 1986, Chaos: Scientific American, v. 255. n. 6, p. 46-57.

Du Boys, M.P.. 1879. Etudes du regime et l'action exercee par les eaux sur un lit a fond de graviers indefiniment a fouliable: Annales des Ponts et Chausses, Ser. 5, Vol. 18, pp. 141-195.

Einstein, H.A., I942, Formulas for the transportation of bed-load, Trans. Am. Soc. Civil Engrs. vol.107, p. 561.

Einstein, H.A., 1950, The bed~load function for sediment transportation in open channel flows: U.S. Dept. of Agriculture Tech. Bull., no. 1026. 328

Halbouty, M.T., 1979, Salt domes in the Gulf region, United States and Mexico: Gulf Publishing Company, Houston, 217 p.

Harbaugh, J.W. and G. Bonham-Carter, 1970, Computer simulation in geology: Wiley Interscience, New York, 575 p.

Harlow, F.H., 1964, The Particle-in-cell computer method for fluid dynamics: in B. Alder (ed.), Computational Physics: v. 3, Academic Press, New York, p. 319-343.

Hockney, R.W. and J.N. Eastwood, I981, Computer simulation using particles: McGraw-Hill. New York, 523 p.

Jones, P.H., A.N. Turcan Jr., and H.E. Skibitzke, 1954. Geology and Groundwater resources of southwestern Louisiana: Louisiana Geol. Survey Bull.. n. 30, p. 47-48.

Kalinske, A.A., I947, Movement of sediment as bed load in rivers: Trans. Am. Geophys. Union, vol. 28, no. 4, p. 615.

Landes, K.K-, 1970, Petroleum Geology of the United States: John Wiley and Sons, Inc.. New York, S71 p.

Lapidus. L-, and Pinder. G.F.. 1982, Numerical solution of partial differential equations in science and engineering: John Wiley & Sons, New York, 677 p.

Laursen, E. M., 1956, The application of sediment transport mechanics to stable channel design: Jour. Hydraulics Division, Am. Soc. Civil Engrs., v. 82, n. HY4. 329

Laursen, E. M., 1958, The total sediment load of streams: Proc. Am. Soc. Civil Engrs., vol. 84, no. HYI, p. 1530-1.

Lane, E. W., and E. J. Carlson, 1953, Some factors affecting stability of canals constructed in coarse granular materials: Proc. Minnesota Internat. Hydraulics convention. Joint Meeting of the International Association for Hydraulics Research and Hydraulics Division, Am. Soc. of Civil Engrs. (August 1953), p. 37.

Limes, L.L., and J.C. Stipe, 1959, Occurrence of Miocene oil in south Louisiana: Gulf Coast Assoc. Geol. Soc. Trans.. v. 9, p. 77.

Manning, R.. 1890, Flow of water in open channels and pipes: Trans. Inst. Civil Engrs., Ireland, vol. 20.

Matthews, W.H., and P. Shepard, 1963, Sedimentation of Fraser River delta, British Columbia: Am. Assoc. Petroleum Geol., v. 46, n. 8, p. 14l6-1443.

May, F.E., 1979, Dinoflagellate and acritarch assemblages from the Nanushuk Group (Albian-Cenomanian) and the Torok formation (Albian), Umiat test well ll, NPRA. Northern Alaska: in Ahlbrandt, T.S. (ed.), Preliminary geologic ,petrologic and paleontologic results of the study of Nanushuk Group rocks, North Slope, Alaska: U.S. Geol. Survey Circ. 794. p. ll3-127.

Mav. F.E., and J.A. Stein. 1979, Dinoflaqellate and acritarch assemblages from the Grandstand formation (Middle to upper Albian) of the Nanushuk Group, Simpson Core test 25,National Petroleum Reserve in Alaska: in Ahlbrandt, T.S. (ed.), Preliminary geologic. petrologic and paleontologic results of the study of Nanushuk Group rocks, North Slope.Alaska: U. S. Geol. Survey Circ. 794. p. 32-46.

Mayer-Kress, G-, (ed.), 1986, Dimensions and entropies in chaotic systems: Springer Verlag, Berlin, 382 p.

Meyer-Peter, E., and Muller, R., 1948. Formulas for bedload transport: Proceedings, Third meeting of Intern. Assoc. Hydr. Res., Stockholm, p. 39-64.

Mitchum, R.M.. Jr., 1977, Seismic stratigraphy and global changes in sea level, part ll; Glossary of terms used in seismic stratigraphy: in Seismic Stratigraphy-applications to hydrocarbon exploration: Am. Assoc. Petroleum Geol. Mem. 26, p. 205-212.

Morgridge, D.L., and W.B. Smith, 1972, Geology and discovery of Prudhoe Bay field. eastern Arctic Slope. Alaska: in King. R.E. (ed.). Stratigraphic oil and gas fields classification. exploration methods. and case histories: Am. Assoc. Petroleum Geol. Mem. 16, p. 489-50l.

Perlmutter, H.A., 1987, personal communication. letter dated April 10, 1987. 33l

Prandtl L., 1923, Ergebnisse der Aerodynamischen Versuchsanstalt zu Goettingen: R. Oldenburg, Munich. and Berlin, p.32.

Richmond, B.M., and A.H. Sallenger. Jr., 1984, Cross-shore transport of bimodal sands: in Proceedings of the 19th International Coastal Engineering Conference: Am. Soc. Civil Engrs., New York, p. 209-234.

Richtmyer, R.D. and K.W. Morton. 1967, Difference methods for initial-value problems: Wiley lnterscience, New York, 348 p.

Rickwood. F.K., I970, The Prudhoe Bay Field: in W.L. Adkinson and M.M. Brosge (ed.), Proceedings of the Geological Seminar on the North Slope of Alaska, Pacific Section. Los Angeles, Am. Assoc. Petroleum Geol., p. L1-L l1.

Roacne, P.J., 1972, On artificial viscosity: Jour. Computational Physics, v. 10. p. l69-l84.

Robinson, F.M., and F.R. Collins, 1959. Core test, Sentinel Hill area and test well, Fish Creek area, Alaska: U.S. Geol. Survey Prof. Paper 305-l, p. 485-521.

Robinson, F.M., 1959, Test wells, Simpson area, Alaska: U.S. Geol. Survey Prof. Paper 305-J, p. 523-568.

Robinson, F.M., 1964, Core tests, Simpson area, Alaska: U.S. Geol. Survey Prof. Paper 305-L, p. 645-730.

Sangree . J.B.. and J.M. Widmier, 1977. Seismic Stratigraphy and global changes in sea level. Part 9: Seismic interpretation of clastic depositional facies: in C. E. Payton (ed.), Seismic stratigraphy - Applications to hydrocarbon exploration: Am. Assoc. of Petroleum Geol. Hem. 26, Tulsa, Oklahoma.

Saxena, R.S., 1976. Modern Mississippi delta-depositional-environments and processes: a guidebook prepared for the Am. Assoc. Petroleum Geol./Soc. Econ. Paleontologists and Mineralogists field trip-Mississippi delta flight. Am. Assoc. of Petroleum Geol., New Orleans, I25 p.

Scott. N., 1986, Modern vs. ancient braided stream deposits: A comparison between simulated sedimentary deposits and the Ivishak formation of the Prudhoe Bay Field, Alaska: M.S. Thesis, Department of Applied Earth Sciences. Stanford University.

Schuster, H.G., 1985. Deterministic chaos, an introduction: VCH Publishers, lnc.

Shannon, Robert E.. 1975, Systems simulation, the art and science: Prentice Hall, Inc., Englewood Cliffs, New Jersey.

Shields. I.A., 1936, Anwendung der Ahnlichkeitsmechanik und der Turbulenzforschung auf Geschiebebewegung: Mitteilungen der Preussischen Versuchsanstalt fur Wasserbau und Schiffbau, Heft 26, Berlin. Available also as translation by w.P. Ott and J.C. van Uchelen, S.C.S. Cooperative Laboratory, California Institute of Technology. Pasadena, Calif.

Sloss, L.L., 1962, Stratigraphic models in exploration: Jour. Sedimentary Petrology, v. 32, pp. 415-422.

Strahler, A.N., 1952, Mathematical models in geomorphology: Geol. Soc. of Am. Bull., v. 63, pp. 923-938.

Tailleur, I.L., 1969, Rifting speculation on the geology of Alaska's North Slope: Oil Gas J., vol. 67, p. 128-130.

Tetzlaff, D.M., 1983, Computer mapping of seismic reflectors in the coastal region of the National Petroleum Reserve in Alaska: Math. Geol., v. 17, n. 4, pp. 445-480.

Thomas, 1976, HEC-6, scour and deposition in rivers and reservoirs: U.S. Army Corps of Engineers, Hydrologic Engineering Center, publication 723-G2-L247O.

Trowbridge, A.C., 1930, Building of Mississippi delta: Am. Assoc. Petroleum Geo]. Bull., v. 14, n. 7, p. 867-901.

Vail, P.R., R.M. Mitchum, Jr., and S. Thompson, III, I977, Seismic stratigraphy and global changes in sea level, part 4; Global cycles of relative changes of sea level: in Seismic Stratigraphy - applications to hydrocarbon exploration: Am. Assoc. Petroleum Geol. Mem. 26, p. 83-97.

Vanoni. V.A.. and G.N. Nomicos, 1960, Resistance properties of sediment-laden streams: Trans. Am. Soc. Civil Engrs., v. I25, P. 1140.

Yalin. M.S., 1963, An expression for bed-load transportation: Proc. Am. Soc. Civil Engrs., v. 89, no. HY3, p. 221.

Appendix A
GLOSSARY

The glossary below defines some of the important technical terms used in this dissertation. Some definitions apply only in the context of the dissertation, but others are in accord with their general scientific use, and are provided as a convenience to the reader.

Anisotropic: A medium in which physical properties vary according to direction.

Armor layer: A layer of relatively coarse material formed naturally on a stream bed by the removal of finer material.

Bed load: Sediment that moves by saltation (jumping), rolling or sliding, and remains within two or three grain diameters above the bed (see also "suspended load").

Bed-materia| load: Part of the sediment load composed of particles of the same size as those in the bed (see also "wash load").

Cell: The portion of a surface or of a volume representing an elementary constituent of a grid. Cells in SEDSIM are either squares or rectangular blocks.

Cell boundary: The line or surface defining the border or edge of a cell.

Chaotic process: A process whose outcome or behavior can only be predicted by having perfect knowledge of the initial state, but that can be considered random if knowledge is not complete. While a chaotic process is actually not random, it behaves much as a random processes.

Continuity equation: An equation that states that no mass can be lost or gained, but only transferred from one place to another.

Deterministic: A process whose outcome or behavior can be predicted from the initial conditions and a set of rules defining how those conditions will change or evolve.

Eulerian: A method of defining flow in which properties of the flow are given at points that are fixed in space.

Finite-difference procedures: Numerical techniques that employ regular grids and approximate differential equations with algebraic expressions that express differences between values of variables at grid nodes.

Finite-element procedures: Numerical techniques that employ grids that may be irregular, and approximate differential equations with algebraic expressions that stem from integrating a variable throughout a cell.

Fixed surface: A surface that does not change shape or position.

Fiow: The type of motion characteristic of fluids, usually represented by a continuous vector field that indicates velocity at each point. Also, a moving volume of fluid.

Flow-velocity profile: A function representing the distribution of velocities along a vertical line through the flow.

Fluid element: A movable point representing a volume of fluid.

Free surface: A surface that bounds a fluid and is free to move as determined by forces within the fluid. Usually applied to the air-water interface in an open channel.

Grid: A mesh or partition into which a surface or a volume can be divided.

Grid element: A cell or a node.

Grid, Fixed: A grid that does not change shape with time.

Grid, regular: A grid in which all the cells have the same shape and size. even if their orientation is different.

Homogeneous: A medium in which physical properties are the same for any portion of the medium.

Homogeneous sediment: An aggregate of particles that has the same physical properties everywhere when observed in bulk, without necessarily having grains that are all identical to each other.

Isotropic: A medium in which physical properties are the same regardless of direction.

Iteration: Each of a number of repetitive steps used in finding a numerical solution to a set of partial differential equations.

Lagrangian: A method of defining flow in which properties of the flow are given at points that move with the fluid.

Model: A representation of a real system, either in the form of a scaled down physical reproduction, or in the form of a conceptual or theoretical description, often embodied as a computer program.

Modeling: The process of building a model to reproduce the behavior of a real system.

Momentum equation: An equation balancing specific factors that affect the changes in the motion of an elementary mass of fluid.

Node or grid point: The point occupied by one or more grid cell vertices.

Random: A process whose outcome or behavior cannot be completely predicted from the initial conditions. but rather depends on unpredictable factors.

Sediment-transport equation: An equation defining how much sediment is carried by the flow according to upstream supply, flow conditions. and bed composition.

Rigid surface: A surface that bounds a fluid and does not move appreciably as compared to the flow velocity. A channel bed, for example, is a rigid surface because. Although erosion or deposition can cause it to move, it does so extremely slowly. (See also "fixed surface".)

Sediment type: A fraction of a sediment mixture composed of particles that are alike in physical characteristics (size, shape, density).

Simulation: The process of running experiments with a model, usually with the purpose of understanding or predicting the behavior of the system that the model reproduces.

Suspended load: Sediment that is supported by upward components of turbulent motion, remaining in suspension for an appreciable time. Bed load and suspended load constitute total load.

System: A mechanism that is characterized by a set of components and the relationships and interactions between the components.

Total load: The total amount of sediment that is being moved by the flow. Total load is equal to bed load plus suspended load, or bed-material load plus wash load.

Uniform sediment: Sediment that is composed of a single type, and whose particles are alike in size, shape, and density.

Variable, continuous: A variable that takes values at every point on a line, surface. or in space.

Variable. discrete: A variable that takes values at a set of points that are separated from each other.

Viscosity: A property of a fluid defining the fluid's resistance to shear.

Wash load: The part of the sediment load composed of particles that are smaller than the particles composing the bed. The amount of wash load is usually determined by upstream conditions. The wash load plus the bed-material load is equal to the total load.

Appendix B
NOTATION CONVENTIONS

Physical quantities:

The following is a list of physical quantities used in this dissertation. The table indicates the quantity by name, the symbol that represents it in the text, and the corresponding units in the International System (SI).

Quantity	Symbols in text	Units (SI)
Area	A	m^{2}
Acceleration	a	m / s^{2}
Coefficient of bottom friction	c_1	dimensionless
Coefficient of lateral friction	c_2	kg (m / s) m / s
Coefficient of transport	c_t	$m \ s^{2/} kg$
Coefficient of sediment transportabillity	f_1 or $f_{1, Ks}$	dimensionless
Coefficient of erosion-deposition	f_2 or $f_{2, Ks}$	m / s
Coefficient of movement treshold	f_3	$kg \ m / s^{2}$
Coefficients of basement decomposition	$f_{4,,Ks}$	dimensionless
Coefficient of transportability to fall velocity	c_f	s / m
Density	ρ	kg / m^3
Energy	E	$kg \ m^2 / s^{2}$
Flow depth	h	m
Flow surface elevation	H	m
Flow velocity (3 dimensions)	q	m / s, m / s, m / s
Flow velocity components	u, v, w	m / s, m / s, m / s
Flow velocity (2-dimensions)	Q	m / s, m / s
Fluid density	q	kg / m^3

Froude number	F_n	dimensionless
Gravity	g	m / s ^{2}
Manning's roughness	n	S *m* $^{1/3}$
Mass	m	kg
Momentum	M	kg m / s
Number of columns, current column number	M, J	dimensionless
Number of rows ,current row number	N, i	dimensionless
Number of elements, current element number	L, k	dimensionless
Number of sed. types, current type	$N_{s,}$ K_s	dimensionless
Position (2 dimensions)	X	m, m
Power	P	kg m ^{2} / s ^{2}
Pressure	p	kg / (m s ^{2})
Reynold's number	R_n	dimensionless
Sediment concentration	l	dimensionless
Sediment particle diameter	d	m
Sediment particle fall velocity	W	m /s
Sediment transport capacity	ƛ	dimensionless
Sediment transport rate	Q_s	kg / (m s)
Sediment type index	K_s	dimensionless
Shear stress	τ	kg / (m s ^{2})
Specific weight	γ	kg (m ^{2} / s ^{2})
Time	t	m
Topographic elevation	Z	s
Viscosity	μ	kg / (m s)
Viscosity. kinematic	ν	m ^{2} / s
Volume	V	m ^{3}

Mathematical operators:

The following table explains the notation utilized throughout the text of mathematical operators:

$$\nabla f \;=\; \frac{\partial f}{\partial x} i + \frac{\partial f}{\partial y} j + \frac{\partial f}{\partial z} k$$

$$\nabla \vec{q} \;=\; \frac{\partial \vec{q}}{\partial x} + \frac{\partial \vec{q}}{\partial y} + \frac{\partial \vec{q}}{\partial z}$$

$$\nabla^2 f \;=\; \frac{\partial^2 f}{\partial x^2} + \frac{\partial f^2}{\partial y^2} + \frac{\partial^2 f}{\partial z^2}$$

$$\nabla^2 \vec{q} \;=\; \frac{\partial^2 \vec{q}}{\partial x^2} + \frac{\partial^2 \vec{q}}{\partial y^2} + \frac{\partial^2 \vec{q}}{\partial z^2}$$

$$\nabla \cdot \vec{q} \;=\; \frac{\partial u}{\partial x} i + \frac{\partial v}{\partial y} j + \frac{\partial w}{\partial z} k \qquad \vec{q} = (u, v, w)$$

$$(\vec{q} \cdot \nabla) \vec{r} \;=\; u \frac{\partial \vec{r}}{\partial x} + v \frac{\partial \vec{r}}{\partial y} + w \frac{\partial \vec{r}}{\partial z}$$

$$\frac{D \vec{q}}{Dt} \;=\; \frac{\partial \vec{q}}{\partial t} + (\vec{q} \cdot \nabla) \vec{q}$$

Mathematical symbols:

d = derivative
∂ = partial derivative
D = derivative following fluid motion
$\int$ = integral
$\oint$ = curvilinear integral
$\cdot$ = scalar product
$\sum$ = summation
| | = absolute value
Δ = finite increment

Appendix C
COMPUTER SOFTWARE

Listing of Program SEDCYC3

Program SEDCYC3 simulates flow, erosion, and deposition of up to four sediment types. A complete listing of the main program, plus the subroutines in alphabetical order, is provided. To generate a data file for SEDCYC3, the user would build a short main program that calls subroutine WRITDF. Parameters then can be assigned inside the main program, or the file written by WRITDF can be edited so as to write in the parameters.

```
C.....PROGRAM SEDCYC3
      IMPLICIT COMPLEX (C)
      CHARACTER*72 IT
      COMMON /BLK1/LBIT(50,41,61)
      COMMON IT,T0,TR,TD,DT,TB,TE,TID,TF,FLD,SWD,VIS,ROU,DV,CVC,CWV,
     & SDI(4),SDD(4),BD(4),FCO(5),
     & TI,LI,CPI(2Q),CVI(20),SLI(20,4),TEV,LEV,CPEV(20),
     & DX,N,M,NQ,QX(10,4),QY(10,4),QZ(10,4),
     & ZT(41,61),ZB(41,61),DZZ,L,CP(5000),CV(5OD0),SL(5000,4),
     & FEN(41,61) ,CVN(41,61),SUB(41,61),ZT1(41,61),SDER(41,61),
     & NY,G,DX2,DZ,DM,FF,FB,F3,F4,VST(4),FU(4),FD(4),TC(4),FAC
      F1=3.1E+07
      E=1.00001
C.....READ
      OPEN (20,FILE='for20.d',FORM='FORMATTED')
      REWIND (20)
      CALL READDF3
      CLOSE (20)
C.....OPEN MESSAGE FILE
      OPEN (25,FILE='for25.d',FORM='FORMATTED')
      REWIND (20)
      WRITE (25,1) T0,TR,L
      FORMAT (1X,' TIME=',F15.7,' YEARS OF ',F15.7,' YEARS'/
     & 'L=',I6)
      CLOSE (25)
      OPEN (22,FILE='for22.d',FORM='UNFORMATTED')
      REWIND (22)
      CALL FILTER3 (-1)
      IF (T0.NE.0.) GOTO 2
      CALL NEWNOD3
      CALL WRITGU3
      IF (TR-T0.LT.0.0000001) STOP
    2 T=T0
      T1=DT*TB/F1
      T2= (TE+TID)*TF
      NYET=INT((TR-T0)/T2-0.00001)
      NYT=TE*F1/DT/TB
      CALL INFLOW3
C.....ENTER MAIN LOOPS
      TYE=0.
      DO 100 NY=0,NYET
      CALL SET3
      DO 10 NY=O,NYT
      TY=(NY+1)*T1
      CALL NEWNOD3
      CALL NEWELM3
      CALL FILTER3 (1)
      IF (TI.LE.TE.AND.AMOD(TY*E,TI).LT.T1.AND.TI.GT.0.) CALL INFLOW3
      T0=T+TYE+TY
      IF (TD.LE.TE.AND.AMOD(TY*E,TD) .LT.T1.AND.TD.GT.0.) CALL WRITGU3
   10 CONTINUE
      TYE=(NYE+1)*T2
      T0=T+TYE
      IF (TF.GT.1.001) CALL EXTRAP3
      IF (TI.GT.TE.AND.AMOD(TYE*E,TI).LT.T2) CALL INFLOW3
      IF (TD.GT.TE.AND.AM0D(TYE*E,TD).LT.T2) CALL WRITGU3
C.....WRITE CURRENT TIME
      OPEN (25,FILE:'for25.d',FORM='FORMATTED')
      REWIND (25)
      WRITE (25,1) T0,TR,L
      CLOSE (25)
  100 CONTINUE
C.....END
      OPEN (21, FILE=' for21.d' , FORM='FORMATTED')
      REWIND (21)
      CALL WRITDF3
      CLOSE (21)
      STOP
      END
C--------------------------------------------------------------------------------
      SUBROUTINE EXTRAP3
C.....EXTRAPOLATES TIME SINCE LAST CALL SET BY FACTOR F (F>1.)
      IMPLICIT COMPLEX (C)
      DIMENSION LC(800)
      CHARACTER*72 IT
      COMMON /BLK1/LBIT(50,41,61)
      COMMON IT,T0,TR,TD,DT,TB,TE,TID,TF,FLD,SWD,VIS,ROU,DV,CVC,CWV,
     & SDI(4),SDD(4),BD(4),FCO(5),
     & TI,LI,CPI(2Q),CVI(20),SLI(20,4),TEV,LEV,CPEV(20),
     & DX,N,M,NQ,QX(10,4),QY(10,4),QZ(10,4),
     & ZT(41,61),ZB(41,61),DZZ,L,CP(5000),CV(5OD0),SL(5000,4),
     & FEN(41,61) ,CVN(41,61),SUB(41,61),ZT1(41,61),SDER(41,61),
     & NY,G,DX2,DZ,DM,FF,FB,F3,F4,VST(4),FU(4),FD(4),TC(4),FAC
C.....ENTER MAIN LOOPS
      DO 10 I=1,N
      DO 10 J=1,M
      ZTN=ZT(I,J)+(ZT(I,J)-ZT1(I,J))*TF
      IF (ZTN.LE.ZT(I,J)) GOTO 9
      K=(ZT(I,J)-ZB(I,J))/DZZ+0.99999
      K1=(ZT1(I,J)-ZB(I,J))/DZZ+O.99999
      IF (K1.LE.0) K1=1
      K2=(ZTN-ZB(I,J))/DZZ+0.99999
      DO 5 KK=K1,K
      K11=K1+1
      LC(K11)=0;
    5 CALL SEDNOD3 (I,J,KK,LC(K11))
      KK=0
      DO 6 KL=K+1,K2
      KK=KK+1
      IF (KK.GT.K) KK=1
    6 CALL SEDNOD3 (I,J,KL,LC(KK))
    9 ZT(I,J)=ZTN _
      IF (ZTN.LT.ZB(I,J)) ZB(I,J)=ZTN
   10 CONTINUE
      RETURN
      END
C------------------------------------------------------------------------------
      SUBROUTINE FILTER3 (IFLAG)
C.....APPLIES TIME AND SPACE FILTERS TO0 VELDCITIES AND FLUID LEVELS
C     IFLAG=1 ADD VARIABLES
C     IFLAG=0 DIVIDE TO FIND AVERAGE
C     IFLAG=-1 INITIALIZE TO 0
      IMPLICIT COMPLEX (C)
      CHARACTER*72 IT
      COMMON /BLK1/LBIT(50,41,61)
      COMMON IT,T0,TR,TD,DT,TB,TE,TID,TF,FLD,SWD,VIS,ROU,DV,CVC,CWV,
     & SDI(4),SDD(4),BD(4),FCO(5),
     & TI,LI,CPI(2Q),CVI(20),SLI(20,4),TEV,LEV,CPEV(20),
     & DX,N,M,NQ,QX(10,4),QY(10,4),QZ(10,4),
     & ZT(41,61),ZB(41,61),DZZ,L,CP(5000),CV(5OD0),SL(5000,4),
     & FEN(41,61) ,CVN(41,61),SUB(41,61),ZT1(41,61),SDER(41,61),
     & NY,G,DX2,DZ,DM,FF,FB,F3,F4,VST(4),FU(4),FD(4),TC(4),FAC
      COMMON /FIL/CV1(41,61),FE1(41,61),NFT
      IF (IFLAG.EQ.0) GOTO 5
      IF (IFLAG.EQ.-1) GOTO 2
      NFT=NFT+1
C.....ADD CURRENT GRID TO PREVIOUS ONE
      DO 3 I=1,N
      DO 3 J=1,M
      CV1(I,J)=CV1(I,J)+CVN(I,J)
    3 FE1(I,J)=FE1(I,J)+FEN(I,J)
      RETURN
C.....FIND TIME AVERAGES
    5 IF (NFT.EQ.O) RETURN
      DO 4 I=1,N
      DO 4 J=1,M
      CVN(I,J)=CV1(I,J)/NFT
    4 FEN(I,J)=FE1(I,J)/NFT
C.....FIND SPATIAL AVERAGES
      IF (NFS.LT.1) RETURN
      DO 11 IFS=1,NFS
      DO 10 I=1,N
      DO 1O J=1,M
      CV2=(0.,0.)
      FE2=0.
      NS=0
      IF (I.LE.1) GOTO 6
      CV2=CV2+CVN(I-1,J)
      FE2=FE2+FEN(I-1,J)
      NS=NS+1
    6 IF (I.GE.N) GOTO 1
      CV2=CV2+CVN(I+1,J)
      FE2=FE2+FEN(I+1,J)
      NS=NS+1
    7 IF (J.LE.1) GOTO 8
      CV2=CV2+CVN(I,J-1)
      FE2=FE2+FEN(I,J-1)
      NS=NS+1
    8 IF (J.GE.M) GOTO 9
      CV2=CV2+CVN(I,J+1)
      FE2=FE2+FEN(I,J+1)
      N5=NS+1
    9 CV1(I,J)=(CVN(I,J)*2.+CV2)/(2+NS)
   10 FE1(I,J)=(FEN(I,J)*2.+FE2)/(2+NS)
C.....EQUALIZE
```

```
      DO 11 I=1,N
      DO 11 J=1,M
      CVN(T,J)=CV1(I,J)
   11 FEN(I,J)=FE11(I,J)
C.....INITIALIZE TO 0
    2 DO 1 I=1,N
      DO 1 J=1,M
      CV1(I,J)=(0.,0.)
    1 FE1(I,J)=0.
      NFT=0
      RETURN
      END
C-------------------------------------------------------------------------------
      SUBROUTINE HSLOP3(CPOS,ZE,CS,I,J,ICALL1,IFL)
C.....CALCULATES HEIGHT AND SLOPE AT A GIVEN POSITION
      IMPLICIT COMPLEX (C)
      CHARACTER*72 IT
      COMMON /BLK1/LBIT(50,41,61)
      COMMON IT,T0,TR,TD,DT,TB,TE,TID,TF,FLD,SWD,VIS,ROU,DV,CVC,CWV,
     & SDI(4),SDD(4),BD(4),FCO(5),
     & TI,LI,CPI(2Q),CVI(20),SLI(20,4),TEV,LEV,CPEV(20),
     & DX,N,M,NQ,QX(10,4),QY(10,4),QZ(10,4),
     & ZT(41,61),ZB(41,61),DZZ,L,CP(5000),CV(5OD0),SL(5000,4),
     & FEN(41,61) ,CVN(41,61),SUB(41,61),ZT1(41,61),SDER(41,61),
     & NY,G,DX2,DZ,DM,FF,FB,F3,F4,VST(4),FU(4),FD(4),TC(4),FAC
C.....SET PARAMETERS
      R1=(FLD-SWD)/SWD
      R2=(SWD-FLD)/FLD
      IFL=0
C.....FIND CELL AND CHECK FOR OUT OF BOUNDS
      JC=REAL(CPOS)/DX+1
      IF (JC.LT.1) RETURN
      IC=N-AIMAG(CPOS)/DX
      IF (JC.LT.M.AND.IC.GE.1.AND.1C.LT.N) GOTO 1
      CPOS=CMPLX(-DX,-DX)
      RETURN
C.....FIND NODE
    7 J=REAL(CPOS)/DX+1.5
      I=N-AIMAG(CPOS)/DX+O.5
      ICALL=ICALL1
      I1=1
      J1=J
C.....FIND RELATIVE POSITION IN CELL
      PCX=REAL(CPOS)/DX-JC+1
      PCY=AIMAG(CPOS)/DX-N+IC+1 .
C.....SET PARAMETERS FOR SURFACE GEOMETRY
      A2=ZT(IC,JC)
      A3=ZT(IC,JC+1)
      A4=ZT(IC+1,JC+1)
      A1=ZT(IC+1,JC)
      ZZ=A2+A4-A1-A3
      ZEA=A1+(A4-A1)*1pcx+(A2-A1)*PCY-ZZ*PCX*PCY
      CSA=CMPLX(A1-A4+ZZ*PCY,A1-A2+ZZ*PCX)/DX
      IF (ICALL.EQ.2) GOTO 2
      FEN(I,J)=FEN(I,J)-1.
    2 B2=FEN(IC,JC)
      B3=FEN(IC,JC+1)
      B4=FEN(IC+1,JC+1)
      B1=FEN(IC+1,JC)
      FEN(I1,J1)=FEN(I1,J1)+1.
      ZZ=B2+B4-B1-B3
      ZEB=(B1+(B4-B1)*PCX+(B2-B1)*PCY-ZZ*PCX*PCY)*DZ
      CSB=CMPLX(B1-B4+ZZ*PCY,B1-B2+ZZ*PCX)/DX*DZ
      ZE=ZEA+ZEB
      CS=CSA+CSB
      IF (SWD.LE.FLD) GOTO 10
      IF (ZEB*R2.LT.ZE) RETURN
      ZE=ZEB*R2
      CS=CSB*R2
      IFL=1
      RETURN
   10 IF (ZEA.GT.-ZEB) RETURN
      ZE=ZE*R1
      CS=CS*R1
      RETURN
      END
C-------------------------------------------------------------------------------
      SUBROUTINE INFLOW3
C.....ALLOCATES NEW ELEMENTS FLOWING INTO THE SYSTEM
      IMPLICIT COMPLEX (C)
      CHARACTER*72 IT
      COMMON /BLK1/LBIT(50,41,61)
      COMMON IT,T0,TR,TD,DT,TB,TE,TID,TF,FLD,SWD,VIS,ROU,DV,CVC,CWV,
     & SDI(4),SDD(4),BD(4),FCO(5),
     & TI,LI,CPI(2Q),CVI(20),SLI(20,4),TEV,LEV,CPEV(20),
     & DX,N,M,NQ,QX(10,4),QY(10,4),QZ(10,4),
     & ZT(41,61),ZB(41,61),DZZ,L,CP(5000),CV(5OD0),SL(5000,4),
     & FEN(41,61) ,CVN(41,61),SUB(41,61),ZT1(41,61),SDER(41,61),
     & NY,G,DX2,DZ,DM,FF,FB,F3,F4,VST(4),FU(4),FD(4),TC(4),FAC
      KI=0
C.....USE ELEMENTS THAT ARE OUT OF BOUNDS
      DO 1 K=1,L
      IF (KI.GE.LI) RETURN
      IF (REAL(CP(K)).GE.0.) GOTO 1
      KI=KI+1
      CP(K)=CPI(KI)
      CV(K)=CVI(KI)
      DO 5 LIT=1,4
    5 SL(K,LIT)=SLI(KI,LIT)
      IF (KI.GE.LI) RETURN
    1 CONTINUE
      K=L
C.....ALLOCATE NEW ELEMENTS
      KI1=KI+1
      DO 2 KI=KI1,LI
      K=K+1
      IF (K.GT.5000) GOTO 3
      CP(K)=CPI(KI)
      CV(K)=CVI(KI)
      DO 2 LIT=1,4
    2 SL(K,LIT)=SLI(KI,LIT)
      L=K
      RETURN
    3 OPEN (24,FILE='for24.d',FORM='FORMATTED')
      WRITE (24,4)
    4 FORMAT (' CANNOT ALLOCATE ANY MODE ELEMENTS')
      STOP
      END
C-------------------------------------------------------------------------------
      SUBROUTINE NEWELM3
```

```
C.....FINDS NEW POSITIONS AND VELOCITIES OF FLUID ELEMENTS
      IMPLICIT COMPLEX (C)
      CHARACTER*72 IT
      COMMON /BLK1/LBIT(50,41,61)
      COMMON IT,T0,TR,TD,DT,TB,TE,TID,TF,FLD,SWD,VIS,ROU,DV,CVC,CWV,
     & SDI(4),SDD(4),BD(4),FCO(5),
     & TI,LI,CPI(2Q),CVI(20),SLI(20,4),TEV,LEV,CPEV(20),
     & DX,N,M,NQ,QX(10,4),QY(10,4),QZ(10,4),
     & ZT(41,61),ZB(41,61),DZZ,L,CP(5000),CV(5OD0),SL(5000,4),
     & FEN(41,61) ,CVN(41,61),SUB(41,61),ZT1(41,61),SDER(41,61),
     & NY,G,DX2,DZ,DM,FF,FB,F3,F4,VST(4),FU(4),FD(4),TC(4),FAC
C.....DEFINE SCALAR PRODUCT
      SCAPRO(C1,C2)=REAL(C1)*REAL(C2)+AIMAG(C1)*AIMAG(C2)
C.....SET CONSTANTS
      BDT=1.-FCO(5)
C.....ENTER MAIN DO LOOP, ONCE PER EACH ELEMENT
      DO 1 K=1,L
C.....FIND HEIGHT AND SLOPE AND CHECK FOR OUT OF BOUNDS
      CP0=CP(K)
      IF (REAL(CP(K)).LT.0.) GOTO 7
C.....FIND RELATIVE FRICTION COEFFICIENTS
      SB=DX2/(FEN(I,J)+1.)
      SF=(DX2-SB)*DZ/DX
      CVE=CVN(I,J)*SF/(SB+SF)
      F2=VIS*(SF+ROU+SB)/(SF+SB)
      CVT=CV(K)-CVE
      SS=CABS(CS)
      SQ=SQRT(1.+SCAPRO(CS,CS))
      CVF=0
      IF (SS.NE.0..AND.F2.NE.0.)
     &     CVF=SQRT(DM*G/F2*SS/SQ)*CS/SS
      CVS=G*CS/SQ*DT
      IF (F2.NE.0.) CVT=CVF+(CVT+CVS-CVF)*EXP(-F2*CABS(CVT-CVF)*DT/DM)
      IF (F2.EQ.0.) CVT=CVT+CVS
      CVT=CVT+CVE
C.....FIND TRANSPORT CAPACITY DIFFERENCE TCD
      IF (I.LE.1.0R.I.GE.N.OR.J.LE.1.0R.J.GE.M) GOTO 9
      V=CABS(CVN(I,J))
      DDV=CABS(CVN(I,J))**2*FB*SB*DT/DM
      SLTX=SL(K,1)/TC(1)+SL[K,2)/TC(2)+SL(K,3)/TC(3)+
     & SL(K,4)/TC(4)
      TCMAX=(DV/TC(1)+DV/TC(2)+DV/TC(3)+DV/TC(4))/4./100.
      TCD=AMIN1((2.*V*DDV+DDV*DDV)/(2.*DT)*DM,TCMAX)*TB-SLTX
C.....UPDATE VELOCITY AND POSITION
    9 CVW=CVT
    2 CVM=(CV(K)+CVW)/2.
      CPW=CP(K)+CVM*DT/SQ
C.....ERODE OR DEPOSIT
      JC=REAL(CP(K))/DX+L
      IC=N-AIMAG(CP(K))/DX
      II=0
      JJ=0
      IF (REAL(CV(K)).LT.0.) JJ=1
      IF (AIMAG(CV(K)).GT.0.) II=1
      J=JC+JJ
      I=IC+II
      IF (I.LE.1.0R.I.GE.N.OR.J.LE.1.0R.J.GE.M) GOTO 5
      ZD1=ZT(I,J)-ZB(I,J)
    6 IF (TCD.LT.-0.00001.AND.SDER(I,J).LT.0.001) GOTO 5
      IF (TCD.GT.0.00001.AND.IFL.NE.1.AND.SDER(I,J).GT.-0.001) GOTO 4
      GOTO 17
C.....ERODE (TCD POSITIVE)
    4 K1=ZD1/DZZ+0.9999
   14 IF (K1.LE.0) GOTO 30
      LIT=0
      CALL SEDNOD3 (I,J,K1,LIT)
      ZER=TCD*TC(LIT)/DX2*FU(LIT)
      IF (ZER.LT.O.) GOTO 17
      IF (INT((ZD1-ZER)/DZZ+D.9999).GE.K1) GOTO 20
C.....ERODE TO CELL BOTTOM
      DZREM=ZD1-(K1-1)*DZZ
      SL(K,LIT)=5L(K,LIT)+DZREH*DX2
      ZT(I,J)=ZT(I,J)-DZREM
      TCD=TCD-DZREM*DX2/TC(LIT)/FU(LIT)
      IF (TCD.LE.0.) GOTO 17
      ZD1=ZD1-DZREM
      K1=K1-1
      GOTO 14
C.....ERODE CELL FRACTION
   20 SL(K,LIT)=SL(K,LIT)+ZER*DX2
      ZT(I,J)=ZT(I,J)-ZER
      GOTO 17
C.....ERODE BASEMENT
   30 ZER=TCD*FAC*BDT
      DO 21 LIT=1,4
   21 SL(K,LIT)=SL(K,LIT)*ZER*DX2*BD(LIT)
      ZT(I,J)=ZT(I,J)-ZER
      ZB(I,J)=ZT(I,J)
      GOTO 17
C.....DEPOSIT (TCD NEGATIVE)
C.....LOOP ONCE PER LITHOLOGY
    3 DO 38 LT=1,4
      LIT=LT
      K1=(ZT(I,J)-ZB(I,J))/DZZ+1
      SDP=-TCD*TC(LIT)*FD(LIT)
      ZDP=SDP/DX2
      IF (SDP/FD(LIT).LT.SL(K,LIT)) GOTO 40
C.....DEPOSIT WHOLE LITHOLOGY
      IF (SL(K,LIT).LE.0.00001) GOTO 38
      ZT(I,J)=ZT(I,J)+SL(K,LIT)/DX2*FD(LIT)
      SL(K,LIT)=SL(K,LIT)*(1.-FD(LIT))
      K2=(ZT(I,J)-ZB(I,J))/DZZ+1
      DO 35 K3=K1,K2
   35 CALL SEDNOD3 (I,J,K3,LIT)
      TCD=TCD+SL(K,LIT)/TC( LIT)
   38 CONTINUE
      GOT0 17
C.....DEPOSIT LITH FRACTION
   40 K1=(ZT(I,J)-ZB(I,J))/DZZ+1
      SL(K,LIT)=SL(K,LIT)-SDP
      ZT(I,J)=ZT(I,J)+ZDP
      K2=(ZT(I,J)-ZB(I,J))/DZZ-1
      DO 45 K3=K1,K2
   45 CALL SEDNOD3 (I,J,K3,LIT)
   17 CONTINUE
    5 CV(K)=CVW
      CPO=CP(K)
      IF (CABS(CPO-CPN).LT.DX.OR.IERR1.EQ.1) GOTO 15
      OPEN (24 , FILE='for24.d', FORM='FORMATTED')
      REWIND (24)
      WRITE (24,8) T0,K,CPO,CPW,CVW,R,AB,VS,ZDIF,FEN(I,J)
    8 FORMAT (' WARNING: TIME INCREMENT 1 on FACT 1 T00 HIGH'/
     &' T0,K,CPO,CPW,CVW,R,AB,VS,ZDIF,FEN(I,J)'/
     &1X,F8.5,I2,1X,6F6.0,2E10.2/1X,3F5.1)
      IERR1=1
      CLOSE (24)
   15 CP(K)=CPW
C.....COMMENT IN NEXT LINE MUST BE ELIMINATED TO PLOT REAL-TIME PATHS
C.....CALL PLTPAT3 (CPO,K,1PLT,K)
      IF (ZEW.LT.0.) CP(K)=CP(K)+(CVC+CWV/(-ZEW+FEN(I,J)*DZ))*DT
    7 CONTINUE
      RETURN
      END
C--------------------------------------------------------------------------------
      SUBROUTINE NEWNOD3
C.....UPDATE NODE PARAMETERS
      IMPLICIT COMPLEX (C)
      CHARACTER*72 IT
      COMMON /BLK1/LBIT(50,41,61)
      COMMON IT,T0,TR,TD,DT,TB,TE,TID,TF,FLD,SWD,VIS,ROU,DV,CVC,CWV,
     & SDI(4),SDD(4),BD(4),FCO(5),
     & TI,LI,CPI(2Q),CVI(20),SLI(20,4),TEV,LEV,CPEV(20),
     & DX,N,M,NQ,QX(10,4),QY(10,4),QZ(10,4),
     & ZT(41,61),ZB(41,61),DZZ,L,CP(5000),CV(5OD0),SL(5000,4),
     & FEN(41,61) ,CVN(41,61),SUB(41,61),ZT1(41,61),SDER(41,61),
     & NY,G,DX2,DZ,DM,FF,FB,F3,F4,VST(4),FU(4),FD(4),TC(4),FAC
C.....INITIALIZE TO 0
      DO 5 I=1,N
      DO 5 J=1,M
      CVN(I,J)=(0.,0.)
    5 FEN(I,J)=0.
      NEA=0
C.....ENTER MAIN D0 LOOP
      DO 10 K=1,L
C.....CHECK FOR OUT OF BOUNDS
      IF (REAL(CP(K)).LT.0.) GOTO 10
      NEA=NEA+1
C.....FIND NODE
      J=REAL(CP(K))/DX+1.5
      I=N-AIMAG(CP(K)/DX+0.5
C.....ADD TO NODE VELOCITY AND NO. OF ELEMENTS
      CVN(I,J)=CVN(I,J)+CV(K)
      FEN(I,J)=FEN(1,J)+1.
   10 CONTINUE
      IF (NEA.EQ.0)) L=0
C.....FIND AVERAGES
      DO 20 I=1,N
      D0 20 J=1,M
   20 IF (FEN(I,J).NE.0.) CVN(I,J)=CVN(I,J)/FEN(I,J)
C.....FIND SECOND DERIVATIVES
      DO 10 I=1,N
      DO 30 J=1,M
      I1=MAX0(1,I-1)
      J1=MAX0(1,J-1)
      I2=MIN0(N,I+1)
      J2=MIN0(M,J+1)
   20 SDER(I,J)=(ZT(I,J)-(ZT(I1,J)+ZT(I2,J)+ZT(I,J1)+ZT(I,J2))/4.)/DX
      RETURN
      END
C--------------------------------------------------------------------------------
```

```
      SUBROUTINE READDF3
C.....READS FORMATTED DATA FILE
      IMPLICIT COMPLEX (C)
      CHARACTER*72 IT
      CHARACTER*4 WORD
      DIMENSION LIT (800)
      COMMON /BLK1/LBIT(50,41,61)
      COMMON IT,T0,TR,TD,DT,TB,TE,TID,TF,FLD,SWD,VIS,ROU,DV,CVC,CWV,
     & SDI(4),SDD(4),BD(4),FCO(5),
     & TI,LI,CPI(2Q),CVI(20),SLI(20,4),TEV,LEV,CPEV(20),
     & DX,N,M,NQ,QX(10,4),QY(10,4),QZ(10,4),
     & ZT(41,61),ZB(41,61),DZZ,L,CP(5000),CV(5OD0),SL(5000,4),
     & FEN(41,61) ,CVN(41,61),SUB(41,61),ZT1(41,61),SDER(41,61),
     & NY,G,DX2,DZ,DM,FF,FB,F3,F4,VST(4),FU(4),FD(4),TC(4),FAC
      READ (20,1,ERR=10,END=10)
     & IT,T0,TR,TD,DT,TB,TE,TID,TF,FLD,SWD,VIS,ROU,DV,CVC,CWV,
     & (5DI(K),K=1,4),(SDD(K),K=1,4),(BD(K),K=1,4),
     & (FCO(K),K=1,5),TI,LI
    1 FORMAT (A72///8(11X,F8.0/)//5(11X,F8.0/)2(11X,2FS.0/)
     & ///3(11X,4F8.0/),11X,5F8.0///11X,F8.0/11X,I8/)
      IF (LI.GT.0) READ (20,6,ERR=10,END=10)
     & (CPI(K),CVI(K),(SLI(K,L1),L1=1,4),K=1,LI)
     & FORMAT (1X,8F8.0)
      READ (20,24,ERR=10,END=10) TEV,LEV
   24 FORMAT (//11X,F8.0/11X,I8/)
      IF (LEV.GT.0) READ (20,4,ERR=10,END=10) (CPEV(LEVI),LEVI=1,LEV)
      READ (20,1,ERR=10,END=10) DX,N,M,NQ
    7 FORMAT (//11X,F8.0/11X,I8/11X,I8///11X,I8/)
      IF (NQ.GT.0) READ (20,4,ERR=10,END=10)
     & ((QX(K,L1),QY(K,L1),QZ(K,L1),L1=1,4),K=1,NQ)
    4 FORMAT (1X,3F8.0)
C.....READ SURFACE GRID AND BASEMENT GRID
      READ (20,8,ERR=10,END=10)
    8 FORMAT (/)
      DO 2 I=1,N
    2 READ (20,3,ERR=10,END=10) (ZT(I,J),J=1,M)
    3 FORMAT (1x,10r-1.0)
      READ (20,9,ERR=10,END=10) WORD
    9 FORMAT (/1X,A4)
      IF (WORD.NE.'NOBA') GOTO 38
      DO 33 I=1,N
      DO 33 J=1,M
   33 ZB(I,J)=ZT(I,J)
      READ (20,48,ERR=10,END=10) DZZ
   48 FORMAT (/11X,F8.0)
      GOTO 19
   38 DO 12 I=1,N
   12 READ (20,3,ERR=10,END=10) (ZB(I,J),J=1,M)
C.....READ LITHOLOGY
      READ (20,18,ERR=10,END=10) DZZ
   18 FORMAT (//11x,F8.0)
      DO 15 I=1,N
      DO 15 J=1,M
      READ (20,14,ERR=10,END=10) KL,(LIT(JKL) ,JKL=1,KL)
   14 FORMAT (1X,I3,1X,12(70I1/))
      DO 13 JKL=1,KL
   13 CALL SEDNOD3 (I,J,JKL,LIT(JKL))
   15 CONTINUE
C.....READ FLUID ELEMENTS
   19 READ (20,5,ERR=10,END=10) L
```

```
    5 FORMAT (//11X,I8/)
      IF (L.GT.0) READ (20,17,ERR=10,END=10) L
     & (CP(K),CV(K),(SL.(K,KS),KS=1,4),K=1,L)
   17 FORMAT (1X,8F8.0)
C.....FIND PARAMETERS
      DZ=DV/DX/DX
      G=9.81
      DX2=DX*DX
      DM=DV*FLD
      FF=VIS
      FB=ROU*FF
      IF (F3.EQ.0.) F3=0.2E-10
      F4=.750
      DO 23 K1=1,4
      FU(K1)=1.-FCO(K1)
      VST(K1)=AMIN1(1895.*(SDD(K1)-FLD)**0.8*SDI(K1)**1.4,
     & 4.88*SQRT((SDD(K1)-FLD)*SDI(K1)))
      FD(K1)=AMIN1(1.,VST(K1)*DT/DZ)
   23 TC(K1)=1./SDI(K1)*F3
      FAC=(1.-FCO(5))/DX2/(BD(1)/TC(1)+BD(2)/TC(2)+BD(3)/TC(3)+
     & BD(4)/TC(4))
      RETURN
C.....ERRORS
   10 OPEN (24,FILE='for24.d',FORM='FORMATTED')
      REWIND(24)
      WRITE (24,101) T0,TR,L
  101 FORMAT (1X,' TIME=',F15.7,' YEARS OF ',F15.7,' YEARS'/
     & ' L=',I6)
      WRITE (24,11)
   11 FORMAT (' SUBROUTINE READDF3 FOUND ERROR IN DATA FILE')
      CLOSE (24)
      STOP
      END
C-------------------------------------------------------------------------------
      SUBROUTINE SEDNOD3 (I,J,K,LIT)
C.....CAUSES EROSION OR DEPOSITION TO OCCUR ON NODE
C     I=ROW OF NODE
C     J=COL OF NODE
C     K=CELL, IF 0, NEGATIVE OR > 800, ERROR IS RETURNED
C     LIT=LITHOLOGY: 1, 2, 3, OR 4. IF 0 or NEGATIVE, LIT IS RETURNED
      IMPLICIT COMPLEX (C)
      CHARACTER*72 IT
      COMMON /BLK1/LBIT(50,41,61)
      COMMON IT,T0,TR,TD,DT,TB,TE,TID,TF,FLD,SWD,VIS,ROU,DV,CVC,CWV,
     & SDI(4),SDD(4),BD(4),FCO(5),
     & TI,LI,CPI(2Q),CVI(20),SLI(20,4),TEV,LEV,CPEV(20),
     & DX,N,M,NQ,QX(10,4),QY(10,4),QZ(10,4),
     & ZT(41,61),ZB(41,61),DZZ,L,CP(5000),CV(5OD0),SL(5000,4),
     & FEN(41,61) ,CVN(41,61),SUB(41,61),ZT1(41,61),SDER(41,61),
     & NY,G,DX2,DZ,DM,FF,FB,F3,F4,VST(4),FU(4),FD(4),TC(4),FAC
C.....ERODE
      IF (K.LE.800.AND.K.GT.0.AND.LIT.GE.0.AND.LIT.LE.4) GOT0 2
      OPEN (24,FILE='for24.d' ,FORM='FDRMATTED’)
      REWIND(24)
      WRITE (24,11) T0,TR,L
   11 FORMAT (1X,' TIME=',F15.7,' YEARS OF ’,F15.7,' YEARS'/
     & ' L=',I6)
      WRITE (24,12) K,LIT
   12 FORMAT (' SED. COLUMN < 1 OR > 800, K=',I4,' LIT=',I1)
      CLOSE (24)
      CALL WRITGU3
      STOP
    2 LW=(K+15)/16
      LB=2*K+14-16*LW
      IF (LIT.GT.0) GOTO 1
      LIT=IBITS(LBIT(LW,I,J),LB,2)+1
      RETURN
C.....DEPOSIT
    1 IF((LIT-1)/2.EQ.1) THEN
      LBIT(LW,I,J)=IBSET(LBIT(LW,I,J),LB+1)
      ELSE
      LBIT(LW,I,J)=IBCLR(LBIT(LW,I,J),LB+1)
      ENDIF
      IF(MOD(LIT,2).EQ.0) THEN
      LBIT(LW,I,J)=IBSET(LBIT(LW,I,J),LB)
      ELSE
      LBIT(LW,I,J)=IBCLR(LBIT(LW,I,J),LB)
      ENDIF
      RETURN
      END
C---------------------------------------------------------------------
      SUBROUTINE SET3
C.....SETS TIME EXTRAPOLATION
      IMPLICIT COMPLEX (C)
      CHARACTER*72 IT
      COMMON /BLK1/LBIT(50,41,61)
      COMMON IT,T0,TR,TD,DT,TB,TE,TID,TF,FLD,SWD,VIS,ROU,DV,CVC,CWV,
     & SDI(4),SDD(4),BD(4),FCO(5),
     & TI,LI,CPI(2Q),CVI(20),SLI(20,4),TEV,LEV,CPEV(20),
     & DX,N,M,NQ,QX(10,4),QY(10,4),QZ(10,4),
     & ZT(41,61),ZB(41,61),DZZ,L,CP(5000),CV(5OD0),SL(5000,4),
     & FEN(41,61) ,CVN(41,61),SUB(41,61),ZT1(41,61),SDER(41,61),
     & NY,G,DX2,DZ,DM,FF,FB,F3,F4,VST(4),FU(4),FD(4),TC(4),FAC
      DO 1 I=1,N
      DO 1 J=1,M
    1 ZT1(I,J)=ZT(I,J)
      RETURN
      END
C---------------------------------------------------------------------
      SUBROUTINE WRITDF3
C.....WRITES FORMATTED DATA FILE
      IMPLICIT COMPLEX (C)
      CHARACTER*72 IT
         DIMENSION LIT(800)
      COMMON /BLK1/LBIT(50,41,61)
      COMMON IT,T0,TR,TD,DT,TB,TE,TID,TF,FLD,SWD,VIS,ROU,DV,CVC,CWV,
     & SDI(4),SDD(4),BD(4),FCO(5),
     & TI,LI,CPI(2Q),CVI(20),SLI(20,4),TEV,LEV,CPEV(20),
     & DX,N,M,NQ,QX(10,4),QY(10,4),QZ(10,4),
     & ZT(41,61),ZB(41,61),DZZ,L,CP(5000),CV(5OD0),SL(5000,4),
     & FEN(41,61) ,CVN(41,61),SUB(41,61),ZT1(41,61),SDER(41,61),
     & NY,G,DX2,DZ,DM,FF,FB,F3,F4,VST(4),FU(4),FD(4),TC(4),FAC
C.....WRITE GENERAL DATA
      WRITE(21,1)
     & IT,T0,TR,TD,DT,TB,TE,TID,TF,FLD,SWD,VIS,ROU,DV,CVC,CWV,
     & SDI(K,K=1,4),(SDD(K),K=1,4),(BD(K),K=1,4),
     & (FCO(K),K=1,5),TI,LI
    1 FORMAT (A72//' RUN PARAMETERS:'/' START TIM=',E8.2,' Y'/
     & ' END TIM=',E8.2,' Y'/' TIM/DISPL=',E8.2,' Y'/' TIM INCR1=',
     & E8.2,' S'/' TIM FACT1=',E8.2/' TIM INCR2=',E8.2,' Y'/
     & ' TIM IDLE =',E8.2,' Y'/' TIMFACT2=',E8.2//
     & ' GENERAL PHYSICAL PARAMETERS:'/'FLOW DENS=',F8.0,' KG/M3'/
     & ' SEA DENS =',F8.0,' KG/M3'/' FLOW VISC=',E8.2,' NS/M2'/
     & ' ROUGHNESS=',F8.4/'EL VOLUME=',E8.2,' M3'/' CURR(X,Y)=',2E8.2,
     & ' M/S'/' WAVE(X,Y)=',2E8.2,' M2/S',
     & ' SEDIMENT PRAMETERS:'/15X,'S1',6X,'S2',6X,'S3',6X,'S4',5X,
     & 'BAS'/' DIAMETER =',4E8.2,'  ----- M'/' DENSITY  =',4F8.0,
     & '  -----  KG/M3'/' BAS DECAY=',4F8.3,'  -----'/' COHESION =',
     & 5E8.2//' SOURCES:'/' INTERVAL =',E8.2,' Y'/' # SOURCES=',I8/
     & '   X(M)    Y(M)   XV9M/S0 YV(M/S)  S1(M3)  S2(M3)',
     & '  S3(M3)  S4(M3)')
      IF (LI.GT.0) WRITE (21,6)
     & (CPI(K),CVI(K),(SLI(K,L1),L1=1,4),K=1,LI)
    6 FORMAT (1X,4F8.0,4E8.2)
      WRITE (21,20) TEV,LEV
   20 FORMAT (/' EVAPORATION (UNUSED AT PRESENT)'/
     & ' INTERVAL =',E8.2,' Y’/' # OF ELEM=',I8/'   X-POS   Y-POS')
      IF (LEV.GT.0) WRITE (21,6) (CPEV(LEVI),LEV1'=1,LEV)
      WRITE (21,7) DX,N,M,NQ
    7 FORMAT (/' TOPOGRAPHY:'/' GRID SIDE=',F8.1, 'M','/' NROWS   =',
     & I8/' NCOLS    =',I8//' TECTONICS (UNUSED AT PRESENT):'
     & /' # QUADS  =',I8/'   X(M)    Y(M)  SUBS(M/Y)')
      IF (NQ.GT.0) WRITE (21,4)
     & ((QX(K,L1),QY(K,L1),QZ(K,L1),L1=1,4) ,K=1,NQ)
    4 FORMAT (1X,2FB.0,E8.2)
C.....WRITE SURFACE GRID AND BASEMENT GRID
      WRITE (21,8)
    8 FORMAT (/' GRID nouns ELEVATION (SURFACE) (M)')
      DO 2 I=1,N
      WRITE (21,3)) (ZT(I,J),J=1,M)
    3 FORMAT (1x,10F7.1)
      WRITE (21,19)
   19 FORMAT (/' GRID NODES ELEVATION (BASEMENT) (M)’)
      DO 12 I=1,N
   12 WRITE (21,3) (ZB(I,J),J=1,N)
C.....WRITE LITHOLOGY
      WRITE (21,18) DZZ
   18 FORMAT (/' LITHOLDGIC COLUMNS:'/' LCELL DEP=',F8.3)
      DO 15 1=1,N
      DO 15 J=1,M
      KL=INT((ZT(I,J)-ZB(I,J))/DZZ+0.99999)
      DO 13 JKL=1,KL
      LIT(JKL)=0
   13 CALL SEDNOD3 (I,J,JKL,LIT(JKL))
      WRITE (21,14) KL,(LIT(JKL),JKL=1,KL)
   14 FORMAT (1X,I3,1X,I2(70I1/))
   15 CONTINUE
C.....WRITE FLUID ELEMENTS
      DO 22 K=1,L
      DO 22 KS=1,4
   22 SL(K,KS)=SL(K,KS)/TB
      WRITE (21,5) L
    5 FORMAT (/' ELEMENT POSITIONS AND VELOCITIES'/' # OF ELEM:',I8/
     & '   X(M)    Y(M)   XV(M/S) YV(M/S)  S1(M3)  S2(M3)',
     & '   S3(M3)   S4(M3)')
      IF(L.GT.0) WRITE (21,17)
     & (CP(K),CV(K),(SL(1(,KS),KS=1,4),K=1,L)
   17 FORMAT (1X,8F8.0)
      RETURN
      END
```

```
C-------------------------------------------------------------------------------
      SUBROUTINE WRITGU3
C.....WRITES OUTPUT FILE FOR GRAPHICS
      IMPLICIT COMPLEX (C)
      CHARACTER*72 IT
         DIMENSION WRT (100)
      COMMON /BLK1/LBIT(50,41,61)
      COMMON IT,T0,TR,TD,DT,TB,TE,TID,TF,FLD,SWD,VIS,ROU,DV,CVC,CWV,
     & SDI(4),SDD(4),BD(4),FCO(5),
     & TI,LI,CPI(2Q),CVI(20),SLI(20,4),TEV,LEV,CPEV(20),
     & DX,N,M,NQ,QX(10,4),QY(10,4),QZ(10,4),
     & ZT(41,61),ZB(41,61),DZZ,L,CP(5000),CV(50D0),SL(5000,4),
     & FEN(41,61) ,CVN(41,61),SUB(41,61),ZT1(41,61),SDER(41,61),
     & NY,G,DX2,DZ,DM,FF,FB,F3,F4,VST(4),FU(4),FD(4),TC(4),FAC
C.....INITIALIZE
      CALL FILTER3 (0)
      EA=0
C.....WRITE
      IF(T0.NE.0.) GOTO 19
C.....WRITE GENERAL DATA
      WRITE (22)
     & IT,T0,TR,TD,DT,TB,TE,TID,TF,FLD,SWD,VIS,ROU,DV,CVC,CWV,
     & SDI(K,K=1,4),(SDD(K),K=1,4),(BD(K),K=1,4),
     & (FCO(K),K=1,5),TI,LI
      IF (LI.GT.0) WRITE (22)
     & (CPI(K),CVI(K),(SLI(K,L1),L1=1,4),K=1,LI)
      WRITE (22) TEV,LEV
      IF (LEV.GT.0) WRITE (22) (CPEV(LEVI),LEVI=1,LEV)
      WRITE (22) DX,N,M,NQ
      IF (NQ.GT.0) WRITE (22)
     & ((QX(K,L1),QY(K,L1),QZ(K,L1),L1=1,4),K=1,NQ)
   19 WRITE(22) T0
      DO 8 I=1,N
    8 WRITE (22) (ZT(I,J),J=1,M)
      DO 2 I=1,N
    2 WRITE (22) (ZB(I,J),J=1,M)
C.....WRITE LITHOLOGY
      WRITE (22) DZZ
      DO 9 I=1,N
      DO 9 J=1,M
      KL=(INT((ZT(I,J)-ZB(I,J))/DZZ+0.99999)+15)/16
    9 WRITE (22) KL,(LBIT(K,I,J),K=1,KL)
C.....WRITE # OF FLUID ELEMENTS
      DO 10 I=1,N
      DO 29 J=1,M
      EA=EA+FEN(I,J)
   29 WRT(J)=FEN(I,J)
   10 WRITE (22) (WRT(J),J=1,M)
      WRITE (22) EA
      DO 14 I=1,N
      DO 13 J=1,M
   13 WRT(J)=REAL(CVN(I,J))
   14 WRITE (22) (WRT(J),J=1,M)
      DO 18 I=1,N
      DO 17 J=1,M
   17 WRT(J)=AIMAG(CVN(I,J))
   18 WRITE (22) (WRT(J),J=1,M)
      RETURN
      END
```

Listing of program SEDSHO3

Program SEDSHO3 produces the graphic output for the multiple-sediment model, SEDSIM3. A listing of the program and its subroutines is provided. There are subroutines that are hardware dependent and that are utilized by SEDSHO3, but they are not included in the listing:

- OPENPLOT opens a plot and sets plotting scales
- PLOT draws a line or moves a pen
- OPENPANL opens a panel or color-filled polygon
- CHARS draws characters
- CLOSPLOT closes a plot

The user should reokace the calls to these subroutines by their equivalents on the particular system employed.

```
      PROGRAM SEDSHO3
      IMPLICIT COMPLEX (C)
      CHARACTER*1 ANS,AN(6),BS
      CHARACTER*8 BLANK,FIL1,FILN
      CHARACTER*72 IT
      COMMON /BLK1/LBIT(50,41,61)
      COMMON IT,T0,TR,TD,DT,TB,TE,TID,TF,FLD,SWD,VIS,ROU,DV,CVC,CWV,
     & SDI(4),SDD(4),BD(4),FCO(5),
     & TI,LI,CPI(20),CVI(20),SLI(20,4),TEV,LEV,CPEV(20),
     & DX,N,M,NQ,QX(10,4),QY(10,4),QZ(10,4) ,
     & ZT(41,61),ZB(41,61),DZZ,L,
     & FEN(41,61),CVN(41,61),SUB(41,61),ZT(41,61),NY
     & /MAP/IPLT,IPEN,IPT,NROWS,NCOLS,
     & ZZ(82,122),XLEN,YLEN,ZSCL,SCLH,SCLV,X0,Y0,Z0,AZ,EL,DS,REF
      DATA BLANK/'        '/
      SAVE /MAP/
C.....INITIALIZE
      DO 5 JK=1,5
    5 AN(JL()='Y'
      AN(3)='N'
      AN(6)='N'
      FIL1='for22.d '
      UA=1.
      UD=0.
      REF=0.
      VEX=10.
      NF=1
      AZ=45.
      EL=30.
      NS=1
      XPOS=0.
      YPOS=0.
      STRK=45.
      IFG=0
      FILN=BLANK
      FENMIN=0.00001
      NDC=0
      BS=CHAR(8)
  500 FORMAT (A1)
  501 FORMAT (F10.0)
C.....SET PARAMETERS
    2 WRITE (6,601)
  601 FORMAT (' CHANGE PARAMETERS?(YES/NO/QUIT)=',$)
      READ (5,500) ANS
      IF (ANS.EQ.'Q'.DR.ANS.EQ.'Q') STOP
      IE (ANS.NE.'Y'.AND.ANS.NE.'Y') GOTO 102
      WRITE (6,502) FIL1,(BS,LL=1,8)
  502 FORMAT (' DATA FILE = '),a8,8a1,$)
      READ (5,503) FILN
  503 FORMAT (A8)
      WRITE (6,508) UA,UD,(BS,LL=1,11)
  508 FORMAT (' UNIT CURRENT (M/S), UNIT DEPTH (M) =',2F6.1,11A1,$)
      READ (5,* ,ERR=21) UA,UD
   21 WRITE (6,505) VEX,REF,(BS,LL=1,LL)
  505 FORMAT (' VERT. EXAGGERATION, REF. LEVEL =',F5.1,F7.1,11A1,$)
      READ (5,*  ,ERR=22) VEX,REF
   22 WRITE (6,512) NF,AZ,EL,(BS,LL=1,10)
  512 FORMAT (' PERSPECTIVE #, AZIMUTH, ELEVATION : ',I1,F5.0,F4.0,
     & 10A1 $)
      READ (5,*   ,ERR=210) NF,AZ,EL
      IF (NF.GT.2) GOTO 22
      IF (NF.LT.1) GOTO 22
  210 WRITE (6,510) NS,XPOS,YPOS,STRK,(BS,LL=1,2U)
  510 FORMAT (' SECTION 19, X-POS, Y-POS, STRIKE = ',IL,2F7.0,F5.0,
     & 20A1 5)
      READ (5,* ,ERR=102) NS,XPOS,YPOS,STRK
      WRITE (6,514) THCK,(B5,LL=1,6)
  514 FORMAT (' FACIES THICKNESS =',F6.2,6A1,$)
      READ (5,515) THCK
  515 FORMAT (F10.0)
      IF (NS.GT.2) GOTO 210
      IF (NS.LT.1) GOTO 210
C .. .-OPEN FILE IF NECESSARY
  102 IF ((FILN.EQ.BLANK.OR.FILN.EQ.FIL1).AND.IFG.EQ.1) GOTO 101
      IF (FILN.NE.BLANK.AND.FILN.NE.FIL1) FIL1=FILN
      OPEN (22,FILE=FIL1,FORM:'UNFORMATTED')
      REWIND (22)
      IFG=1
C....SET SURFACE DISPLAYS
  101 WRITE (6,602)
  602 FORMAT (' CHANGE DISPLAYS?(Y/N/Q)=',$)
      READ (5,500) ANS
      IF (ANS.EQ.'Q'.OR.ANS.EQ.'q') STOP
      IF (ANS.NE.'Y'.A.ND.ANS.NE.'y') GOTO 300
      WRITE (6,603) AN(1),BS
  603 FORMAT ('   1. CONTOUR MAP?(Y/N)=',2A1,$)
      READ (5,500) ANS
      IF (ANS.NE.' ') AN(1)=ANS
      WRITE (6,604) AN(2),BS
  504 FORMAT ('   2. VELOCITY AND DEPTH PLOT?(Y/N)=',2A1,$)
      READ (5,500) ANS
      IF (ANS.NE.' ') AN(2)=ANS
      WRITE (6,605) AN(3),BS
  605 FORMAT ('   3. FISHNET DIAGRAM?(Y/N)=',2A1,$)
      IF (ANS.NE.' ') AN(3)=ANS
      WRITE (6,606) AN(4),BS
  606 FORMAT ('   4. AGE CROSS SECTION?(Y/N)=',2A1,$)
```

```
      IF (ANS.NE.' ') AN(4)=ANS
      WRITE (6,607) AN(5),BS
  607 FORMAT ('   5. SED-TYPE CROSS SECTION?(Y/N)=',2A1,$)
      READ (5 500) ANS
      IF (ANS.NE.' ') AN(5)=ANS
      WRITE (6,610) AN(6),BS
  610 FORMAT ('   6. FACIES MAPS?(Y/N)=',2A1,$)
      READ (5,500) ANS
      IF (ANS.NE.' ') AN(6)=ANS
  300 WRITE (6,608)
  608 FORMAT (' STARTING TIME (YR)=',$)
      READ (5,50L,ERR=300) TNDS
      WRITE (6,609)
  609 FORMAT (' ENDING TIME (YR)=',$)
      READ (5,501,ERR=300) TNDE
      IF (TNDE.EQ.0..AND.TNDS.EQ.0.) GOTO 2
C.....PROCESS
  310 REWIND (22)
      NDC=0
  312 CALL READGU3 (IF1,0)
      IF (IF1.EQ.1) GOTO 2
      NY=-1
  350 CALL READGU3 (IF1,1)
      TR=TNDE
      NY=NY+1
      IF (IF1.EQ.1.0R.T0.GT.TNDE*1.0001) GOTO 2
  325 NDC=NDC+1
      IF (T0.LT.TNDS) SGOTO 350
  330 IF (AN(1).EQ.’Y'.OR.AN(3).EQ.'Y'.OR.AN(1).EQ.'y'.OR.AN(3).EQ.'y')
     & CALL MAPCYC3 (2,1,0,VEX)
      IPLT=100+NY
      IPEN=3
      IF (AN(1).NE.'Y'.AND.AN(1).NE.'y') GOTO 335
      IF (NY.EQ.0) CALL PLTGRD (1,1)
      CALL MAP2D
  335 IPLT=20D+NY
      IF (AN(2).EQ.'Y'.OR.AN(2).EQ.'y')
     & CALL PLTNOD3 (IPLT,5,D,FENMIN,UA,UD)
      IPLt=200+NF*100+NY
      IPEN=6
      IF (AN(3).EQ.'Y'.DR.AN(3).EQ.'Y') CALL MAP3D
      IFL=0
      IF (TNDE-T0.LT.TD) IFL=1
      IF (AN(4).EQ.’Y'.OR.AN(4).EQ.'y')
     & CALL CRSSEC3 (NS,VEX,XPOS,YPOS,STRK,REF,0,IFL,IF1)
      IF (AN(5).EQ.'Y'.OR.AN(5).EQ.'y')
     & CALL CRSSEC3 (NS,VEX,XPOS,YPOS,STRK,REF,1,IFL,IFU)
      IF (AN(6).EQ.'Y'.OR.AN(6).EQ.'y') CALL FACIES] (THCK)
      IF (IF1.EQ.1) GOTO 210
      WRITE (6,199) T0
  199 FORMAT (' TIME :',F15.7,' YEARS')
      GOTO 350
      END
C-------------------------------------------------------------------------------
      SUBROUTINE CRSSEC3 (NS,VEX,XPOS,YPOS,STRKL,REF,LITAGE,IFL,IFU
C.....DRAWS CNOSS SECTION SHOWING AGE OF SEDIMENT
C     NS = SRCTION NUMBER (1 OR 2)
C     VEX = VERTICAL EXAGGERATION FOR CROSS SECTION
C     LITAGE = 0 DRAW AGE, = 1 DRAW SEDIMENT TYPE
C     IFL = 1 IF DISPLAY IS LAST IN SSQUENCE
```

```
C      SLEN = SECTION LENGTH (METERS, OBJECT SCALE)
C      SLENM = SECTION LENGTH (INCHES, MAP SCALE)
C      XSEC = X POSITION IN SECTION (INCHES, MAP SCALE)
C      YSEC = Y (VERTICAL) POSITION IN SECTION (INCHES, MAP SCALE)
C      YSEC1 = SAME AS YSEC, BUT ONE SURFACE DOWN
C      DZZ = HEIGHT OR ONE LITHOLOGY BLOCK
       IMPLICIT COMPLEX (C)
       CHARACTER*72 IT
       CHARACTER*2 AB(4)
       CHARACTER*6 LEG
       DIMENSION IND(11),XS(2),YS(2),FLIT(4),YSEC(101),YSEC1(101)
C.....FOR STANDARD FORTRAN CHANGE 'EXTENDED BLOCK' TO 'COMON',
       COMMON /BLK1/LBIT(50,41,61)
       COMMON IT,T0,TR,TD,DT,TB,TE,TID,TF,FLD,SWD,VIS,ROU,DV,CVC,CWV,
      & SDI(4),SDD(4),BD(4),FCO(5),
      & TI,LI,CPI(20),CVI(20),SLI(20,4),TEV,LEV,CPEV(20),
      & DX,N,M,NQ,QX(10,4),QY(10,4),QZ(10,4) ,
      & ZT(41,61),ZB(41,61),DZZ,L,
      & FEN(41,61),CVN(41,61),SUB(41,61),ZT(41,61),NY
       DATA IND/-2,-3,-4,-5,-6,-7,-8,-9,-12,-14,-15/ ,PI/3.1415926/,
      & AB/'A ','A''','B','B'''/
       TIM=TR-T0
       IF1=0
       D=2.1*(1-LITAGE)
C.....SKIP IF DISPLAY NOT 0
       IF (NY.NE.0) GOTO 35
C.....INITIALIZE
       E=DX/1000.
       ND=100
       XLEN=6.87/MAX0(N-1,M-1)
       YLEN=XLEN
       ZSCL=XLEN/DX*VEX
       XLE=2.*DX/VEX
       XD=0.25
       YD=0.25
       FLIT(1)=0.
       FLIT(2):0.
       FLIT(3)=0.
       FLIT(4)=0.
       SHFT=-REF*ZSCL
C.....CONVERT STRIKE TO 1ST HALF AND TO RADIANS AND ROTATE BY PI
       STRK=AMOD(STRK1,180.)
       IF (STRK.LT.0.) SRRX=STRK+180.
       IF (STRK.EQ.0.) STRK=0.01
       IF (STRK.EQ.90.) STRK:90.01
       STRK=(90.-STRK)/180.*PI
.....FIND END POINTS OR SECTION XS(L),YS(1),XS(2),YS(2)
       XMAX=(M-1)*DX-E
       YMAX=(N-1)*DX-E
       TANS=TAN(STRK)
       XL=XPOS-YPOS/TANS
       YL=YPO5-XPOS*TANS
       X2=XPOS+(YMAX-YPOS)/TANS
       Y2=YPOS+(XMAX-XPOS)*TAN5
       I=1
       IF (Y1.LE.0..OR.Y1.GT.XMAX) GOTO 11
       XS(I)=E
       YS(I)=Y1
       I=2
   11 IF (X2.LE.0..OR.X2.GT.XMAX) GOTO 12
```

```
      XS(1)=X2
      YS(I)=YMAX
      IF (I.EQ.2) GOTO 44
      I=2
   12 IF (X1.LT.0..OR.X1.GE.XMAX) GOTO 13
      XS(I)=X1
      YS(I)=E
      IF(I.EQ.2) GOTO 44
      I=2
   13 XS(I)=XMAX
      YS(I)=Y2
      IF (I.EQ.2) GOTO 44
      WRITE (6,17)
   17 FORMAT (' SECTION NOT IN AREA, TRY AGAIN')
      IF1=1
      RETURN
C.....REVERSE POINTS IF NECESSARY
   44 IF (XS(2).GT.XS(1)) SOME 45
      XT=XS(1)
      YT=YS(1)
      XS(1)=XS(2)
      YS(1)=YS(2)
      XS(2)=XT
      YS(2)=YT
C.....FIND CONSTANTS
   45 SLEN=SQRT((XS(1)-XS(2))**2+(YS(1)-YS(2))**2)
      DSEC=5LEN/ND
      SLENH=SLEN/DX*XLEN
      XSECU=SLENM/ND
C.....DRAW LINE ON MAP
      IPLT=13+(NS*2+LITAGE)
      CALL OPENPLOT (IPLT,1,13.75,13.75.-1.,15.,-5.,11.)
      CALL PLOT (IPLT,XS(1)/DX*XLEN,Y5(1)/DX*YLEN,0)
      CALL PLOT (IPLT,XS(2)/DX*XLEN,YS(2)/DX*YLEN,1)
C.....DRAW LABELS AT ENDS OF SECTION LINE
      X=XS(1)/DX*XLEN+0.1*COS(STRK+1.25*PI)
      Y=YS(1)/DX*YLEN+0.1*SIN(STRK+1.25*PI)
      CALL PLOT (IPLT,X,Y,0)
      CALL CHARS (PLT,STRK*180./PI,0.1,0.,0.,1.,1,2,AB(2*NS-1))
      X=XS(2)/DX*XLEN+0 071*COS(STRK-PI/2.)
      Y=YS(2)/DX*YLEN+0.071*SIN(STRK-PI/2.)
      CALL PLOT (IPLT,X,Y,O)
      CALL CHARS (IPLT,STRK*180./PI,0.1,0.,0.,1.,1,2,AB(2*NS))
      CALL CLOSPLOT (IPLT)
C.....DRAW INITIAL PANEL
   30 IPLT=3OU+(NS*2+LITAGE)*100
      CALL OPENPLOT (IPLT,1,13.75,13.75,
     & -1./2.,15./2.,-0.1-D,(-0.1-D+16.)/2.+(-0.1-D)/2.)
      CALL PLOT (IPLT,0.,0.,0)
      CALL OPENPANL (1,1)
      CALL PLOT (IPLT,SLENM,0.,1)
      CALL PLOT (IPLT,SLENM,2.,1)
      CALL PLOT (IPLT,0.,2.,1)
      CALL CLOSPANL
.....DRAW LABELS AT ENDS OR SECTION PANEL
      CALL PLOT (IPLT,-0.1,0.,0)
      CALL CHARS (IPLT,0.,0.1,0.,0.,1.,1,2,AB(2*NS-1))
      CALL PLOT (IPLT,SLENM,0,0)
      CALL CHARS (IPLT,0.,0.1,0.,0.,1.,1,2,AB(2*NS))
C.....ENCODE SCALE
```

```
      WRITE (LEG,19) XLE
   19 FORMAT (F5.L,'m')
C.....DRAN VERTICAL SCALE
  102 CALL PLOT (IPLT,-0.15,XD+1.-YLEN,0)
      CALL PLOT (IPLT,-0.15,XD+1.+YLEN,1)
      CALL PLOT (IPLT,-.20,XD+0.7,0)
      CALL CHARS (IPLT,90.,0.1,0.,0.,1.,1,6,LEG)
      CALL PLOT (IPLT,-.35,XD+0.4,0)
      CALL CHARS (IPLT,90.,0.L,0.,0.,1.,1,11,'Vert. Scale')
      CALL PLOT (IPLT,SLENM+0.1,0.3,0)
      IF (LITAGE.EQ.0) CALL CHARS (IPLT,0.,0.1,0.,0.,1.,1,3,'AGE')
      IF (LITAGE.EQ.1) CALL CHARS (IPLT,0.,0.1,0.,0.,1.,1,3,'SED')
C.....FIND YSEC AND YSEC1 ARRAYS
   35 DO 215 KD=1,ND+1
      X=XS(1)+(KD-1)*DSEC*COS(STRK)
      Y=YS(1)+(KD-1)*DSEC*SIN(STRK)
C.....FIND CELL (IC,JC) AND PROPORTIONS OF INFLUENCE (FJ,FI)
      JC=X/DX+1
      IC=N-INT(Y/DX)
      FJ=X/DX-INT(X/DX)
      FI=1.-(Y/DX-INT(Y/DX))
      YSEC(KD) =((ZT(IC,JC)*(1-FI)
     &        +ZT(IC+1,JC)*FI)*(1-FJ)
     &       +(ZT(IC,JC+1)*(1-FI)
     &      +ZT1(1C+1,JC+1)*FI)*FJ)*ZSCL
      YSEC1(KD)=((ZT1(IC,JC)*(1-FI)
     &        +ZT1(IC+1,JC)*FI)*(1-FJ)
     &       +(ZT1(IC,JC+1)*(1-FI)
     &      +ZT1(1C+1,JC+1)*FI)*FJ) *ZSCL
  215 CONTINUE
C.....OPEN AGE OR SED-TYPE PLOT
      IPLT=300+(NS*2+LITAGE)*100+NY
      IF (NY.GT.0)
    & CALL OPENPLOT (IPLT,1,13.75,13.75,
    & -1./2.,15./2.,-0.1-D,(-0.1-D+16.)/2.+(-0.1-D)/2.)
      IF (LITAGE.EQ.0) SOTO 135
C.....START SED-TYPE PLOT
      DO 15 KD=1,ND
      IF (YSEC(KD).LE.YSEC1(KD).AND.YSEC(KD+1).LE.YSEC1[KD+1)) GOTO 15
      FLIT(1)=0.
      FLIT(2)=0.
      FLIT(3)=0.
      FLIT(4)=0.
      DO 14 1N=-1,0
C ....FIND LITHOLOGY AND COLOR (COLOR INDEX IS GRAPHIC SOFTW. DEPEND.)
      X=XS(1)+(KD+ID)*DSEC*COS(STRK)
      Y=YS(1)+(KD+ID)*DSEC*SIN(STRK)
C.....FIND CELL (IC,JC) AND (FJ,FI) FOR SEGMENT END
      JC=X/D`+1
      IC=N-INT(Y/DX)-1
      FJ=X/DX-INT(X/DX)
      FI=1.-(Y/DX-INT(Y/DX))
      DO 14 II=0,1
      NO 14 JJ=0,1
      ZH=(ZT(IC+II,JC+JJ)-ZB(IC+II,JC+JJ) )/DZZ
      ZH1=(ZT1(1C+II,JC+JJ)-SUB(1C+II,JC+JJ)*TD-ZB(IC+II,JC+JJ)/DZZ
      IF (ZH1.GE.ZH.OR.ZH.LE.0.) GOTO 14
      NH=ZH+1
      NH1=ZH1+1
      FACT=(1-II+(2*II-1)*FI)*(1-JJ+(2*JJ-1)*FJ)/(NH-NH1+1)
      DO 24 KH=NH1,NH
      LIT=0
      IF (KH.LE.0) KH=1
      CALL SEDNO13 (IC+II,JC+JJ,KH,LIT)
      FLIT(LIT =FLIT(LIT)+FACT
   24 CONTINUE
   14 CONTINUE
      FLITOT=FLIT(1)+FLIT(2)+FLIT(3)+FLIT(4)
      IF (FLITOT0T.LE.0.1) GOTO 15
      IMAX=5-INT(FLIT(4)/FLITOT*4.9999)
      INDCOL=111
      IF(IMAX.EQ.1) GOTO 16
      IND1=MIN0(IMAX,INT(FLIT(1)/AMAX1(FLIT(1)+FLIT(2),FLIT(1)+FLIT(3))
     & *(2*IMAX-1.0001)+1))
      IND2=MIN0(IMAX,INT(FLIT(2)/AMAX1(FLIT(1)+FLIT(2),FLIT(2)+FLIT(3))
     & *(2*IMAX-1.0001)+1))
      IND3=MIN0(IMAX,INT(FLIT(3)/AMAX1(FLIT(1)+FLIT(3),FLIT(2)+FLIT(3))
     & *(2*IMAX-1.0001)+1))
      INDCOL=IND1*100+IND2*10+IND3
C.....DRAW SEDIMENT TYPE PANEI5
   16 CALL PLOT(IPLT,XSECU*(KD-1),YSEC(KD)+SHFT,0)
      CALL OPENPANL(INDCOL,0)
      CALL PLOT(IPLT,XSECU*(KD-1),YSEC1(KD)+SHFT,0)
      CALL PLOT(IPLT,XSECU*KD,YSEC1(KD+1)+SHFT,0)
      CALL PLOT(IPLT,XSECU*KD,YSEC(KD+1)+SHFT,0)
      CALL CLOSPANL
   15 CONTINUE
C.....DRAW AGE PANELS OR LITH MASKING PANEL
  135 CALL PLOT (IPLT,0.,2.,0)
      ICC=MOD(NY,10)+1
      IF (IFL.EQ.1.0R.LITAGE.EQ.1) 1CC=11
      CALL OPENPANL (IND(ICC),1)
      DO 115 KD=1,ND+1
  115 CALL PLOT (IPLT,XSECU*KD-1),YSEC(KD)+SHFT,1)
      CALL PLOT (IPPLT,SLENM,2.,0)
      CALL CLOSPANL
      CALL CLOSPLOT (IPLT)
C.....DRAW SEA LEVEL
      IF (SHFT.LE.0..OR.NY.NE.0) RETURN
      IPLT=30+(NS*2+LITAGE)*10
      CALL OPENPLOT (IPLT,1,13.75,13.75,
     & -1./2.,15./2.,-0.1-D,(-0.1-D+16.)/2.+(-0.1-D)/2.)
      CALL PLOT (IPLT,0.,SHFT,0)
      CALL PLOT (IPLT,SLENM,SHFT,5)
      CALL CLOSPLOT (IPLT)
      RETURN
      END
C--------------------------------------------------------------------------------
      SUBROUTINE DRBOTT
      COMMON /MAP/IPLT,IPEN,IPT,NROWS,NCOLS,
     & ZZ(82,122),XLEN,YLEN,ZSCL,SCLH,SCLV,X0,Y0,Z0,AZ,EL,DS,REF
     & /PERS/SINAZ,COSAZ,SINEL,COSEL
      SAVE /MAP/,/PERS/
      DO 1 K=1,4
      JINC=(K-1)/2
      IINC=MOD(K,4)/2
      IP=(K+2)/4*IPEN
      X1=JINC*XLEN*NCOLS
      Y1=IINC*YLEN*NROWS
      CALL PERSP (X1,YL,REF,X2,Y2,Z2,IFLAG)
      CALL PLOT (IPLT,X2,Y2,IP)
      IF (K.EQ.1) CALL OPENPANL (-15,1)
    1 IF (K(.EQ.4) CALL CLOSPANL
      RETURN
      END
C-------------------------------------------------------------------------------
      SUBROUTINE DRCELL(I,J)
      COMMON /MAP/IPLT,IPEN,IPT,NROWS,NCOLS,
     & ZZ(82,122),XLEN,YLEN,ZSCL,SCLH,SCLV,X0,Y0,Z0,AZ,EL,DS,REF
      /PERS/SINAZ,COSAZ,INEL,COSEL
      SAVE /MAP/,/PERS/
      DO 1 K=1,4
      JINC=(K-1)/2
      IINC=1-MOD(K,4)/2
      IP=(K+2)/4*IPEN
      X1=(J-1+JINC)*XLEN
      Y1=(NROWS-I-IINC)*YLEN
      ZL=Z(I+IINC,J+JINC)
      CALL PERSP (X1,Y1,Z1,X2,Y2,Z2,IFLAG)
      CALL PLOT (IPLT,X2,Y2,IP)
      IF (K.EQ.1) CALL OPENPANL (-15,1)
      IF (K.EQ.4) CALL CLOSPANL
      RETURN
      END
C-------------------------------------------------------------------------------
      SUBROUTINE DRSCAL
C.....DRAWS SCALE
      COMMON /MAP/IPLT,IPEN,IPT,NROWS,NCOLS,
     & ZZ(82,122),XLEN,YLEN,ZSCL,SCLH,SCLV,X0,Y0,Z0,AZ,EL,DS,REF
     & /PERS/SINAZ,COSAZ,SINEL,COSEL
      SAVE /MAP/,/PERS/
      CHARACTER*6 STRNG(3)
      LSCLH=SCLH*4
      LSCLV=SCLV*4
      WRITE (STRNG,10) LSCLH, LSCLH,LSCLV
   10 FORMAT (2(I5,'m'/)I4,'m ')
      CALL PERSP ((NCOLS+7)*XLEN,((NROWS-1)/2-2)*YLEN,0.,
     & XP1,YPL,ZP1,IFLAG)
      CALL PERSP ((NCOLS+7)*XLEN,((NROWS-1)/2+2)*YLEN,0.,
     & XP2,YP2,ZP2,IFLAG)
      CALL PERSP ((NCOLS+3)*XLEN,((NROWS-1)/2*2)*YLEN,0.,
     & XP3,YP3,ZP3,IFLAG)
      CALL PERSP ((NCOLS+7)*XLEN,((NROWS-1)/2-2*YLEN,4.*XLEN/ZSCL,
     & XP4,YP4,ZP4,IFLAG)
      CALL PLOT (IPLT,XP1,YP1,0)
      CALL PLOT (IPLT,XP2,YP2,1)
      CALL CHARS (IPLT,0.,0.1,0.,0.,1.,1,6,
      CALL PLOT (IPLT,XP1,YP1,0)
      CALL PLOT (IPLT,XP3,YP3,1)
      CALL CHARS (IPL‘I‘,0.,0.1,0.,0.,1.,1,6,
      CALL PLOT (IPLT,XP1,YP1,0)
      CALL PLOT (IPLT,XP4,YP4,1)
      CALL CAMS (IPLT,0.,0.1,0.,0.,1.,1,6,
      RETURN
         END
C-------------------------------------------------------------------------------
      SUBROUTINE DRSIDE (IXY,N)
C.....DRAWS SIDE OR SLICE OF BLOCK DIAGRAM
C     IXY=0 TO DRAW X-AXIS SIDE, 1 TO DRAW Y-AXIS SIDE
C     N=ROW OR COLUMN NUMBER
```

```
      COMMON /MAP/IPLT,IPEN,IPT,NROWS,NCOLS,
     & ZZ(82,122),XLEN,YLEN,ZSCL,SCLH,SCLV,X0,Y0,Z0,AZ,EL,DS,REF
     & /PERS/SINAZ,COSAZ,SINEL,COSEL
      SAVE /MAP/,/PERS/
      IF (IXY.EQ.1) GOTO 2
      Y1=(NROWS-N)*YLEN
      CALL PERSP (0.,Y1,REF,X2,Y2,Z2,IFLAG)
      CALL PLOT (IPLTR,X2,Y2,0)
      CALL OPENPANL(-15,1)
      DO 1 J=1,NCOLS
      X1=(J-1)*XLEN
      Z1=Z(N,J)
      CALL PERSP (X1,Y1,Z1,X2,Y2,Z2,IFLAG)
    1 CALL PLOT (IPLT,X2,Y2,IPEN)
      CALL PERSP (X1,Y1,REF,X2,Y2,Z2,IFLAG)
      CALL PLOT (IPLT,X2,Y2,IPEN)
      CALL CLOSPANL
      RETURN
    2 X1=(N-1)*YLEN
      Y1=(NROWS-1)*YLEN
      CALL PERSP (X1,Y1,REF,X2,Y2,Z2,IFLAG)
      CALL PLOT (IPLT,X2,Y2,0)
      CALL OPENPANL(-15,1)
      DO 3 1=1,NROWS
      Y1=(NROWS-I)*XLEN
      Z1=Z(I,N)
      CALL PERSP (X1,Y1,Z1,X2,Y2,Z2,IFLAG)
    3 CALL PLOT (IPLT,X2,Y2,IPEN)
      CALL PERSP (X1,Y1,REF,X2,Y2,Z2,IFLAG)
      CALL PLOT (IPLT,X2,Y2,IPEN)
      CALL CLOSPANL
      RETURN
      END
C-------------------------------------------------------------------------------
      SUBROUTINE FACIES (THCK)
C.....DRAWS FACIES MAP
C     THCK= THICKNESS TO BE DRAWN, IF 0 LAST CYCLE'S
C            DEPOSIT IS DRAWN
C     DZZ = HEIGHT OF ONE LITHOLOGY BLOCK
      IMPLICIT COMPLEX (C)
      CHARACTER*72 IT
      DIMENSION FLIT(4)
      COMMON /BLK1/LBIT(50,41,61)
      COMMON IT,T0,TR,TD,DT,TB,TE,TID,TF,FLD,SWD,VIS,ROU,DV,CVC,CWV,
     & SDI(4),SDD(4),BD(4),FCO(5),
     & TI,LI,CPI(20),CVI(20),SLI(20,4),TEV,LEV,CPEV(20),
     & DX,N,M,NQ,QX(10,4),QY(10,4),QZ(10,4),
     & ZT(41,61),ZB(41,61),DZZ,L,
     & FEN(41,61),CVN(41,61),SUB(41,61),ZT(41,61),NY
      COMON /PLT/XMN,YMM,XMX,YMX,XSCL,YSCL,LPEN,MS,IXT,IYT
      MS=1
      TIM=TR-T0
      IF1=0
C.....SKIP IF DISPLAY NOT 0
C.....INITIALIZE
C     NC=CELL MULTIPLICITY
      NC=6
      DNC=1./NC/2.
      XYLEN=6.87/MAX0(N-1,M-1)
      IPLT=0
      CALL OPENPLOT (IPLT,1,13.75,13.75,-1.,15.,-5.,11 )
C.....ENTER MAIN LOOPS
   35 DO 215 IC=1,N-1
      DO 214 JC=1,M-1
      DO 213 ID=1,NC
      DO 212 JD=1,NC
      FJ=(JD*2.-1)*DNC
      F1=(ID*2.-1.)*DNC
      Y=(N-IC)-FI
      X=(JC-1)+FJ
C.....FIND CELL (IC,JC) AND PROPORTIONS OF INFLUENCE (FJ,FI)
      YSEC =((ZT(IC,JC)*(1-FI)
     &     +ZT(IC+L,JC)*FI)*(1-FJ)
     &    +(ZT(IC,JC+1)*(1-FI)
     &   +ZT(IC+L,JC+1)*FI)*FJ)
      YSEC1 =((ZT1(IC,JC)*(1-FI)
     &      +ZT1(1C+1,JC)*FI)*(1-FJ)
     &     +(ZT1(1C,JC+1)*(1-FI)
     &    +ZT1(IC+1,JC+1)*F1)*FJ)
C.....START SED-TYPE CELL
      IF (YSEC.LE.YSEC1.AND.THCK.LE.0.) GOTO 212
      FLIT(1)=0.
      FLIT(2)=0.
      FLIT(3)=0.
      FLIT(4)=0.
C.....FIND LITHOLDGY AND COLOR (COLOR INDEX IS GRAPHIC SOFTW. DEPEND.)
      DO 15 II=0,1
      DO 14 JJ=0,1
      ZH=(ZT(IC+II,JC+JJ)-ZB(IC+II,JC+JJ))/DZZ
      IF (THCK.LE.O)
     & ZH1=(ZTL(IC+II,JC+JJ)-SUB(IC+II,JC+JJ)*TD-ZB(IC+II,JC4-JJ) )/DZZ
      IF (THCK.GT.0.) ZH1=ZH-THCK/DZZ
      IF (ZH1.LT.0.) ZH1=0.
      IF (ZH1.GE.ZH.OR.ZH.LE.0.) GOTO 14
      NH=ZH+1
      NH1=ZH1+1
      FACT=(1-II+(2*II-1)*FI)*(1-JJ+(2*JJ-1)*FJ)/(NH-NH1+1)
      IF (NH.LE.0) NH=1
      DO 24 KH=NH1,NH
      LIT=0
      CALL SEDNO13 (IC+II,JC+JJ,KH,LIT)
      FLIT(LIT)=FLIT(LIT)+FACT
   24 CONTINUE
   14 CONTINUE
   15 CONTINUE
      FLITOT=FLIT(1)+FLIT(2)+FLIT(3)+FLIT(4)
      IF (FLITOT.LE.0.1) GOTO 212
      IMAX=5-INT(FLIT(A)/FLITOT*4.9999)
      INDCOL=111
      IF (IMAX.EQ.1) GOTO 16
      IND1=MIN0(IMAX,INT(FLIT(1)/AMAX1(FLIT(1)+FLIT(2),FLIT(1)+FLIT(3))
     & *(2*IMAX-1.0001)+1))
      IND2=MIN0(IMAX,INT(FLIT(2)/AMAX1(FLIT(1)+FLIT(2),FLIT(2)+FLIT(3))
     & *(2*IMAX-1.0001)+1))
      IND3=MIN0(IMAX,INT(FLIT(3)/AMAX1(FLIT(1)+FLIT(3) FLIT(2)+FLIT(3))
     & *(2*IMAX-1.0001)+1))
      INDCOL=IND1*100+IND2*10+IND3
C.....DRAW SEDIMENT TYPE CELLS
   16 CALL PLOT (IPLT,(X-DNC)*XYLEN,(Y+DNC)*XYLEN,0)
      CALL OPENPANL (INDCOL,0)
      CALL PLOT (IPLT,(X+DNC)*XYLEN,(Y+DNC)*XYLEN,0)
      CALL PLOT (IPLT,(X+DNC)*XYLEN,(Y-DNC)*XYLEN,0)
      CALL PLOT (IPLT,(X-DNC)*XYLEN,(Y-DNC)*XYLEN,0)
      CALL CLOSPANL
  212 CONTINUE
  213 CONTINUE
  214 CONTINUE
  215 CONTINUE
      CALL CLOSPLOT (IPLT)
      RETURN
      END
C-------------------------------------------------------------------------------
      SUBROUTINE MAP2D
C.....SUBROUTINE TO PLOT A CONWOUN MAP FROM RECTANGULAR GRID.
C      Z = ARRAY CONTAINING Z VNNUNS
C`     TG = ARRAY INDICATING WNSWNZX SNCUNUR IS TAGGED
      CHARACTER*10 LABEL
      CHARACTER*6 STRNG
      LOGICAL TG
      COMMON /MAP/IPLT,IPEN,IPT,NROWS,NCOLS,
     & ZZ(82,122),XLEN,YLEN,ZSCL,SCLH,SCLV,X0,Y0,Z0,AZ,EL,DS,REF, /TAG/TG(82,122)
      SAVE /MAP/,/TAG/
C.....INITIALIZE
      DO 6 I=1,NROWS
      DO 6 J=1,NCOLS
    6 TG(I,J)=.FALSE.
C.....OPEN PLOT
      XMAX=(NCOLS-1)*XLEN
      YMAX=(NROWS-1)*YLEN
      CALL OPENPLOT (IPLT,1,13.75,13.75,-1.,15.,-5.,11.)
C.....DRAW BOX
      CALL PLOT (IPLT,0.,0.,0)
      CALL OPENPANL (-15,1)
      CALL PLOT (IPLT,XMAX,0.,IPEN)
      CALL PLOT (IPLT,XHAX,YMAX,IPEN)
      CALL PLOT (IPLT,0.,YMAX,IPEN)
      CALL PLOT (IPLT,0.,0.,IPEN)
      CALL CLOSPANL
C.....FIND Z EXTREMA
      ZMAX=Z(1,1)
      ZMIN=ZMAX
      NO 1 I=1,NROWS
      NO 1 J=1,NCOLS
      ZMAX=AMAX1(ZMAX,Z(I,J))
    1 ZMIN=AMIN1(ZMIN,Z(I,J))
C.....FIND CONTOURING INTERVAL
      ZRANG=ZMAX-ZMIN
      IF (ZRANG.EQ.0.) GOTO 110
      CINT=ZRANG/20.
      CMAG=ALOG10(CINT)
      MAG=CMAG
      IF (CMAG.LT.0.) MAG=MAG-1
      CMANT=CMAG-MAG
      IVAL=10.**CMANT+0.5
      IF (IVAL.EQ.3) IVAL=2
      IF (IVAL.GE.4.AND.IVAL.LE.6) IVAL=5
      IF (IVAL.LT.7) GOTO 2
      IVAL=1
      MAG=MAG+1
    2 CINT=10.**MAG*IVAL
```

```
      CMIN=INT(ZMIN/CINT)*CINT
      IF (ZMIN.GT.0.) CMIN=CMIN+CINT
      CMAX=INT(ZMAX/CINT)*CINT
      IF (ZMAX.LT.0.) CMAX=CMAX-CINT
      NCON=(CNAX-CMIN)/CINT+1.1
C.....ENTER MAIN DO LOOP, ONCE PER CONTOUR
      DO 100 IC=L,NCON
      CONT=CMIN+CINT*(IC-1)
      WRITE (LABEL,5) CONT
    5 FORMAT (G10.4)
C.....SPECIFY PEN FOR THICK CONTOURS
      IF(MOD(INT(CONT/CINT),5).EQ.0) IPEN=IPEN
C.....ENTER SECONDARY DO LOOPS, ONCE PER HORIZ. SEGMENT, TG SEGMENTS
      DO 30 I=2,NROWS-1
      DO 30 J=1,NCOLS-1
   30 TG(I-1,J)=Z(I,J).LE.CONT.AND.Z(I,J+L).GT.CONT
C.....PLOT CONTOURS
C.....ENTER 4 INDEPENDENT DO LOOPS (ONCE PER EACH EDGE)
C.....TOP EDGE
      DO 40 J=1,NCOLS-1
      IL=1
      I2=1
      J1=J
      J2=J1+1
      IF (Z(I1,J1).LE.CONT.AND.Z(I2,J2).GT.CONT)
     +CALL PLTCON (CONT,I1,J1,I2,J2,LABEL)
   40 CONTINUE
C.....RIGHT EDGE
      DO 50 1=1,NROWS-1
      J1=NCDIS
      J2=NCOLS
      I1=I
      I2=I1+1
   50 IF (Z(I1,J1).LE.CONT.AND.Z(I2,J2).GT.CONT)
     +CALL PLTCON (CONT,I1,J1,I2,J2,LABEL)
C.....BOTTOM EDGE
      DO 60 J=1,NCOLS-L
      I1=NROWS
      I2=NROWS
      JZ=NCOLS-J
      J1=J2+L
   60 IF (Z(IL,JL).LE.CONT.AND.Z(I2,J2).GT.CONT)
     +CALL PLTCON (CONT,I1,JL,I2,J2,LABEL)
C.....LEFT EDGE
      DO 70 1=1,NROWS-1
      J1=1
      J2=1
      I2=NROWS-1
      I1=I2+1
   70 IF (Z(I1,J1).LE.CONT.AND.Z(I2,J2).GT.CONT)
     +CALL PLTCON (CONT,IL,J1,I2,J2,LABEL)
C.....ENTER NESTED NO LOOPS FOR CLOSED CONTOURS
      DO 80 I=2,NROWS-1
      DO 80 J=1,NCOLS-1
      I1=I
      I2=I1
      J1=J
      J2=J1+1
  80  IF (TG(I1-1,J1))
     +CALL PLTCON (CONT,I1,J1,I2,J2,LABEL)
  100 CONTINUE
C.....DRAW SCALE
  110 CALL PLOT (IPLT,0.5,-0.15,0)
      CALL PLOT (IPLT,XLEN*4+0.5,-0.15,0)
      LEG=4*SCLH
      WRITE (STRNG,13) LEG
   13 FORMAT (I5,'M')
      CALL PLOT (IPLT,0.4,-0.30,0)
      CALL CHARS (IPLT,D.,0.L,0.,0.,L.,1,6,STRNG)
      CALL PLOT (IPLT,D.1,-0.45,0)
      CALL CHARS (IPLT,0.,0.1,0.,0.,L.,1,12,'H0RIZ. SCALE')
      CALL PLOT (IPLT,1.B,-0.45,0)
      CALL CHARS (IPLT,0.,0.1,0.,0.,1.,1,18,'CONTOURS IN METERS')
C.....CLOSE PLOT
      CALL CLOSPLOT (IPLT)
      RETURN
      END
C--------------------------------------------------------------------------------
      SUBROUTINE MAP3D
C.....MAKES BLOCK DIAGRAM FROM SQUARE OR RECTANGULAR GRID
      COMMON /MAP/IPLT,IPEN,IPT,NROWS,NCOLS,
     & Z(82,122),XLEN,YLEN,ZSCL,SCLH,SCLV,X0,Y0,Z0,AZ,EL,DS,REF
     & /PERS/SINAZ,COSAZ,SINEL,COSEL
      SAVE /MAP/,/PERS/
C.....NROWS,NCOLS: NUMBER OF ROWS AND CONUNNS OR NODES
C     Z= ARRAY CONTAINING Z VANUNS
C     X0,Y0,Z0= CODRDINATES OR CENTER OR VIEW (INCHES
C     AZ= AZIMUTH OR OBSERVER (CLOCKWISE FROM Y AXIS (NORTH))
C     EL= ELEVATION ON OBSERVER (UP FROM HORIZONTAL)
C     DS= DISTANCE FROM OBSERVER TO CENTER OF VIEW (INCHES)
C     XLEN,YLEN= LENGTH OF SIDES OR EACH CELL (INCHES)
C     ZSCL=VERTICAL SCALE IN INCHES PER UNIT
C.....INITIALIZE
      SINAZ=SIN(AZ*3.1416/180.)
      COSAZ=COS(AZ*3.141S/1S0.)
      SINEL=SIN(EL*3.14L6/180.)
      COSEL=COS(EL*3.1416/180.)
C.....FIND POSITION OF OBSERVER
      XOBS=X0+DS*SINAZ*COSEL
      YOBS=Y0+DS*COSAZ*COSEL
      ZOBS=Z0+DS*SINEL
      IOBS=NROWS-INT(YOBS-YLEN+1001.)+1000
      JOBS=INT(XOBS/XLEN+1001.)-1000
C.....OPEN PLOT
      CALL OPENPLOT (IPLT,1,13.75,13.15,-16.,5.,-10.5, 10.5)
C.....ENTER 4 DO LOOPS TO DRAW CORNER AREAS
      DO 10 I=1,MIN0(IOBS-1,NROWS-1)
      DO 10 J=NCOLS-L,MAX0(JOBS+1,1),-1
   10 CALL DRCELL(I,J)
      DO 11 J=NCOLS-1,MAX0(JOBS+L,1),-1
      DO 11 I=NROWS-1,MAX0(IOBS+1,1),-1
   11 CALL DRCELL(I,J)
      DO 12 I=NROWS-1,MAX0(IOBS+1,1),-1
      DO 12 J=1,MIN0(JOBS-1,NCOLS-1)
   12 CALL DRCELL(I,J)
      DO 13 J=1,MIN0(JOBS-1,NCOLS-1)
      DO 13 I=1,MIN0(IOBS-1,NROWS-1)
   13 CALL DRCELL(I,J)
C.....DRAW ROW AND COLUMN OF OBSERVER
         IF (JOBS.LT.1.0R.JOBS.GT.NCOLS-1) GOTO 16
      DO 14 I=1,MIN0(IOBS-1,NROWS-1)
   14 CALL DRCELL(I,JOBS)
      DO 15 I=NROWS-1,MAX0(IOBS+1,1),-1
   15 CALL DRCELL(I,JOBS)
   16 IF (IOBS.LT.1.0R.IOBS.GT.NROWS-1) GOTO 19
      DO 17 J=NCOLS-L,MAX0(JOBS+L,L),-L
   17 CALL DRCELL(IOBS,J)
      DO 18 J=1,MIN0(JOBS-1,NCOLS-1)
   18 CALL DRCELL(IOBS,J)
C.....DRAW CENTER CELL
   19 IF (JOBS.GE.1.AND.JOBS.LE.NCOLS.AND.IOBS.GE.1.AND.IOBS.LE.NCOLS)
     & CALL DRCELL(IOBS,JOBS)
C.....DRAW SIDES
      IF (JOBS.LT.1) CALL DRSIDE (1,1)
      IF (JOBS.GT.NCOLS) CALL DRSIDE (1,NCOLS)
      IF (IOBS.LT.1) CALL DRSIDE (0,1)
      IF (IOBS.GT.NROWS) CALL DRSIDE(0,NROWS)
C.....DRAW BOTTOM
      IF (ZOBS.LT.0) CALL DRBOTT
C.....DRAW SCALE
      CALL DRSCAL
C.....CLOSE PLOT
      CALL CLOSPLOT (IPLT)
      RETURN
      END
C-------------------------------------------------------------------------------
      SUBROUTINE MAPCYC3 (IF,K1,K2,VEX)
C.....BUILDS GRID TO BE MAPPED
C     K1=1 ADD TOPOGRAPHY TO MAPPED QUANTITY K1=0 DON'T ADD
C     K2=1 ADD WATER DEPTH TO MAPPED QUANTITY, K2=0 DON'T ADD
C     VEX = VERTICAL EXAGGERATIDN FOR PERSPECTIVE DIAGRAM
C     IF = CELL MULTIPLICITY
      IMPLICIT COMPLEX (C)
      CHARACTER*72 IT
C     FOR STANDARD FORTRAN CHANGE 'EXTENDED BLOCK' TO 'COMMON',
      COMMON IT,T0,TR,TD,DT,TB,TE,TID,TF,FLD,SWD,VIS,ROU,DV,CVC,CWV,
     & SDI(4),SDD(4),BD(4),FCO(5),
     & TI,LI,CPI(20),CVI(20),SLI(20,4),TEV,LEV,CPEV(20),
     & DX,N,M,NQ,QX(10,4),QY(10,4),QZ(10,4) ,
     & ZT(41,61),ZB(41,61),DZZ,L,
     & FEN(41,61),CVN(41,61),SUB(41,61),ZT(41,61),NY,
      COMMON /MAP/IPLT,IPEN,IPT,NROWS,NCOLS,
     & ZZ(82,122),XLEN,YLEN,ZSCL,SCLH,SCLV,X0,Y0,Z0,AZ,EL,DS,REF
C.....SET CONSTANTS
      SCLH=DX/IF
      SCLV=SCLH/VEX
      NCOLS=(M-1)*IF+1
      NROWS=(N-1)*IF+1
C.....JUMP TO APPROPRIATE SECTION OR PROGRAM
      IF (IF.EQ.0) RETURN
      IF (IF/2) 20,10,10
C.....REDUCE GRID SIDE
   10 DO 1 I3=1,NROWS-1
      DO 1 J3=1,NCOLS-1
      I1=MOD(I3-1,IF)
      J1=MOD(J3-1,IF)
      I2=(I1-1)/IF+1
      J2=(J3-1)/IF+1
      I4=(I3-1+IF/2)/IF+1
      J4=(J3-1+IF/2)/IF+1
```

```
    1 ZZ(I3,J3)=(ZT(I2,J2)*(IF-I1)*(IF-J1)+ZT(I2+1,J2)*I1*(IF-J1)+
     & ZT(I2,J2+1)*(IF-I1)*J1+ZT(I2+1,J2+1)*I1*J1)/(IF*IF)
C.....DO LAST COLUMN EXCEPT LAST ELEMENT
      DO 2 I3=1,NROWS-1
      I1=MOD(I3-1,IF)
      I2=(I3-1)/IF+1
      I4=(I3-1+IF/2)/IF+1
    2 ZZ(I3,NCOLS)=(ZT(I2,M)*(IF-I1)+ZT(I2+1,M)*I1)/IF
C.....DO LAST ROW EXCEPT LAST ELEMENT
      DO 3 J3=L,NCOLS-1
      J1=MOD(J3-1,IF)
      J2=(J3-1)/IF=+1
      J4=(J3-1+IF/2)/IF+1
    3 ZZ(NROWS,J3)=(ZT(N,J2)*(IF-J1]+ZT(N,J2+1)*J1)/IF
C.....DO LAST ELEMENT
      ZZ(NROWS,NCOLS)=ZT(N,M)
      GOTO 30
C.....INCREASE GRID SIDE
   20 DO 5 I1=1,(N-1)/(-IF)+1
      DO 5 J1=1,(M-1)/(-IF)+1
    5 ZZ(I1,J1)=ZT((I1-1)*(-IF)+1,(J1-1)*(-IF)+1)
C.....MAP
   30 XLEN=6.87/MAX0(NROWS-1,NCOLS-1)
      YLEN=XLEN
      ZSCL=XLEN/DX*VEX*IF
      X0=(NCOLS-1)*XLEN/2.
      Y0=(NROWS-1)*YLEN/2.
      Z0=0.
      NS=(X0+Y0)*2.
C.....AZ MUST DIFFER BY 4 DEGREES BETWEEN VIEW OF EACH EYE
      RETURN
      END
C-------------------------------------------------------------------------------
      SUBROUTINE PERSP (XI,YI,ZI,XP,YP,ZP,IFLAG)
C.....TRANSFOMS (X,Y,Z) IN SPACE TO (XP,YP) ON A PLANE, ZP IS THE
C     DISTANCE FROM 0BSERVER'S PLANE.
C     (X0,Y0,Z0)=COORDINATES OF CENTER OF VIEW (COMMONLY CENTER OF
C                OBJECT BEING VIEWED)
C     AZ=AZIMUTH OF OBSERVER (CLOCKWISE FROM Y AXIS (NORTH)
C     EL=ELEVATION OF VIEWER (UP MOM HORIZONTAL)
C     DS=DISTANCE OF VIEWER FROM CENTER OR VIEW
C     IFLAG=1 IF ERROR OCCURS (I.E. IF POINT BEHIND VIEWER)
      COMMON /MAP/IPLT,IPEN,IPT ,NROWS,NCOLS,Z(82,122),XLEN,
     & YLEN,ZSCL,SCLH,SCLV,X0,Y0,Z0,AZ,EL,DS,REF
     & /PERS/SINAZ,COSAZ,SINEL,COSEL
      SAVE /MAP/,/PERS/
      IFLAG=0
C.....TRANSLATE
      X1=XI-X0
      Y1=YI-Y0
      Z1=ZI*ZSCL-Z0
C.....ROTATE AZIMUTH
      X2=-COSAZ*X1+SINAZ*Y1
      Y2=-SINAZ*X1-COSAZ*Y1
      Z2=Z1
C.....ROTATE ELEVATION
      X3=X2
      Y3=SINEL*Y2+COSEL*Z2
      Z3=-COSEL*Y2+SINEL*Z2
C.....TRANSFORM FOR PERSPECTIVE
```

```
      ZP=DS-Z3
      IF (ZP.GT.0.) GOTO 1
      IFLAG=1
      RETURN
    1 C=DS/ZP
      XP=X3*C
      YP=Y3*C
      RETURN
      END
C-------------------------------------------------------------------------------
      SUBROUTINE PLTARR (IPLT,X1,Y1,X2,Y2,Z,IPEN)
C.....PLOTS ARROW BETWEEN TWO POINTS
      DATA PI/3.1415926/
      ARG(Z1,Z2)=ATAN(Z2/Z1)+PI*(0.5-SIGN(0.5,Z1))
C.....PLOT ARROW SHAFT
      CALL PLOT (IPLT,X1,Y1,0)
      CALL PLOT (IPLT,X2,Y2,IPEN)
C.....PLOT ARROW HEAD
      IF (X1.EQ.X2.AND.Y2.GE.Y1) ANG=-PI/2.
      IF (X1.EQ.X2.AND.Y2.LT.Y1) ANG=PI/2.
      IF (X1.NE.X2) ANG=ARG(X1-X2,Y1-Y2)
      XP=X2+0.05*COS(ANG+D.4)
      YP=Y2+0.05*SIN(ANG+0.4)
      CALL PLOT(IPLT,XP,YP,0)
      CALL PLOT(IPLT,X2,Y2,IPEN)
      XP=X2+0.05*COS(ANG-0.4)
      YP=Y2+0.05*SIN(ANG-0.4)
      CALL PLOT (IPLT,XP,YP,IPEN)
C.....PLOT DEPTH SEGMENT ACROSS ARROW
      XZ1=(X1+X2-SIN(ANG)*Z)/2
      YZ1=(Y1+Y2+COS(ANG)*Z)/2
      XZ2=XZ1+SIN(ANG)*Z
      YZ2='LZ1-CO5(ANG)*Z
      CALL PLOT (IPLT,XZ1,YZ1,0)
      CALL PLOT (IPLT,XZ2,YZ2,IPEN-1)
      RETURN
      END
C-------------------------------------------------------------------------------
      SUBROUTINE PLTCON (CONT,IL,J1,I2,J2,LABEL)
C.....PLOTS A SINGLE CONTOUR LINE STARTING AT SEGMENT (I1,J1) (I2,J2)
C.....PLOTTED CONTOUR STARTS TO THE RIGHT OF SEGMENT
C     IDL=1 WHILE LABEL IS BEING DRAWN, 0 ELSE
C     I1=1 WHEN A LABEL HAS ALREADY BEEN DRAWN, 0 ELSE
C     CLV=CONTOUR LENGTH OF LAST VECTOR
C     CCLL=CUM. CONT. LENGTH SINCE LAST LAEEL
C     CCLT=CONT. LENGTH SINCE START OF CONTOUR (USED FOR TICKS)
C     CLL=CONT. LENGTH OF LABEL
C     CLBL=CONT. LENGTH BETWEEN LABELS
C     CLBT=CONT. LENGTH BETWEEN TICKS
C     XTICK1(I),YTICK1(I),XTICK2(I),YTICK2(I)= COORDS. OF TICKS
C     XTEMP(I),YTEMP(I)= COORDS. OR TEMPORARY VECTORS
      DIMENSION XTICK1(16),YTICK1(L6),XTICK2(16),YTICK2(16),XT(16),
    & YT(16)
      CHARACTER*5 LABEL
      LOGICAL TG
      COMMON /MAP/IPLT,IPEN,IPT,NROWS,NCOLS,
     & ZZ(82,122),XLEN,YLEN,ZSCL,SCLH,SCLV,X0,Y0,Z0,AZ,EL,DS,REF,/TAG/TG(82,122)
      SAVE /MAP/,/TAG/
C.....SET PARAMETERS ANB INITIALIZE
      CLL=0.35
      CLBL=6.
      CLBT=0.5
      CCLT=0.4
      CCLL=5.5
      HGT=0.06
      IDL=0
      IL=0
      IFIRST=0
      IT=0
C.....FIND INCREMENTS
    5 INCI=J2-J1
      INCJ=I1-I2
C.....FIND DISTANCE OF INTERSECTION ALONG SEGMENT
      D=(CONT-Z(I1,J1))/(Z(I2,J2)-Z(I1,J1))
      IF (D.GT.1.) D=1.
      IF (CONT-Z(I1,J1).EQ.0..OR.D.LT.0.) D=0.
C.....FIND NEW X,Y
      XN=XLEN*(J1-1+D*INCI)
      YN=YLEN*(NROWS-I1+D*INCJ)
      IF (IFIRST.EQ.0) GOTO 1
      DX=XN-X
      DY=YN-Y
      CLV=SQRT(DX**2+DY**2)
      IF (ABS(CLV).LT.0.00001) GOTO 3
      IF (DX.EQ.0.) DX=0.00001
      TANV=DY/DX
      CCLL=CCLL+CLV
C.....FIND TICKS IF NECESSARY
      IF (IL.NE.0) GOTO 8
      CCLT=CCLT+CLV
      NTICK=MIN0(INT(CCLT/CLBT),6
      DO 9 ITICK=(CCLT-CLV)/CLBT+1,NTICK
      XTICK1(ITICK)=X+(CLBT*(ITICK)-CCLT+CLV)*DX/CLV
      YTICK1(ITICK)=Y+(CLBT*(ITICK)-CCLT+CLV)*DY/CLV
      XTICK2(ITICK)=XTICK1(ITICK)+DY*0.05/CLV
    9 YTICK2(ITICK)=YTICK1(ITICK)-DX*0.05/CLV
C.....DRAW LABEL IF NECESSARY
C.....CHECK FOR LABEL START AND DRAW CONTOUR UP TO LABEL
    8 IF (CCLL.LW.CLBL.OR.IDL.EQ.1) GOTO 2
      XL1=X+(CLBL-CCLL+CLV)*DX/CLV
      YL1=Y+(CLBL-CCLL+CLV)*DY/CLV
      CALL PLOT (IPLT,XL1,YL1,IPEN)
      IDL=1
C.....CHECK FOR LABEL END AND DRAW LABEL
    2 IF(IDL.NE.1) GOTO 7
      DSL=SQRT((XN-XL1)**2+(YN-YL1)**2)
      IF (DSL.LT.CLL) GOTO 4
      DX1=XL1-X
      IF (DX1.EQ.0.) DX1=0.00001
      ALPHA=ABS(ATAN((YL1-Y)/DX1)-ATAN(TANV)
      IF ((XL1-X)*DX.LT.0.) ALPHA=:3.1416-ALPHA
      B=SQRT((XL1-X)**2+(YL1-Y)**2)
      P=B*COS(ALPHA)
      IF (P.GT.100.) P=100.
      RAD=P**2-B**2+CLL**2
      IF (RAD.LT.0.)RAD=0.
      A=P+SQRT (RAD)
      XL2=X+A*DX/CLV
      YL2=Y+A*DY/CLV
      ANG=ATAN((YL2-YL1)/(XL2-XL1))*180./3.1416
      IF (XL2.LT.XL1) GOTO 11
      XL3=XL1
      YL3=YLL
      GOTO 12
   11 XL3=XL2
      YL3=YL2
   12 XL3=XL3+(YL2-YL1)*SIGN(1.,XL2-XL1)/CLL*HGT/2.
      YL3=YL3-ABS(XL2-XL1)/CLL*HGT/2.
      CALL PLOT (IPLT,XL3,YL3,0)
      CALL CHARS (IPLT,ANG,HGT,0.,0.,1.,IPEN,5,LABEL)
      CALL PLOT (IPLT,XL2,YL2,0)
      IDL=O
      IL=1
      IT=0
      CCLL=CCLL-CLBL-CLL
      GOTO 8
C.....MOVE PEN (FIRST TIME) OR DRAW VECTOR
    7 IP=IFIRST*IPEN
      CALL PLOT (IPLT,XN,YN,IP)
    4 X=XN
      Y=YN
      IF (IDL.EQ.O) GOTO 3
      IT=IT+1
      XT(IT)=X
      YT(IT)=Y
C.....UNTAG SEGMENT AT END OE VECTOR AND RETURN IF NECESSARY
    3 IF (I1.EQ.I2.AND.(I1+INCI.GT.NROWS.OR.I1+INCI.LT.1)) GOTO 40
      IF (J1.EQ.J2.AND.(J1+INCJ.GT.NCOLS.OR.J1+INCJ.LT.1)) GOTO 40
      IF (I1.NE.I2.OR.I1.EQ.1.OR.I1.EQ.NROWS.OR.J1.GT.J2) GOTO 6
      IF (.NOT.TG(IL-L,J1)) GOTO 40
      TG(I1-1,J1)=.FALSE.
C.....INDICATE THAT FIRST MOVE IS DONE
    6 IFIRST=1
C.....FIND GEOMETRIC CONDITION OF NEXT VECTOR
      IA=0
      IB=0
      IF (Z(I2+INCI,J2+INCJ).LE.CONT) IA=1
      IF (Z(I1+INCI,J1+INCJ).GT.CONT) IB=2
      IC=IA+IB
      GOTO (10,20,30),1C
C.....NEITHER BACK NOR FRONT (I.E. SIDE ONLY)
      I1=I1+INCI
      I2=I2+INCI
      J1=J1+INCJ
      J2=J2+INCJ
      GOTO 5
C.....FRONT ONLY
   10 I1=11+INCI-INCJ
      J1=JL+INCI+INCJ
      GOTO 5
C.....BACK ONLY
   20 I2=I2+INCI+INCJ
      J2=J2-INCI+INCJ
      GOTO 5
C.....BOTH BACK AND FRONT
   30 DL=(CONT-Z(I1+INCI,J1+INCJ))/(Z(I2+INCI,J2+INCJ)-Z(I1+INCI,
     + J1+INCJ))
      IF (D1-D) 10,10,20
C.....RETURN SEQUENCE
C.....DRAW STORED CONTOUR IF LABEL WASN'T FINISHED
```

```
   40 IF (IDL.EQ.0) GOTO 42
      DO 41 I=1,IT
   41 CALL PLOT (IPLT,XT(I),YT(I),IPEN)
C.....DRAW TICKS IF NO LABEL HAS BEEN DRAWN OR LABEL WASN'T FINISHED
   42 IF (IL.EQ.1.AND.IDL.EQ.0) RETURN
      DO 43 ITICK=1,NTICK
      CALL PLOT (IPLT,XTICK1(ITICK),YTICK1(ITICK),0)
   43 CALL PLOT (IPLT,XTICK2(ITICK),YTICK2(ITICK),IPEN)
      RETURN
      END
C-------------------------------------------------------------------------------
      SUBROUTINE PLTCRS (IPLT,X,Y,IPEN)
C.....PLOTS CROSS AT POSITION (X,Y)
      CALL PLOT (IPLT,X-0.05,Y,0)
      CALL PLDT (IPLT,X+0.05,Y,IPEN)
      CALL PLOT (IPLT,X,Y-0.05,0)
      CALL PLOT (IPLT,X,Y+0.05,IPEN)
      RETURN
      END
C-------------------------------------------------------------------------------
      SUBROUTINE PLTGRD (IPLT,IPEN)
C.....OPENS PLOT AND PLOTS GRID
      IMPLICIT COMPLEX (C)
      CHARACTER*72 IT
C.....FOR STANDARD FORTRAN CHANGE 'EXTENDED BLOCK' TO 'COMMON',
      COMMON IT,T0,TR,TD,DT,TB,TE,TID,TF,FLD,SWD,VIS,ROU,DV,CVC,CWV,
     & SDI(4),SDD(4),BD(4),FCO(5),
     & TI,LI,CPI(20),CVI(20),SLI(20,4),TEV,LEV,CPEV(20),
     & DX,N,M,NQ,QX(10,4),QY(10,4),QZ(10,4) ,
     & ZT(41,61),ZB(41,61),DZZ,L,
     & FEN(41,61),CVN(41,61),SUB(41,61),ZT(41,61),NY
C.....OPEN PLOT
      XYLEN=6.87/MAX0(M-1,N-1)
      CALL OPEN-PLOT (IPLT,1,13.75,13.75,-1.,15.,-5.,11.)
      XHX=(M-1)*XYLEN
      YMX=(N-1)*XYLEN
C.....DRAW GRID ON BOX
      DO 1 J=1,M
      X=(J-1)*XYLEN
      CALL PLOT (IPLT,X,0.,0
    1 CALL PLOT (IPLT,X,YMX,IPEN)
      DO 2 I=1,N
      Y=(I-1)*XYLEN
      CALL PLOT (IPLT,0.,Y,0)
    2 CALL PIDT (IPLT,XMX,Y,IPEN)
      CALL CLOSPLOT(IPLT)
      RETURN
      END
C-------------------------------------------------------------------------------
      SUBROUTINE PLTNOD3 (IPLT,IPEN,K1,FENMIN,UAR,UDP)
C.....PLOTS VELOCITY VECTORS AT EACH NODE
C     K1=0 PLOTS VELOCITY ARROWS
C`    K`=1 PLOTS FLOW ARROWS
      IMPLICIT COMPLEX (C)
      CHARACTER*72 IT
      CHARACTER*80 STRNG
C.....FOR STANDARD FORTRAN CHANGE 'EXTENDED BLOCK' TO 'COMMON',
      COMMON /BLK1/LBIT(50,41,61)
      COMMON IT,T0,TR,TD,DT,TB,TE,TID,TF,FLD,SWD,VIS,ROU,DV,CVC,CWV,
     & SDI(4),SDD(4),BD(4),FCO(5),
     & TI,LI,CPI(20),CVI(20),SLI(20,4),TEV,LEV,CPEV(20),
     & DX,N,M,NQ,QX(10,4),QY(10,4),QZ(10,4) ,
     & ZT(41,61),ZB(41,61),DZZ,L,
     & FEN(41,61),CVN(41,61),SUB(41,61),ZT(41,61),NY
C.....SET PARAMETERS
      XYLEN=6.87/MAX0(M-1,N-1)
      SCALE=XYLEN/UAR
      SCALZ=0.
      IF (UDP.NE.0.) SCALZ=XYLEN/UDP
C.....OPEN PLOT AND DRAW GRID
      CALL OPENPLOT (IPLT,1,13.75,13.75,-1.,15.,-5.,11.)
C.....ENTER MAIN NESTED LOOPS (ONCE PER NODE)
      DO 1 I=1,N
      DO 1 J=1,M
      IF (FEN(I,J).LT.FENMIN) GOTO 1
      X=(J-1)*XYLEN
      Y=(N-I)*XYLEN
C.....PLOT CROSS IF VELOCITY IS 0.
      IF (CVN(I,J).EQ.(0.,0.)) CALL PLTCRS(IPLT,X,Y,IPEN)
C.....PLOT ARROW
      IF (K1.EQ.O) GOTO 4
      XD=REAL(CVN(I,J))*SCALE/2.*(FEN(I,J)*DZ)
      YD=AIMAG(CVN(I,J))*SCALE/2.*(FEN(I,J)*DZ)
      GOTO 5
    4 XD=REAL(CVN(I,J))*SCALE/2.
      YD=AIMAG(CVN(I,J))*SCALE/2.
    5 ZZ=DZ*SCALZ*FEN(I,J)
      CALL PLTARR (IPLT,X-XD,Y-YD,X+XD,Y+YD,ZZ,IPEN)
    1 CONTINUE
C.....PLOT POSITION OF SOURCES
      DO 2 K=1,LI
      X=REAL(CPI(K))/DX*XYLEN
      Y=AIMAG(CPI(K))/DX*XYLEN
      CALL PLTCRS (IPLT,X,Y,IPEN)
      WARMS (STRNG,10) K
   10 FORMAT (12)
    2 CALL CHARS (IPLT,U.,D.1,D.,0.,L.,5,2,STRNG)
C.....PLOT SCALE
      ZZ=XYLEN
      CALL PLTARR (IPLT,(M-2)*XYLEN-.3,-0.15,(M-1)*XYLEN-.3,-0.15,ZZ
     & IPEN)
      WRITE (STRNG,13) UAR
   13 FORMAT (F4.0,' M/S')
      CALL PLOT (IPLT,(M-2)*XYLEN-.6,-0.30,0)
      CALL CHARS (IPLT,0.,0.1,0.,0.,1.,1,8,STRNG)
      CALL PLOT (IPLT,(M-2)*XYLEN-0.7,-0.45,0)
      CALL CHARS (IPLT,0.,0.1,0.,0. ,1,11,'VELOC. SCALE')
      CALL CLOSPLOT (IPLT)
      RETURN
      END
C-----------------------------------------------------------------------------
      SUBROUTINE PLTPAT3 (CPO,K,IPLT,IPEN)
C.....PLOTS PATHS OR INDIVIDUAL FLUID ELEMENTS
C     XYLEN=LENGTH IN INCHES OF CELL SIDE
      IMPLICIT COMPLEX (C)
      CHARACTER*72 IT
      COMMON IT,T0,TR,TD,DT,TB,TE,TID,TF,FLD,SWD,VIS,ROU,DV,CVC,CWV,
     & SDI(4),SDD(4),BD(4),FCO(5),
     & TI,LI,CPI(20),CVI(20),SLI(20,4),TEV,LEV,CPEV(20),
     & DX,N,M,NQ,QX(10,4),QY(10,4),QZ(10,4) ,
     & ZT(41,61),ZB(41,61),DZZ,L,
     & FEN(41,61),CVN(41,61),SUB(41,61),ZT(41,61),NY
      COMMON /PPAT/F1,NYT,XYLEN,ICALL
      SAVE /PPAT/
C.....OPEN PLOT
      IF (K.NE.1.OR.NY.NE.0) GOTO 2
      F1=3.1E+07
      IF (ICALL.NE.1) IPLT=2
      ICALL=1
      NYT=TE*F1/DT/TB
      XYLEN=6.87/MAX0(M-1,N-1)/DX
      CALL OPENPLOT (IPLT,1,13.75,13.75,-1.,15.,-5.,11.)
    2 X1=REAL(CPO)*XYLEN
      IF (X1.LT.0.) GOTO 1
      Y1=AIMAG(CPO)*XYLEN
      X2=REAL(CP(K))*XYLEN
      IF (X2.LT.0.) GOTO 1
      Y2=AIMAG(CP(K))*XYLEN
      IF (CPO.EQ.CP(K)) CALL PLTCRS (IPLT,X1,Y1,IPEN)
      IF (CPO.NE.CP(K)) CALL PLTARR (IPLT,X1,Y1,X2,Y2,0.,IPEN)
    1 IF (K.LT.L.OR.NY.LT.NYT) RETURN
      CALL CLOSPLOT (IPLT)
      IPLT=IPLT+1
      RETURN
      END
C-----------------------------------------------------------------------------
      SUBROUTINE READGU3 (IFL,IF2)
C.....READS FROM UNFORMATTED GRAPHIC FILE
C     IF1=1 IF END OF FILE IS FOUND
C     IF2=1 DON'T READ GENERAL DATA
      IMPLICIT COMPLEX (C)
      CHARACTER*8 BLANK
      DIMENSION RD(61)
C.....FOR STANDARD FURTRAN CHANGE 'EXTENDED BLOCK' TO 'COMNON' ,
      CHARACTER*72 IT
      COMMON /BLK1/LBIT(50,41,61)
      COMMON IT,T0,TR,TD,DT,TB,TE,TID,TF,FLD,SWD,VIS,ROU,DV,CVC,CWV,
     & SDI(4),SDD(4),BD(4),FCO(5),
     & TI,LI,CPI(20),CVI(20),SLI(20,4),TEV,LEV,CPEV(20),
     & DX,N,M,NQ,QX(10,4),QY(10,4),QZ(10,4) ,
     & ZT(41,61),ZB(41,61),DZZ,L,
     & FEN(41,61),CVN(41,61),SUB(41,61),ZT(41,61),NY
      DATA BLANK/'        '/
      IF1=0
      IF (IF2.EQ.1) GOTO 19
C.....READ DATA FILE
      READ (22,ERR=10,END=20)
     & IT,T0,TR,TD,DT,TB,TE,TID,TF,FLD,SWD,VIS,ROU,DV,CVC,CWV,
     & (5DI(K)K=1,4),(SDD(K),K=1,4),(BD(K),K=1,4),
     & (FCO(K),K=1,5),TI,LI
      IF (LI.GT.0) READ (22,ERR=10,END=20)
     & (CPI(K),CVI(K),(SLI(X,L1),L1=1,4),K=1,LI)
      READ (22,ERR=10,END=20) TEV,LEV
      IF (LEV.NE.0) READ (22,ERR=10,END=20) (CPEV(LEVI),LEVI=1,LEV)
      READ (22,ERR=10,END=20) DX,N,M,NQ
      IF (NQ.GT.0) READ (22,ERR=10,END=20)
     & ((QX(K,L1),QY(K,L1),QZ(K,L1),L1=1,4),K=1,NQ)
      RETURN
C.....READ DATA FOR CURRENT CYCLE
   19 READ (22,ERR=10,END=99) T0
```

```
      DO 28 I=1,N
      IF (T0.EQ.0.) GOTO 27
      DO 1 J=1,M
    1 ZT1(I,J)=ZT(I,J)
   27 READ (22,ERR=10,END=20) (ZT(I,J),J=1,M)
   28 CONTINUE
      DO 2 I=1,N
      READ (22,ERR=10,END=20) (ZB(I,J),J=1,M)
      IF (T0.NE.0.) GOTO 2
      DO 35 J=1,M
   35 ZT1(I,J)=ZB(I,J)
    2 CONTINUE
C.....READ LITHOLOGY
      READ (22,ERR=10,END=20) DZZ
      DO 29 I=1,N
      DO 29 J=1,M
   29 READ (22,ERR=10,END=20) KL,(LBIT (K,I,J),K=1,KL)
      DO 9 I=1,N
    9 READ (22,ERR=10,END=20) (FEN(I,J),J=1,M)
      READ (22,ERR=10,END=20) EA
      DO 31 I=1,N
      READ (22,ERR=10,END=20) (RD(J),J=1,M)
      DO 31 J=1,M
   31 CVN(I,J)=CMPLX(RD(J),0.)
      DO 12 I=1,N
      READ (22,ERR=10,ERR=20) (RD(J),J=1,M)
      DO 12 J=1,M
   12 CVN(I,J)=CVN(I,J)+CMPLX(0.,RD(J))
      RETURN
   10 WRITE (6,11)
   11 FORMAT (' SUBROUTINE READGU FOUND ERROR IN GRAPHIC FILE’)
      STOP
   20 WRITE (6,21)
   21 FORMAT (' SUEROUTINE READGU FOUND EOF IN GRAPHIC FILE’)
      STOP
   99 IF1=1
      RETURN
      END
C-------------------------------------------------------------------------------
      SUBROUTINE SEDNO13 (I,J,K,LIT)
C     I=ROW OF NODE
C     J=COL OF NODE
C     K=CELL, IF 0, NEGATIVE OR > 800, ERROR IS RETURNED
C     LIT=LITHOLOGY: 1, 2, 3, OR 4. IF 0 OR NEGATIVE, LIT IS RETURNED
      IMPLICIT COMPLEX (C)
      CHARACTER*72 IT
      COMMON /BLK1/LBIT(50,41,61)
      COMMON IT,T0,TR,TD,DT,TB,TE,TID,TF,FLD,SWD,VIS,ROU,DV,CVC,CWV,
     & SDI(4),SDD(4),BD(4),FCO(5),
     & TI,LI,CPI(20),CVI(20),SLI(20,4),TEV,LEV,CPEV(20),
     & DX,N,M,NQ,QX(10,4),QY(10,4),QZ(10,4) ,
     & ZT(41,61),ZB(41,61),DZZ,L,
     & FEN(41,61),CVN(41,61),SUB(41,61),ZT(41,61),NY
C.....ERODE
      IF (K.LE.800.AND.K.GT.0.AND.LIT.GE.0.AND.LIT.LE.4) GOTO 2
      OPEN (24,FILE='FOR24.D',FORM:'FORMATTED')
      REWIND(24)
      WRITE (24,11) T0,TR,L
   11 FORMAT (1X,' TIME:',F15.7,' YEARS OF ',F15.7,' YEARS'/
      & ' L=',I6)
      WRITE (24,12) K,LIT
   12 FORMAT (' SED. COLUMN < 1 OR > 800, K=',I4,' LIT=',I1)
      CLOSE (24)
      STOP
    2 LW=(K+15)/16
      LB=2*K+14-16*LW
      IF (LIT.GT.0) GOTO 1
      LIT=IBITS(LBIT(LW,I,J),LB,2)+1
      RETURN
C.....DEPOSIT
    1 IF((LIT-1)/2.EQ.1) THEN
      LBIT(LW,I,J)=IBSET(LBIT(LW,I,J),LB+1
      ELSE
      LBIT(LW,I,J)=IBCLR(LBIT(LW,I,H),LB+1
      ENDIF
      IF(MOD(LIT,2).EQ.0) THEN
      LBIT(LW,I,J)=IBSET(LBIT(LW,I,H),LM
      ELSE
      LBIT(LW,I,J)=IBCLR(LBIT(LW,I,J),LB
      ENDIF
      RETURN
      END
C--------------------------------------------------------------------------------
```